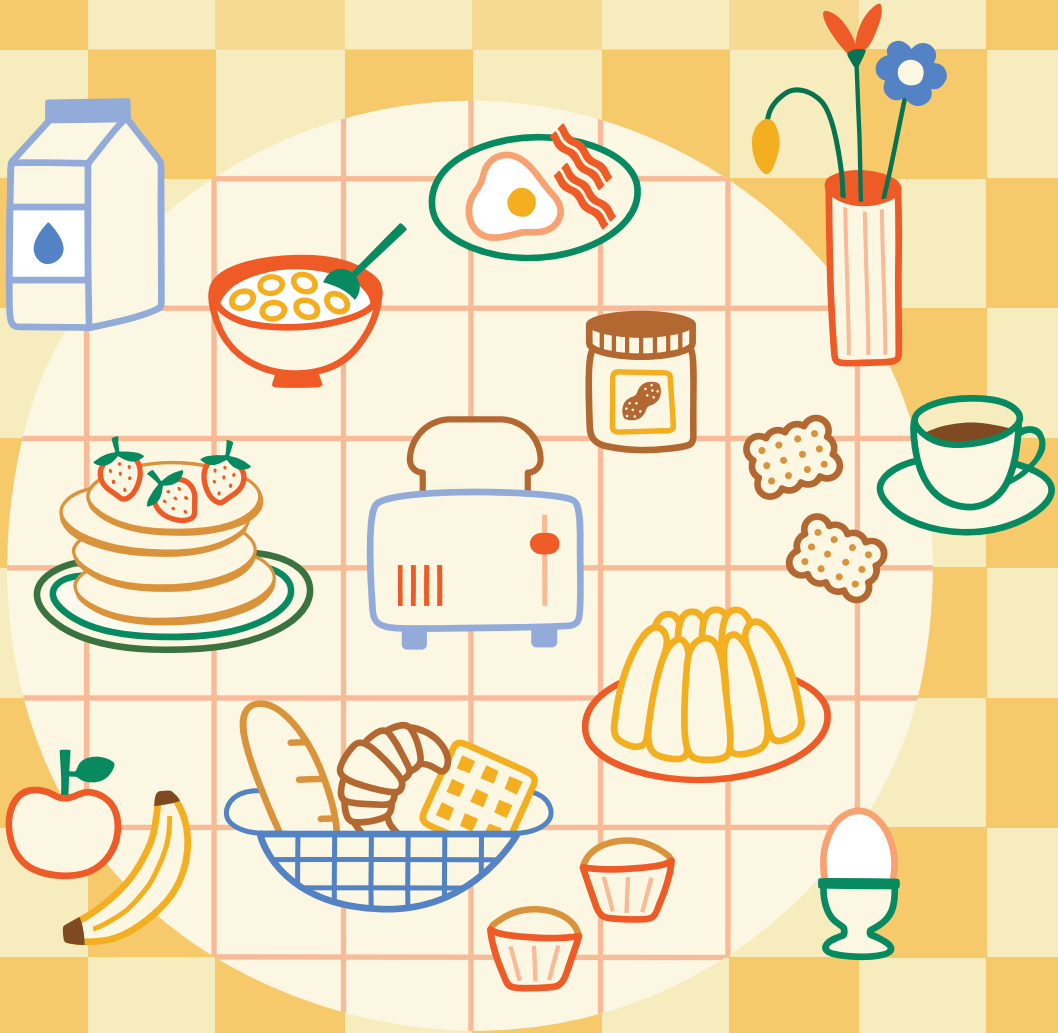
IN VITRO INSIGHTS INTO

DIETARY ADVANCED GLYCATION END PRODUCTS AND THEIR IMPACT ON INTESTINAL HEALTH



FLEUR A.C. JANSEN

Propositions

1. A low-glycemic index diet is more important to general health than a low-advanced glycation end product (AGE) diet.
   (this thesis)
2. Binding of AGEs to receptor for AGEs (RAGE) is routinely misinterpreted as evidence of RAGE activation.
   (this thesis)
3. Plasma micronutrient values within the reference range do not reflect optimal health status.
4. The habitual ending that "more research is needed" often hides the honest conclusion that "no further research is warranted".
5. Genuine scientific consensus can only emerge when researchers have the courage to be vulnerable.
6. The current fragmentation of household and employment structures complicates the design of social policy.
7. The act of dressing lightly is an underappreciated but effective strategy for weight control.

Propositions belonging to the thesis, entitled

In vitro insights into dietary advanced glycation end products and their impact on intestinal health

Fleur A.C. Jansen
Wageningen, 9 July 2026

IN VITRO INSIGHTS INTO

DIETARY ADVANCED GLYCATION END PRODUCTS AND THEIR IMPACT ON INTESTINAL HEALTH

FLEUR A.C. JANSEN

Thesis committee

Promotor
Prof. Dr Vincenzo Fogliano
Professor of Food Quality and Design
Wageningen University & Research

Co-promotors
Dr Tamara Hoppenbrouwers
Assistant Professor in Food Quality and Design
Wageningen University & Research

Dr Klaske van Norren
Associate Professor in Human Nutrition and Health
Wageningen University & Research

Dr Josep Rubert Bassedas
Assistant Professor in Human Nutrition and Health
Wageningen University & Research

Other members
Prof. Dr Hans Bouwmeester, Wageningen University & Research
Dr Chantal Fradin, Université de Lille, Lille, France
Dr Kristiaan Wouters, Maastricht University
Dr Coen Govers, Wageningen University & Research

This research was conducted under the auspices of the VLAG Graduate School (Biobased, Biomolecular, Chemical, Food and Nutrition Sciences).

In vitro insights into dietary advanced glycation end products and their impact on intestinal health

Fleur A.C. Jansen

Thesis

submitted in fulfilment of the requirements for the degree of doctor
at Wageningen University
by the authority of the Rector Magnificus,
Prof. Dr C. Kroeze,
in the presence of the
Thesis Committee appointed by the Academic Board
to be defended in public
on Thursday 9 July 2026
at 10.30 a.m. in the Omnia Auditorium.

Fleur A.C. Jansen
In vitro insights into dietary advanced glycation end products and their impact on intestinal health.
186 pages.

PhD thesis, Wageningen University, Wageningen, The Netherlands (2026)
With references, with summary in English

DOI: 10.18174/681620

Table of contents

Chapter 1	General introduction	**7**
Chapter 2	Dietary advanced glycation end products interacting with the intestinal epithelium: what do we really know?	**23**
Chapter 3	Protein-bound dietary advanced glycation end products cross the intestinal barrier: organoid models suggest paracellular transport as predominant route	**45**
Chapter 4	Seeking standardized *in vitro* models of AGE-RAGE signaling in the physiological perspective of glycated dietary proteins	**79**
Chapter 5	Role of LPS in RAGE activation: confounder or co-factor?	**125**
Chapter 6	General discussion	**147**
Chapter 7	English summary	**173**
Appendices	Acknowledgements	**178**
	About the author	**181**
	List of publications	**182**
	Training activities	**184**



1

General introduction

History of the Maillard reaction

In 1912, the French physician and organic chemist Louis-Camille Maillard described a non-enzymatic reaction between amino acids and sugars [1]. Under the influence of only heat, free amino groups in proteins, either at the N-terminus or as part of a side-chain, react with the carbonyl group of a reducing sugar, such as glucose (Figure 1.1). As a result, covalent adducts are formed, mainly on lysine and arginine residues. Well-known examples of such adducts are N(6)-carboxymethyllysine (CML), N(6)-carboxyethyllysine (CEL), glucosepane, pentosidine, and methylglyoxal-derived hydroimidazolone-1 (MG-H1). These adducts are collectively referred to as advanced glycation end products (AGEs), although they differ in their specific characteristics. Certain AGEs can form cross-links, connecting two amino acids by a covalent bond either within the same protein or between different proteins. These cross-links alter the tertiary structure of proteins and promote the formation of protein aggregates. In addition, some AGEs are autofluorescent, contributing to the characteristic browning of the Maillard reaction [2]. Although originally named after its discoverer, the Maillard reaction is nowadays also widely recognized as (protein) glycation, appearing relevant in both food and health research.

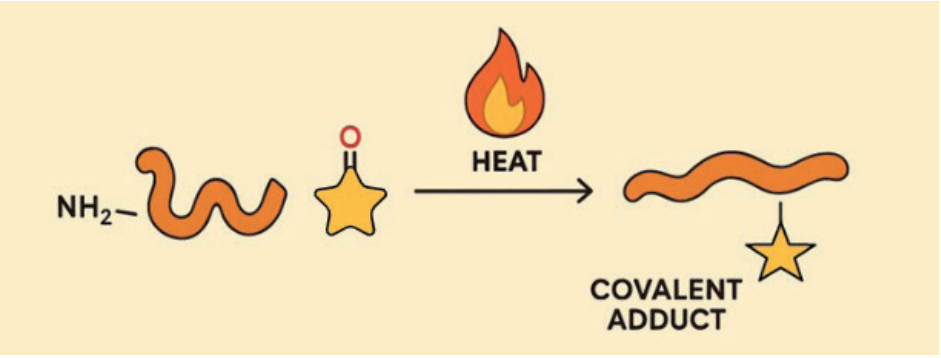


Figure 1.1: Graphical image of the Maillard reaction. Free amino groups in proteins (NH2) react with carbonyl groups (=O) of reducing sugars, under the presence of heat, forming covalent adducts on the proteins known as advanced glycation end products (AGEs).

Maillard reaction in food research

In the decades following Maillard's original publication, glycation research largely focused on food quality. Scientists linked the Maillard reaction to reduced nutritional value of milk proteins [3,4], non-enzymatic browning of fruits [5], and the development of off-flavors in skim milk during storage [3]. They also identi-

fied moisture content, temperature and time as key factors influencing these processes. Next to its role in off-flavor formation, the Frenchman Patron [6,7] proposed in the early 1950s that the Maillard reaction would also be responsible for the desirable aromas, flavors and textures in foods such as beer, cheese, and bread (Figure 1.2). Shortly thereafter, the American chemist Hodge described the mechanism of the reaction [8], enabling scientists to start linking specific flavors and odors to distinct Maillard reaction products. Together, these discoveries marked the beginning of flavor science.

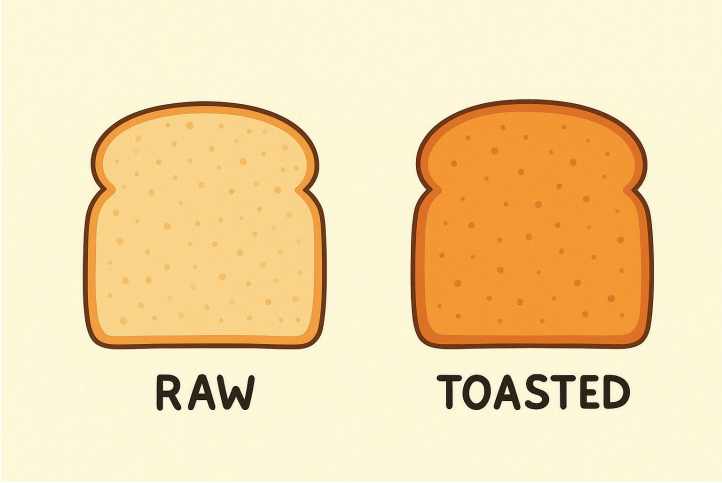


Figure 1.2: Change in appearance of bread by heating. Advanced glycation end products are formed through the Maillard reaction, resulting in a golden-brown color of the toasted bread.

Maillard reaction in health research

It became apparent that protein glycation is also relevant beyond food quality and design with the discovery of elevated hemoglobin A1c (HbA1c) levels in diabetic patients in the late 1960s [9]. This variant of hemoglobin contains a glucose-modified N-terminal of the β-chain, providing clear evidence that protein glycation also occurs at 37°C in the human body, as originally suggested by Louis-Camille Maillard. Because glycation of this N-terminal is accelerated by elevated blood glucose levels, HbA1c levels are still used as a clinical marker by physicians to monitor long-term glycemic control in diabetic patients. Following this discovery, Monnier and Cerami [10] linked the Maillard reaction to age-related pigmentation and clouding of the human lens, known as cataract, which is more profound in individuals with diabetes. Since then, a growing body of evidence suggests that

protein glycation is correlative or causative with (chronic complications of) various diseases, such as diabetes, neurodegenerative disorders, and atherosclerosis.

Endogenous Maillard reaction in ageing and disease

Inevitably, the Maillard Reaction occurs within our body, driven by temperature and substrate availability, leading to the formation of endogenous AGEs. Its role in ageing and disease manifestation is widely recognized and can be divided into three mechanisms: 1) oxidative stress, 2) modification of long-lived proteins, and 3) AGE-RAGE interaction.

Oxidative stress

In the early stages of the Maillard reaction, a free amino group reacts with a reducing sugar to form an unstable intermediate (a Schiff base), which then rearranges into a more stable Amadori product (e.g. fructoselysine). This Amadori product can subsequently follow different pathways, mainly depending on pH and temperature: it may undergo further rearrangements leading to the formation of AGEs, or its carbonyl group can get oxidized and cleaved to form α-dicarbonyl compounds such as methylglyoxal. These aldehydes are very reactive and therefore short-lived. They react not only with proteins, forming AGEs, but also with lipids and nucleic acids. This is known as carbonyl stress, which in turn triggers inflammation and oxidative stress. The formation of these α-dicarbonyl compounds is however not limited to the Maillard reaction. They are also formed during other metabolic pathways, like glycolysis and lipid peroxidation, making carbonyl stress an inevitable part of life [11]. Therefore, according to the free radical theory of ageing, oxidative stress is believed to be the primary source of physiological (i.e. normal ageing) and pathological damage to cells and tissues.

Modification of long-lived proteins

Throughout life, proteins in the human body undergo random glycation. The formation of glycation-induced cross-links alters protein tertiary structures and promotes protein aggregation, impairing protein function. To maintain optimal functioning, the body continuously degrades and replaces proteins, however these protein turnover rates vary widely, ranging from a few minutes to decades. Frequently replaces proteins include regulatory proteins, enzymes and hormones, whereas proteins that provide structure to tissues are hardly replaced. These structural proteins are called long-lived proteins, with collagen being a prominent

example with a half-life of 117 years [12]. Because they are rarely renewed, glycation leads to progressive formation of dysfunctional aggregates in these tissues contributing to age-related health deterioration [13]. One example, as already mentioned earlier, is cataract. When crystallin in the eye lens becomes glycated, the lens gets cloudy due to the formation of both fluorescent adducts and protein aggregates resulting in impaired vision [12]. Another condition linked to glycation of long-lived proteins, in this case the extracellular matrix protein elastin, is the loss of elasticity of the skin and arterial walls [14]. Here, glycation directly compromises protein function leading to tissue deterioration. For other proteins, glycation primarily interferes with their clearance. Meaning that, while otherwise their turnover rate is considered quite fast, they now start to accumulate in the tissue. A well-known example of such a protein is amyloid-β. Impaired clearance of this protein is linked to the formation of plaques that are observed in neurodegenerative disorders like Alzheimer's [15]. In summary, glycation of proteins in the human body impairs their ability to function properly, which affects health, especially when these proteins have a slow turnover rate or are prone to impaired clearance.

AGE-RAGE interaction

In 1992, a cell surface-associated protein was identified that binds glycated proteins and therefore mediates the interaction of AGEs with cells. It was named the receptor for advanced glycation end products: RAGE [16,17]. This transmembrane receptor is widely expressed and consists of three main domains: an extracellular domain, transmembrane domain, and a cytoplasmic tail. Since the extracellular domain was found to interact not only with protein-bound AGEs but also with other molecules like multiple damage-associated molecular patterns (DAMPs) [18–20], it has been described a multiligand pattern recognition receptor. Such receptors do not bind one specific ligand, but recognize a combination of common features within different ligands. In the case of RAGE, these features include a net negative charge at neutral pH and a tendency to oligomerize. In the years following the discovery of RAGE, it became evident that inflammatory stimuli directly enhance its expression, leading to RAGE being upregulated in several diseases [21,22]. Subsequently, a role for RAGE in immune responses was demonstrated as RAGE deletion in a mouse knockout model reduced sepsis lethality [23]. In this context, AGE-RAGE interaction would induce inflammation through NF-κB signaling facilitated by Diaphanous-1 (DIAPH1) binding to RAGE's cytosolic tail [24–26] (Figure 1.3). In summary, RAGE is proposed as a central

mediator connecting endogenous AGE formation to the manifestation of different diseases related to inflammation.

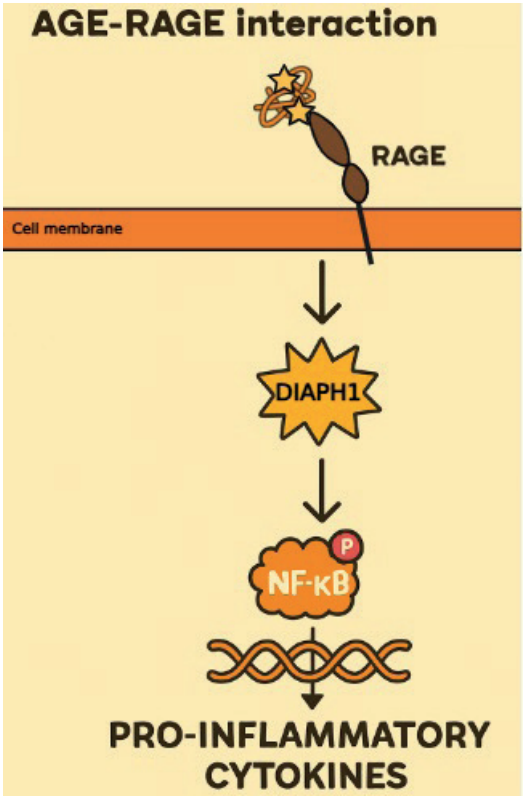


Figure 1.3: Graphical image of inflammatory responses induced by AGE-RAGE interactions. When a RAGE ligand like protein-bound AGEs binds to the receptor, an NF-κB signaling cascade is initiated by DIAPH1 binding to RAGE's cytosolic tail, leading to the production of pro-inflammatory cytokines.

Dietary AGEs: a link between diet and health?

Whereas the role of endogenous AGEs in ageing and disease is widely recognized, interest in the potential health effects of dietary AGE consumption only emerged after the Western diet was linked to an increased risk of several non-communicable diseases, including cardiovascular diseases, neurodegenerative disorders and diabetes type 2 [27,28]. As the Western diet is characterized by high intake of processed foods, attention quickly shifted to processing-related factors and dietary AGEs became of interest because of their known detrimental effects when formed endogenously [29]. However, even though they are structur-

ally comparable, dietary AGEs and endogenous AGEs cannot be considered the same in terms of biological activity since dietary AGEs enter the body through the digestive tract while endogenous AGEs are generated within the body and thereby directly affect body protein functionality.

Most AGEs in food are protein-bound [30] and much research has focused on how glycation affects protein digestion and the subsequent bioavailability of amino acids. The amino acid availability from highly glycated proteins was shown to be largely preserved, except for lysine [31,32], which is the amino acid being particularly susceptible to glycation. Early studies indicated that dietary AGEs could contribute to the endogenous AGE pool as they were shown bioavailable upon digestion in both animals and humans [33,34]. Subsequent mice studies showed adverse effects of a high-AGE diet on insulin resistance, atherosclerosis and longevity [35–38]. In humans, high dietary AGE intake in humans was associated with elevated systemic markers of oxidative stress and inflammation [39,40]. Moreover, the reaction was shown to generate toxic compounds in heated foods, such as acrylamide [41]. Together, these findings suggest that lowering AGE intake would be beneficial for healthy ageing and lead to the publication of for example "The AGE-less diet" [42], a Health & Nutrition Book explaining how to lower your daily AGE consumption to improve health and slow down the ageing process.

However, this narrative has become more nuanced by recent findings. New techniques were developed to quantify AGEs in food and biological samples. The abovementioned studies used the enzyme-linked immunosorbent assay (ELISA) which is a commonly used and cost-effective method to detect and quantify specific proteins of interest. However, since it relies on antibody-antigen interactions, it is sensitive to cross-reactivity and matrix effects. When mass spectrometry (MS) techniques were developed, discrepancies were shown between these two methods especially for foods high in fat such as butter, cheese, and olive oil [43–45]. Since MS techniques are considered more specific and accurate, as well as providing a superior sensitivity, current food databases are relying on this method [43,46]. Accordingly, a 4-week dietary intervention study was conducted in healthy, overweight individuals based on these databases [47]. Although a clear increase in plasma AGE levels was observed upon a high AGE diet, this diet did not change insulin sensitivity, vascular function, or overall inflammation. In addition, while dietary AGEs contribute to the endogenous pool of AGEs as they are shown bioavailable, recent mice studies showed that these effects are reversible [48,49]. By feeding mice a high AGE diet, tissue AGE levels increased,

but these levels dropped again when switched to a low AGE diet, showing body clearance. In addition, these studies did not show disease development specific to the high AGE diet. Taken together, these results add more layers of complexity to the initial viewpoint of dietary AGEs contributing to systemic inflammation and an accelerated ageing process.

Current research gaps: dietary AGEs and intestinal health

Since dietary AGEs have been shown to be bioavailable, much research has focused on their potential systemic health effects. However, depending on the protein source and food processing methods, also a fraction of dietary proteins remains undigested [50,51]. Little is known about the potential health impact of these intact glycated proteins. As they are considered hardly bioavailable, the intestine is the first, and possibly the only, organ to interact with them. Although glycated proteins have been shown to undergo microbial fermentation in the colon [52–55], their direct effects on the intestinal epithelium remain largely unexplored. Since protein-bound AGEs have been shown to be capable of binding to RAGE [56,57], chronic exposure of the intestinal epithelium to these proteins could potentially trigger inflammation through this mechanism. Given the central role of intestinal health in overall wellbeing, such effects may have broader health implications. For instance, impaired gut barrier function, often referred to as a “leaky gut”, can promote low-grade systemic inflammation [58], a condition associated with many age-related and metabolic diseases [59,60]. Accordingly, intestinal health may represent a critical link between dietary AGEs and systemic health outcomes.

Aim and outline of this thesis

In summary, the consumption of dietary AGEs has been linked to increased systemic inflammation and a higher risk for non-communicable diseases, such as diabetes and cardiovascular diseases. Recent findings suggest that in healthy individuals, free and dipeptide-bound dietary AGEs are absorbed but efficiently cleared from the body. No direct detrimental health effects were observed in this regard. However, the potential impact of such a diet on the intestine remains largely unknown. The intestinal epithelium is the first, and possibly the only tissue to encounter intact, undigested glycated proteins, which can interact with RAGE. Because intestinal health is known to influence overall wellbeing, this

may represent one pathway through which dietary AGEs exert indirect systemic effects. **Therefore, the thesis aims to increase our understanding of how intact glycated dietary proteins affect intestinal health at the epithelium and immune level, using *in vitro* models.**

A visual outline of the thesis is represented in Figure 1.4. In **Chapter 2**, the current literature on dietary AGEs, their digestion, and their interaction with the intestine is reviewed. Both *in vivo* and *in vitro* studies are discussed, with emphasis on their methodological approaches. The chapter also provides recommendations for future *in vitro* study design and identifies knowledge gaps that require further investigation. The insights from this position paper formed the basis for Chapters 3, 4, and 5. **Chapter 3** examines the translocation of glycated beta-lactoglobulin (BLG) across the intestinal epithelium. Human ileum-derived organoids were cultured as two-dimensional monolayers on transwell inserts to form an epithelial barrier. To explore the potential involvement of Microfold (M) cells in the translocation of intact proteins across this barrier, an additional model was investigated in which the differentiation factors RANKL and TNFα were added to the medium to promote M cell differentiation. The passage of beta-lactoglobulin was measured by ELISA and Western blot analysis. **Chapter 4** focusses on dietary AGE-RAGE interaction in the context of inflammation. Glycated BLG was characterized for AGE content, aggregation pattern, and sRAGE affinity. Its inflammatory potency was assessed using primary immune cells in which surface RAGE expression was confirmed. Comparable experiments were performed with both in-house and commercially glycated bovine serum albumin (BSA). **Chapter 5** focusses on LPS as potential co-factor for RAGE activation. The same primary cell model was used as in Chapter 4. The DAMPs high mobility group box 1 (HMGB1) and amyloid-β (Aβ) were used as RAGE agonists and combined with different doses of LPS, whereafter inflammatory responses were measured by qPCR and ELISA methods. In addition, pre-liminary results were shown using an immune cell line with an incorporated NF-κB-inducible luciferase reporter construct. In the last chapter, **Chapter 6**, the results of the previous chapters are discussed and integrated with respect to the current literature, providing a broader perspective on the potential role of dietary AGEs in health.

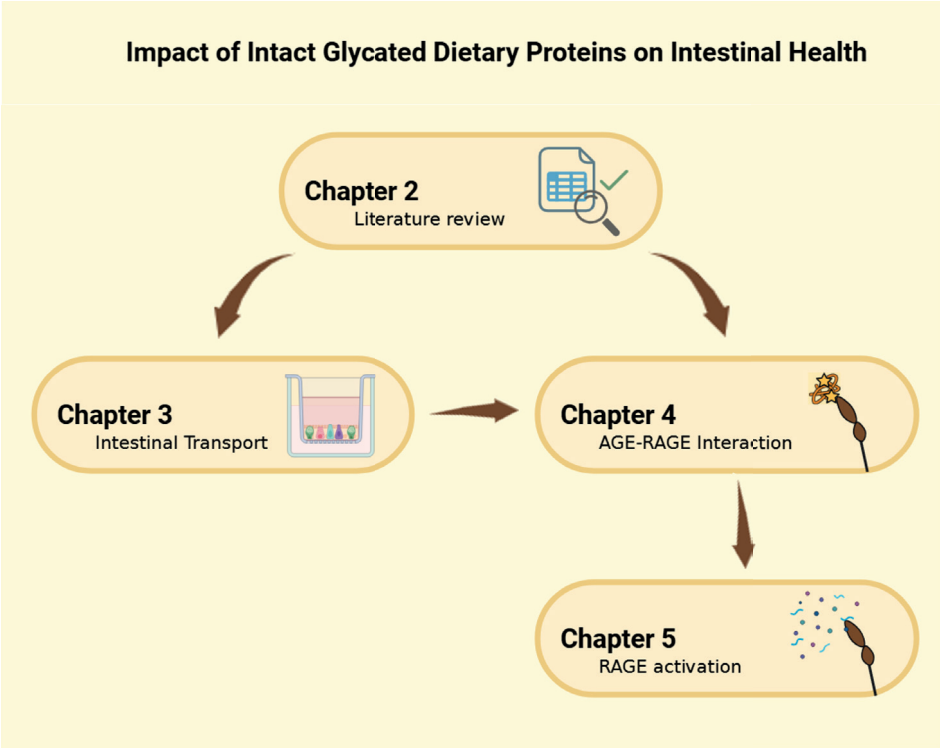


Figure 1.4: Overview of thesis outline. This thesis is divided in four chapters with the aim to better understanding how intact glycated dietary proteins affect intestinal health. Chapter 2 summarizes the current literature on dietary AGEs and their interaction with the intestine, with emphasis on methodological approaches. These insights form the basis for research Chapters 3, 4, and 5.

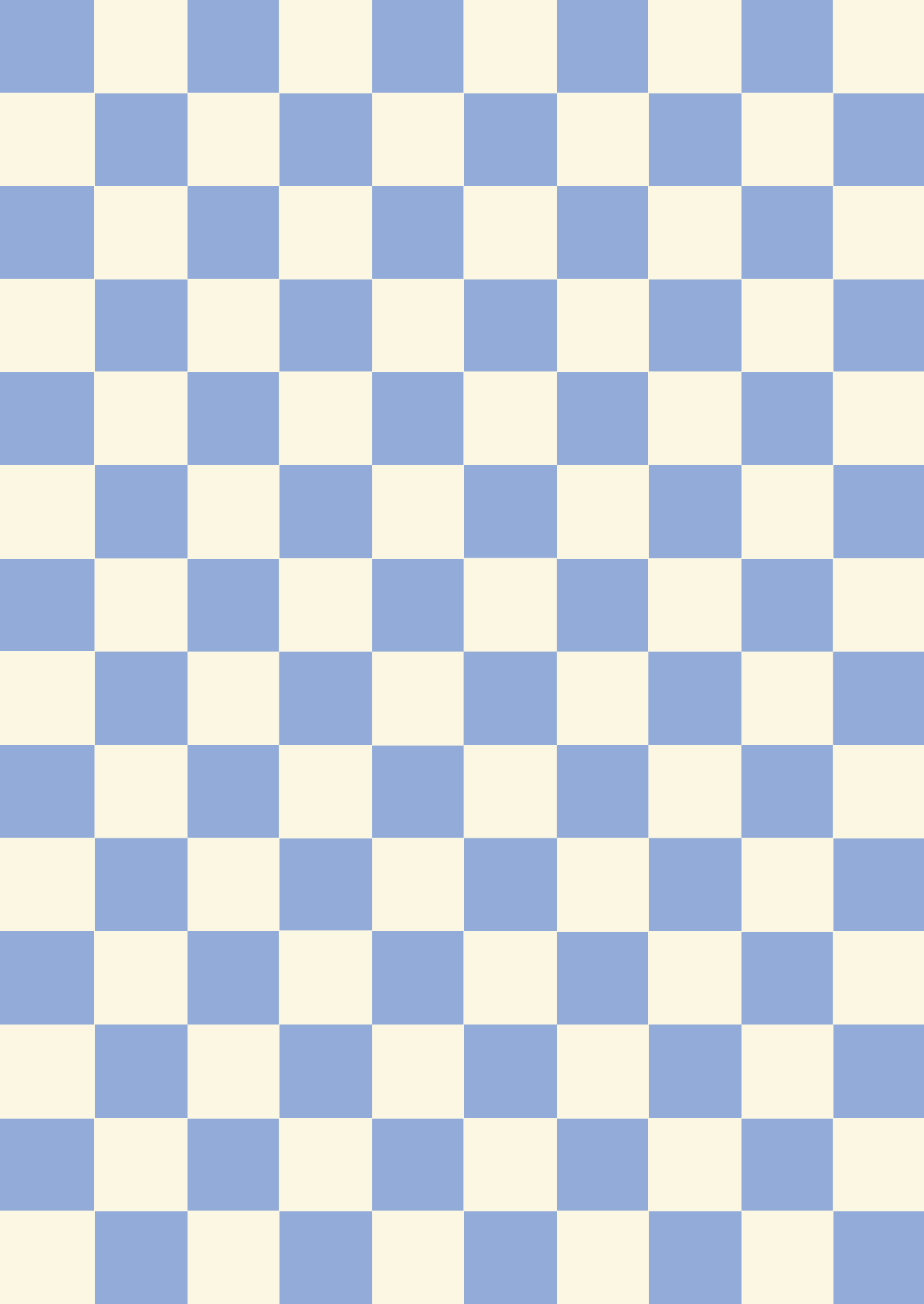
References

1. Maillard L-C. Action des acides amines sur les sucres : formation des melanoidines par voie methodique. C R Seances Soc Biol Fil 1912;154:66–8.
2. Perrone A, Giovino A, Benny J, Martinelli F. Advanced Glycation End Products (AGEs): Biochemistry, Signaling, Analytical Methods, and Epigenetic Effects. Oxid Med Cell Longev 2020;2020. https://doi.org/10.1155/2020/3818196.
3. Henry KM, Kon SK, Lea CH, Smith JAB, White JCD. Deterioration on storage of dried skim milk. Nature 1946;158:348–9. https://doi.org/10.1038/158348A0;KWRD.
4. Greaves EO, Morgan AF, Loveen MK. The Effect of Amino-Acid Supplements and of Variations in Temperature and Duration of Heating Upon the Biological Value of Heated Casein: Two Figures. J Nutr 1938;16:115–28. https://doi.org/10.1093/JN/16.2.115.
5. Weast C, Mackinney G. Nonenzymatic darkening of fruits and fruit products. Ind Eng Chem 1941;33:1408–12. https://doi.org/10.1021/IE50383A017.
6. Patron A. Recherches sur le brunissement non enzymatique des fruits et des produits de fruits en conserve. Fruits d'Outre-Mer 1950;5:167–207.
7. Patron A. La reaction de Maillard et le brunissement non-enzymatique dans l'industrie alimentaire. Indust Agr Alim 1951;68:251–6.
8. Hodge JE. Dehydrated Foods, Chemistry of Browning Reactions in Model Systems. J Agric Food Chem 1953;1:928–43. https://doi.org/10.1021/JF60015A004.
9. Rahbar S. Hemoglobin H disease in two Iranian families. Clinica Chimica Acta 1968;20:381–5. https://doi.org/10.1016/0009-8981(68)90293-3.
10. Monnier VM, Cerami A. Nonenzymatic Browning in Vivo: Possible Process for Aging of Long-Lived Proteins. Science (1979) 1981;211:491–3. https://doi.org/10.1126/SCIENCE.6779377.
11. Fournet M, Bonté F, Desmoulière A. Glycation Damage: A Possible Hub for Major Pathophysiological Disorders and Aging. Aging Dis 2018;9:880. https://doi.org/10.14336/AD.2017.1121.
12. Toyama BH, Hetzer MW. Protein homeostasis: live long, won't prosper. Nat Rev Mol Cell Biol 2013;14:55–61. https://doi.org/10.1038/nrm3496.
13. Monnier VM, Sell DR. Prevention and Repair of Protein Damage by the Maillard Reaction In Vivo. Https://HomeLiebertpubCom/Rej 2006;9:264–73. https://doi.org/10.1089/REJ.2006.9.264.
14. Forbes JM, Yee LTL, Thallas V, Lassila M, Candido R, Jandeleit-Dahm KA, et al. Advanced Glycation End Product Interventions Reduce Diabetes-Accelerated Atherosclerosis. Diabetes 2004;53:1813–23. https://doi.org/10.2337/DIABETES.53.7.1813.
15. Sasaki N, Fukatsu R, Tsuzuki K, Hayashi Y, Yoshida T, Fujii N, et al. Advanced Glycation End Products in Alzheimer's Disease and Other Neurodegenerative Diseases. Am J Pathol 1998;153:1149. https://doi.org/10.1016/S0002-9440(10)65659-3.
16. Schmidt AM. Isolation and characterization of two binding proteins for advanced glycosylation end products from bovine lung which are present on the endothelial cell surface. Journal of Biological Chemistry 1992;267:14987–97. https://doi.org/10.1016/S0021-9258(18)42137-0.
17. Neeper M, Marie Schmidt A, Brett J, Du YanQ S, Wangll F, Pan Y-CE, et al. Cloning and Expression of a Cell Surface Receptor for Advanced Glycosylation End Products of Proteins. J Biol Chem 1992;267:14998–5004.
18. Schmidt AM, Yan S Du, Yan SF, Stern DM. The multiligand receptor RAGE as a progression factor amplifying immune and inflammatory responses. Journal of Clinical Investigation 2001;108:949. https://doi.org/10.1172/JCI14002.
19. Hofmann MA, Drury S, Fu C, Qu W, Taguchi A, Lu Y, et al. RAGE mediates a novel proinflammatory axis: A central cell surface receptor for S100/calgranulin polypeptides. Cell 1999;97:889–901. https://doi.org/10.1016/S0092-8674(00)80801-6.
20. Hori O, Brett J, Slattery T, Cao R, Zhang J, Chen JX, et al. The Receptor for Advanced Glycation End Products (RAGE) Is a Cellular Binding Site for Amphoterin. Journal of Biological Chemistry 1995;270:25752–61. https://doi.org/10.1074/jbc.270.43.25752.

21. Li J, Schmidt AM. Characterization and functional analysis of the promoter of RAGE, the receptor for advanced glycation end products. Journal of Biological Chemistry 1997;272:16498–506. https://doi.org/10.1074/jbc.272.26.16498.
22. Ramasamy R, Shi FY, Schmidt AM. RAGE: Therapeutic target and biomarker of the inflammatory response - The evidence mounts. J Leukoc Biol 2009;86:505–12. https://doi.org/10.1189/jlb.0409230.
23. Liliensiek B, Weigand MA, Bierhaus A, Nicklas W, Kasper M, Hofer S, et al. Receptor for advanced glycation end products (RAGE) regulates sepsis but not the adaptive immune response. J Clin Invest 2004;113. https://doi.org/10.1172/JCI200418704.
24. Schmidt AM, Hori O, Brett J, Yan S Du, Wautier JL, Stern D. Cellular receptors for advanced glycation end products. Implications for induction of oxidant stress and cellular dysfunction in the pathogenesis of vascular lesions. Arterioscler Thromb 1994;14:1521–8. https://doi.org/10.1161/01.ATV.14.10.1521.
25. Marie Schmidt A, Hori O, Cao R, Du Yan S, Brett J, Wautier J-L, et al. RAGE A Novel Cellular Receptor for Advanced Glycation End Products. Diabetes 1996;45:77–80.
26. Hudson BI, Kalea AZ, Del Mar Arriero M, Harja E, Boulanger E, D'Agati V, et al. Interaction of the RAGE cytoplasmic domain with diaphanous-1 is required for ligand-stimulated cellular migration through activation of Rac1 and Cdc42. Journal of Biological Chemistry 2008;283:34457–68. https://doi.org/10.1074/jbc.M801465200.
27. Van Dam RM, Rimm EB, Willett WC, Stampfer MJ, Hu FB. Dietary patterns and risk for type 2 diabetes mellitus in U.S. men. Ann Intern Med 2002;136:201–9. https://doi.org/10.7326/0003-4819-136-3-200202050-00008.
28. Menotti A, Kromhout D, Blackburn H, Fidanza F, Buzina R, Nissinen A. Food intake patterns and 25-year mortality from coronary heart disease: cross-cultural correlations in the Seven Countries Study. The Seven Countries Study Research Group. Eur J Epidemiol 1999;15:507–15. https://doi.org/10.1023/A:1007529206050.
29. Uribarri J, Woodruff S, Goodman S, Cai W, Chen X, Pyzik R, et al. Advanced Glycation End Products in Foods and a Practical Guide to Their Reduction in the Diet. J Am Diet Assoc 2010;110:911. https://doi.org/10.1016/J.JADA.2010.03.018.
30. Yuan X, Nie C, Liu H, Ma Q, Peng B, Zhang M, et al. Critical Reviews in Food Science and Nutrition Comparison of metabolic fate, target organs, and microbiota interactions of free and bound dietary advanced glycation end products Comparison of metabolic fate, target organs, and microbiota interactions of free and bound dietary advanced glycation end products. Food Sci Nutr 2021;63:3612–33. https://doi.org/10.1080/10408398.2021.1991265.
31. Nyakayiru J, Van Lieshout GAA, Trommelen J, Van Kranenburg J, Verdijk LB, Bragt MCE, et al. The glycation level of milk protein strongly modulates post-prandial lysine availability in humans. British Journal of Nutrition 2020;123:545–52. https://doi.org/10.1017/S0007114519002927.
32. van Lieshout GA, Trommelen J, Nyakayiru J, van Kranenburg J, Senden JM, Gijsen AP, et al. Protein glycation compromises the bioavailability of milk protein-derived lysine in vivo in healthy adult males: a double-blind, randomized cross-over trial. Am J Clin Nutr 2025. https://doi.org/10.1016/J.AJCNUT.2025.01.025.
33. Koschinsky T, He C, Mitsuhashi T, Bucala R, Liu C, Buenting C, et al. Orally absorbed reactive glycation products (glycotoxins): an environmental risk factor in diabetic nephropathy. Proc Natl Acad Sci U S A 1997;94:6474–9. https://doi.org/10.1073/PNAS.94.12.6474.
34. He C, Sabol J, Mitsuhashi T, Vlassara H. Dietary glycotoxins: inhibition of reactive products by aminoguanidine facilitates renal clearance and reduces tissue sequestration. Diabetes 1999;48:1308–15. https://doi.org/10.2337/DIABETES.48.6.1308.
35. Cai W, He JC, Zhu L, Chen X, Zheng F, Striker GE, et al. Oral Glycotoxins Determine the Effects of Calorie Restriction on Oxidant Stress, Age-Related Diseases, and Lifespan. Am J Pathol 2008;173:327–36. https://doi.org/10.2353/AJPATH.2008.080152.
36. Lin RY, Choudhury RP, Cai W, Lu M, Fallon JT, Fisher EA, et al. Dietary glycotoxins promote diabetic atherosclerosis in apolipoprotein E-deficient mice. Atherosclerosis 2003;168:213–20. https://doi.org/10.1016/S0021-9150(03)00050-9.

37. Hofmann SM, Dong HJ, Li Z, Cai W, Altomonte J, Thung SN, et al. Improved Insulin Sensitivity Is Associated With Restricted Intake of Dietary Glycoxidation Products in the db/db Mouse. Diabetes 2002;51:2082–9. https://doi.org/10.2337/DIABETES.51.7.2082.
38. Sandu O, Song K, Cai W, Zheng F, Uribarri J, Vlassara H. Insulin Resistance and Type 2 Diabetes in High-Fat–Fed Mice Are Linked to High Glycotoxin Intake. Diabetes 2005;54:2314–9. https://doi.org/10.2337/DIABETES.54.8.2314.
39. Uribarri J, Cai W, Peppa M, Goodman S, Ferrucci L, Striker G, et al. Circulating Glycotoxins and Dietary Advanced Glycation Endproducts: Two Links to Inflammatory Response, Oxidative Stress, and Aging. The Journals of Gerontology: Series A 2007;62:427–33. https://doi.org/10.1093/GERONA/62.4.427.
40. Vlassara H, Cai W, Goodman S, Pyzik R, Yong A, Chen X, et al. Protection against Loss of Innate Defenses in Adulthood by Low Advanced Glycation End Products (AGE) Intake: Role of the Antiinflammatory AGE Receptor-1. J Clin Endocrinol Metab 2009;94:4483–91. https://doi.org/10.1210/JC.2009-0089.
41. Stadler RH, Blank I, Varga N, Robert F, Hau J, Guy PA, et al. Acrylamide from Maillard reaction products. Nature 2002 419:6906 2002;419:449–50. https://doi.org/10.1038/419449a.
42. Vlassara H, Woodruff S, Striker G. Dr. Vlassara's AGE-less Diet. New York: Square One Publishers; 2017.
43. Scheijen JLJM, Clevers E, Engelen L, Dagnelie PC, Brouns F, Stehouwer CDA, et al. Analysis of advanced glycation endproducts in selected food items by ultra-performance liquid chromatography tandem mass spectrometry: Presentation of a dietary AGE database. Food Chem 2016;190:1145–50. https://doi.org/10.1016/J.FOODCHEM.2015.06.049.
44. Assar SH, Moloney C, Lima M, Magee R, Ames JM. Determination of N ε-(carboxymethyl) lysine in food systems by ultra performance liquid chromatography-mass spectrometry. Amino Acids 2009;36:317–26. https://doi.org/10.1007/S00726-008-0071-4/TABLES/5.
45. Charissou A, Ait-Ameur L, Birlouez-Aragon I. Evaluation of a gas chromatography/mass spectrometry method for the quantification of carboxymethyllysine in food samples. J Chromatogr A 2007;1140:189–94. https://doi.org/10.1016/J.CHROMA.2006.11.066.
46. Boiko A, Fiore A, Hay A, Troise AD, De Pascale S, Scaloni A, et al. The glycation database: from the Maillard reaction in foods to biomolecular insight. Abertay University 2022.
47. Linkens AMA, Houben AJHM, Niessen PM, Wijckmans NEG, de Goei EEC, Van den Eynde MDG, et al. A 4-week high-AGE diet does not impair glucose metabolism and vascular function in obese individuals. JCI Insight 2022;7. https://doi.org/10.1172/JCI.INSIGHT.156950.
48. van Dongen KCW, Linkens AMA, Wetzels SMW, Wouters K, Vanmierlo T, van de Waarenburg MPH, et al. Dietary advanced glycation endproducts (AGEs) increase their concentration in plasma and tissues, result in inflammation and modulate gut microbial composition in mice; evidence for reversibility. Food Research International 2021;147:110547. https://doi.org/10.1016/J.FOODRES.2021.110547.
49. Nogueira Silva Lima MT, Delayre-Orthez C, Howsam M, Jacolot P, Niquet-Léridon C, Okwieka A, et al. Early- and life-long intake of dietary advanced glycation end-products (dAGEs) leads to transient tissue accumulation, increased gut sensitivity to inflammation, and slight changes in gut microbial diversity, without causing overt disease. Food Research International 2024;195:114967. https://doi.org/10.1016/J.FOODRES.2024.114967.
50. Bartlett A, Kleiner M. Dietary protein and the intestinal microbiota: An understudied relationship. IScience 2022;25:105313. https://doi.org/10.1016/J.ISCI.2022.105313.
51. Xie Y, Wang C, Zhao D, Zhou G, Li C. Processing Method Altered Mouse Intestinal Morphology and Microbial Composition by Affecting Digestion of Meat Proteins. Front Microbiol 2020;11:528031. https://doi.org/10.3389/FMICB.2020.00511/BIBTEX.
52. Zhao D, Sheng B, Wu Y, Li H, Xu D, Nian Y, et al. Comparison of Free and Bound Advanced Glycation End Products in Food: A Review on the Possible Influence on Human Health. J Agric Food Chem 2019;67:14007–18. https://doi.org/10.1021/acs.jafc.9b05891.
53. Hellwig M, Diel P, Eisenbrand G, Grune T, Guth S, Henle T, et al. Dietary glycation compounds – implications for human health. Crit Rev Toxicol 2024:1–133. https://doi.org/10.1080/10408444.2024.2362985.

54. Hellwig M, Bunzel D, Huch M, Franz CMAP, Kulling SE, Henle T. Stability of Individual Maillard Reaction Products in the Presence of the Human Colonic Microbiota. J Agric Food Chem 2015;63:6723–30. https://doi.org/10.1021/ACS.JAFC.5B01391.
55. Bui TPN, Troise AD, Nijsse B, Roviello GN, Fogliano V, de Vos WM. Intestinimonas-like bacteria are important butyrate producers that utilize Nε-fructosyllysine and lysine in formula-fed infants and adults. J Funct Foods 2020;70:103974. https://doi.org/10.1016/J.JFF.2020.103974.
56. Xie J, Reverdatto S, Frolov A, Hoffmann R, Burz DS, Shekhtman A. Structural Basis for Pattern Recognition by the Receptor for Advanced Glycation End Products (RAGE). Journal of Biological Chemistry 2008;283:27255–69. https://doi.org/10.1074/JBC.M801622200.
57. Xue J, Rai V, Singer D, Chabierski S, Xie J, Reverdatto S, et al. Advanced glycation end product recognition by the receptor for AGEs. Structure 2011;19:722–32. https://doi.org/10.1016/j.str.2011.02.013.
58. Witkamp RF, van Norren K. Let thy food be thy medicine....when possible. Eur J Pharmacol 2018;836:102–14. https://doi.org/10.1016/j.ejphar.2018.06.026.
59. Thevaranjan N, Puchta A, Schulz C, Naidoo A, Szamosi JC, Verschoor CP, et al. Age-Associated Microbial Dysbiosis Promotes Intestinal Permeability, Systemic Inflammation, and Macrophage Dysfunction. Cell Host Microbe 2017;21:455-466.e4. https://doi.org/10.1016/j.chom.2017.03.002.
60. Escalante J, Artaiz O, Diwakarla S, McQuade RM. Leaky gut in systemic inflammation: exploring the link between gastrointestinal disorders and age-related diseases. Geroscience 2024;47:1. https://doi.org/10.1007/S11357-024-01451-2.



2

Dietary advanced glycation end products interacting with the intestinal epithelium: what do we really know?

Fleur A.C. Jansen [1] · Vincenzo Fogliano [1] · Josep Rubert [1, 2 #] · Tamara Hoppenbrouwers [1, 3 #]

1 Department of Food Quality and Design, Wageningen University & Research, Wageningen, The Netherlands
2 Nutritional Biology, Division of Human Nutrition, Wageningen University & Research, Wageningen, The Netherlands
3 Food and Biobased Research, Wageningen University & Research, Wageningen, The Netherlands
Shared last author

Molecular Metabolism, 2023; 73: 101734

Abstract

Background: Advanced Glycation End products (AGEs) are a heterogeneous group of stable reaction products formed when amino acids, peptides, or proteins are glycated by the non-enzymatic Maillard Reaction. The formation and accumulation of these products *in vivo* are linked to many inflammation-based pathological outcomes and part of the pathophysiology of non-communicable diseases like eye cataracts and Alzheimer's disease. Since our diet contains high levels of the same compounds, it has been questioned whether their consumption is also detrimental to health. However, this is still under debate. In this context, the intestinal epithelium is an important target tissue since it is chronically exposed to relatively high concentrations of dietary AGEs.

Scope of review: This review summarizes the current evidence on the impact of dietary AGEs on the intestinal epithelium and critically reflects on its methodology.

Major conclusions: In healthy rodent models, an inflammation-independent impaired intestinal barrier function is claimed; however, dietary AGEs showed anti-inflammatory activity in IBD models. *In vitro* studies could be a valuable tool to unravel the underlying mechanisms of these effects, however the available studies face some limitations, e.g. lack of the physicochemical characterization of the glycated proteins, the inclusion of the proper controls and the dose-dependency of the effect. In addition, studies using more advanced *in vitro* models like intestinal organoids and co-cultures with immune cells exposed to gut microbial metabolites derived from the fermentation of AGEs are still needed.

Introduction

Advanced Glycation End products (AGEs) are a heterogeneous group of stable reaction products from the Maillard Reaction. This reaction is a non-enzymatic process in which simple sugars (e.g. glucose) react with free amino groups leading to glycation of amino acids, peptides, and proteins, i.e. covalent bonding between the sugar molecules and free amino groups [1]. In the case of AGEs, the reacting amines are part of lysine or arginine residues. Well-known lysine-based AGEs are carboxymethyllysine (CML) and carboxyethyllysine (CEL), while a frequently studied arginine-based AGE is methylglyoxal-derived hydroimidazolone 1 (MG-H1). In addition to this characteristic, AGEs can be distinguished based on whether their formation facilitates protein cross-linking. For example, the AGE pentosidine acts as a covalent cross-link between lysine and arginine residues [2]. Since the Maillard Reaction is a non-enzymatic process driven by temperature, AGEs are formed endogenously (*in vivo*) as well as exogenously (food processing), admittedly at different rates [3].

Endogenous vs exogenous AGEs

Although their chemical structures are similar, endogenous and exogenous AGEs were approached differently in research. Where endogenously formed AGEs are investigated for their role in the pathophysiology of several non-communicable diseases, exogenously formed AGEs have mainly been investigated in relation to palatability and protein digestibility. However, recently, scientist started questioning whether the consumption of these AGEs may also contribute to several diseases generating an ample debate [3–6].

Endogenously, the Maillard Reaction causes body protein misfolding and aggregation, respectively, dependent on whether the formation occurs within the same protein or between different proteins [3]. Although these proteins become dysfunctional, they are not always cleared properly. This accumulation of misfolded and aggregated proteins contributes to several non-communicable age-related diseases, such as cataracts, Alzheimer's disease, and atherosclerosis [7–9]. In addition, endogenous AGEs are described to activate the Receptor for Advanced Glycation End products (RAGE). Upon RAGE induction, a variety of intracellular signaling pathways have been described to be activated, among which pathways involved in cell survival and apoptosis (e.g. ERK1/2, PI3K/Akt, Caspase 8) and inflammation (NF-kB, JNK) [10]. Together, endogenous AGEs are considered

to be involved in disease pathology by generating dysfunctional proteins and inducing pro-inflammatory signaling.

Exogenously, the Maillard Reaction is essential for developing the food's color, taste, and odor while cooking. Especially high-temperature processed low-moisture foods such as bakery products have been described to contain high levels of these dietary AGEs [3,11]. Much research has been performed on their effect on protein digestibility and, subsequently, the bioavailability of amino acids. *In vitro* research shows that the digestibility of food proteins decreases with the level of glycation since aggregates are formed and lysine and arginine would no longer be available for cleavage by pepsins. As a result, these studies suggest that free AGEs and dipeptides can be considered (partially) bioavailable, while large glycated peptides and proteins would hardly be bioavailable [12–14]. However, reduced bioavailability of amino acids from glycated proteins was not observed in a clinical setting, except for lysine [15]. The latter could also be related to glycation-induced structural changes interfering with the employed detection method, leading to an underestimation of the amount of absorbed lysine. In another study, Van Dongen et al. [16] investigated the digestibility of glycated proteins and bioavailability of protein-bound AGEs in mice. Mice were fed a baked chow diet, containing more protein-bound CML but less free CML than the standard chow diet. The authors observed increased levels of free and protein-bound CML in plasma. On top of that, the authors also quantified other AGEs (CEL and MG-H1) in different tissues (liver and kidney). Overall, the results were inconsistent. For example, free MG-H1 was elevated in plasma, liver, and kidney, but protein-bound MG-H1 did not increase. By contrast, CEL was not elevated in the liver. This suggests tissue-dependent effects and discrepancies between various AGEs. The increased levels of reactive oxoaldehydes in the baked chow diet could be a confounding factor since they may promote endogenous formation of AGEs. Interestingly, all effects observed in this study were shown to be reversible by switching back to a normal chow diet. To sum up, *in vitro* research shows decreased digestibility of glycated proteins, but *in vivo* studies suggest that the bioavailability of (modified) amino acids from these glycated proteins is not hampered. However, more research is required in this respect.

Next to the bioavailability of dietary AGEs, many researchers also focused on the potential systemic health effects they exert after being absorbed. For example, in the mice study discussed before [16], the authors also measured inflammatory markers in plasma and showed that the inflammatory z-score was elevated by

the baked chow diet suggesting a pro-inflammatory effect. However, none of the inflammatory biomarkers included in this score varied with diet when measured individually. Next to mice studies, several human intervention trials have been performed to link the consumption of dietary AGEs to human health and disease. Since tissue accessibility in humans is limited, results are mainly directed toward indirect measures such as systemic oxidative stress and inflammation. Collectively these studies claimed that long-term restriction of dAGE consumption could improve health [17–20]. However, since they prepared low- and high-AGE diets using different cooking techniques, other variables could have been affected as well, for example caloric density, micronutrient content, and formation of other Maillard Reaction Products [21]. Recently, an intervention study has investigated diets different in AGE content without them being prepared via different cooking methods. Instead, the intervention diets were composed of different food items, varying in AGE levels, while being energy- and macronutrient-matched. In contrast to the previous intervention studies, they did not observe differences between the diets [22]. Thus, whether the absorption of dietary AGEs, like the formation of endogenous AGEs, is part of disease pathologies is still under debate and a critical evaluation of the experimental design should be performed before drawing dietary recommendations.

Interaction of dietary protein-bound AGEs with the intestinal epithelium

Besides potentially exerting these systemic health effects after absorption, dietary AGEs might also interact with the intestinal epithelial cells directly. These cells are chronically exposed to relatively high levels of glycated proteins [13] that are hypothesized to exert a pro-inflammatory effect via interaction with membrane-bound receptors, mainly RAGE [23]. Tessier et al. [24] employed [$^{13}C_2$]-glyoxylic acid glycated bovine serum albumin-fed mice, showing that CML was accumulated at a high deposition rate in the ileum and colon. They showed that this accumulation was RAGE-independent. Unfortunately, due to the limited amount of tissue available, the authors were not able to qualify the CML accumulation in the tissue in terms of free versus protein-bound and intra- versus extracellular, nor could they access the physiological effects of this accumulation. Therefore, it is difficult to formulate a statement on the consequences of and mechanisms underlying tissue deposition of CML. Since glycated proteins are considered hardly bioavailable, the formation of free AGEs and dipeptides upon partial digestion of these proteins

is potentially involved as they are described to be (partially) bioavailable, either via passive diffusion, paracellular transport or absorption via for example PEPT1 [14,25]. In theory, endocytic uptake and intracellular degradation of undigested glycated proteins and large peptides could also be involved [26]. However, this has mainly been shown in conditions of cellular stress when cells use the protein as a source of amino acids and energy [27]. Overall, protein-bound dietary AGEs may have other (indirect) modes of action than solely acting via membrane-bound receptors like RAGE, possibly also dependent on the inflammatory state.

Animal studies on dietary protein-bound AGEs and the intestinal epithelium

Human intervention studies have yet to be performed in this field. Nevertheless, a few *in vivo* animal studies investigated the effect of glycated proteins on the intestinal epithelium as a (secondary) outcome measure (see Table 2.1). Except for one study, they all used healthy rodent models exposed to high levels of AGEs, either by heating the diet or supplementing it with glycated proteins. Increasing the exposure to AGEs by heating the diet has some disadvantages, due to the introduction of uncontrolled variables. For example, micronutrient content may change, caloric density increases due to water loss, and other (possibly toxic) compounds unrelated to AGEs are formed. The study of Qu et al. [28] kept these limitations to a minimum by adjusting for the water loss and adding vitamins and minerals into the pellet only after the heat treatment. In addition, they quantified both free and protein-bound CML in the food pellets after heating with advanced mass spectrometry techniques. In this way the effectiveness of the glycation protocol was checked and dose comparison between studies was made possible. This analysis showed that most dietary AGEs formed were protein-bound. The authors observed that the histomorphology score of the colon deteriorated with intervention time, affecting the intestinal architecture and distorting intestinal crypts, depleting Goblet cells, and making cellular arrangements looser. However, tissue inflammation was not evident. In addition, the expression of the tight junction proteins ZO-1 and Occludin in the colonic epithelium was decreased after 18 weeks of intervention. This decreased expression of tight junction proteins could be indicative of the development of a leaky gut, which was also suggested by a modest increase of plasma LPS levels. Unfortunately, no direct measurement of gut permeability, for instance, by the FITC-Dextran method, was performed. In line with these results, Cao et al. [29] observed a reduced gene expression of the

same tight junction proteins in colonic tissue after increasing the consumption of AGEs in mice by adding extensively glycated fish protein (dry glycation, 55°C, 24 h) to the diet. In addition, this study showed increased colonic gene expression of RAGE, but did not find an effect on pro-inflammatory cytokines in the colonic tissue. When they supplemented the mice's diet with lightly or moderately glycated fish protein (dry glycation, 55°C, resp. 6 and 12 h), these effects were not observed or observed in a reverse direction. Together, these two studies suggest that increased consumption of AGEs leads to increased intestinal permeability independent of inflammation but dependent on the degree of protein glycation. In comparison, two studies using healthy rodent models increased the AGEs intake only by heating the diet without controlling the other variables. They showed varying effects on the gene expression of multiple tight junction proteins in the jejunum and ileum [30] and no effect on colonic inflammation in terms of mast cell infiltration and the neutrophil marker myeloperoxidase (MPO) activity [31]. Next to this healthy model, Al Amir et al. [31] also looked at a DSS-induced colitis model, in which he observed less mast cell infiltration and lower MPO activity when mice were pre-exposed to an AGEs-rich diet. These intervention effects increased with prolonged heating of the diet. Overall, the current *in vivo* studies suggest that consumption of glycated proteins affects the intestinal epithelium differently depending on their degree of glycation and the inflammatory state of the intestine. However, the amount of data is limited and results should be verified in various models.

Overall, data from animal studies suggests that in healthy models dietary AGEs mainly affect tight junction expression and thus intestinal barrier integrity without directly inducing inflammation, while in a model for inflammatory bowel disease they showed a protective effect against inflammation (see Figure 2.1). Under healthy conditions, RAGE is expressed on the lateral side of epithelial cells beneath the tight junctions [32] and paracellular transport of protein-bound AGEs is unlikely since the space between epithelial cells is too narrow [33]. Since especially protein-bound AGEs have affinity for RAGE, the proposed effect of dietary AGEs on tight junction expression and gut barrier integrity is probably RAGE-independent. The effects are more likely to be caused by intracellular signaling of AGEs being absorbed through passive diffusion, active transport, or endocytosis [14,25,26]. Under inflammatory conditions, RAGE is also expressed on the basolateral membrane intestinal and intestinal permeability is increased [32], wherefore bigger proteins could pass the barrier paracellularly and bind RAGE.

Table 2.1: Summary of *in vivo* animal studies published on the effect of glycated proteins on the intestinal epithelium

***In vivo* animal studies**													
	Synthesis conditions					Experimental conditions					Observed effects		
Model	Heating	Reducing agent	Temper-ature	Time	Character-ization	Background animal	Disease	Type of treatment	Duration	Control group	Tight junctions	Inflam-mation	Reference
Heated diet	Dry	N.A.	160°C	1 hr	NBT assay LC-MS/MS[1]	C57BL/6 mice	None	Standard diet	24 weeks	Non-heated diet[6]	↕	X	[30]
	Wet	N.A.	150°C	1.5 hrs	None	Balb/c mice	None	Standard diet	3 weeks	Non-heated diet	X	–	[31]
	Wet	N.A.	150°C	4 hrs	None	Balb/c mice	None	Standard diet	3 weeks	Non-heated diet	X	–	[31]
	Wet	N.A.	150°C	1.5 hrs	None	Balb/c mice	DSS-induced colitis	Standard diet	3 weeks	Non-heated diet	X	↓	[31]
	Wet	N.A.	150°C	4 hrs	None	Balb/c mice	DSS-induced colitis	Standard diet	3 weeks	Non-heated diet	X	↓	[31]
	Dry	N.A.	125°C	3 hrs	LC-MS/MS[2]	Sprague-Dawley rats	None	Standard diet	18 weeks	Non-heated diet[7]	↓	X	[28]

Glycated protein	Dry	Glucose	55°C	6 hrs	Fluorescent intensity LC-MS/MS[3]	C57BL/6 mice	None	Fish protein	15 weeks	Non-heated fish protein with glucose[8]	↑	↓	[29]
	Dry	Glucose	55°C	12 hrs	Fluorescent intensity LC-MS/MS[4]	C57BL/6 mice	None	Fish protein	15 weeks	Non-heated fish protein with glucose[8]	-	-	[29]
	Dry	Glucose	55°C	24 hrs	Fluorescent intensity LC-MS/MS[5]	C57BL/6 mice	None	Fish protein	15 weeks	Non-heated fish protein with glucose[8]	↓	-	[29]

↑ = upregulated, ↓ = downregulated, ↕ = ambiguous, − = no effect, X = not investigated.
[1] 4.87 µg CML/g chow, 1.38 µg CEL/g chow, 43.49 µg MG-H1/g chow;
[2] 39 ng free CML/g chow, 14.45 µg protein-bound CML/g chow;
[3] 21 µg Furosine/mg protein, 8.29 ng CML/mg protein, 0.54 ng CEL/mg protein;
[4] 26.2 µg Furosine/mg protein, 12.76 ng CML/mg protein, 1.88 ng CEL/mg protein;
[5] 2.84 µg Furosine/mg protein, 13.31 ng CML/mg protein, 3.96 ng CEL/mg protein;
[6] 2.58 µg CML/g chow, 0.89 µg CEL/g chow, 34.51 µg MG-H1/g chow;
[7] 5 ng free CML/g chow, 2.79 µg protein-bound CML/g chow;
[8] 0.6 µg Furosine/mg protein, 1.05 ng CML/mg protein, 0.24 ng CEL/mg protein.

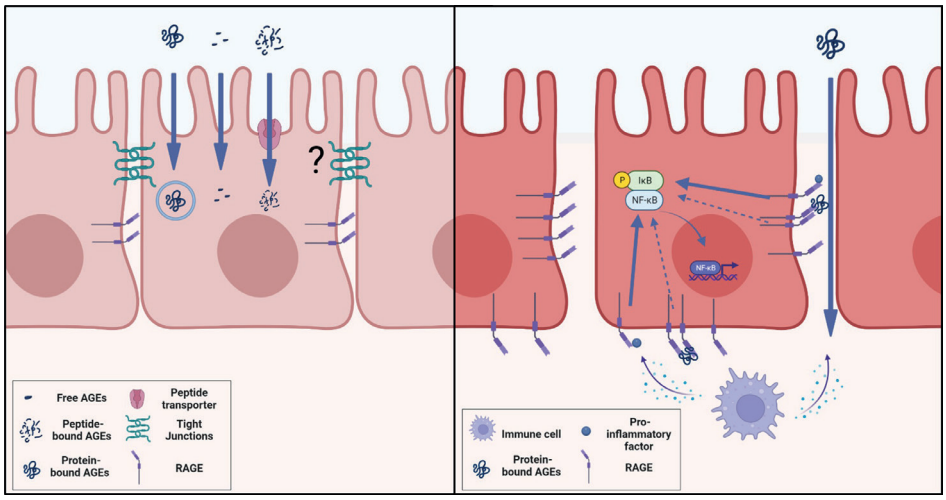


Figure 2.1: Hypothesis on how dietary Advanced Glycation End products (AGEs) affect intestinal epithelial cells under homeostatic (left panel) and inflammatory conditions (right panel), based on results of *in vivo* rodent studies. Under homeostatic conditions, dietary AGEs seem to increase intestinal permeability independent from inflammation, while RAGE is expressed on the lateral side of epithelial cells underneath the tight junctions. Since especially protein-bound AGEs have affinity for RAGE, it is unlikely that this effect is induced in a RAGE-dependent manner as cellular arrangements under homeostatic conditions are too tight for proteins to pass the barrier paracellularly. It is more likely that the effect is induced by intracellular signaling of AGEs, being absorbed via passive diffusion, active transport or endocytosis. In case of inflammation, the intestinal barrier function is hampered. Therefore, in addition to the intracellular signaling mentioned above, protein-bound AGEs would be able to interact with RAGE, which is expressed on lateral as well as basolateral side under these conditions. Although data is limited, AGEs seem to have a protective effect on inflammation, suggesting that they would act as a partial agonist or antagonist on RAGE for NF-κB activation or enhance scavenging or RAGE agonists by exaggerating RAGE shedding. Figure created with BioRender.com.

Treatment with a RAGE-specific inhibitor has been shown to protect mice from DSS-induced colitis [34], so the protective effect of dietary AGEs shown by Al Amir et al. [31] might be mediated by these compounds acting as a partial agonist or even antagonist to RAGE. On the other hand, dietary AGEs may act anti-inflammatory through stimulating RAGE shedding. RAGE shedding has been observed in active IBD, leading to increased levels of sRAGE [35]. As sRAGE scavenges RAGE agonists, dietary AGEs exaggerating the RAGE shedding observed in IBD might further dampen RAGE activation. In conclusion, the impact of dietary AGEs on intestinal epithelial cells might deviate between healthy and diseased models and might depend on the size of the AGEs and whether enterocytes can internalize them.

In vitro studies on dietary protein-bound AGEs and the intestinal epithelium

Next to the rodent studies, *in vitro* studies have been performed to understand better the mechanisms behind the effects of glycated proteins on the intestinal epithelium (Table 2.2). Different model proteins have been used: mainly bovine serum albumin (BSA) but also peanut 7S globulin and casein. Studies investigating the glycation of casein primarily focused on its potential pro-inflammatory properties. Jing et al. [36] showed that glycated casein decreased proliferation and antioxidant enzyme activity in an Int-407 *in vitro* model, but not in a Caco-2 model. Comparing these cell lines, Int-407 cells were considered healthy since they are cultured from normal embryonic intestinal tissue, whereas Caco-2 cells originate from a colon carcinoma. Later on, Int-407 was shown to be derived by HeLa contamination [37], so strictly, it cannot be considered a healthy intestinal model anymore. Another study used a cell line cloned from Caco-2, C2BBe1, and reported that glycated casein increased proliferation, oxidative stress, and IL-8 secretion compared to native casein [38]. In this polarized monolayer, activation of the pro-inflammatory NF-kB and Akt-mTORC signaling pathways was also observed. These inconsistent results about the inflammatory properties of glycated proteins can be due to different protein aggregation patterns and AGE levels. Aggregated proteins are described to have an increased affinity for the RAGE receptor [39,40], however, aggregation can be caused by heat-induced protein unfolding as well as glycation-dependent protein cross-linking [41]. It has not yet been described whether RAGE affinity and epithelial responses depend on the nature of aggregation, i.e. AGEs being present or absent. Therefore, future studies focussing on the inflammatory properties of glycated proteins on the intestinal epithelium should be conducted after a detailed physicochemical characterization of the glycated protein. In addition, when studying the inflammatory properties of biological macromolecules, it is important to check for possible endotoxin contamination in the sample as this can interfere with the measurement. Unfortunately, in general, this confounder is often overlooked.

Next to pro-inflammatory properties, potential cancer-promoting effects of glycated proteins have been studies as well [42–45]. They all used BSA as model protein and colon-cancer-derived immortalized cell lines expressing relatively high levels of RAGE (HCT116, SW620, and LoVo) [45]. Three of these four studies showed that observed cancer-promoting effects were (partially) RAGE-dependent [42,44,45]. In this respect, Wang et al.[42] described RAGE-dependent upregulation

Table 2.2: Summary of *in vitro* studies published on the effect of glycated proteins on intestinal epithelial cells

***In vitro* studies**															
	Synthesis conditions						Exposure conditions			Controls		Observed effects			
Protein	Heating	Reducing agent	Temperature	Time	Characterization	Cell line	Concentration of protein	Time	Medium	Native	Heated	Proliferation	Inflammation / oxidative stress	Cancer promotion	Reference
Bovine Serum Albumin	Wet	Glucose	37°C	8 weeks	Fluorescent intensity	HCT116	50 µg/mL	12–48 hrs	No	No	Yes	–	X	↑	[42]
	Wet	Glyceraldehyde	37°C	10 days	None	HCT116	200 µg/mL	24 hrs	No	No	Yes	X	X	↑	[43]
	Wet	Glucose	37°C	8 weeks	None	HCT116	200 µg/mL	24 hrs	No	No	Yes	↑	X	↑	[44]
	Wet	Glucose	37°C	8 weeks	None	SW620	200 µg/mL	72 hrs	No	No	Yes	X	X	↑	[45]
	Wet	Glucose	37°C	8 weeks	None	LoVo	200 µg/mL	72 hrs	No	No	Yes	X	X	↑	[45]
Casein	Wet	Glucose / Fructose	55°C	18 days	Colorimetric index Available lysine	Caco-2	0.5–2.0 mg/mL	3 hrs	Yes	Yes	No	–	–	X	[36]
	Wet	Glucose / Fructose	55°C	18 days	Colorimetric index Available lysine	Int-407	0.5–2.0 mg/mL	3 hrs	Yes	Yes	No	↓	↓	X	[36]
	Wet	Mixture of glucose, fructose and lactose	70°C*	30 min	LC-MS/MS[1] Size exclusion chromatography Fluorescent intensity ELISA	C2BBe1	200 µg/mL	3–24 hrs	No	Yes[2]	No	↑	↑	X	[38]

Peanut 7S globulin	Dry	Glucose	37°C	7 days	OPA assay SDS-PAGE Colorimetric index Fluorescent intensity	Caco-2	500 µg/mL (proliferation) / 25 µg/mL (inflammation)	Resp. 1.5 and 24 hrs	Yes	Yes	Yes**	–	↓	X	[47]
	Dry	Glucose	60°C	3 days	OPA assay SDS-PAGE Colorimetric index Fluorescent intensity	Caco-2	500 µg/mL (proliferation) / 25 µg/mL (inflammation)	Resp. 1.5 and 24 hrs	Yes	Yes	Yes**	↑	↓	X	[47]
	Dry	Glucose	145°C	20 min	OPA assay SDS-PAGE Colorimetric index Fluorescent intensity	Caco-2	500 µg/mL (proliferation) / 25 µg/mL (inflammation)	Resp. 1.5 and 24 hrs	Yes	Yes	Yes**	↑	↓	X	[47]

↑ = upregulated, ↓ = downregulated, ↕ = ambiguous, – = no effect, X = not investigated.
* Mimicking ultra-high-temperature processing of milk: 70°C for 30 min, followed by 135°C for 8 seconds and stored for 90 days at 25°C. ** Outcomes compared to heated controls.
[1] 267 µg total AGEs/mg protein.
[2] 11 µg total AGEs/mg protein.

of the oncogene MDM2 and inactivation of related tumor suppressors p53 and Rb, while Lin et al. [43] showed increased translocation of β-catenin, which has been described to promote transcription of several oncoproteins [46], accompanied with the upregulation of RAGE. In addition, H. Chen et al. [44] and R. Deng et al. [45] showed a RAGE-dependent increase of the expression of proteins involved in respectively cell proliferation (ChREBP) and cancer cell migration (Sp1 and MMP2). Related to these outcomes, these studies also showed increased cell proliferation and increased invasion and migration rates, respectively. So, overall, these studies suggest cancer-promoting properties of glycated BSA, however, their methodology faces some limitations. For example, the studies used heated BSA as a negative control, while preferably a native BSA and medium control would be included as well since Teodorowicz et al. [47] showed that glycated protein increased proliferation (and decreased inflammation) compared to the native and heated protein, while there was no or an opposite effect on these parameters compared to the medium control, when investigating the effect of glycated peanut 7S globulin on a Caco-2 model. In addition, these studies did not always check for dose-dependency, which would prove causality, nor did they include a compound known to promote cancer, preferably through RAGE, as a positive control. Therefore, it is hard to make a statement about the potency of glycated BSA in inducing the observed effect. So, although evidence seems to suggest that glycated BSA has a cancer-promoting effect in immortalized cancer colon-derived cell lines, the results should be interpreted with caution.

Studies on dietary free AGEs and the intestinal epithelium

The abovementioned studies investigated dietary protein-bound AGEs. In general, this research focused on their effects on the colonic epithelium, related to the reduced digestibility and bioavailability of these proteins shown *in vitro*. Apart from this, some *in vivo* and *in vitro* studies investigated the effects of free AGEs, mainly free CML, in Caco-2 cells [48–50] and rodent models [51]. For the *in vitro* studies, Holik et al. [49] and Wu et al. [50] differentiated the Caco-2 cells to produce a small intestinal-like phenotype, while Z. Chen et al. [48] did not differentiate the cells. Wu et al. [50] showed increased ROS generation, MAPK and NF-κB protein expression, and decreased ZO-1 protein expression, while Holik et al. [43] reported no effect on proliferation. In comparison, Z. Chen et al. [48] observed increased proliferation but exposed the cells to 20 mM free CML

which is a 40-times higher concentration than tested by Holik et al. [49] and Wu et al. [50]. *In vivo*, potential pro-inflammatory effects of free CML, as suggested by the *in vitro* study of Wu et al. [50], were not observed in a healthy nor in a colitis mouse model [51]. Since free CML was shown to lack affinity for RAGE [39] but can enter the cells by passive diffusion [52], its potential cellular effects are more likely to be initiated by intracellular interactions with proteins and/or receptors. In this case, the mTOR pathway may be a potential candidate since it stimulates proliferation in the presence of amino acids [53]. However, current literature is not conclusive as to which pathways and processes might be affected by free AGEs in the intestinal epithelium.

Concluding remarks and future research

Taken together, *in vitro* studies are a valuable tool to understand underlying mechanisms of observations made *in vivo*, however the design of the currently available *in vitro* studies face some limitations and should therefore be interpreted with caution. Future *in vitro* studies focusing on the biological properties of dietary AGEs should only be conducted after a detailed physicochemical characterization of the glycated protein and the quantification of endotoxins in the sample. If endotoxins are detected, it has to be confirmed that the *in vitro* model of interest is not affected by their presence, otherwise the endotoxins in the sample need to be removed or neutralized before conducting any experiment on this model. In addition, based on its research question and hypothesis, future studies should consider carefully which negative and positive controls to include. When glycating a protein of interest, reducing sugars react with free amino groups of the target protein under the influence of heat. So, for the negative controls, future studies should not only control for the effect of a reducing sugar modifying the protein by including a heated protein control, but also for the effect of heating a protein and the presence of the protein itself, respectively by including a native protein and medium control. Besides, especially when the reducing sugar used is highly potent, the sample needs to be checked for any residues of this reactant as this could affect the cells. Considering the positive controls, a compound already known to induce the hypothesized outcome must be included. When this outcome is expected to be RAGE dependent, the positive control should also be described in the literature to act through RAGE. Lastly, dose-dependency between exposure and outcome must be shown to prove causality. In summary, since the glycation process introduces many additional variables and the generated AGEs are a

heterogeneous group of compounds, it is of paramount importance to characterize the glycated protein thoroughly and to check and control for all possible confounders that might be introduced in the *in vitro* model.

Until now, all these *in vitro* studies use immortalized cell lines from colon cancer origin, mainly Caco-2. Although these cells are widely used and accepted as a model for intestinal epithelial cells, it cannot be excluded that they might respond differently from healthy epithelial cells [54], for example when RAGE appears to be differently expressed on or distributed over the cell membrane. Therefore, using intestinal organoids as a model could be the next step to increase the external validity of *in vitro* studies. In addition, the interaction between dAGEs and the gut microbiota should be considered as a variable to control, as dAGEs are subject to microbial fermentation [55,56]. As gut microbial metabolites are known to interact with the intestinal epithelium and exert immunomodulatory properties, exposure to gut microbial metabolites derived from the fermentation of AGEs and co-cultures with immune cells would be necessary to cover the interplay between epithelial cells, the microbiome, and mucosal immune system [57]. By operating a more advanced *in vitro* model, such studies could be more effectively translated to human studies limiting the use of experimental animals as much as possible.

References

1. Perrone A, Giovino A, Benny J, Martinelli F. Advanced Glycation End Products (AGEs): Biochemistry, Signaling, Analytical Methods, and Epigenetic Effects. Oxid Med Cell Longev 2020;2020. https://doi.org/10.1155/2020/3818196.
2. Ahmad S, Akhter F, Shahab U, Rafi Z, Sajid Khan M, Nabi R, et al. Do all roads lead to the Rome? The glycation perspective! 2017. https://doi.org/10.1016/j.semcancer.2017.10.012.
3. Delgado-Andrade C, Fogliano V. Dietary Advanced Glycosylation End-Products (dAGEs) and Melanoidins Formed through the Maillard Reaction: Physiological Consequences of their Intake. Annu Rev Food Sci Technol 2018;9:271–91. https://doi.org/10.1146/ANNUREV-FOOD-030117-012441.
4. Poulsen MW, Hedegaard R V., Andersen JM, de Courten B, Bügel S, Nielsen J, et al. Advanced glycation endproducts in food and their effects on health. Food and Chemical Toxicology 2013;60:10–37. https://doi.org/10.1016/J.FCT.2013.06.052.
5. Koschinsky T, He C, Mitsuhashi T, Bucala R, Liu C, Buenting C, et al. Orally absorbed reactive glycation products (glycotoxins): an environmental risk factor in diabetic nephropathy. Proc Natl Acad Sci U S A 1997;94:6474–9. https://doi.org/10.1073/PNAS.94.12.6474.
6. Vlassara H, Cai W, Crandall J, Goldberg T, Oberstein R, Dardaine V, et al. Inflammatory mediators are induced by dietary glycotoxins, a major risk factor for diabetic angiopathy. Proc Natl Acad Sci U S A 2002;99:15596–601. https://doi.org/10.1073/PNAS.242407999.
7. Ashrafian H, Zadeh EH, Khan RH. Review on Alzheimer's disease: Inhibition of amyloid beta and tau tangle formation. Int J Biol Macromol 2021;167:382–94. https://doi.org/10.1016/J.IJBIOMAC.2020.11.192.
8. Moreau KL, King JA. Protein Misfolding and Aggregation in Cataract Disease and Prospects for Prevention. Trends Mol Med 2012;18:273. https://doi.org/10.1016/J.MOLMED.2012.03.005.
9. Ursini F, Davies KJA, Maiorino M, Parasassi T, Sevanian A. Atherosclerosis: another protein misfolding disease? Trends Mol Med 2002;8:370–4. https://doi.org/10.1016/S1471-4914(02)02382-1.
10. Koch M, Chitayat S, Dattilo BM, Schiefner A, Diez J, Chazin WJ, et al. Structural Basis for Ligand Recognition and Activation of RAGE. Structure 2010;18:1342. https://doi.org/10.1016/J.STR.2010.05.017.
11. Scheijen JLJM, Clevers E, Engelen L, Dagnelie PC, Brouns F, Stehouwer CDA, et al. Analysis of advanced glycation endproducts in selected food items by ultra-performance liquid chromatography tandem mass spectrometry: Presentation of a dietary AGE database. Food Chem 2016;190:1145–50. https://doi.org/10.1016/J.FOODCHEM.2015.06.049.
12. Zhao D, Li L, Le TT, Larsen LB, Xu D, Jiao W, et al. Digestibility of glycated milk proteins and the peptidomics of their in vitro digests. J Sci Food Agric 2019;99:3069–77. https://doi.org/10.1002/JSFA.9520.
13. van der Lugt T, Venema K, van Leeuwen S, Vrolijk M, Opperhuizen A, Bast A. Gastrointestinal digestion of dietary advanced glycation endproducts using an in vitro model of the gastrointestinal tract (TIM-1). Food Funct 2020;11:6297–307. https://doi.org/10.1039/D0FO00450B.
14. Zhao D, Sheng B, Wu Y, Li H, Xu D, Nian Y, et al. Comparison of Free and Bound Advanced Glycation End Products in Food: A Review on the Possible Influence on Human Health. J Agric Food Chem 2019;67:14007–18. https://doi.org/10.1021/acs.jafc.9b05891.
15. Nyakayiru J, Van Lieshout GAA, Trommelen J, Van Kranenburg J, Verdijk LB, Bragt MCE, et al. The glycation level of milk protein strongly modulates post-prandial lysine availability in humans. British Journal of Nutrition 2020;123:545–52. https://doi.org/10.1017/S0007114519002927.
16. van Dongen KCW, Linkens AMA, Wetzels SMW, Wouters K, Vanmierlo T, van de Waarenburg MPH, et al. Dietary advanced glycation endproducts (AGEs) increase their concentration in plasma and tissues, result in inflammation and modulate gut microbial composition in mice; evidence for reversibility. Food Research International 2021;147:110547. https://doi.org/10.1016/J.FOODRES.2021.110547.

17. Baye E, Kiriakova V, Uribarri J, Moran LJ, de Courten B. Consumption of diets with low advanced glycation end products improves cardiometabolic parameters: meta-analysis of randomised controlled trials. Scientific Reports 2017 7:1 2017;7:1–9. https://doi.org/10.1038/s41598-017-02268-0.
18. Clarke R, Dordevic A, Tan S, Ryan L, Coughlan M. Dietary Advanced Glycation End Products and Risk Factors for Chronic Disease: A Systematic Review of Randomised Controlled Trials. Nutrients 2016;8. https://doi.org/10.3390/NU8030125.
19. Kellow N, Savige G. Dietary advanced glycation end-product restriction for the attenuation of insulin resistance, oxidative stress and endothelial dysfunction: a systematic review. Eur J Clin Nutr 2013;67:239–48. https://doi.org/10.1038/EJCN.2012.220.
20. Puyvelde K Van, Mets T, Njemini R, Beyer I, Bautmans I. Effect of advanced glycation end product intake on inflammation and aging: a systematic review. Nutr Rev 2014;72:638–50. https://doi.org/10.1111/NURE.12141.
21. Pouillart P, Mauprivez H, Ait-Ameur L, Cayzeele A, Lecerf J, Tessier F, et al. Strategy for the study of the health impact of dietary Maillard products in clinical studies: the example of the ICARE clinical study on healthy adults. Ann N Y Acad Sci 2008;1126:173–6. https://doi.org/10.1196/ANNALS.1433.040.
22. Linkens AMA, van Best N, Niessen PM, Wijckmans NEG, de Goei EEC, Scheijen JLJM, et al. A 4-Week Diet Low or High in Advanced Glycation Endproducts Has Limited Impact on Gut Microbial Composition in Abdominally Obese Individuals: The deAGEing Trial. Int J Mol Sci 2022;23:5328. https://doi.org/10.3390/IJMS23105328.
23. Ott C, Jacobs K, Haucke E, Navarrete Santos A, Grune T, Simm A. Role of advanced glycation end products in cellular signaling. Redox Biol 2014;2:411–29. https://doi.org/10.1016/J.REDOX.2013.12.016.
24. Tessier FJ, Niquet-Léridon C, Jacolot P, Jouquand C, Genin M, Schmidt A-M, et al. Quantitative assessment of organ distribution of dietary protein-bound 13C-labeled Nε-carboxymethyllysine after a chronic oral exposure in mice. Mol Nutr Food Res 2016;60:2446–56. https://doi.org/10.1002/MNFR.201600140.
25. Snelson M, Coughlan MT. Dietary Advanced Glycation End Products: Digestion, Metabolism and Modulation of Gut Microbial Ecology. Nutrients 2019;11: 215. https://doi.org/10.3390/NU11020215.
26. Dubois C, Litke R, Rianha S, Paul-constant C, Lo Guidice JM, Taront S, et al. Exposure of caenorhabditis elegans to dietary nε-carboxymethyllysine emphasizes endocytosis as a new route for intestinal absorption of advanced glycation end products. Nutrients 2021;13. https://doi.org/10.3390/NU13124398/S1.
27. Frei E. Albumin binding ligands and albumin conjugate uptake by cancer cells. Diabetol Metab Syndr 2011;3:11. https://doi.org/10.1186/1758-5996-3-11.
28. Qu W, Yuan X, Zhao J, Zhang Y, Hu J, Wang J, et al. Dietary advanced glycation end products modify gut microbial composition and partially increase colon permeability in rats. Mol Nutr Food Res 2017;61:1700118. https://doi.org/10.1002/MNFR.201700118.
29. Cao C, Tang M, Zhao N, Dong S, Wu H. Effects of fish protein with glycation extent on gut microbiota and colonic barrier function in mice fed a high-fat diet. J Funct Foods 2021;85:1756–4646. https://doi.org/10.1016/J.JFF.2021.104636.
30. Snelson M, Tan SM, Clarke RE, De Pasquale C, Thallas-Bonke V, Nguyen TV, et al. Processed foods drive intestinal barrier permeability and microvascular diseases. Sci Adv 2021;7:1–16. https://doi.org/10.1126/sciadv.abe4841.
31. Al Amir I, Dubayle D, Héron A, Delayre-Orthez C, Anton PM. Maillard reaction products from highly heated food prevent mast cell number increase and inflammation in a mouse model of colitis 2017;48:26–32. https://doi.org/10.1016/J.NUTRES.2017.10.005.
32. Zen K, Chen CX-J, Chen Y-T, Wilton R, Liu Y. Receptor for Advanced Glycation Endproducts Mediates Neutrophil Migration across Intestinal Epithelium. The Journal of Immunology 2007;178:2483–90. https://doi.org/10.4049/JIMMUNOL.178.4.2483.
33. Snoeck V, Goddeeris B, Cox E. The role of enterocytes in the intestinal barrier function and antigen uptake. Microbes Infect 2005;7:997–1004. https://doi.org/10.1016/J.MICINF.2005.04.003.

34. Body-Malapel M, Djouina M, Waxin C, Langlois A, Gower-Rousseau C, Zerbib P, et al. The RAGE signaling pathway is involved in intestinal inflammation and represents a promising therapeutic target for Inflammatory Bowel Diseases. Mucosal Immunol 2019;12:468–78. https://doi.org/10.1038/S41385-018-0119-Z.
35. Bramhall M, Rich K, Chakraborty A, Logunova L, Han N, Wilson J, et al. Differential Expression of Soluble Receptor for Advanced Glycation End-products in Mice Susceptible or Resistant to Chronic Colitis. Inflamm Bowel Dis 2020;26:360–8. https://doi.org/10.1093/IBD/IZZ311.
36. Jing H, Kitts DD. Redox-related cytotoxic responses to different casein glycation products in Caco-2 and Int-407 cells. J Agric Food Chem 2004;52:3577–82. https://doi.org/10.1021/JF035512M/SUPPL_FILE/JF035512MSI20040309_014253.PDF.
37. Lacroix M. Persistent use of "false" cell lines. Int J Cancer 2008;122:1–4. https://doi.org/10.1002/IJC.23233.
38. Geicu OI, Stanca L, Voicu SN, Dinischiotu A, Bilteanu L, Serban AI, et al. Dietary AGEs involvement in colonic inflammation and cancer: insights from an in vitro enterocyte model. Sci Rep 2020;10:1–14. https://doi.org/10.1038/s41598-020-59623-x.
39. Zenker HE, Teodorowicz, Malgorzata Ewaz A, van Neerven JR, Savelkoul HF, De Jong NW, Wichers HJ, et al. Binding of CML-Modified as Well as Heat-Glycated β-lactoglobulin to Receptors for AGEs Is Determined by Charge and Hydrophobicity. Int J Mol Sci 2020;21:1–16. https://doi.org/10.3390/IJMS21124567.
40. Xie J, Reverdatto S, Frolov A, Hoffmann R, Burz DS, Shekhtman A. Structural Basis for Pattern Recognition by the Receptor for Advanced Glycation End Products (RAGE). Journal of Biological Chemistry 2008;283:27255–69. https://doi.org/10.1074/JBC.M801622200.
41. Deng Y, Govers C, Bastiaan-net S, Hulst N Van Der, Hettinga K, Wichers HJ. Hydrophobicity and aggregation , but not glycation , are key determinants for uptake of thermally processed β -lactoglobulin by THP-1 macrophages. Food Research International 2019;120:102–13. https://doi.org/10.1016/j.foodres.2019.01.038.
42. Wang P, Lu YC, Li YF, Wang L, Lee SC. Advanced Glycation End Products Increase MDM2 Expression via Transcription Factor KLF5. J Diabetes Res 2018;2018. https://doi.org/10.1155/2018/3274084.
43. Lin JA, Wu CH, Yen GC. Breadfruit flavonoid derivatives attenuate advanced glycation end products (AGEs)-enhanced colon malignancy in HCT116 cancer cells. J Funct Foods 2017;31:248–54. https://doi.org/10.1016/J.JFF.2017.01.050.
44. Chen H, Wu L, Li Y, Meng J, Lin N, Yang D, et al. Advanced glycation end products increase carbohydrate responsive element binding protein expression and promote cancer cell proliferation. Mol Cell Endocrinol 2014;395:69–78. https://doi.org/10.1016/J.MCE.2014.07.021.
45. Deng R, Wu H, Ran H, Kong X, Hu L, Wang X, et al. Glucose-derived AGEs promote migration and invasion of colorectal cancer by up-regulating Sp1 expression. BBA - General Subjects 2017;1861:1065–74. https://doi.org/10.1016/j.bbagen.2017.02.024.
46. Shang S, Hua F, Hu ZW. The regulation of β-catenin activity and function in cancer: therapeutic opportunities. Oncotarget 2017;8:33972. https://doi.org/10.18632/ONCOTARGET.15687.
47. Teodorowicz M, Fiedorowicz E, Kostyra H, Wichers H, Kostyra Z. Effect of Maillard reaction on biochemical properties of peanut 7S globulin (Ara h 1) and its interaction with a human colon cancer cell line (Caco-2). Eur J Nutr 2013;52:1927–38. https://doi.org/ 10.1007/s00394-013-0494-x.
48. Chen Z, Kondrashina A, Greco I, Gamon LF, Lund MN, Giblin L, et al. Effects of Protein-Derived Amino Acid Modification Products Present in Infant Formula on Metabolic Function, Oxidative Stress, and Intestinal Permeability in Cell Models. J Agric Food Chem 2019;67:5634–46. https://doi.org/10.1021/ACS.JAFC.9B01324.
49. Holik AK, Lieder B, Kretschy N, Somoza MM, Ley JP, Hans J, et al. The advanced glycation end product Nε-carboxymethyllysine and its precursor glyoxal increase serotonin release from Caco-2 cells. J Cell Biochem 2018;119:2731–41. https://doi.org/10.1002/JCB.26439.

50. Wu Q, Chen Y, Ouyang Y, He Y, Xiao J, Zhang L, et al. Effect of catechin on dietary AGEs absorption and cytotoxicity in Caco-2 cells. Food Chem 2021;355. https://doi.org/10.1016/J.FOODCHEM.2021.129574.
51. Aljahdali N, Gadonna-Widehem P, Delayre-Orthez C, Marier D, Garnier B, Carbonero F, et al. Repeated Oral Exposure to N e-Carboxymethyllysine, a Maillard Reaction Product, Alleviates Gut Microbiota Dysbiosis in Colitic Mice. Dig Dis Sci 2017;62:3370–84. https://doi.org/10.1007/s10620-017-4767-8.
52. Grunwald S, Krause R, Bruch M, Henle T, Brandsch M. Transepithelial flux of early and advanced glycation compounds across Caco-2 cell monolayers and their interaction with intestinal amino acid and peptide transport systems. British Journal of Nutrition 2006;95:1221–8. https://doi.org/10.1079/BJN20061793.
53. Takahara T, Amemiya Y, Sugiyama R, Maki M, Shibata H. Amino acid-dependent control of mTORC1 signaling: A variety of regulatory modes. J Biomed Sci 2020;27:1–16. https://doi.org/10.1186/S12929-020-00679-2/FIGURES/4.
54. Sambuy Y, de Angelis I, Ranaldi G, Scarino ML, Stammati A, Zucco F. The Caco-2 cell line as a model of the intestinal barrier: influence of cell and culture-related factors on Caco-2 cell functional characteristics. Cell Biol Toxicol 2005;21:1–26. https://doi.org/10.1007/S10565-005-0085-6.
55. Hellwig M, Bunzel D, Huch M, Franz CMAP, Kulling SE, Henle T. Stability of Individual Maillard Reaction Products in the Presence of the Human Colonic Microbiota. J Agric Food Chem 2015;63:6723–30. https://doi.org/10.1021/ACS.JAFC.5B01391.
56. Bui TPN, Troise AD, Nijsse B, Roviello GN, Fogliano V, de Vos WM. Intestinimonas-like bacteria are important butyrate producers that utilize Nε-fructosyllysine and lysine in formula-fed infants and adults. J Funct Foods 2020;70:103974. https://doi.org/10.1016/J.JFF.2020.103974.
57. Rubert J, Schweiger PJ, Mattivi F, Tuohy K, Jensen KB, Lunardi A. Intestinal Organoids: A Tool for Modelling Diet–Microbiome–Host Interactions. Trends in Endocrinology & Metabolism 2020;31:848–58. https://doi.org/10.1016/J.TEM.2020.02.004.

3

Protein-bound dietary advanced glycation end products cross the intestinal barrier: organoid models suggest paracellular transport as predominant route

Fleur A.C. Jansen [1] · Susanne Lotstra [2] · Vincenzo Fogliano [1] · Josep Rubert [1, 2] · Tamara Hoppenbrouwers [1, 3] · Klaske van Norren [2]

1 Department of Food Quality and Design, Wageningen University & Research, Wageningen, The Netherlands
2 Nutritional Biology, Division of Human Nutrition, Wageningen University & Research, Wageningen, The Netherlands
3 Food and Biobased Research, Wageningen University & Research, Wageningen, The Netherlands

Submitted

Abstract

During food processing, protein glycation leads to the formation of advanced glycation end products (AGEs). Most dietary AGEs are protein-bound and some of them become bioavailable after digestion as free AGEs or small peptides. However, recent evidence suggests that some intact glycated proteins may also be absorbed. Since protein-bound AGEs can bind RAGE, unlike the free or small peptide-bound forms, this could trigger inflammation. To further investigate whether intact glycated proteins cross the intestinal barrier, we used a conventional ileum air–liquid interface (ALI) model mimicking the normal ileum villous epithelium (VE). Considering the potential immunomodulatory properties of glycated proteins, in addition, a recently developed ALI model mimicking the follicle-associated epithelium (FAE) above the Peyer's Patches was also adopted. Beta-lactoglobulin (BLG) was modified through different thermal protocols including glycation and its translocation across the ALI models was assessed using ELISA and Western blot. Results showed that the FAE model has increased M cell expression and lowered transepithelial resistance (TEER), consistent with increased FITC-Dextran permeability, compared to the VE model. BLG crossed both epithelial barriers, however greater overall passage was observed in the FAE model (23.4% vs. 4.4%; compared to blank transwell). This passage was independent of the protein's heat-modification and a strong inverse exponential relationship with TEER was observed, suggesting paracellular transport as the main mechanism. In the FAE model the ratio of translocated protein monomers to high-molecular-weight structures was higher for glycated BLG than for aggregated BLG (3.6 vs. 1.0), which may be related to M cell-specific activity. In summary, the majority of translocation across the epithelial barrier likely occurred paracellularly, but also some M cell-mediated transcellular transport might have been involved. This leaves open the possibility that glycated proteins may also interact with cell types beyond the epithelium, such as intestinal immune cells, thereby potentially activating RAGE.

Introduction

During food processing, dietary proteins react with reducing sugars in the presence of heat which is known as protein glycation. As a result, a heterogenous group of stable amino acid modifications are formed: dietary Advanced Glycation End products (AGEs). These dietary AGEs are especially present in high-temperature processed, low-moisture foods such as bakery products [1] and for many years, they were mainly investigated in relation to their influence on food palatability and protein digestibility [2]. However, when the degree of food processing started to get linked more often to negative health effects of certain foods, also the role of dietary AGEs within this association became of interest [3].

In our diet, AGEs are predominantly present in a protein-bound form [4]. Like all proteins, they are digested and get absorbed in the form of single amino acids or dipeptides [5–7]. Although *in vitro* studies suggest that glycation slightly reduces the digestibility of these proteins [8,9], postprandial intervention studies showed that amino acid availability from highly glycated proteins is largely preserved, except for lysine [10,11]. This reduced bioavailability of lysine likely reflects its frequent modification during glycation, whereas other amino acids are less affected. These glycation-modified amino acids themselves have also been shown to remain bioavailable, since several studies reported that an increased habitual intake of dietary AGEs leads to raised AGE levels in plasma, urine, and tissues [12–15]. This is supported by data showing elevated levels of free AGEs in plasma directly after a high AGE meal [16]. However, some intervention studies also showed increased levels of protein-bound AGEs [12,17]. This distinction is important because it may affect how diet influences health: free AGEs do not bind to RAGE, while large peptide- and protein-bound AGEs do which is suggested to promote inflammation [18,19]. This rise in protein-bound AGEs in plasma was hypothesized to be indirectly related to AGE consumption, by increased endogenous formation through ingestion of reactive precursors (e.g. oxoaldehydes such as glyoxal and methyl-glyoxal) [12]. However, a recent *in vivo* study using *C. Elegans* suggests that glycated proteins of the undigested fraction might also be absorbed directly by enterocytes [20]. It would therefore be of interest to explore this mechanism further *in vitro*.

Current *in vitro* studies on the intestinal absorption of dietary AGEs typically focus on the uptake of dietary AGEs in free, di- or tripeptide form [6,7,21,22]. They employ Caco-2-cell-derived monolayers as experimental models, as these monolayers

express key intestinal enzymes and transporters involved in peptide transport, like peptide transporter 1 (PEPT1). However, this traditional model for intestinal barrier research is derived from colon carcinoma, which limits its translatability. For instance, it displays non-physiological resilience to inflammatory stimuli [23]. In recent years, organoid models have emerged as a more physiologically relevant alternative, as they are derived from human biopsies and preserve the diversity of cell types present *in vivo* [24]. Among these, differentiated organoid-derived monolayers have become the preferred model for studying transport mechanisms, as they closely recapitulate the barrier properties of the villous epithelium (VE) [23] while providing easy access to both the apical and basolateral compartments.

Since intact glycated proteins are thought to have immunomodulatory properties, their transport by specialized Microfold (M) cells is also of interest. These cells, located in the follicle-associated epithelium (FAE), transcytose macromolecules from the lumen to the underlying Peyer's patches, playing a key role in immune surveillance [25,26]. However, similar to the villous epithelium *in vivo*, conventional organoid-derived monolayers contain relatively few M cells [27]. Their expression can however be increased *in vitro* by applying RANKL [28], which is a differentiation factor expressed by subepithelial stromal cells beneath the FAE. It induces M cell-specific genes and markers, such as the surface marker glycoprotein 2 (GP2), in RANK-expressing epithelial cells [29,30]. Adding TNFα may further support this differentiation process, possibly by acting synergistically with RANKL through simultaneous activation of canonical and non-canonical NF-κB pathways [31]. Applying these differentiation factors in an *in vitro* culture therefore creates an FAE-like barrier, enabling to investigate the functional properties of this specialized epithelial domain. Nevertheless, beyond the characterization of different cell types [32], these models have not yet been applied in functional assays.

This study aimed to investigate the translocation of intact glycated food proteins across an intestinal barrier. To this end, the model protein beta-lactoglobulin (BLG) was modified using different thermal protocols, including glycation, and applied on an air-liquid interface (ALI) model mimicking the normal ileum VE. In addition to this conventional VE model, the novel RANKL and TNFα-differentiated ALI model mimicking FAE was also adopted, as FAE is hypothesized to be involved in the selective transport of glycated proteins. Translocation of BLG across these ALI models was assessed by ELISA and Western Blot.

Results

Enhanced M cell expression in follicle-associated epithelium (FAE) model compared to villous epithelium (VE) model

Based on literature [32], M cell differentiation was induced in the ALI model by basolateral stimulation with RANKL and TNFα between day 7 and 14 of culture (further referred to as FAE model). At the end of this differentiation period, GP2 staining was performed to identify mature M cells. A higher intensity of this staining was observed in the FAE model compared to the VE model, as shown in the confocal overview image (Supplementary Figure S3.1), confirming previous reports in literature. An enlarged section of this image shows that the GP2 staining is distributed in organized cell-shaped structures in the FAE model whereas the VE model shows fainter and primarily speckled signals (Figure 3.1). In case of the FAE model, these structures are typically located in areas of lower-lying cellular structures. When comparing Z-stack images (Figure 3.2), the FAE model shows GP2 staining on the cell surface, while the VE model shows only staining inside the cell. This confirms that ALI models express more mature M cells when differentiated with RANKL/TNFα.

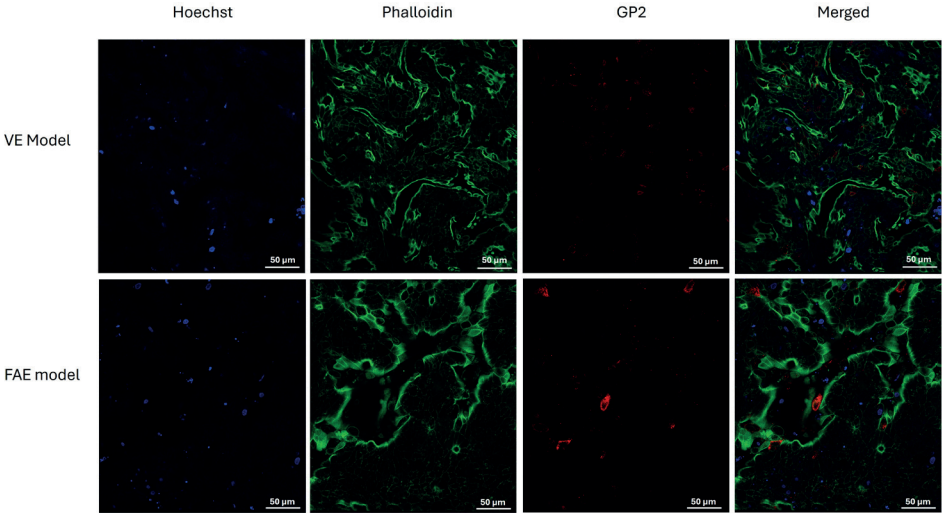


Figure 3.1: M cell expression in ALI models by RANKL/TNFα differentiation. ALI model was either differentiated with commercial medium (VE model) or with RANKL/TNFα-enriched commercial medium (FAE model). Blue dye – Nuclei (Hoechst); Green dye – Actin filaments (Phalloidin); Red dye – Microfold cells (GP2).

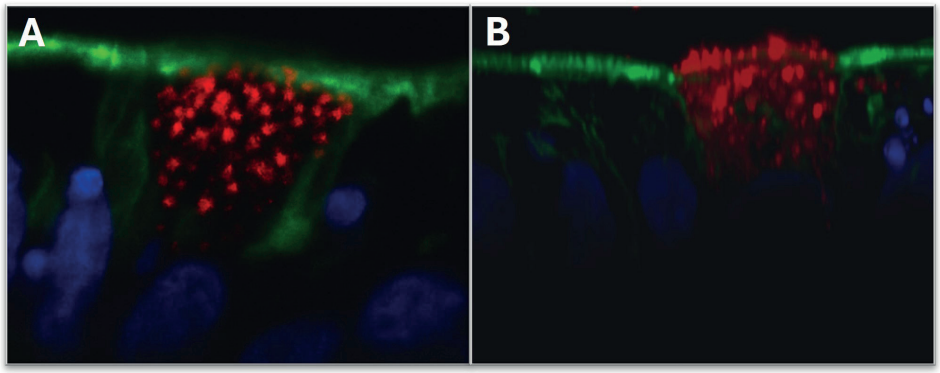


Figure 3.2: Confocal Z-stack image of M cell expression in ALI models by RANKL/TNFα differentiation. ALI model was either differentiated with commercial medium (**A**; VE model) or with RANKL/TNFα-enriched commercial medium (**B**; FAE model). Blue dye – Nuclei (Hoechst); Green dye – Actin filaments (Phalloidin); Red dye – Microfold cells (GP2).

Transepithelial resistance and FITC-dextran transport in the FAE model

Having confirmed increased M cell differentiation in the FAE model, we next assessed functional parameters that have not yet been described. Interestingly, clear and reproducible differences were observed between the FAE and VE model with respect to the temporal evolution of TEER during differentiation (interaction effect; $p<0.001$), shown in Figure 3.3. For the VE model, TEER values gradually increased over time and stabilized to an average value of 556.9 ± 109 Ω*cm^2.

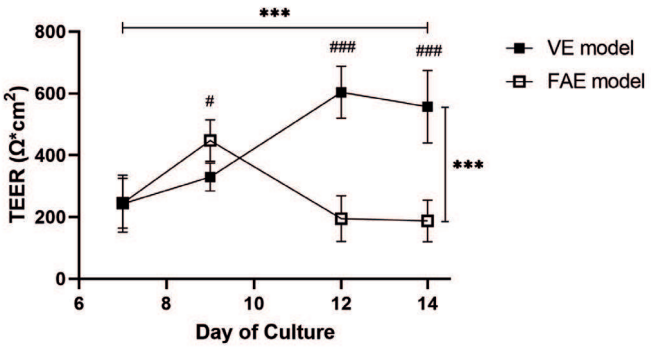


Figure 3.3: TEER values (Ω*cm2) over time of ALI models. To induce the differentiation of Microfold-like cells, the commercial differentiation medium of the ALI model was enriched with RANKL and TNFα from day 7 to day 14 of culture (FAE model). In parallel, a conventional model was cultured under identical conditions, but without enrichment of the medium (VE model). Data is mean values ± SD obtained from seven independent cultures. Two-way repeated measure ANOVA indicated significant model difference, time difference, and model*time interaction effects (all $p<0.001$; ***). Pairwise comparisons (LSD) indicated significant differences between models at specific time points (p-value; #<0.05, ###<0.001).

Upon basolateral stimulation with RANKL and TNFα, TEER values initially increased but started to drop after day 7 and stabilized at 187.9 ± 63 Ω*cm^2. Therefore, TEER of the FAE model is significantly lower compared to the VE model at the end of the differentiation period (day 14) ($p<0.001$). Given the reproducibility and minimal variability of these measurements, the observed values likely reflect altered barrier properties associated with the RANKL/TNFα differentiation protocol.

To assess paracellular transport in both models, permeability assays with FITC-Dex10 (10 kDa) and FITC-Dex150 (150 kDa) were performed and compared to the maximal FITC-Dextran permeability, which was defined through a Matrigel-coated blank transwell. For both FITC-Dex10 (Figure 3.4A) and FITC-Dex150 (Figure 3.4B), its concentration in the basolateral compartment of the ALI models increased over time (main effect; resp. $p<0.001$ and $p=0.006$) and differences in permeability between the models were observed (main effect; resp. $p=0.002$ and $p=0.09$). The FAE model showed significantly reduced permeability to FITC-Dex10 and FITC-Dex150 compared to the blank transwell (resp. $p=0.009$ and $p=0.034$). In turn, the VE model showed even lower permeability than the FAE model (resp. $p=0.013$ and $p=0.017$). The low variability observed in these measurements indicates that barrier integrity was maintained in both models (Figure 3.4) even though TEER decreased after the permeability assay (Supplementary Figure S3.2).

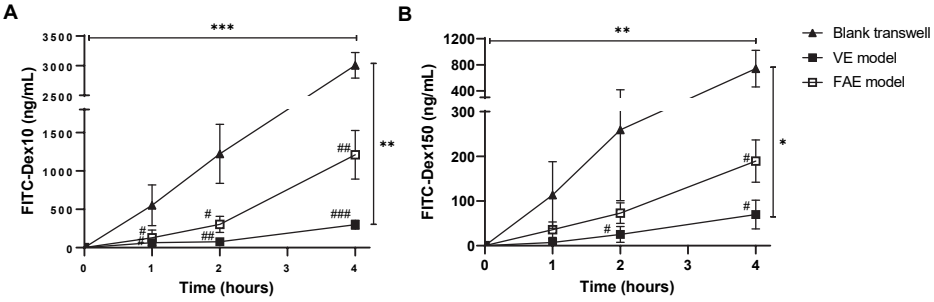


Figure 3.4: Concentration (ng/mL) of FITC-Dextran 10kDa **(A)** and FITC-Dextran 150kDa **(B)** in the basolateral compartment of ileum ALI model after apical exposure. VE and FAE model were compared to a blank transwell. Data is mean values ± SD obtained from four independent experiments. Two-way repeated measure ANOVA indicated significant model difference, time difference, and model*time interaction effects (p-value; *<0.05, **<0.01, ***<0.001). Pairwise comparisons (LSD) indicated significant differences when compared to blank transwell at specific time points (p-value; #<0.05, ##<0.01, ###<0.001).

When the dextran passage was expressed as a percentage of its maximum passage, it showed a non-linear inverse relationship with the corresponding TEER values (Figure 3.5A; individual datapoint). Furthermore, when averaging this

scatter plot for type of dextran and ALI model, Figure 3.5B again shows higher passage of FITC-Dextrans in the FAE model compared to the VE model (main effect; p=0.004) and a trend towards higher passage of the smaller FITC-Dex10 compared to FITC-Dex150 was observed in the FAE model (p=0.082). Both observations are expected in the context of the tight junction-regulated, paracellular transport mechanism of FITC-Dextrans. In summary, because of lower tightness of its monolayer (determined by TEER), the amount of paracellular transport of FITC-Dextrans is higher in the FAE model compared to the VE model.

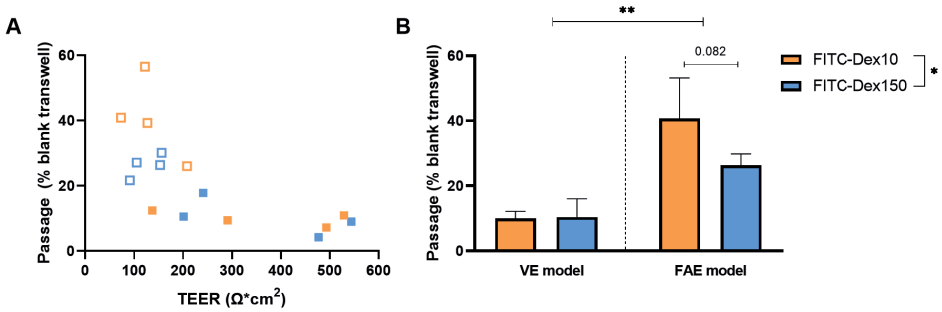


Figure 3.5: Passage of FITC-Dex10 (orange) and FITC-Dex150 (blue) in a VE model (closed squares) and FAE model (open squares), expressed as percentage of passage through a blank transwell. Data shown as individual data points expressed against TEER values **(A)** or as mean values ± SD **(B)**, obtained from four independent experiments. Two-way repeated measure ANOVA indicated a significant model and FITC-Dextran differences (p-value; *<0.05, **<0.01). Pairwise comparisons (LSD) indicated showed a trend towards higher passage of FITC-Dex10 compared to FITC-Dex150 in the FAE model (p=0.082).

Transepithelial passage of heat-modified dietary proteins

To answer the research question whether intact glycated proteins can pass an intestinal barrier, the common food protein BLG (18 kDa) was used as a model and tested both in its native form as well as after heat-treatment. To mimic the types of protein modifications formed during food processing, native BLG was heated following different protocols: moderate temperature (heated BLG), moderate temperature in the presence of glucose (glycated BLG), and higher, denaturing temperatures (aggregated BLG). As shown in Figure 3.6, the glycated and aggregated BLG preparations represented a highly heterogenous mixture, containing fractions that varied strongly in MWs. Compared to native BLG, the MW of the BLG monomers in the glycated BLG preparation increased, due to reaction with the sugar moieties. This reaction also leads to protein crosslinking, forming dimers, trimers and high MW structures. In comparison, the MW of the monomers in the aggregated BLG preparation is still comparable to the native

protein, while high MW structures are formed as a result of thermal unfolding of the protein and strong physical aggregation phenomena. Together, these BLG preparations allowed evaluation of the impact of protein modifications and MW on intestinal translocation.

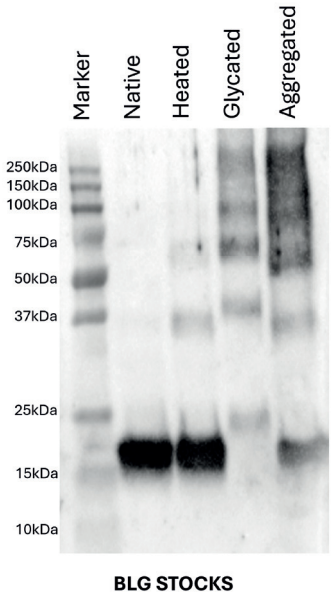


Figure 3.6: Western blot of differently heat-modified beta-lactoglobulin (BLG) stocks.

For quantification of the total amount of protein passing the epithelial layer, basolateral BLG concentrations were measured by ELISA and results are shown in Figure 3.7A. The concentrations of glycated BLG were multiplied by factor 2.5 to correct for underestimation of the sample by the assay (Supplementary Figure S3.3). When comparing the different models, significant differences in protein passage were observed (main effect; p=0.006): the VE model showed lower passage of proteins compared to the FAE model (p=0.023) while both models showed decreased passage compared to the blank transwell (resp. p=0.003 and p=0.011). Upon exposure to these heat-modified proteins, inflammatory responses were not observed and TEER changes were not different from vehicle control (resp. Supplementary Figure S3.4 and S3.5). When the BLG passage was expressed as a percentage of the passage through a blank transwell (Figure 3.7B), no significant differences between the heat-modified proteins were observed, nor an interaction effect between the proteins and ALI models. This suggest a-specific translocation; most variation in protein passage is likely explained by

differences in TEER and thereby differences in the tight junction-regulated, paracellular transport mechanism between the ALI models. This is supported by the strong inverse exponential relationship observed between protein passage and its corresponding TEER values (Figure 3.7C). In summary, BLG passage seems strongly dependent on paracellular transport, which is influenced by TEER. However, also in the VE model, showing highest TEER values, all BLG preparations reached the basolateral compartment.

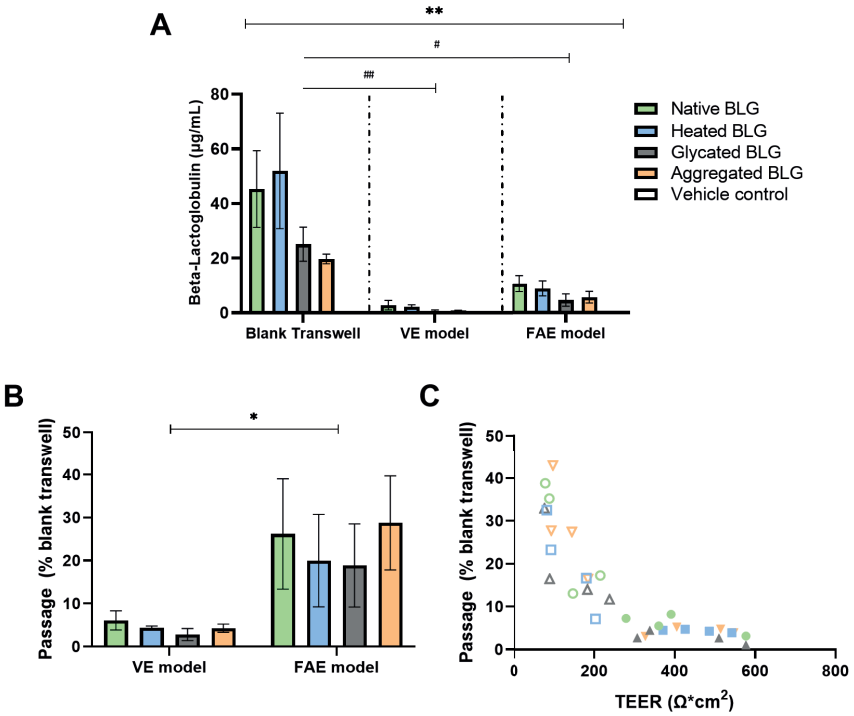


Figure 3.7: Concentration of differently heat-modified beta-lactoglobulin (BLG) in the basolateral compartment of ileum ALI model after apical exposure. Absolute values (µg/mL) were measured by ELISA **(A)**, and expressed as percentage of passage through a blank transwell **(B)**. These data is shown as mean values ± SD obtained from four independent experiments. Two-way repeated measure ANOVA indicated a significant model differences (p-value; *<0.05, **<0.01). Pairwise comparisons (LSD) indicated showed a lower passage in the VE and FAE model compared to the blank transwell trend (p-value; #<0.05, ##<0.01). Individual data points (%) from these experiments are also plotted against corresponding TEER values, for both VE model (closed symbols) and FAE model (open symbols) **(C)**.

Considering the highly heterogenous nature of the glycated and aggregated BLG preparation with respect to MW, Western blot analysis was performed to identify whether only the monomeric or also the high MW fractions of these samples were able to pass the monolayer (resp. Figure 3.8A and 3.8B). Relative quantification of

the passage of the monomers (~20 kDa) and high MW structures (100–250 kDa) was performed based on the volume intensity of these fractions, normalized to the vehicle control (medium) and referred against the maximum passage defined by a blank transwell. In this respect, the glycated sample was not detectable in the basolateral compartment of the VE model, suggesting lower sensitivity of this assay compared to the previous ELISA. The relative passage of the monomeric and high MW fractions of the aggregated sample was resp. 13.6% and 11.8%, providing a monomer:high MW-ratio of 1.15. As expected based on the ELISA data, the observed percentages were higher in the FAE model. For the glycated sample, basolateral intensity values of 100% (monomers) and 28.1% (high MW structures) were measured in the FAE model, providing a monomer:high MW-ratio of 3.6. For the aggregated sample, this ratio was 1.04 (41.7% monomers vs. 40% high MW structures). The higher ratio for glycated BLG suggests that the FAE model handles this sample differently from aggregated BLG, which may be related to M cell-specific activity.

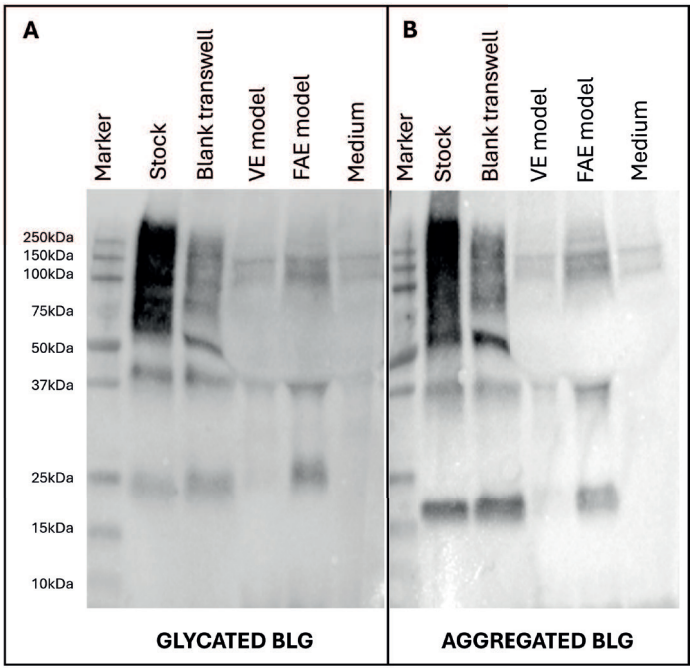


Figure 3.8: Western blot of glycated and aggregated BLG stock present in the basolateral compartment of different ALI models after a permeability assay (resp. **A** and **B**). Passage of the monomers (~20 kDa) and high MW structures (100–250 kDa) in the permeability assays was analysed based on the volume intensity of these fractions, normalized to the vehicle control (medium) and referred against the maximum passage defined by a blank transwell. Blots shown are obtained with pooled samples from four independent experiments.

Discussion

In this research, we investigated the translocation of an intact, undigested food protein, beta-lactoglobulin (BLG), across an intestinal epithelial barrier, and explored whether this process was influenced by thermal processing of this protein (protein glycation). We employed a conventional ileum ALI model representing villous epithelium (VE), alongside a recently developed RANKL-TNFα differentiated ALI variant that mimics the specialized follicle-associated epithelium (FAE) regions of the ileum.

Translocation of BLG across the villous epithelium

The ileal surface is mainly covered by VE, interspersed with specialized regions of FAE. The VE plays a key role in digestion and absorption of nutrients and consists of enterocytes combined with entero-endocrine cells, goblet cells, and Paneth cells. When studying the bioavailability of glycated proteins, most previous studies have focussed on the transport of single amino acids and dipeptides after digestion [6,7,21,22] since intact proteins are generally assumed to remain unabsorbed [5]. However, recent *in vivo* findings in the nematode *Caenorhabditis elegans* challenge this assumption [20] as they showed that intact glycated proteins were endocytosed by the worm's enterocytes. When employing the conventional VE model, being abundant in enterocytes, glycated BLG was also observed to pass the epithelial barrier. This translocation was not limited by size, as both BLG monomers and high MW structures were observed to cross the epithelial barrier, neither was it affected by thermal processing of the protein.

The primary mechanism involved is suggested to be paracellular transport, since a strong inverse exponential relationship was observed between BLG passage and the corresponding TEER values of the monolayer [33]. This implies that the amount of protein translocation depends on the permeability of the barrier, which increases under specific circumstances like strenuous exercise, illness, or medication use [34]. Therefore, the observation that the amount of peanut-derived large peptides and proteins in human plasma increase upon exercise [35] supports the suggestion that passage of big protein structures, for example glycated BLG, occurs through paracellular transport. This implies that glycated proteins pass the barrier unchanged by moving through intercellular spaces, in contrast to the glycated proteins likely being degraded by lysosomes within the enterocytes of the *C. Elegans* model. Potentially, this degradation is driven by a lack of alternative energy and/or amino acid sources, however mimicking these

circumstances in an ALI model would attenuate cell viability and is not considered physiologically relevant. Together, this suggests that glycated proteins would be able to cross the intestinal barrier unchanged, leaving open the possibility that these proteins may also interact with cell types beyond the epithelium, such as intestinal immune cells, thereby potentially activating RAGE.

Translocation of BLG across the follicle-associated epithelium

Considering the potential immunomodulatory properties of glycated proteins, it is also interest to investigate whether glycated proteins can pass the FAE as these specialized ileal regions play a key role in mucosal immune surveillance [29]. Therefore, FAE differs both morphologically and physiologically from surrounding VE. For example, because the expression of goblet cells is lower, the mucus layer covering the FAE is considered thinner. In addition, the M cells present in the FAE can recognize specific macromolecules through several receptors (e.g. GP2) and selectively transport them from the lumen to the underlying Peyer's patches [26]. These cells have shorter and fewer microvilli on their apical surface and contain pocket-like basolateral invagination of the plasma membrane harboring immune cells [36]. Together with the more porous basal lamina of FAE, these features facilitate fast translocation of luminal macromolecules to immune cells within the Peyer's patches [37]. M cells are however difficult to identify and isolate from *ex vivo* tissue [25]. Therefore, recently, methods have been developed to increase the expression of M cells in *in vitro* enteroid models, using specific differentiation factors like RANKL [27,32,38,39]. These cultures were previously shown to exhibit a gene expression profile closely resembling that of M cells *in vivo* [28], however functional parameters were not yet described for enteroid monolayers. In our study, we confirmed increased M cell expression in our FAE model, and we are the first to report on functional characteristics of these monolayers, underscoring the novelty of this work.

This strength also brings about the main limitation of this study. Because data on the permeability of *in vitro* FAE-like monolayers are currently lacking in literature, we are unable to externally validate our finding that their permeability is higher than that of VE monolayers. Importantly, however, this observation was highly reproducible within our experimental set-up and similar data are present for another *in vitro* FAE model: Caco-2/B-lymphocyte co-culture [40–43]. Similar to our findings, these studies reported increased translocation of paracellular markers (e.g. mannitol, FITC-Dextrans) and approximately 50% lower TEER values compared

with a conventional Caco-2 monoculture [41,42,44]. For example, des Rieux et al. [42] reported an average TEER value of 174 Ω*cm^2 for the co-culture versus 322 Ω*cm^2 for the monoculture. Despite the reproducibility of our experiments and the observed similarities with other FAE-like models, we acknowledge that additional validation is required to determine whether these models accurately reflect the physiological FAE barrier properties.

This external validation would include examining *ex vivo* FAE tissue. Since this is a niche field and specialized techniques are required regarding the identification and isolation of this tissue, few studies are available, predominantly from the same research group [44–47]. In the two studies concerning healthy human FAE tissue [44,45], Ussing chamber experiments showed that the passage of bacterial strains, which is considered transcellular transport, was clearly increased in FAE tissue compared to VE tissue, while permeability to a paracellular marker (^{51}Chromium-EDTA) was not significantly different between the two tissues. A trend towards higher paracellular permeability in FAE was however observed, which is in line with our observations *in vitro*. Nevertheless, the differences in TEER and paracellular permeability between our FAE and VE models were substantially larger, which may reflect the simplified nature of the *in vitro* system. Unlike *ex vivo* tissue, our monolayers consist of solely epithelial cells and lack stromal and immune components. Future studies should aim to incorporate additional structures to create an *in vitro* model that represents the *in vivo* barrier even more closely.

Regarding the transport of glycated proteins in our study, passage across the epithelial barrier was more pronounced in the FAE model than in the VE model. Because a strong inverse exponential relationship was observed with the corresponding TEER, this is likely related to increased paracellular transport [33]. However, some M cell-mediated transcellular transport might have contributed as well, as a higher monomer:high MW translocation ratio was observed for glycated BLG compared to aggregated BLG. This suggests that glycated BLG monomers might be selectively transported via transcytosis by the M cells. Other studies have also reported increased cellular uptake upon protein glycation [20,48], which supports this finding and suggests that glycation might promote a specific recognition of proteins by epithelial cells. Future studies could further investigate selective M cell-mediated endocytosis by using labelled food proteins, potentially combined with IgA co-incubation to help localize the M cells [29].

Conclusion

In summary, translocation of (glycated) BLG is already visible in the conventional VE models, and appears to occur mainly via paracellular routes, implying that passage increases when gut barrier integrity is compromised. Notably, this translocation is not limited to protein monomers, as larger protein aggregates also reached the basolateral side regardless of their thermal modifications. Our data further suggests that some M cell-mediated transcellular transport of glycated monomers may occur, however these findings are preliminary and warrant further investigation. Overall, glycated proteins appear capable of crossing the intestinal barrier, leaving open the possibility that they may interact with cell types beyond the epithelium, such as intestinal immune cells, thereby potentially activating RAGE.

Materials & methods

Materials

All stocks and reagents were prepared and stored according to manufacturer instructions. The materials below are applicable to all protocols unless stated otherwise. From Merck Life Sciences (Darmstadt, Germany), Dulbecco's Phosphate Buffered Saline (DPBS) without Ca^{2+} and Mg^{2+} (#D857), Bovine Serum Albumin (BSA) (#A3912) and Matrigel (Growth Factor Reduced; #CLS356231) were purchased. Matrigel was thawed at 4°C and kept on ice until use. From VWR International (Boxmeer, The Netherlands), TC-treated flat bottom 24-well plates (#734-2325) and transparent 0.4 µM pore diameter 24-well Thincerts (#82050-022) were purchased. Advanced DMEM/F12 (#12634-010), Penicillin-Streptomycin (P/S; 10,000 U/mL) (#15140122), TrypLE Express Enzyme (#12604013), Recombinant human sRANK Ligand (RANKL) (#310-01), and Recombinant Murine TNFα (#315-01A) were obtained from ThermoFisher Scientific (Waltham, MA, USA). RANKL and TNFα were reconstituted in sterile 0.1% BSA-dH2O at resp. 200 µg/mL and 50 µg/mL, stored at -20°C. Repeated freeze-thaw cycles were avoided. IntestiCult™ Intestinal Organoid Growth and Differentiation medium (resp. OGM and ODM) (resp. #06010 and #100-0214) and Y-27632 Rho-kinase inhibitor (#72304) were purchased from STEMCELL technologies (Vancouver, Canada). All solutions used for culturing, with the exception of TrypLE, were supplemented with 1% P/S and Rho-kinase inhibitor at a working concentration of 10 µM.

Human ileal organoid culture

To establish 3D organoid cultures from human ileal tissue, commercially available organoids were purchased at Merck (#SCC339; Prep ht-105-I), which were generated from the healthy ileal tissue of a 19-year-old male donor. Briefly, organoids were thawed, resuspended in 5 mL of Advanced DMEM/F12 and spun down at 500*g for 5 min at 4°C, after which the supernatant was discarded, and the organoid pellet was resuspended in undiluted Matrigel. Domes of this organoid-Matrigel mixture were seeded in a 24-wells plate, one dome (35 µL) per well. Plates were incubated at 37°C, 5% CO_2, and, after Matrigel solidification, 500 µL OGM per well was added. OGM was refreshed every other day.

Organoid passaging was performed at day 7. The 3D organoids were harvested by resuspending the domes, using the old culture medium. Domes were scraped free of the well bottom and broken up by pipetting up and down three times. These dome-medium mixtures were then collected in a 15 mL tube (#62.554.502; Sarstedt, Nümbrecht, Germany) and spun down at 500*g for 5 min at 4°C. After centrifugation, the supernatant was discarded and 1 mL of ice-cold DPBS was added to the dome pellet. To generate organoid fragments for passaging, the pellet was resuspended by vigorously pipetting up and down 30 times. Then, an extra 4 mL of ice-cold DPBS was added, and the suspension was centrifuged at 500*g for 5 min at 4°C. Undiluted Matrigel was added to the pellet and new 35 µL domes were made in a new 24-wells plate, as described above. General subculturing ratio was 1:4 to 1:6, depending on the size of the organoids and fragment generation efficacy. Passage number did not exceed 10.

To seed the 3D organoids as 2D monolayers, 24-well Thincert transwell inserts were coated 4% Matrigel, diluted in Advanced DMEM/F12, 100 µL per insert, for 1 h at 37°C. After coating, remaining liquid was removed and a single cell suspension was seeded obtained from the 3D cultures. To this end, 3D organoids were harvested by scraping as described above, collected in a 15 mL tube and spun down at 500*g for 5 min at 4°C. Supernatant was discarded, and, if an opaque layer of Matrigel remained, this was also removed through careful pipetting. Next, 1 mL of TrypLE™ Express Enzyme was added to the pellet and incubated for 10–15 min in a 37°C waterbath, with periodic gentle agitation. After incubation, the organoids were dislodged into single cells by vigorous pipetting. To deactivate the TrypLE, 3 mL of OGM was added, and the single-cell suspension was spun down at 500*g for 5 min at 4°C. Of the supernatant, 3 mL was discarded, leaving 1 mL in which the pellet was resuspended. Cell concentration was measured using the TC-20 Cell

Counter (Bio-Rad; Hercules, CA, USA), and the live-cell count was used to prepare a dilution of 5.0*10^5 cells/mL in OGM. Per Matrigel-coated transwell, 200 µL of the suspension was added apically, and 500 µL of OGM was added basolaterally. The transwell inserts were then incubated stationary at 37°C, 5% CO_2. After 48h (day 2), the OGM was refreshed (apical and basolateral), and the plate was placed onto a rotational shaker, set at 100 rpm, and incubated at 37°C, 5% CO_2. On day 5, at which the monolayers had typically reached confluency, the apical medium was removed and the basolateral OGM was replaced with ODM, 500 µL per well.

From day 7 onwards, the monolayers were exposed basolaterally to a combination of RANKL and TNFα to induce the differentiation of M-like cells in the 2D transwell system (FAE model), following an adaptation of the protocol by Fasciano et al. [32]. Briefly, every other day, the ODM was replaced and freshly enriched with RANKL and TNFα at final concentrations of 200 and 50 ng/mL, respectively. In parallel, monolayers were differentiated with regular ODM as a VE model. At day 14, characteristics of the models were defined (immunostaining, epithelial resistance and permeability assays) and the transepithelial passage of FITC-Dextrans and dietary proteins was assessed. When visual disturbances (e.g. holes) were absorbed in either the VE or FAE monolayer, cultures were excluded from these experiments. This was the case for two out of nine cultures.

Functional characterization of monolayers

Epithelial resistance

To assess the resistance to passive ion flow across the monolayers during differentiation, the TEER of the monolayers was measured at day 7, 9, 12, and 14 of culturing. At day 14, TEER was measured at baseline and at the end of the experiment. Measurements were performed at RT with resp. 300 µL and 1000 µL of advanced DMEM/F12 on the apical and basolateral side. The device used was the Millicell® ERS 3.0 Digital VoltOhmMeter (Merck Life Sciences, Darmstadt, Germany). Values were corrected for the resistance value of a Matrigel-coated blank transwell and expressed as multiplied by surface area (Ω*cm^2).

Immunostaining

For the visualization of cellular markers, the protocol described by Fasciano et al. [32] was followed. Briefly, 2D ileal organoid monolayers cultured and stimulated as described above were fixed with 4% paraformaldehyde (#252549; Merck Life Sciences, Darmstadt, Germany) in DPBS, 500 µL basolaterally and 300 µL apically, for 15 min at RT. Afterwards, the solution was removed through careful pipetting and the monolayers were washed three times with DPBS (300 µL apical, 500 µL basolateral), and either wrapped in parafilm and stored at 4°C for future use, or used immediately.

To immunostain for M cell marker GP2 and F-actin stain Phalloidin, fixed monolayers were blocked with 5% BSA in DPBS for 30 min at RT. Blocking solution was added to both sides of the transwell (100 µL apical, 500 µL basolateral). After blocking, the mouse anti-GP2 primary antibody (#D277-3; MBL International, Schaumburg, IL, USA) was added to the apical side at a dilution of 1:100 in 1% BSA in DPBS (100 µL) and incubated for 1 h at RT. Basolateral side contained 500 µL DPBS. After primary antibody incubation, the monolayers were washed as described above. Secondary stain solution, containing Alexa Fluor 594 goat anti-mouse secondary antibody (#A-11005), Alexa Fluor Phalloidin 488 (#A12379) and Hoechst 33342 (#H3570) (ThermoFisher Scientific, Waltham, MA, USA) at resp. 1:200, 1:100 and 1:2000 dilution to 1% BSA + 0.1% Triton (#X100; Merck Life Sciences, Darmstadt, Germany) in DPBS was added apically (100 µL). The monolayers were incubated with secondary staining solution for 30 min at RT, in the dark. Basolateral side contained 500 µL DPBS. Afterwards, the monolayers were washed again.

For visualization, the transwell membranes were transferred onto glass microscope slides as follows. After staining, the transwell cups were turned upside down and the membranes were cut out using the tip of a scalpel blade. To prevent ragged edges, the cut-out circular membrane was further cut into a square by placing the membrane monolayer-side-up onto a glass cutting board and using the scalpel blade to cut off the round edges, leaving the middle square. Using tweezers, the square was transferred onto the microscope slide, covered with a drop of Imsol Mount (#4058; Avantor/VWR, Radnor, PA, USA), and a cover slide. Images were acquired using a Stellaris STED Microscope equipped with a HC PL APO CS2 86x/1.20 water immersion objective (Leica Microsystems BV, Amsterdam, NL). All images were processed using LAS X software (Leica Microsystems BV, Amsterdam, NL).

Permeability assays

To check the tightness of the monolayer, a permeability assay was performed with Lucifer Yellow (LY) (#L0144), FITC-Dextran 10 kDa (FITC-Dex10) (#FD10S) and FITC-Dextran 150 kDa (FITC-Dex150) (#FD150S) (Merck Life Sciences, Darmstadt, Germany) for the VE model, FAE model and Matrigel-coated blank transwell. The polysaccharides were reconstituted in DPBS at 500 µg/mL and cultures were exposed apically to 10 µL of these solutions for 4 h, placed onto a rotational shaker (100 rpm) and incubated at 37°C, 5% CO_2. As a vehicle control, DPBS was included. During this experiment, basolateral ODM samples (50 µL) were taken after 1 h, 2 h and 4 h. Fluorescence of the LY samples was measured in a black 96-well plate (#237105; ThermoFisher Scientific, Waltham, MA, USA) at λexc 425 nm and λem 515 nm using a Spectramax® M2 (Molecular Devices, San Jose, CA, USA), while FITC-Dex samples were measured at λexc 485 nm and λem 528 nm. Values were corrected for vehicle control. Concentrations in the basolateral medium were determined by interpolating these OD values against a standard curve of the stock solution (10 µg/mL to 5 ng/mL).

Experimental acceptability

Further criteria for experimental acceptability were defined as 1) average baseline TEER value of the VE model higher than 500 Ω*cm^2, based on reference data from STEMCELL Technologies, 2) no significant drop of TEER (≤50%) after the experiment in the VE model, and 3) LY passage in the FAE model not within one standard deviation of the blank transwell. These criteria lead to the exclusion of 43% of the cultures (3 out of 7) (Supplementary Figure S3.6).

Transepithelial passage of modified dietary proteins

Protein glycation and characterization

Four differently modified BLG samples were prepared: native, heated, glycated, and aggregated BLG. To this end, BLG (#L0130; Merck Life Sciences, Darmstadt, Germany) was dissolved to 10 mg/mL in DPBS with or without 16 mM D-glucose (#G7021; Merck Life Sciences, Darmstadt, Germany). These solutions were lyophilized in aliquots of 500 µL in 5.0 mL Sterile Eppendorf® tubes (#525-0982; Avantor/VWR, Radnor, PA, USA). For the native BLG, no heating protocol was applied, while the lyophilized aliquots for the heated and glycated BLG were heated in a Memmert Environmental Chamber (#10861-384; Avantor/VWR, Radnor, PA, USA) at 60°C and 40% humidity for 24 h, to approach temperatures reached during food

processing without denaturing BLG. The lyophilized aliquots for the aggregated BLG were heated at 90°C and 40% humidity for 20 h, to approach the degree of aggregation in the glycated sample without AGEs being formed. Afterwards, all samples were redissolved in 500 µL DPBS. Residual glucose was removed by 10 kDa MWCO, Amicon™ Filter (#UFC9010; Merck Life Sciences, Darmstadt, Germany) according to manufacturer protocol. For each sample, final protein concentration was determined by DUMAS, to be able to account for potential losses. The conversion factor of 6.38 was applied. Samples were stored at -20°C. Samples were characterized by absorbance/fluorescence measurements, LC-MS/MS quantification of intact lysine/CML/CEL/Furosine, and OPA assay according to the protocols described by Jansen et al. [49]. Results are shown in Supplementary Table S3.1.

Transepithelial passage of modified dietary proteins

Cell culture experiment

In parallel with the FITC-Dextrans, translocation of the modified BLG samples was assessed for the VE culture, the FAE culture and Matrigel-coated blank transwells. The cultures were exposed apically to 10 µL of the undiluted stocks (in duplicate). As vehicle control, DPBS was included. Cultures were placed onto a rotational shaker (100 rpm) and incubated at 37°C, 5% CO_2. After 4 h, basolateral ODM samples were collected and stored at -20°C. Measurements on the basolateral samples as described below were only performed when the experiment was considered acceptable based on the experimental criteria mentioned above.

Inflammation

IL-8 concentration was determined with the human IL-8 Duoset ELISA kit (#DY208; Bio-Techne, Minneapolis, MN, USA). Manufacturer protocol was followed, however TMB substrate, supersensitive, for ELISA (#T4444; Merck Life Sciences, Darmstadt, Germany) was used as substrate solution. Samples were measured undiluted. Absorbance was measured at 450 nm and 540 nm using a Spectramax® M2. For data analysis, the OD values (450–540 nm) of technical duplicates were averaged and corrected for the blank. Sample concentrations were determined by interpolating these OD values against the standard curve by GraphPad Prism 9 (GraphPad Software, La Jolla, CA).

Beta-Lactoglobulin ELISA

Beta-Lactoglobulin concentration was measured by ELISA (#E11-125; Fortis Life Sciences, Boston, MA, USA), according to manufacturer protocol. Samples were diluted 500–2000 times. Absorbance was measured at 450 nm and 540 nm using a Spectramax® M2. For data analysis, the OD values (450–540 nm) of technical duplicates were averaged and corrected for the blank. Sample concentrations were determined by interpolating these OD values against the standard curve by GraphPad Prism. For samples with an average OD value below the LLOQ, the concentration was considered zero.

Beta-Lactoglobulin Western Blot

Beta-Lactoglobulin Western Blots were performed for the BLG stocks and for the experimental supernatants, according to the following protocol. All materials were purchased from Bio-Rad (Hercules, CA, USA) unless stated otherwise. 10 µL of NuPAGE™ LDS sample buffer (#NP0007; ThermoFisher, Waltham, MA, USA) and 4 µL of NuPAGE™ Sample Reducing Agent (#NP0009; ThermoFisher, Waltham, MA, USA) were added to 30 µL of 50X diluted BLG stock samples or undiluted basolateral supernatant. For the latter, supernatants from the individual experiments were pooled (blank transwell, VE model, FAE model and vehicle control) and a reference sample was included being the specific BLG stock diluted with deionized water to its average basolateral concentration in the blank transwell as determined by the BLG ELISA. These mixtures were heated for 10 min at 70°C and loaded on an 8–16% Mini-PROTEAN® TGX™ Precast protein 12-well Gel (#4561105) (20 µL/well). As a reference, 10 µL prestained protein standard (#1610377) was loaded. This gel was run with Tris/Glycine/SDS buffer (#1610772) at 120V in a Mini-PROTEAN Tetra Cell until the dye front reached the bottom of the gel. The gel was rinsed in deionized water and the proteins were transferred to a membrane by using a Trans-Blot® Turbo™ Mini 0.2 µM PVDF Transfer Pack (#1704156) with a Trans-Blot® Turbo™ Transfer System (settings: 1.3 A, 25 V, 7 min). Afterwards, membranes were washed for 5 min in deionized water and blocked with 20 mL 5% equine serum (#H1138; Merck Life Sciences, Darmstadt, Germany) in TBS containing 0.1% Tween-20 (TBST). After incubating 1h at RT on a roller, blocking buffer was discarded and 10 mL of primary antibody (#PA5-97512; ThermoFisher Scientific, Waltham, MA, USA) diluted 1:1000 in 5% horse-serum TBST was added. Membranes were incubated for 1 h at RT on a roller and washed 3X for 10 min with TBST. 10 mL of secondary antibody (#31460; ThermoFisher Scientific, Waltham, MA, USA) diluted 1:5000 in 5% horse-serum TBST was added

and after incubating 1 h at RT on a roller, membranes were washed 6X for 5 min with TBST. Membranes were incubated for 1 min with 2 mL Clarity Western ECL substrate (#1705061) and imaged by ChemiDoc MP machine. To quantify the passage of the different weight fractions of the glycated and aggregated BLG, the volume (intensity) was determined for the monomer fraction as well as high molecular weight (MW) fraction by ImageLab software (Supplementary Figure S3.7). The values were corrected for the intensity of the background (medium) and expressed as percentage of the volume observed for the blank transwell.

Statistical analysis

All cell culture experiments were repeated 4 times (n=4). Results are stated as mean ± SD from these independent experiments, unless stated otherwise. Two-way repeated measure analysis of variance (ANOVA) was used for statistical analysis in IBM SPSS statistics 25 (SPSS Inc., Chicago, IL, USA). The within-subject factors included being 1) culture model and time or 2) culture model and type of dextran/modified protein. Greenhouse-Geisser corrections were applied to account for potential violations of sphericity due to small sample size. When factors showed significance (p-value of ≤0.05), the LSD method was used for pairwise comparisons. All graphs were created using GraphPad Prism 9 (GraphPad Software, La Jolla, CA).

References

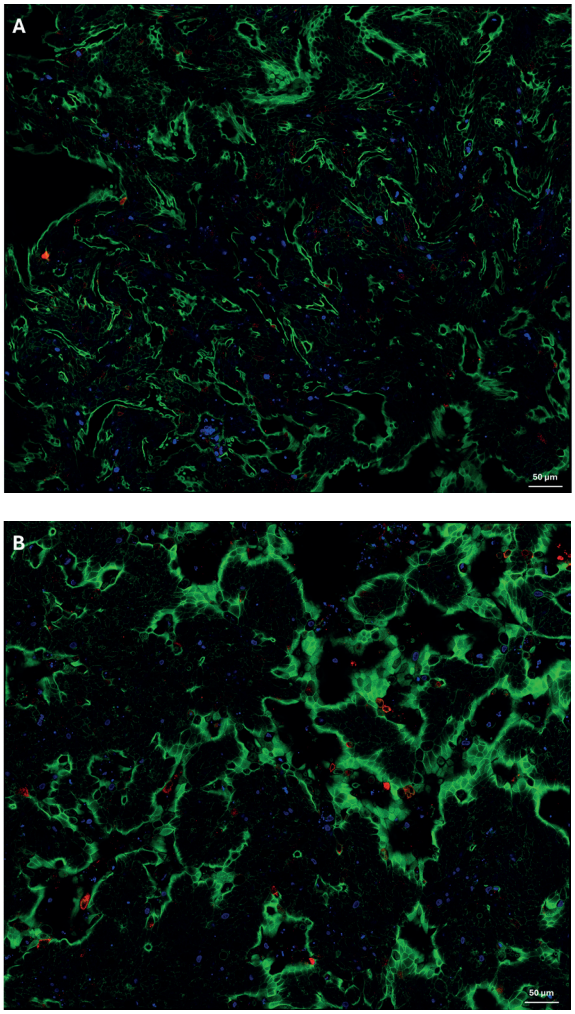
1. Scheijen JLJM, Clevers E, Engelen L, Dagnelie PC, Brouns F, Stehouwer CDA, et al. Analysis of advanced glycation endproducts in selected food items by ultra-performance liquid chromatography tandem mass spectrometry: Presentation of a dietary AGE database. Food Chem 2016;190:1145–50. https://doi.org/10.1016/J.FOODCHEM.2015.06.049.
2. Delgado-Andrade C, Fogliano V. Dietary Advanced Glycosylation End-Products (dAGEs) and Melanoidins Formed through the Maillard Reaction: Physiological Consequences of their Intake. Annu Rev Food Sci Technol 2018;9:271–91. https://doi.org/10.1146/ANNUREV-FOOD-030117-012441.
3. Uribarri J, del Castillo MD, de la Maza MP, Filip R, Gugliucci A, Luevano-Contreras C, et al. Dietary Advanced Glycation End Products and Their Role in Health and Disease. Advances in Nutrition 2015;6:461–73. https://doi.org/10.3945/AN.115.008433.
4. Yuan X, Nie C, Liu H, Ma Q, Peng B, Zhang M, et al. Critical Reviews in Food Science and Nutrition Comparison of metabolic fate, target organs, and microbiota interactions of free and bound dietary advanced glycation end products Comparison of metabolic fate, target organs, and microbiota interactions of free and bound dietary advanced glycation end products. Food Sci Nutr 2021;63:3612–33. https://doi.org/10.1080/10408398.2021.1991265.
5. Zhao D, Sheng B, Wu Y, Li H, Xu D, Nian Y, et al. Comparison of Free and Bound Advanced Glycation End Products in Food: A Review on the Possible Influence on Human Health. J Agric Food Chem 2019;67:14007–18. https://doi.org/10.1021/acs.jafc.9b05891.
6. Hellwig M, Geissler S, Matthes R, Peto A, Silow C, Brandsch M, et al. Transport of Free and Peptide-Bound Glycated Amino Acids: Synthesis, Transepithelial Flux at Caco-2 Cell Monolayers, and Interaction with Apical Membrane Transport Proteins. ChemBioChem 2011;12:1270–9. https://doi.org/10.1002/CBIC.201000759.
7. Grunwald S, Krause R, Bruch M, Henle T, Brandsch M. Transepithelial flux of early and advanced glycation compounds across Caco-2 cell monolayers and their interaction with intestinal amino acid and peptide transport systems. British Journal of Nutrition 2006;95:1221–8. https://doi.org/10.1079/BJN20061793.
8. Van Der Lugt T, Venema K, Van Leeuwen S, Vrolijk MF, Opperhuizen A, Bast A. Gastrointestinal digestion of dietary advanced glycation endproducts using an in vitro model of the gastrointestinal tract (TIM-1). Food Funct 2020;11:6297–307. https://doi.org/10.1039/D0FO00450B.
9. Zhao D, Li L, Le TT, Larsen LB, Xu D, Jiao W, et al. Digestibility of glycated milk proteins and the peptidomics of their in vitro digests. J Sci Food Agric 2019;99:3069–77. https://doi.org/10.1002/JSFA.9520.
10. Nyakayiru J, Van Lieshout GAA, Trommelen J, Van Kranenburg J, Verdijk LB, Bragt MCE, et al. The glycation level of milk protein strongly modulates post-prandial lysine availability in humans. British Journal of Nutrition 2020;123:545–52. https://doi.org/10.1017/S0007114519002927.
11. van Lieshout GA, Trommelen J, Nyakayiru J, van Kranenburg J, Senden JM, Gijsen AP, et al. Protein glycation compromises the bioavailability of milk protein-derived lysine in vivo in healthy adult males: a double-blind, randomized cross-over trial. Am J Clin Nutr 2025. https://doi.org/10.1016/J.AJCNUT.2025.01.025.
12. van Dongen KCW, Linkens AMA, Wetzels SMW, Wouters K, Vanmierlo T, van de Waarenburg MPH, et al. Dietary advanced glycation endproducts (AGEs) increase their concentration in plasma and tissues, result in inflammation and modulate gut microbial composition in mice; evidence for reversibility. Food Research International 2021;147:110547. https://doi.org/10.1016/J.FOODRES.2021.110547.
13. Linkens AMA, van Best N, Niessen PM, Wijckmans NEG, de Goei EEC, Scheijen JLJM, et al. A 4-Week Diet Low or High in Advanced Glycation Endproducts Has Limited Impact on Gut Microbial Composition in Abdominally Obese Individuals: The deAGEing Trial. Int J Mol Sci 2022;23:5328. https://doi.org/10.3390/IJMS23105328.

14. Nogueira Silva Lima MT, Delayre-Orthez C, Howsam M, Jacolot P, Niquet-Léridon C, Okwieka A, et al. Early- and life-long intake of dietary advanced glycation end-products (dAGEs) leads to transient tissue accumulation, increased gut sensitivity to inflammation, and slight changes in gut microbial diversity, without causing overt disease. Food Research International 2024;195:114967. https://doi.org/10.1016/J.FOODRES.2024.114967.
15. Tessier FJ, Niquet-Léridon C, Jacolot P, Jouquand C, Genin M, Schmidt A-M, et al. Quantitative assessment of organ distribution of dietary protein-bound 13C-labeled Nε-carboxymethyllysine after a chronic oral exposure in mice. Mol Nutr Food Res 2016;60:2446–56. https://doi.org/10.1002/MNFR.201600140.
16. Helou C, Lima MTNS, Niquet-Leridon C, Jacolot P, Boulanger E, Delguste F, et al. Plasma Levels of Free Nε-Carboxymethyllysine (CML) after Different Oral Doses of CML in Rats and after the Intake of Different Breakfasts in Humans: Postprandial Plasma Level of sRAGE in Humans. Nutrients 2022;14:1890. https://doi.org/10.3390/NU14091890/S1.
17. Teissier T, Quersin V, Gnemmi V, Daroux M, Howsam M, Delguste F, et al. Knockout of receptor for advanced glycation end-products attenuates age-related renal lesions. Aging Cell 2019;18. https://doi.org/10.1111/ACEL.12850.
18. Xie J, Reverdatto S, Frolov A, Hoffmann R, Burz DS, Shekhtman A. Structural Basis for Pattern Recognition by the Receptor for Advanced Glycation End Products (RAGE). Journal of Biological Chemistry 2008;283:27255–69. https://doi.org/10.1074/JBC.M801622200.
19. Xue J, Rai V, Singer D, Chabierski S, Xie J, Reverdatto S, et al. Advanced glycation end product recognition by the receptor for AGEs. Structure 2011;19:722–32. https://doi.org/10.1016/j.str.2011.02.013.
20. Dubois C, Litke R, Rianha S, Paul-constant C, Lo Guidice JM, Taront S, et al. Exposure of caenorhabditis elegans to dietary nε-carboxymethyllysine emphasizes endocytosis as a new route for intestinal absorption of advanced glycation end products. Nutrients 2021; 13. https://doi.org/10.3390/NU13124398/S1.
21. Hellwig M, Geissler S, Peto A, Knütter I, Brandsch M, Henle T. Transport of free and peptide-bound pyrraline at intestinal and renal epithelial cells. J Agric Food Chem 2009;57:6474–80. https://doi.org/10.1021/JF901224P.
22. Wu Y, Zong M, Zhang Z, Wu Y, Li L, Zhang X, et al. Selective transportation and energy homeostasis regulation of dietary advanced glycation end-products in human intestinal Caco-2 cells. Food Chem 2022;391. https://doi.org/10.1016/J.FOODCHEM.2022.133284.
23. Kollmann C, Buerkert H, Meir M, Richter K, Kretzschmar K, Flemming S, et al. Human organoids are superior to cell culture models for intestinal barrier research. Front Cell Dev Biol 2023;11:1223032. https://doi.org/10.3389/FCELL.2023.1223032/FULL.
24. Boonekamp KE, Dayton TL, Clevers H. Intestinal organoids as tools for enriching and studying specific and rare cell types: advances and future directions. J Mol Cell Biol 2020;12:562. https://doi.org/10.1093/JMCB/MJAA034.
25. Corr SC, Gahan CCGM, Hill C. M-cells: origin, morphology and role in mucosal immunity and microbial pathogenesis. FEMS Immunol Med Microbiol 2008;52:2–12. https://doi.org/10.1111/J.1574-695X.2007.00359.X.
26. Nakamura Y, Kimura S, Hase K. M cell-dependent antigen uptake on follicle-associated epithelium for mucosal immune surveillance. Inflamm Regen 2018;38:15. https://doi.org/10.1186/s41232-018-0072-y.
27. Nickerson KP, Llanos-Chea A, Ingano L, Serena G, Miranda-Ribera A, Perlman M, et al. A Versatile Human Intestinal Organoid-Derived Epithelial Monolayer Model for the Study of Enteric Pathogens. Microbiol Spectr 2021;9. https://doi.org/10.1128/SPECTRUM.00003-21/SUPPL_FILE/SPECTRUM00003-21_SUPP_1_SEQ8.PDF.
28. de Lau W, Kujala P, Schneeberger K, Middendorp S, Li VSW, Barker N, et al. Peyer's Patch M Cells Derived from Lgr5 + Stem Cells Require SpiB and Are Induced by RankL in Cultured "Miniguts" . Mol Cell Biol 2012;32:3639–47. https://doi.org/10.1128/MCB.00434-12.
29. Mabbott NA, Donaldson DS, Ohno H, Williams IR, Mahajan A. Microfold (M) cells: Important immunosurveillance posts in the intestinal epithelium. Mucosal Immunol 2013;6:666–77. https://doi.org/10.1038/MI.2013.30.

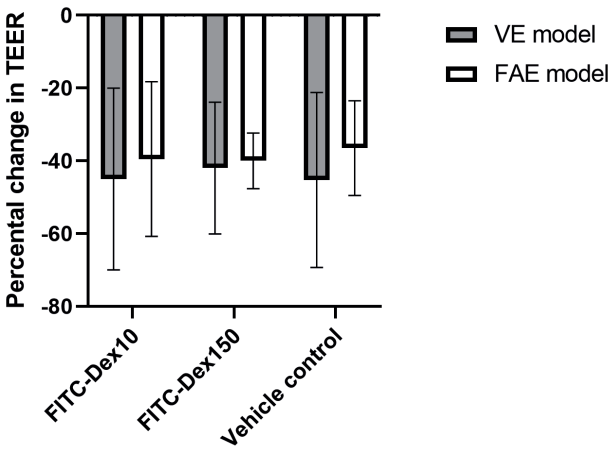
30. Sato S, Pascual DW. M Cell-Targeted Vaccines. Mucosal Vaccines: Innovation for Preventing Infectious Diseases 2020:487–98. https://doi.org/10.1016/B978-0-12-811924-2.00028-6.
31. Wood MB, Rios D, Williams IR. TNF-α augments RANKL-dependent intestinal M cell differentiation in enteroid cultures. Am J Physiol Cell Physiol 2016;311:C498–507. https://doi.org/10.1152/AJPCELL.00108.2016.
32. Fasciano AC, Blutt SE, Estes MK, Mecsas J. Induced Differentiation of M Cell-like Cells in Human Stem Cell-derived Ileal Enteroid Monolayers. JoVE (Journal of Visualized Experiments) 2019;2019:e59894. https://doi.org/10.3791/59894.
33. Helms HC, Waagepetersen HS, Nielsen CU, Brodin B. Paracellular Tightness and Claudin-5 Expression is Increased in the BCEC/Astrocyte Blood–Brain Barrier Model by Increasing Media Buffer Capacity During Growth. AAPS J 2010;12:759. https://doi.org/10.1208/S12248-010-9237-6.
34. Camilleri M. Human Intestinal Barrier: Effects of Stressors, Diet, Prebiotics, and Probiotics. Clin Transl Gastroenterol 2021;12:e00308. https://doi.org/10.14309/CTG.0000000000000308.
35. Janssen Duijghuijsen LM, Van Norren K, Grefte S, Koppelman SJ, Lenaerts K, Keijer J, et al. Endurance exercise increases intestinal uptake of the peanut allergen Ara h 6 after peanut consumption in humans. Nutrients 2017;9. https://doi.org/10.3390/nu9010084.
36. Kanaya T, Ohno H. The Mechanisms of M-cell Differentiation. Biosci Microbiota Food Health 2014;33:91. https://doi.org/10.12938/bmfh.33.91.
37. Radloff J, Falchuk EL, Markov AG, Amasheh S. Molecular characterization of barrier properties in follicle-associated epithelium of porcine Peyer's patches reveals major sealing function of claudin-4. Front Physiol 2017;8:273788. https://doi.org/10.3389/fphys.2017.00579.
38. Alfituri OA, Blake R, Jensen K, Mabbott NA, Hope J, Stevens JM. Differential role of M cells in enteroid infection by Mycobacterium avium subsp. paratuberculosis and Salmonella enterica serovar Typhimurium. Front Cell Infect Microbiol 2024;14:1416537. https://doi.org/10.3389/FCIMB.2024.1416537.
39. Rouch JD, Scott A, Lei NY, Solorzano-Vargas RS, Wang J, Hanson EM, et al. Development of Functional Microfold (M) Cells from Intestinal Stem Cells in Primary Human Enteroids. PLoS One 2016;11:e0148216. https://doi.org/10.1371/JOURNAL.PONE.0148216.
40. Kernéis S, Bogdanova A, Kraehenbuhl JP, Pringault E. Conversion by Peyer's patch lymphocytes of human enterocytes into M cells that transport bacteria. Science (1979) 1997;277:949–52. https://doi.org/10.1126/SCIENCE.277.5328.949.
41. Beloqui A, Brayden DJ, Artursson P, Préat V, Des Rieux A. A human intestinal M-cell-like model for investigating particle, antigen and microorganism translocation. Nat Protoc 2017;12:1387–99. https://doi.org/10.1038/nprot.2017.041.
42. des Rieux A, Fievez V, Théate I, Mast J, Préat V, Schneider YJ. An improved in vitro model of human intestinal follicle-associated epithelium to study nanoparticle transport by M cells. European Journal of Pharmaceutical Sciences 2007;30:380–91. https://doi.org/10.1016/J.EJPS.2006.12.006.
43. Gullberg E, Leonard M, Karlsson J, Hopkins AM, Brayden D, Baird AW, et al. Expression of specific markers and particle transport in a new human intestinal M-cell model. Biochem Biophys Res Commun 2000;279:808–13. https://doi.org/10.1006/bbrc.2000.4038.
44. Keita Å V, Alkaissi LY, Holm EB, Heil SDS, Chassaing B, Darfeuille-Michaud A, et al. Enhanced E. coli LF82 Translocation through the Follicle-associated Epithelium in Crohn's Disease is Dependent on Long Polar Fimbriae and CEACAM6 expression, and Increases Paracellular Permeability. J Crohns Colitis 2019;2020:216–29. https://doi.org/10.1093/ecco-jcc/jjz144.
45. Keita Å V., Gullberg E, Ericson AC, Salim SY, Wallon C, Kald A, et al. Characterization of antigen and bacterial transport in the follicle-associated epithelium of human ileum. Laboratory Investigation 2006;86:504–16. https://doi.org/10.1038/labinvest.3700397.
46. Velin ÅK, Ericson AC, Braaf Y, Wallon C, Söderholm JD. Increased antigen and bacterial uptake in follicle associated epithelium induced by chronic psychological stress in rats. Gut 2004;53:494–500. https://doi.org/10.1136/gut.2003.028506.

47. Radloff J, Falchuk EL, Markov AG, Amasheh S. Molecular characterization of barrier properties in follicle-associated epithelium of porcine Peyer's patches reveals major sealing function of claudin-4. Front Physiol 2017;8. https://doi.org/10.3389/fphys.2017.00579.
48. Perusko M, van Roest M, Stanic-Vucinic D, Simons PJ, Pieters RHH, Cirkovic Velickovic T, et al. Glycation of the Major Milk Allergen β-Lactoglobulin Changes Its Allergenicity by Alterations in Cellular Uptake and Degradation. Mol Nutr Food Res 2018;62. https://doi.org/10.1002/MNFR.201800341.
49. Jansen FAC, Rubert J, van Norren K, Fogliano V, Hoppenbrouwers T. Seeking standardized in vitro models of AGE-RAGE signaling in the physiological perspective of glycated dietary proteins. Int J Biol Macromol 2025;318. https://doi.org/10.1016/j.ijbiomac.2025.144889.

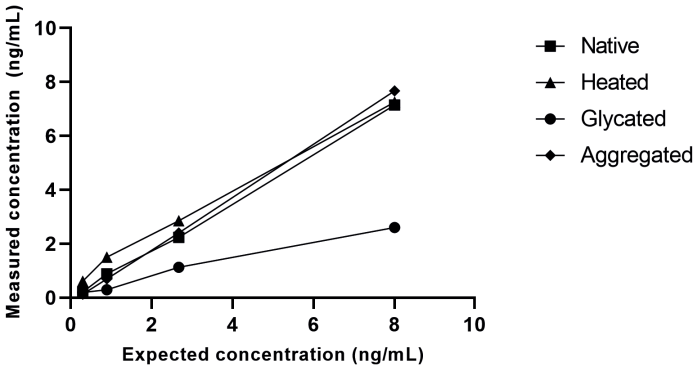
Supplementary materials



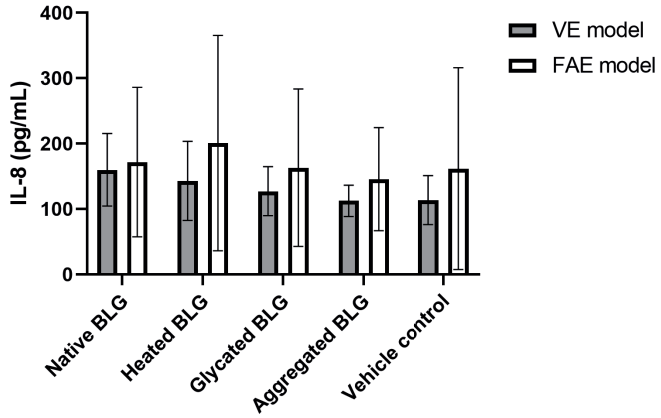
Supplementary Figure S3.1: Confocal overview image. Ileum ALI model was either differentiated with commercial medium (**A**; VE model) or with RANKL/TNFα-enriched commercial medium (**B**; FAE model). Blue dye – Nuclei (Hoechst); Green dye - Actin filaments (Phalloidin); Red dye – Microfold cells (GP2).



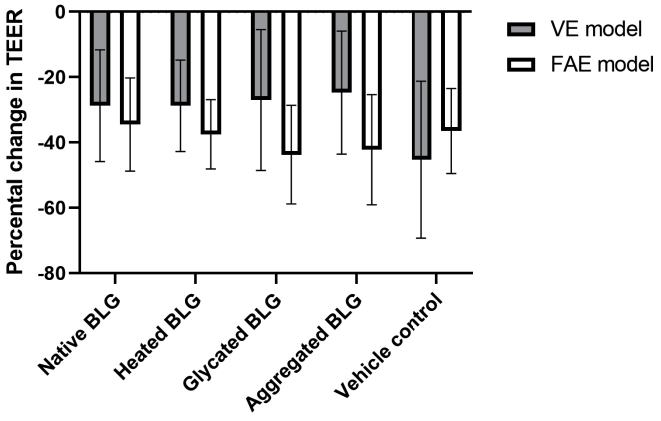
Supplementary Figure S3.2: Percental change in TEER between FITC-Dextrans and vehicle control, for the VE and FAE model. TEER values were measured at baseline and after the 4 h-lasting permeability assay. Data is mean values ± SD obtained from four independent experiments. Two-way repeated measure ANOVA did not show any significant effects for type of dextran or type of model, nor for their interaction ($p>0.05$).



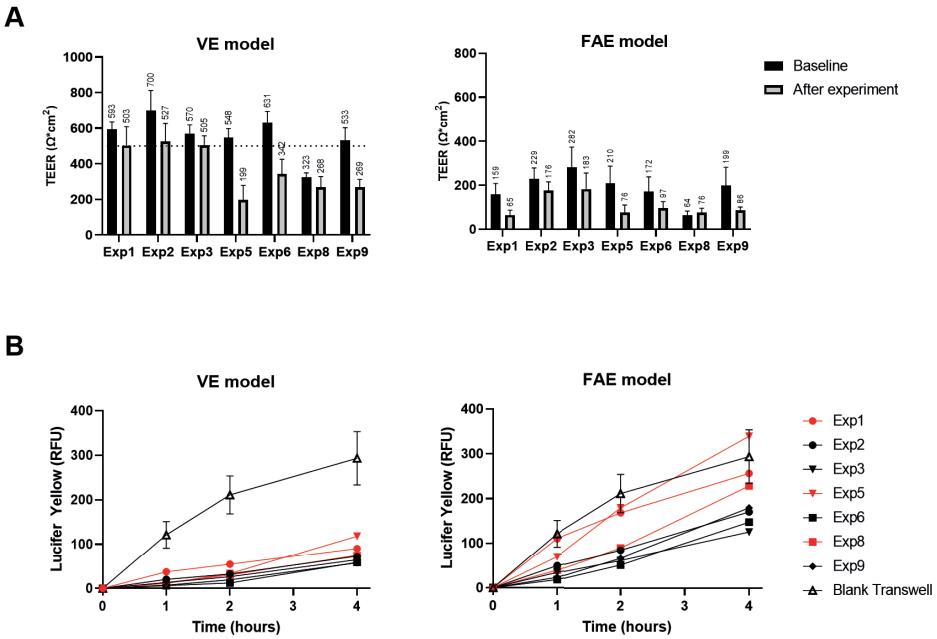
Supplementary Figure S3.3: BLG concentration measured by ELISA vs the expected BLG concentration based on DUMAS.



Supplementary Figure S3.4: Basolateral IL-8 concentration for the VE and FAE model being exposed apically to heat-modified BLGs and vehicle control. Data is mean values ± SD obtained from four independent experiments. Two-way repeated measure ANOVA did not show any significant effects for type of BLG or type of model, nor for their interaction ($p>0.05$).



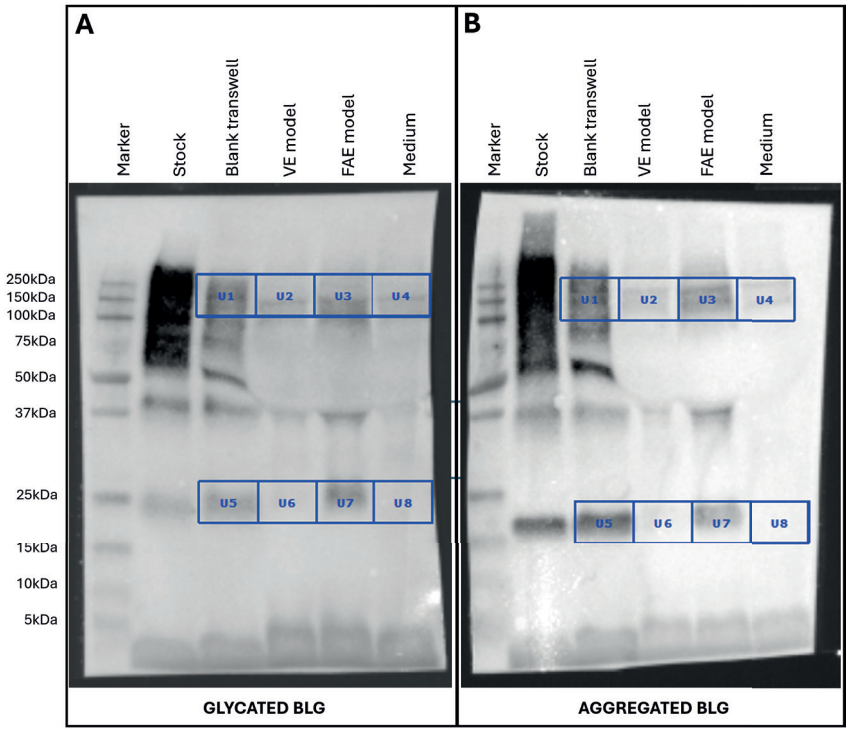
Supplementary Figure S3.5: Percental change in TEER between heat-modified BLGs and vehicle control, for the VE and FAE model. TEER values were measured at baseline and after the 4 h-lasting permeability assay. Data is mean values ± SD obtained from four independent experiments. Two-way repeated measure ANOVA did not show any significant effects for type of BLG or type of model, nor for their interaction ($p>0.05$).



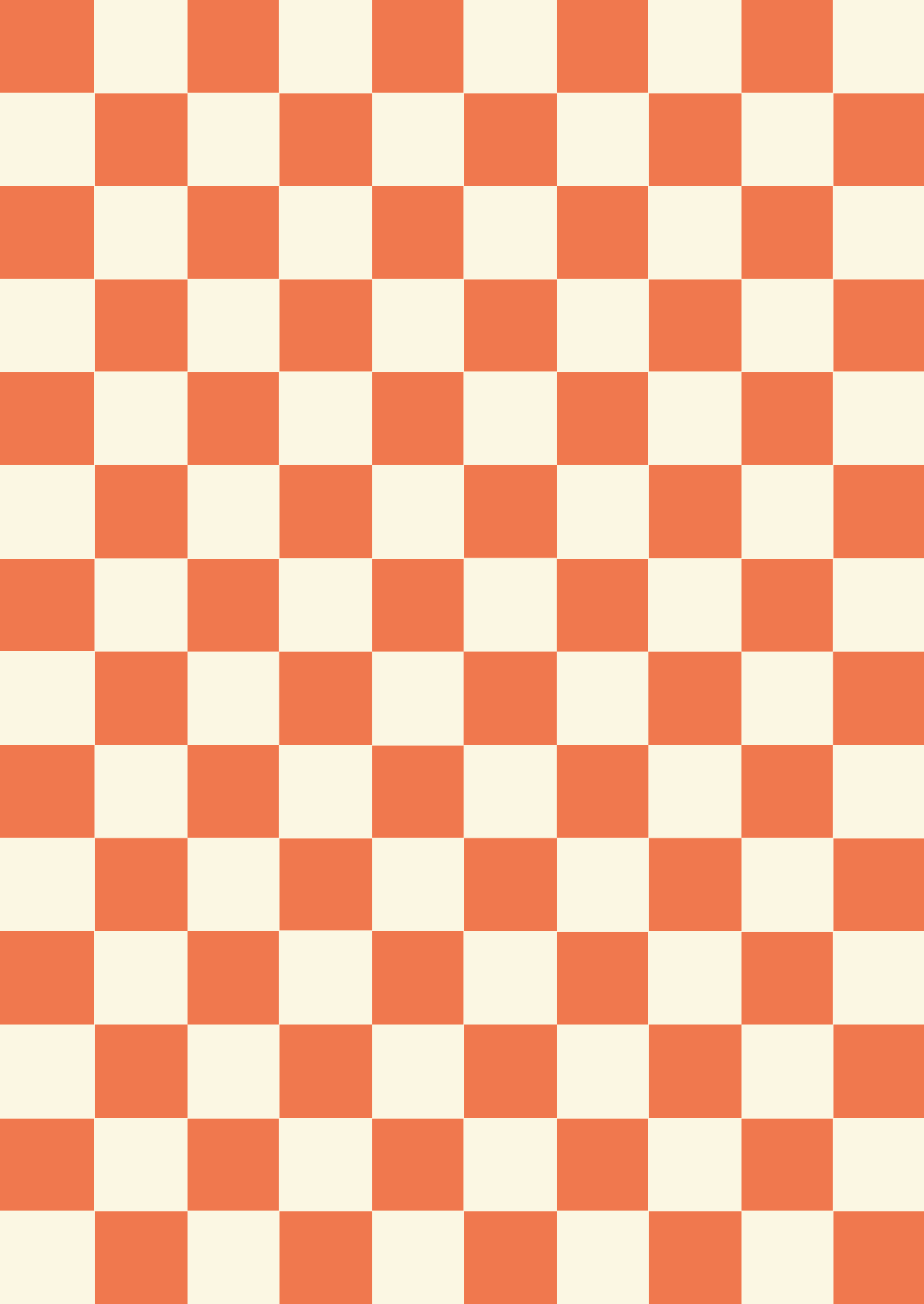
Supplementary Figure S3.6: TEER values (Ω*cm^2) **(A)** and lucifer yellow passage **(B)** in ileum ALI models during 4 h apical exposure. ALI model was either differentiated with commercial medium (VE model) or with RANKL/TNFα-enriched commercial medium (FAE model). Data are presented per experiment.

Supplementary Table S3.1: Fluorescence, absorbance, furosine, CEL, CML, intact lysine, and free amino group content of heat-modified beta-lactoglobulin (BLG). Native BLG was dry heated at 60°C (40% humidity) for 24 h without glucose (heated BLG) or with glucose (glycated BLG). Aggregated BLG was dry heated without glucose at 90°C (40% humidity) for 20 h. Fluorescence (in AU) was measured at 370/440 nm, while absorbance (in AU) was measured at 300 nm and corrected for background values at 600 nm. Furosine, CEL, CML and lysine were quantified with LC-MS/MS and expressed as µg/mg protein. Free amino group content were determined with an OPA assay and expressed relative to native BLG. Data is mean values ± SD obtained from technical duplicate.

	Fluorescence (370/440 nm)	Absorbance (300–600 nm)	LC-MS/MS (µg/mg protein)				Free amino group (relative to BLG)
			Furosine	CEL	CML	Intact lysine	
Native BLG	0.64±0.0001	69±5.9	0.6±0.008	<DL	<DL	74.0±1.3	1.0
Heated BLG	0.70±0.01	195±31.3	1.8±0.02	0.076±0.001	1.7±0.005	63.0±0.5	0.90±0.02
Glycated BLG	2.74±0.05	1159±35.1	33.4±0.48	0.84±0.003	3.0±0.007	33.1±1.2	0.14±0.01
Aggregated BLG	1.01±0.001	808±9.5	0.04±0.002	0.37±0.006	1.3±0.004	83.0±1.5	1.00±0.02



Supplementary Figure S3.7: Western blot detection and quantification of glycated **(A)** and aggregated **(B)** beta-lactoglobulin. Passage of beta-lactoglobulin in VE model (U2, U6) and FAE model (U3, U7) was determined for aggregates (U1–U4) and monomers (U5–U8) by volume intensity corrected for medium background (U4, U8) and calculated as percentage of blank transwell (U1, U5).



4

Seeking standardized *in vitro* models of AGE-RAGE signaling in the physiological perspective of glycated dietary proteins

Fleur A.C. Jansen [1] · Josep Rubert [1, 2] · Klaske van Norren [2] · Vincenzo Fogliano [1] · Tamara Hoppenbrouwers [1, 3]

1 Department of Food Quality and Design, Wageningen University & Research, Wageningen, The Netherlands
2 Nutritional Biology, Division of Human Nutrition, Wageningen University & Research, Wageningen, The Netherlands
3 Food and Biobased Research, Wageningen University & Research, Wageningen, The Netherlands

International Journal of Biological Macromolecules, 2025; 318: 144889

Abstract

Introduction: Advanced Glycation End products (AGEs) are covalent protein adducts formed through the Maillard reaction. High dietary intake might harm human health, however studies on their impact remain inconclusive. A proposed mechanism is that dietary AGEs trigger inflammation by interacting with the AGEs receptor (RAGE). However, *in vitro* studies on dietary AGE-RAGE signaling have reported inconsistent results, probably due to methodological issues. This study aimed to seek a standardized model of dietary AGE-RAGE signaling.

Methods: *In vitro* models were characterized for surface and total RAGE expression using flow cytometry. Both commercially available and in-house prepared dietary AGE preparations were analyzed for AGE levels, aggregation, and LPS content, then tested in the model with the highest surface RAGE expression.

Results: All immortalized cell lines expressed intracellular RAGE, while its surface expression was marginal or even absent. Only M-CSF-differentiated M0 macrophages showed significant surface RAGE expression. Some glycated dietary proteins induced inflammation in this model, but not all. While these proteins showed RAGE affinity in a chemical assay, the inflammatory response could not be reduced by the RAGE antagonist FPS-ZM1. Interestingly, co-incubation with the LPS scavenger PMB reduced inflammation despite negligible LPS levels in the sample.

Conclusion: These results challenge the hypothesis that dietary AGEs cause inflammation via RAGE activation, as glycated dietary proteins alone do not seem to induce acute inflammation. To better understand the biological activity of dietary AGEs, future studies should confirm surface RAGE expression, detail glycation methods and glycated protein characteristics, and account for LPS interference.

Introduction

Advanced Glycation End products (AGEs) are a heterogeneous group of covalent adducts and cross-linking structures in proteins formed by the Maillard Reaction. This reaction, also known as protein glycation, is a non-enzymatic process in which carbonyl groups of reducing sugars react with free amino groups of proteins, namely the side chain of lysine or arginine residues [1]. Since the Maillard Reaction happens non-enzymatically, it is driven by moderately high temperature, but the formation of AGEs also happens continuously on body proteins, although at low velocity. The concentration of AGEs in tissues such as articular collagen and the lens increases with age and was shown to be higher in diabetics [2–4]. This accumulation has been linked to many age-related non-communicable diseases, like cataract and cardiovascular diseases, and diabetes-related complications [1–3].

Multiple mechanisms have been described through which glycation contributes to such disease states. These mechanisms include for example the formation of protein crosslinks, inducing structural changes and possibly affecting protein functionality [1]. In addition, the interaction between AGEs and the AGEs receptor (RAGE) is often mentioned [5–7]. This receptor was first described three decades ago when researchers were searching for recognition sites for AGEs on the cell surface [8,9]. RAGE is a member of the immunoglobulin superfamily of cell surface molecules with a multiligand character [10]. This implies that not only AGEs but also other ligands, mainly damage-associated molecular patterns, can bind to the extracellular region of this transmembrane receptor. Especially the V-domain of the extracellular part of RAGE is involved in the recognition of these ligands. When the receptor gets activated by the binding of a ligand, its cytoplasmic tail initiates an intracellular signaling cascade leading to the production of pro-inflammatory cytokines. Multiple pathways are involved in this signaling cascade, with the NF-κB pathway playing a pivotal role [7]. These series of events starting with AGEs binding to RAGE and ending with the production of pro-inflammatory cytokines is often referred to as AGE-RAGE signaling [11–13].

According to some scholars, dietary AGEs can also trigger AGE-RAGE signaling and high intake of food rich in dietary AGEs would be harmful for human health. Human observational and intervention studies are however inconclusive and the most recent intervention trial failed to find any correlation between the intake of dietary AGEs and several health outcomes [14,15]. When comparing dietary AGEs to endogenous AGEs, a few structural differences can be stated [16], however the

main point is the bioactivity of glycated dietary proteins being affected by their digestion, absorption, distribution, metabolism and excretion. The majority of the dietary AGEs will be absorbed as single amino acids, di- or tripeptides, while a relatively large peptide backbone is required for AGEs to bind to RAGE [17,18]. Therefore, dietary AGE-RAGE interaction could only occur at the intestinal level, or with cells of the intestinal immune system if part of the undigested protein fraction is able to pass the epithelial layer through paracellular transport and/or transcytosis [19–21].

To explore the consequences of dietary AGE-RAGE interaction, *in vitro* models are a frequently used tool. Currently, mixed results have been reported in this regard. Some studies indeed attribute pro-inflammatory properties to dietary AGEs [22–24], whereas other studies show no effect [25,26]. In general, these studies are hard to compare since they did not only investigate different proteins and use different glycation methods, but also tested these glycated proteins in different *in vitro* models. The objective of this study was to seek a standardized *in vitro* model of dietary AGE-RAGE signaling, to enhance our understanding of the biological activity of glycated dietary proteins. We hypothesized that differences in RAGE expression between models and in LPS content between samples are factors to consider.

In this study, different *in vitro* models were characterized using flow cytometry for their surface and total RAGE expression. Inflammatory properties of both commercially available and in-house dietary AGEs preparations (characterized for AGE levels, aggregation, and LPS content) were tested in the model showing highest surface RAGE expression. A RAGE antagonist and an LPS scavenger were included to check the actual involvement of AGE-RAGE signaling when a specific dietary AGEs preparation showed pro-inflammatory properties.

Results

Various immortalized cell lines primarily express RAGE intracellularly

To verify and validate the presence of RAGE at the cell surface, as depicted in the AGE-RAGE signaling hypothesis, its expression was measured using flow cytometry in six immortalized human cell lines (HMC3, THP-1, hCMEC/D3, HBVP, Raji, and Caco-2), that were previously described to express RAGE. An antibody specific for the V-domain of RAGE (epitope mapped by the manufacturer) was used on intact cells to identify RAGE when present as a cell surface receptor. The same protocol

was used on fixated and permeabilized cells to also detect intracellular RAGE (total RAGE). Figure 4.1A shows that, for all cell lines, only a small percentage of cells, ranging from 1.0 to 10.4%, expressed RAGE on its surface. When considering total RAGE expression, this percentage clearly increased and varied from 71.1 to 99.3%. When looking at the fluorescent intensity emitted, i.e. the relative expression level of RAGE per cell, expressed as the median fluorescent intensity (MFI), a similar trend between surface vs. total RAGE was observed: low relative expression level of surface RAGE (62 to 1,362 RFU) compared to total RAGE (6,356 to 180,000 RFU) (Figure 4.1B). Therefore, these data show that RAGE was constitutively expressed intracellularly in immortalized cells while the surface expression only occurred marginally or was even absent.

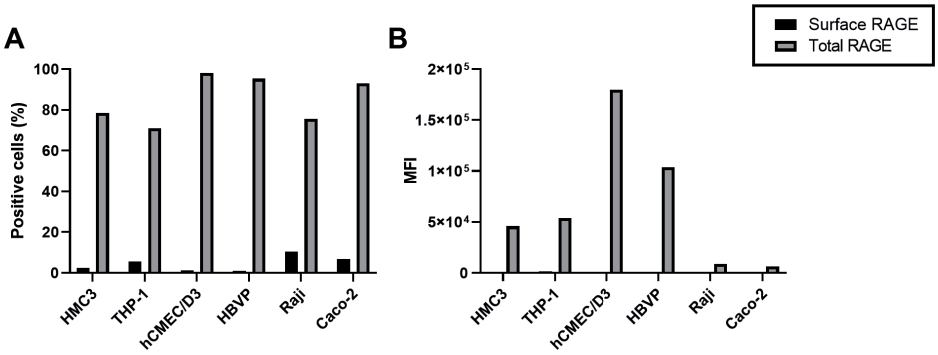


Figure 4.1: Percentage of positive cells **(A)** and median fluorescent intensity (MFI) **(B)** for RAGE measured on the cell surface (black bars) or in totality (grey bars) in different immortalized human cell lines: HMC3 (microglia), THP-1 (monocytes; differentiated to M0 macrophages), hCMEC/D3 (brain endothelial cells), HBVP (brain vascular pericytes), Raji (lymphoblasts) and Caco-2 (intestinal cells). Flow cytometry analysis was performed on cells being fixed and permeabilized to assess total RAGE expression, whereas fixation and permeabilization steps were not applied when assessing surface RAGE expression. All values are relevant to (%) or corrected for (MFI) the unstained control, which implies no staining with the primary RAGE antibody.

Primary monocytes differentiated with M-CSF show increased surface RAGE expression

Next, RAGE levels were determined on primary monocytes, GM-CSF differentiated M0 macrophages, and M-CSF differentiated M0 macrophages. The results are shown in the different panels of Figure 4.2. A substantial amount of primary monocytes was positive for total RAGE (79.3±21.8%), whereas monocytes expressing RAGE on their surface were more scarce (24.4±29.4%) (Figure 4.2A). Differentiation to macrophages did subsequently not affect the percentage of

cell positive for total RAGE (p=0.199), while M-CSF differentiation significantly enhanced the percentage of cells expressing RAGE on its surface (24.4±29.4% vs 68.2±16%, p=0.027). GM-CSF differentiation did not exert this effect (10.8±6.5% vs 24.4±29.4%, p=0.645). In terms of relative expression levels (Figure 4.2B), the enhancing effect of M-CSF differentiation was observed for both total (240% increase, p=0.012) and surface RAGE (1,118% increase, p=0.003). With GM-CSF

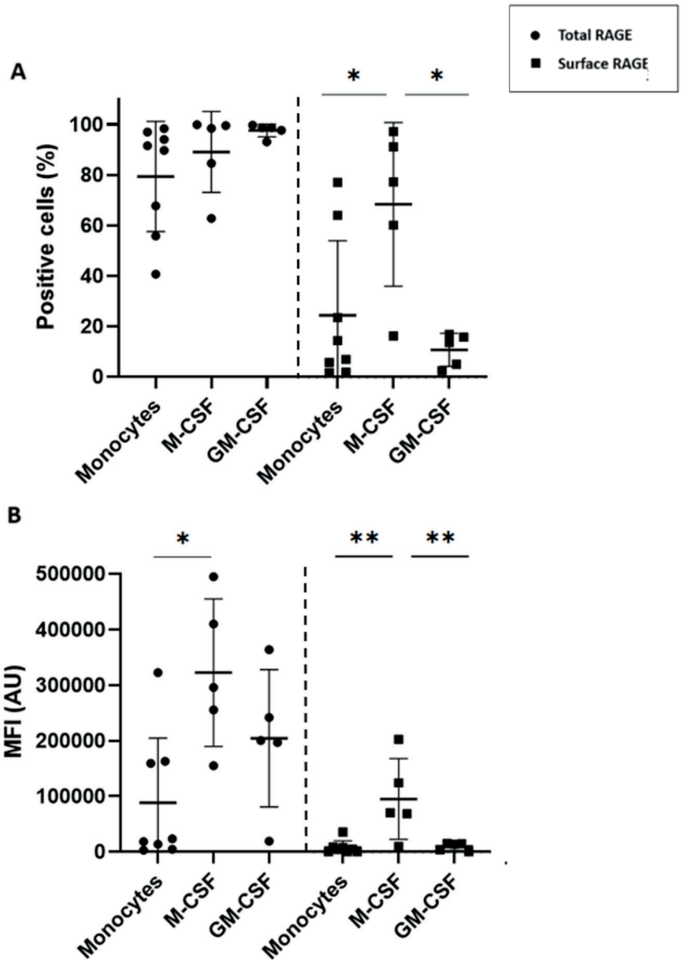


Figure 4.2: Percentage of positive cells **(A)** and median fluorescent intensity (MFI) **(B)** for RAGE in primary monocytes, M-CSF differentiated M0 macrophages, and GM-CSF differentiated M0 macrophages measured in totality (dots) and on the cell surface (squares). Flow cytometry analysis was performed on cells being fixed and permeabilized to assess total RAGE expression, whereas fixation and permeabilization steps were not applied when assessing surface RAGE expression. All values are relevant to (%) or corrected for (MFI) the unstained control, which implies no staining with the primary RAGE antibody. Values are depicted as mean±SD of biological replicates. P-values (*<0.05, **<0.01) are obtained by a multiple comparisons test (Tukey) following ANOVA.

differentiation, no significant changes in the relative expression levels of total or surface RAGE were observed (resp. p=0.254 and p=0.996). All in all, these data showed that primary monocytes express RAGE, but only sporadically on the cell's surface. With M-CSF differentiation, both the percentage of cells expressing surface RAGE as well as its relative expression level increased. This effect proved to be growth factor specific, since it was not observed for GM-CSF. Therefore, the M-CSF differentiated M0 macrophages can be considered a suitable *in vitro* model to study the function of RAGE as a multi-ligand cell surface receptor.

Prolonged heating of beta-lactoglobulin with glucose increases its glycation and aggregation levels

A common dietary protein, BLG, was heated with glucose for a prolonged time and characterized for glycation and aggregation levels before testing its inflammatory potential *in vitro*. This chemical characterization of the glycated BLG is reported in Figure 4.3. These data indicate that the intact lysine content of BLG dropped upon glycation in a time-dependent manner, reaching a maximum of

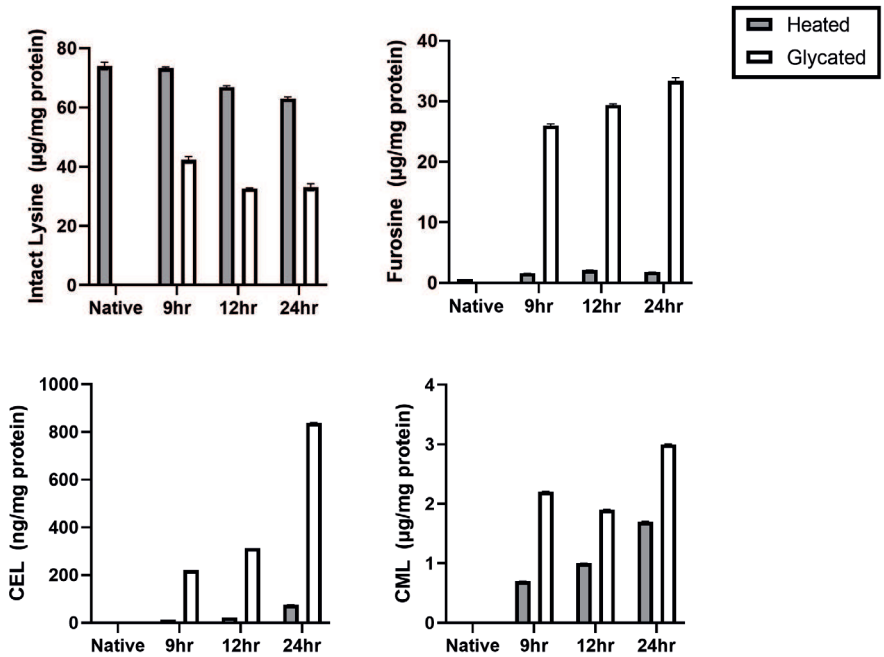


Figure 4.3: Levels of intact lysine, CEL, CML and furosine quantified by LC-MS/MS in beta-lactoglobulin (BLG). BLG was dry heated with glucose for 9, 12 or 24 h at 60°C and 40% humidity (glycated) and compared to non-heated BLG (native) and BLG dry heated at similar conditions but without glucose (heated). Data is mean values ± SD obtained from a technical duplicate.

about 50% after 12 hours. As expected, with the decrease in intact lysine content, the levels of Amadori products (glucosyl-lysine detected as furosine) and AGEs (CEL and CML) increased, as they are formed on lysine residues. Glycation increased furosine and CEL levels over time up to respectively 33.1 µg/mg protein and 838.1 ng/mg protein, compared to resp. 1.8 µg/mg protein and 75.8 ng/mg protein under similar heating conditions. For CML, this difference between heating and glycating conditions was less pronounced, but its level still increased by 45% upon glycation. This result indicates that a substantial amount of the available lysine in the glycated BLG used in the following biological experiments was modified due to the glycation. To quantify this level, based on the data of Figure 4.3, the furosine-to-lysine ratio of the glycated samples was determined to be 20–26%. This

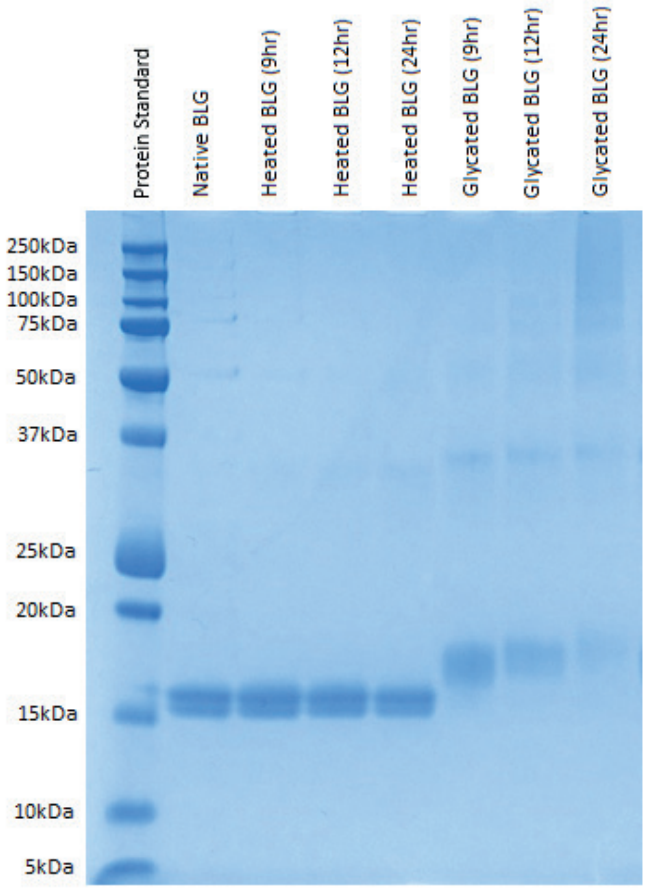


Figure 4.4: SDS-PAGE profile of Beta-Lactoglobulin (BLG). BLG was dry heated with glucose for 9, 12 or 24 h at 60°C and 40% humidity (glycated) and compared to non-heated BLG (native) and BLG dry heated at similar conditions but without glucose (heated).

suggests an estimate average of approximately 3–4 sugar molecules attached per molecule of BLG. The SDS-PAGE gel pattern in Figure 4.4 showing a slight increase in weight of the BLG monomer upon glycation also indicates the formation of AGEs. Furthermore, the number of high molecular weight structures increased over time, demonstrating the aggregation of BLG upon heating. In the presence of glucose, the formation of dimers and high molecular weight aggregates was more pronounced, indicating that glycation accelerates this aggregation process. This phenomenon was particularly evident after 24 hours of heating with glucose. Combined with the furosine-to-lysine ratio of this sample, results indicate a high degree of glycation.

High levels of glycation and aggregation in beta-lactoglobulin correspond to an increased affinity to sRAGE

Next, a competitive sRAGE ELISA was performed with these BLG preparations to investigate their affinity to the receptor in the context of AGE-RAGE signaling. Aβ-42, a well-known RAGE ligand, was used as a positive control for sRAGE binding. Figure 4.5 indicates that the native and all the heated BLG control samples had inhibition values below the detection limit (<25%), whereas the glycated BLG samples dose-dependently inhibited the binding of sRAGE to the plate. As expected, inhibition values increased with prolonged heating time. In combination with the results discussed above regarding the glycation level and aggregation pattern of these preparations (Figures 4.3 and 4.4), it can be argued that the higher the

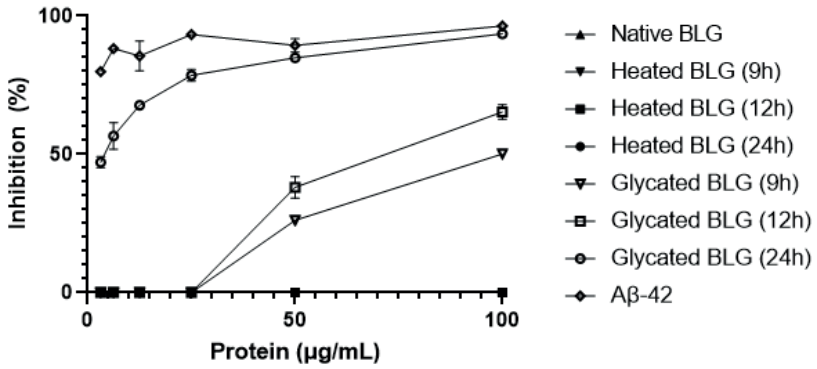


Figure 4.5: Inhibition ELISA for binding of Beta-Lactoglobulin (BLG) to sRAGE. BLG was dry heated with glucose for 9, 12 or 24 h at 60°C and 40% humidity (glycated), and compared to non-heated BLG (native) and BLG dry heated at similar conditions but without glucose (heated). Aβ-42 was included as positive control. All compounds were tested in duplicate as a two-times dilution series from 100 µg/mL to 3.125 µg/mL. Data is mean values±SD obtained from a technical duplicate.

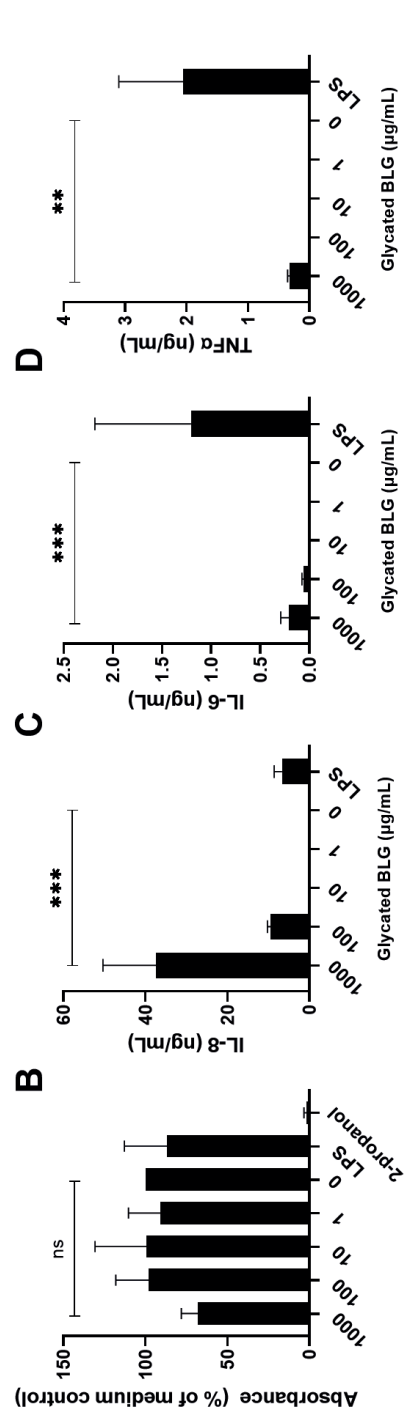


Figure 4.6: Cell viability of M-CSF differentiated M0 macrophages **(A)** and their IL-8 **(B)**, IL-6 **(C)** and TNFα **(D)** secretion upon exposure to glycated beta-lactoglobulin (BLG). BLG was dry heated with glucose for 24 h at 60°C and 40% humidity. Subsequently, M-CSF differentiated monocytes were exposed to this glycated protein for 24 h at 37°C (5% CO_2, saturated humidity) at concentrations ranging from 1,000 µg/mL to 1 µg/mL. LPS (100 ng/mL) was included as positive control. Data is mean values±SD obtained from independent experiments performed with three different donors. P-values (** <0.01, *** <0.001) are obtained by a multiple comparisons test (Tukey) following ANOVA.

modification level of BLG, the higher its affinity to sRAGE. Accordingly, the BLG preparation that was glycated for 24 hours was used in the *in vitro* experiments hereafter (Figures 4.6, 4.7 and 4.8) as it most closely resembled the sRAGE binding capacity of Aβ-42.

Glycated BLG acts pro-inflammatory on surface RAGE-expressing M-CSF differentiated macrophages

To investigate the activation of surface RAGE by dietary AGEs, M-CSF differentiated M0 macrophages were exposed for 24 h to our model sample, 24 h glycated BLG. Experimental data are reported in the different panels of Figure 4.6. Cell viability was not affected (Figure 4.6A, $p=0.287$), while the excretion of several pro-inflammatory cytokines increased in a concentration-dependent manner ($p<0.001$) (Figure 4.6B, C and D). For IL-8, the concentrations dose-dependently increased up to 37.5±13.0 ng/mL, when exposed to 1,000 µg/mL glycated BLG ($p<0.001$; compared to medium control). For IL-6 and TNFα, maximum concentrations of resp. 207.5±86.0 pg/mL and 320.2±38.6 pg/mL were detected (resp. $p<0.001$ and $p<0.01$; compared to medium control). Interestingly, although RAGE is not expressed on the surface of GM-CSF differentiated M0 macrophages, the glycated protein also induced a pro-inflammatory response in this *in vitro* model (data not shown). This suggests mechanisms other than surface RAGE activation being involved.

The RAGE antagonist FPS-ZM1 does not inhibit the inflammatory effect of glycated BLG

Subsequently, M-CSF differentiated M0 macrophages were pre-incubated with a RAGE antagonist to confirm the involvement of RAGE in the observed pro-inflammatory response. The inhibitor FPS-ZM1 did not affect cell viability or act pro-inflammatory at the concentrations used (Supplementary Figure S4.1). Data reported in Figure 4.7 showed that FPS-ZM1 could not block the inflammatory effect. Neither IL-6, IL-8, nor TNFα secretion was lowered when the cells were pre-incubated for 1 hour with this inhibitor (0–20 µM) prior to exposure to the glycated protein (200 µg/mL). Based on this data, surface RAGE does not seem to be involved in the observed pro-inflammatory response, despite the glycated BLG showing affinity to RAGE according to the competitive sRAGE ELISA (Figure 4.5).

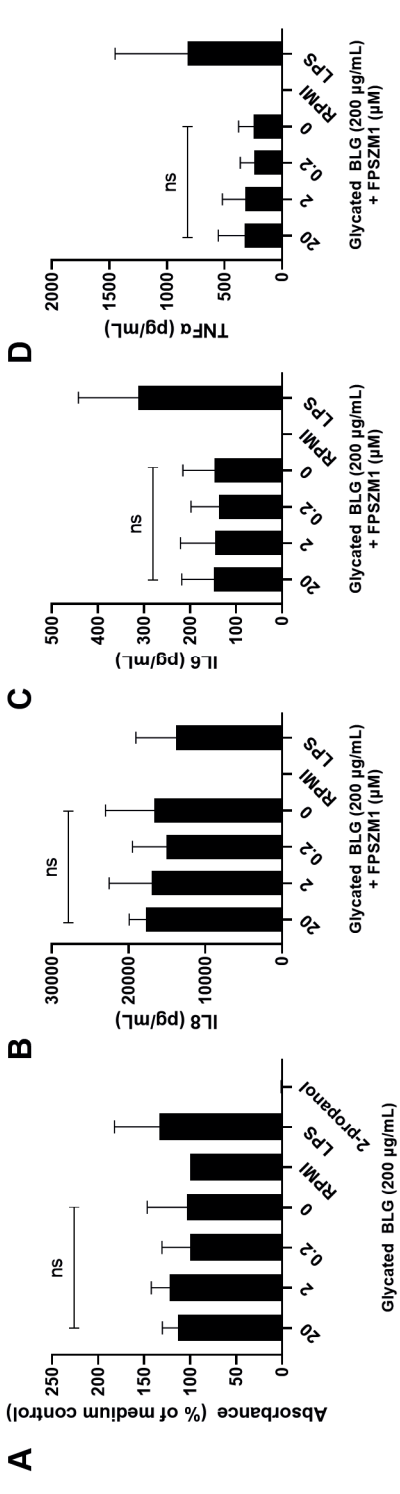


Figure 4.7: Cell viability of M-CSF differentiated M0 macrophages **(A)** and their IL-8 **(B)**, IL-6 **(C)** and TNFα **(D)** secretion upon exposure to glycated beta-lactoglobulin (BLG), after pre-incubation with different concentrations of RAGE inhibitor FPS-ZM1. BLG was dry heated with glucose for 24 h at 60°C and 40% humidity. Subsequently, M-CSF differentiated M0 macrophages were pre-exposed for 1 h to different concentrations of RAGE inhibitor FPS-ZM1 (0–20 µM) before being exposed to this glycated protein for 24 h at 37°C (5% CO_2, saturated humidity) at 200 µg/mL. LPS (1 ng/mL) was included as positive control. Data is mean values ± SD obtained from independent experiments performed with three different donors. P-values are obtained by a multiple comparisons test (Tukey) following ANOVA.

The pro-inflammatory effect of glycated BLG can be inhibited by LPS scavenging

To further explore the inflammatory response of the M-CSF differentiated M0 macrophages induced by the glycated BLG, PMB was added to scavenge potential LPS present in the sample. Supplementary Figure S4.2 indicates that PMB did not affect cell viability or act pro-inflammatory at the concentrations used, while Supplementary Figure S4.3 shows the strong capacity of PMB to block the pro-inflammatory activity of LPS in our cell model. LPS quantification of the sample showed a level of 0.11 EU/mg protein (=16.5 pg/mg protein), which would normally be considered neglectable, however both M-CSF and GM-CSF differentiated M0 macrophages are sensitive to these levels of LPS and respond to them in a pro-inflammatory fashion as shown in Supplementary Figure S4.4. In line with these observations, co-incubation with PMB dose-dependently lowered the pro-inflammatory response induced by glycated BLG in M-CSF differentiated M0 macrophages, as illustrated by the various panels of Figure 4.8. For IL-8 and IL-6, a maximal drop of respectively 60% and 85% was observed when glycated BLG (200 µg/mL) was co-incubated with 10 µg/mL PMB (resp. $p<0.001$ and $p<0.05$) (resp. Figure 4.8B and 4.8C). In the case of TNFα, the secreted levels dropped below the detection limit at this PMB concentration ($p<0.001$) (Figure 4.8D). Supplementary Figure S4.5 shows that the inflammatory response induced by glycated BLG in GM-CSF differentiated M0 macrophages could also be attenuated by PMB. In conclusion, the pro-inflammatory response observed in M0 macrophages was affected by traces of LPS present in the sample.

Cellular responses to commercial glycated proteins varies between manufacturers and batches

In addition to in-house glycated proteins, commercially available glycated proteins were used in many published studies [22,27–32]. Glycated BSA from two different companies (Sigma and Abcam) were characterized and tested on M-CSF differentiated M0 macrophages while being compared to an in-house preparation of glycated BSA. According to the manufacturer information, both preparations were glycated using glycolaldehyde. Data reported in Table 4.1 depicts that the Sigma preparation showed lower levels of glycation than the Abcam and our in-house preparation. In terms of fluorescence and absorbance, the Sigma sample showed values approximately 2.5-times higher than native BSA, which was used as reference sample. In comparison, the Abcam and our in-house glycated sample showed values 13.5- to 27-times higher, respectively.

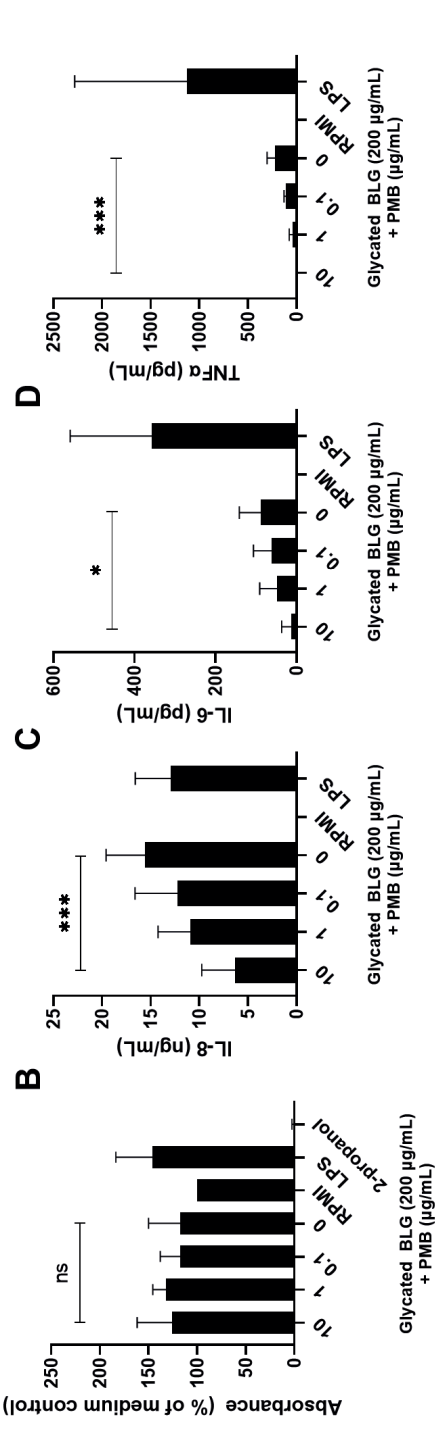


Figure 4.8: Cell viability of M-CSF differentiated M0 macrophages **(A)** and their IL-8 **(B)**, IL-6 **(C)** and TNFα **(D)** secretion upon exposure to glycated beta-lactoglobulin (BLG), co-incubated with different concentrations of polymyxin B (PMB). BLG was dry heated with glucose for 24 h at 60°C and 40% humidity. Subsequently, M-CSF differentiated M0 macrophages were exposed to this glycated protein at 200 µg/mL for 24 h at 37°C (5% CO_2, saturated humidity) co-incubated with different concentrations of LPS scavenger PMB (0–10 µg/mL). LPS (1 ng/mL) was included as positive control. Data is mean values ± SD obtained from independent experiments performed with three different donors. P-values (* <0.05, ***<0.001) are obtained by a multiple comparisons test (Tukey) following ANOVA.multiple comparisons test (Tukey) following ANOVA.

Table 4.1: Fluorescence, absorbance, furosine, CEL, CML, intact lysine, and free amino group content of glycolaldehyde-glycated BSA (10 mg/mL). Preparations were purchased from Abcam, Sigma, or made in-house (10 mg/mL BSA in PBS with 10mM glycolaldehyde for 24 h at 37°C). Native BSA was included as reference. Native BSA was included as reference. Fluorescence (in AU) was measured at 370/440 nm, while absorbance (in AU) was measured at 300 nm and corrected for background values at 600 nm. Furosine, CEL, CML and lysine were quantified with LC-MS/MS and expressed as µg/mg protein. Free amino group content were determined with an OPA assay and expressed relative to the BSA solution. Data is mean values±SD obtained from technical duplicate.

	Fluorescence (370/440 nm)	Absorbance (300–600 nm)	LC-MS/MS (µg/mg protein)				Free amino group content (relative to BSA)
			Furosine	CEL	CML	Intact lysine	
BSA	91±0.71	0.08±0.01	<DL	<DL	<DL	8.40±0.12	1.0
Sigma	244±0.07	0.22±0.001	0.46±0.004	<DL	1.43±0.08	8.10±0.04	0.9±0.01
Abcam	1,631±0.002	2.18±0.05	0.50±0.001	1.27±0.036	4.78±0.01	13.29±0.03	1.4±0.04
In-house	1,241±13.67	1.50±0.03	0.49±0.003	0.90±0.003	4.26±0.22	7.43±0.02	0.7±0.02

Looking at the concentration of single Maillard reaction products, the difference in glycation between the Sigma and the other two samples was most profoundly seen in the CEL and CML content. Next to these differences in the level of glycation, a surprising observation was made for the Abcam sample. This preparation showed higher values than the BSA reference for both the lysine and free amino acid content. This would imply that the protein level of this preparation exceeds the 10 mg/mL that is stated in the formulation. The SDS PAGE gel reported in Figure 4.9 showed a large amount of high molecular weight structures (>250 kDa) for the Abcam as well as for the Sigma preparation, indicating the presence of big aggregates in these solutions. Interestingly, as shown in Figure 4.10, despite these high molecular weight structures, only the in-house preparation showed affinity to sRAGE. When M-CSF differentiated M0 macrophages were exposed to these preparations, no

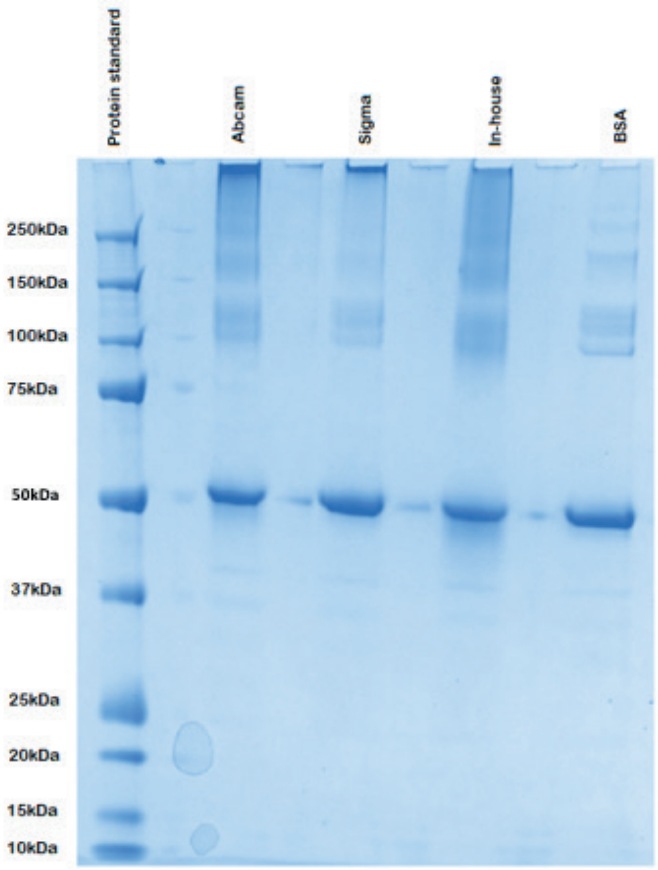


Figure 4.9: SDS-PAGE profile of glycolaldehyde-glycated BSA. Preparations were purchased from Abcam, Sigma, or made in-house (10 mg/mL BSA in PBS with 10 mM glycolaldehyde for 24 h at 37°C). Native BSA was included as reference.

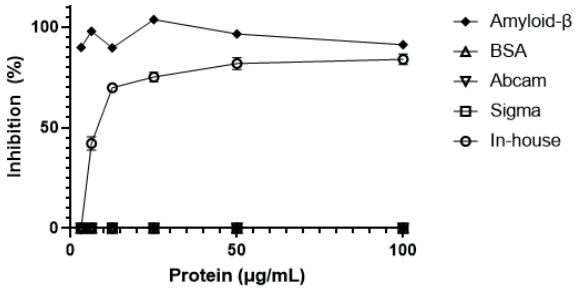


Figure 4.10: Inhibition ELISA for binding of glycolaldehyde-glycated BSA to sRAGE. Three different preparations were tested: one in-house preparations (10 mg/mL BSA in PBS with 10 mM glycolaldehyde for 24 h at 37°C) and two commercial preparations from Abcam and Sigma. Aβ-42 was included as positive control, and native BSA as reference. All compounds were tested in duplicate as a two-times dilution series from 100 µg/mL to 3.125 µg/mL. Data is mean values ± SD obtained from a technical duplicate.

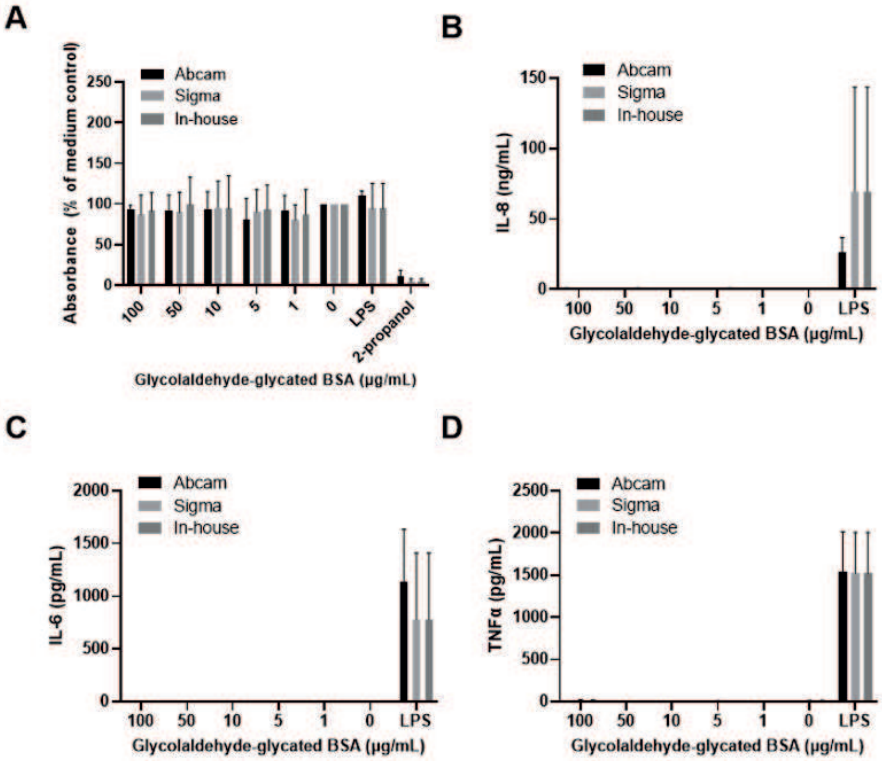


Figure 4.11: Cell viability **(A)** of M-CSF differentiated M0 macrophages and their IL-8 **(B)**, IL-6 **(C)** and TNFα **(D)** secretion upon exposure to different preparations of glycolaldehyde-glycated BSA. Preparations were purchased from Sigma and Abcam, and an in-house preparation was produced by heating 10 mg/mL BSA in PBS with 10 mM glycolaldehyde for 24 h at 37°C. M-CSF differentiated M0 macrophages were exposed to these preparations (100–0 µg/mL) for 24 h at 37°C (5% CO_2, saturated humidity). LPS (1 ng/mL) was included as positive control. Data is mean values ± SD obtained from independent experiments performed with three different donors. P-values are obtained by a multiple comparisons test (Tukey) following ANOVA.

pro-inflammatory effect was induced as shown by Figure 4.11. Interestingly, LPS levels measured in these samples were comparable to the levels measured in the in-house glycated BLG sample discussed before (Supplementary Table S4.1). All in all, glycolaldehyde-glycated BSA did not act pro-inflammatory in the applied model.

Discussion

The objective of this study was to seek a standardized *in vitro* model of dietary AGE-RAGE signaling, to enhance our understanding of the biological activity of glycated dietary proteins. Our data showed that there are three preliminary questions to answer when assessing the inflammatory potential of dietary AGEs *in vitro*:

1. Does the selected cell model express RAGE on the cell surface?
2. Is there solid evidence that LPS is not interfering with the measurements?
3. For both in-house produced and commercially prepared glycated protein samples: are they properly characterized?

RAGE was only expressed as cell surface receptor in specific *in vitro* models

According to the AGE-RAGE signaling hypothesis, RAGE is present on the cell surface as a multi-ligand transmembrane receptor. Although all cell lines and primary cells expressed RAGE in our study, it was mainly expressed intracellularly: the receptor was only expressed on the cell surface in marginal amounts, if not absent. We were able to obtain a model that substantially expressed surface RAGE only after differentiating primary monocytes into M0 macrophages with M-CSF. In the literature, many different *in vitro* models have been used to study the inflammatory properties of dietary AGEs. However, the RAGE expression in these models has not been measured [22–24] or only quantified at total RNA (qPCR) or protein (Western-Blot) levels [25,26]. When quantifying RAGE at total RNA or protein level, it is not possible to discriminate between transmembrane and intracellular receptors. Therefore, although positive results for RAGE expression were obtained, the expression of surface RAGE (as suggested in the AGE-RAGE hypothesis) could not be confirmed in these studies. Our data revealed robust total RAGE expression, thereby confirming the results of earlier studies, but showed minimal to no surface RAGE expression in the characterized models. This result underscores the importance of discriminating between both when validating *in vitro* models, as they might exert different physiological functions.

Intracellular RAGE could, for example, play a role in DNA repair. Papers published by Kumar et al. [33,34] describe that nuclear RAGE is part of an early DNA damage response and that deletion of nuclear RAGE leads to persistent double-strand break signaling, leading to senescence, tissue fibrosis, and oncogenesis. Kumar and others suggest nuclear RAGE is a master regulator of double-strand break [35]. Beside this function, it has been suggested that intracellular RAGE is only used for storage and is translocated to the cell surface upon pathological conditions [36]. This hypothesis is in line with the widespread function of RAGE as a multi-ligand transmembrane receptor activating NF-κB upon binding to AGEs and other RAGE ligands like Aβ-42. This hypothesis was tested in the current study, however not supported by the data. Possibly, surface RAGE has other, more complex functionalities than inducing an inflammatory response upon single ligand binding.

Our observation that only M-CSF, and not GM-CSF, differentiation-induced surface RAGE expression would suggest a potential anti-inflammatory role for surface RAGE, as M-CSF is used to drive macrophage polarization towards the resolving M2 phenotype while GM-CSF promotes the pro-inflammatory M1 phenotype. The observation of Liliensiek et al. [37] that healthy RAGE knockout mice have a slightly pro-inflammatory phenotype supports our suggestion that RAGE might also be involved in the regulation of anti-inflammatory responses. The Nrf2 signaling pathway, a major mechanism against oxidative stress, might be a target in this respect as Raupbach et al. [25] found pyrraline-modified casein activating this transcription factor in HCT116 cells. More in general, RAGE seems to play a role in the innate rather than the adaptive immune response, as RAGE knockout mice showed lower susceptibility to lethal sepsis while antibody subtypes and the titres did not differ compared to wildtype mice [37]. This reduction in mortality was linked to a decreased number of inflammatory cells adherent to the peritoneum instead of a reduced number of inflammatory cells or cytokine levels in the blood. Chavakis et al. [38] described similar findings, showing impaired leukocyte recruitment to the peritoneum in RAGE knockout mice. They suggested that RAGE interacting with the β2-integrin Mac-1 is required for leukocytes to adhere to the endothelium. Collectively, these data suggest that surface RAGE might play a role in (resolving) innate immune responses, immune cell recruitment, and immune cell tissue adhesion, rather than ligand-induced pro-inflammatory receptor signaling.

Important to note, this study focused on the hypothesis of glycated dietary proteins acting pro-inflammatory through receptor signaling. However, these proteins could also lead to cellular stress through other, RAGE-independent, mechanisms. For

example, when specific cell types like macrophages endocytose highly glycated proteins, ubiquitination of these foreign proteins might be hampered due to blockage of the lysine residues by the AGE-modifications. In the absence of ubiquitination, the proteins will not be marked for MHC-I antigen presentation and/or autophagic degradation. At high concentrations, this might lead to the accumulation of aggregates within the cell leading to cellular stress and cell apoptosis [39–41]. Based on the WST-1 results, cell apoptosis in our cell model upon the exposure to the glycated proteins was not observed. However, other glycation methods, longer incubation times and/or higher exposure concentrations might yield different results, so these mechanisms should also be considered when interpreting results in future studies.

RAGE antagonist could not reduce inflammation induced by glycated dietary proteins, while scavenging LPS reduced inflammation even with negligible LPS levels in the sample

Apart from an alternative function in immune cell recruitment and tissue adhesion, ligand-induced pro-inflammatory signaling by RAGE might also be dependent on the presence of co-stimulatory factors alongside its ligands. In our experiments, LPS scavenging drastically reduced the inflammatory response induced by glycated dietary proteins. In this context, LPS could be a confounding factor or play an active role in RAGE-mediated processes. The former is most straightforward as the RAGE antagonist FPS-ZM1 was not able to attenuate the inflammatory response, suggesting no involvement of surface RAGE in the observed effect. However, although this antagonist has been shown effective before in attenuating inflammatory responses *in vitro* [32,42], its effectiveness for inhibiting RAGE activation in the current cell model could not be confirmed due to lack of a positive control. Therefore the involvement of RAGE in the observed effect cannot be ruled out. Our observation that another frequently described RAGE ligand – Aβ-42 – did also not induce inflammation in our model (Supplementary Figure S4.6), despite RAGE affinity being shown by the sRAGE ELISA, reinforces the hypothesis that co-stimulatory factors might be necessary for effective RAGE activation by its described ligands. Since LPS-induced amplification of RAGE-mediated cellular responses has been described before [43,44], the possibility of LPS acting as such a co-stimulatory factor should be considered. To strengthen the conclusions of these studies, using a RAGE knockdown or knockout model would circumvent the possibility of non-effective or cross-reactive antagonists leading to false negative or false positive results, respectively.

Regardless of whether LPS acts as a confounding or co-stimulatory factor, our research stresses the importance of carefully examining it in *in vitro* studies investigating inflammatory processes. Often, *in vitro* studies report their sample being endotoxin free (<1.0 EU/mg protein) according to the manufacturer's or in-house LPS quantification measurements without further consideration. We showed that LPS can still have a significant effect, even though its quantity is below the current safety limits. Interestingly, samples with comparable LPS content did not exhibit the same inflammatory potency. For instance, in the glycated BSA preparations, higher LPS levels seem necessary to induce a pro-inflammatory response. LPS is known to interact with various biomolecules, including proteins, and these interactions can potentially vary depending on the protein of origin or its method of glycation. Such differences may influence the biological activity of LPS or interfere with its accurate quantification [44,45]. Relying solely on an endotoxin-free label or in-house LPS quantification assay to rule out LPS interference might therefore lead to misinterpretation of the results. Since LPS might amplify RAGE-mediated responses, using a LPS scavenger would be more appropriate for detecting LPS interference than a TLR4 inhibitor in this context. Such a scavenger has to be specific for the confounder of interest. In our case, PMB shows high specificity for LPS [46] while, to our knowledge, no data is available suggesting BLG or BSA being retained by PMB. All in all, when investigating the dietary AGE-RAGE signaling hypothesis *in vitro*, LPS interference should be closely monitored to ensure internal validity.

Characterization of in-house produced and commercially prepared glycated proteins

To compare and combine results from different studies, it is important to have a more in-depth characterization of the glycated dietary proteins tested. A few measures to consider are discussed below. Firstly, LC-MS/MS quantification of AGEs should be performed. This is the validated technique to quantify dietary AGEs and with this technique, databases for the AGE content of different foods have been developed to easily calculate AGE content in the diet for human observational and intervention studies [16]. Examples of such databases are the Glycation Database of Abertay University [47] and the AGE database of Maastricht University [48]. For *in vitro* studies, glycated proteins are not obtained directly from foods, but food proteins are being glycated in the lab with specific protocols after being isolated and purified. However, AGE quantification of these proteins is often not provided. In this study, the glycated proteins and their controls were

characterized for CML, CEL, and Furosine. Next to MG-H1, these dietary AGEs are most frequently analyzed as all of them are (derivatives) of (early-stage) non-crosslinking lysine-derived Maillard reaction products [47]. To obtain a more complete overview, it would be favorable to also quantify cross-linking AGEs like pentosidine, glucosepane, MOLD and GOLD [49]. However, currently these AGEs are not yet often quantified in foods [47]. Regarding this aspect, secondly, the aggregation pattern of the glycated proteins should be visualized with SDS-PAGE or any other adequate technique, since RAGE has been described to only bind AGEs when there are coupled to a relatively large peptide backbone, and high molecular weight structures would facilitate oligomerization of the receptor, which is a process involved in signal transduction [17,18,50]. When combining our SDS-PAGE with sRAGE ELISA results, it seems that the presence of high molecular weight structures alone does not predict the protein's affinity to RAGE, as the presence of high molecular weight structures in the glycated BSA preparations did not necessarily correlate with strong inhibition in the ELISA. For more in-depth understanding of this relationship, characterization of samples with a chemical assay like the sRAGE ELISA is not sufficient. In this case, cell-based assays (e.g. fluorescence resonance energy transfer) are preferred, since cellular processes like oligomerization could change the protein's affinity to RAGE [17]. Assessing the glycated protein's affinity to RAGE by a cell-based assay would therefore be our third recommendation for sample characterization in future studies. Lastly, based on our data, it is preferred to study in-house glycated proteins instead of commercial preparations as the purity of the commercial preparations could, in some cases, be questioned. In addition, although using commercially glycated proteins is considered a more standardized and reproducible practice, a full description of commercial glycation methods has not been published and the possibility of significant batch-to-batch variability cannot be excluded. In summary, when studying AGE-RAGE signaling *in vitro*, we suggest to prepare the glycated proteins in-house and subsequently determine its AGE content, aggregation pattern and RAGE affinity with the methods discussed above.

Conclusion

In conclusion, our data challenge the existing *in vitro* models used to study the hypothesis on dietary AGE-RAGE signaling. It shows that surface RAGE expression is limited to specific cell conditions and that the inflammatory response induced by the preparation of glycated protein is drastically reduced when LPS is scavenged. This challenges the hypothesis that dietary protein-bound AGEs act

pro-inflammatory through RAGE activation. Our data indicates that surface RAGE either has a role beyond facilitating ligand-induced cytokine release or requires a co-stimulatory factor for activation with dietary protein-bound AGEs. Therefore, to better understand the biological activity of dietary AGEs, we recommend future *in vitro* studies to show surface RAGE expression in their model, report thoroughly on glycation methods and glycated protein's characteristics, and closely monitor LPS interference in their experiments. *In vitro* studies lacking these rigorous methodological controls are likely to lead to conclusions that do not fully reflect the physiological relevance of dietary AGEs, thereby hampering the creation of scientific consensus.

Materials & methods

Materials

All stocks (e.g. for M-CSF and GM-CSF) were prepared and stored according to manufacturer instructions. The materials mentioned below are applicable to all protocols unless stated otherwise. From Merck Life Sciences (Darmstadt, Germany), Corning® 96-well microplates (#CLS3595), Corning® T75 cell culture flasks (#CLS430641U), Eppendorf® Safe-Lock 1.5 mL microcentrifuge tubes (#T9661), Dulbecco's Phosphate Buffered Saline (DPBS) without Ca^{2+} and Mg^{2+} (#D857), Bovine Serum Albumin (BSA) (#A3912), Dimethyl sulfoxide (DMSO) (#D2650), and Tween 20 (#P1379) were purchased. RPMI-1640-Glutamax medium (#72400-021), Penicillin-Streptomycin (P/S; 10,000 U/mL) (#15140122) and 0.25% Trypsin-EDTA (#25200072) were obtained from ThermoFisher Scientific (Waltham, MA, USA). From Sarstedt (Nümbrecht, Germany), 15 mL and 50 mL sterile screw cap tubes (resp. #62.554.502 and #62.547.254) were purchased. From Avantor/VWR (Radnor, PA, USA), Research Grade Foetal Bovine Serum (FBS) (#HYCLSV30160.03; South American Origin) was purchased which was heat inactivated by heating it for 45 min at 56°C. From Greiner Bio-One (Alphen aan den Rijn, The Netherlands), CELLSTAR 6-well and 12-well microplates (resp. #657160 and #665180) were purchased. UltraPure water was obtained with the Arium 611 VF Water Purifier (Sartorius, Utrecht, The Netherlands).

Culturing cell lines

Different immortalized cell lines were cultured at 37°C (5% CO_2 at saturating humidity) in T75 flasks and, for each cell type, $4.0*10^6$ cells were collected to quantify their RAGE expression by flow cytometry.

HMC3

HMC3 microglial cells (#CRL-3304; ATCC, Manassas, VA, USA) were cultured in DMEM, high glucose, GlutaMAX™ with 4.5 g/L D-Glucose and 110 mg/L sodium pyruvate (#10569010; ThermoFisher Scientific, Waltham, MA, USA), supplemented with 10% non-heat inactivated FBS (#30-2020; ATCC, Manassas, VA, USA) and 1% P/S. For subculturing, twice a week, cells were trypsinised with 2 mL 0.25% trypsin-EDTA for 5–10 min at 37°C until detachment and passaged in a 1:8–1:10 ratio. Passage numbers did not exceed passage 25.

THP-1

Monocytic THP-1 cells (#TIB-202; ATCC, Manassas, VA, USA) were cultured in RPMI-1640-Glutamax, supplemented with 10% FBS and 1% P/S. For subculturing, cells were inoculated at $5.0*10^5$ cells/mL twice a week (total volume 12–30 mL) up to passage 25. To differentiate THP-1 monocytes to M0 macrophages, cells were seeded at $1.0*10^6$ cells/mL in a 12-well plate (1 mL/well), with 100 ng/mL PMA (#P1585; Merck Life Sciences, Darmstadt, Germany) supplemented to the medium. At day 2 of culturing, cells were washed twice with pre-warmed medium and fresh medium was added (1 mL/well). After resting for 5 days, cells were collected by incubating with 0.25% trypsin-EDTA (0.4 ml/well) for 5–10 min at 37°C until detachment. Immediately thereafter, they were resuspended in culture medium to neutralize the trypsin.

hCMEC/D3

The brain microvascular endothelial cell line hCMEC/D3 (#SCC066; Merck Life Science, Darmstadt, Germany) was cultured in EBM-2 Endothelial Cell Growth Basal Medium-2 (#00190860; Lonza, Basel, Switzerland), supplemented with 5% FBS (#11560636; ThermoFisher Scientific, Waltham, MA, USA), 1% P/S, 1% Chemically Defined Lipid Concentrate (#11905031; ThermoFisher Scientific, Waltham, MA, USA), 10 mM HEPES (#15630080; ThermoFisher Scientific, Waltham, MA, USA), 5 µg/ml L-Ascorbic acid (#A4544; Merck Life Science, Darmstadt, Germany), 1.4 µM Hydrocortisone (#H0888; Merck Life Science, Darmstadt, Germany), and 1 ng/ml of basic fibroblast growth factor (#GF003; Merck Life Science, Darmstadt, Germany). The cells were grown in flasks precoated with rat tail collagen type I (#08-115; Merck Life Science, Darmstadt, Germany), diluted 1:20 in DPBS. The collagen solution was left for an hour to solidify at 37°C, and the excess collagen was removed before adding the cells. For subculturing, twice a week, cells were trypsinised with 2 mL 0.25% trypsin-EDTA for 5–10 min at 37°C until detachment and passaged in a 1:6 ratio. Passage numbers did not exceed passage 25.

HBVP

The Human Brain Vascular Pericytes cell line HBVP (#P10363-IM; Innoprot, Derio, Spain) were cultured in Pericyte medium (#P600121; Innoprot, Derio, Spain). This medium was purchased as a kit, including FBS, P/S, and pericyte growth supplement, which were all added according to manufacturer's protocol. For subculturing, twice a week, cells were trypsinised with 2 mL 0.05% trypsin-EDTA (#25300062; ThermoFisher Scientific, Waltham, MA, USA) for 5–10 min at 37°C until detachment and passaged in a 1:6 ratio. Passage numbers did not exceed passage 25.

Raji

The lymphoblast-like cell line Raji (#CCL-86; ATCC, Manassas, VA, USA) was cultured in RPMI-1640-Glutamax, supplemented with 10% FBS, 1% non-essential amino acids (#11140-035; ThermoFisher Scientific, Waltham, MA, USA), and 1% P/S. For maintenance, half of the medium was refreshed every other day and, up to passage 20, cells were subcultured by inoculating $4.0*10^5$ cells/mL when their density reached $3.0*10^6$ cells/mL (total volume 12–30 mL).

Caco-2

The enterocyte cell line Caco-2 (#CRL-2102; ATCC, Manassas, VA, USA) was cultured with DMEM, high glucose (#10569010; ThermoFisher Scientific, Waltham, MA, USA) supplemented with 10% FBS, 1% non-essential amino acids (#11140-035; ThermoFisher Scientific, Waltham, MA, USA), and 1% P/S. For subculturing, twice a week, cells were trypsinised with 2 mL 0.25% trypsin-EDTA for 5–10 min at 37°C until detachment and passaged in a 1:3–1:6 ratio. Cells were used between passage 45 and 55.

Monocyte isolation

Per donor, 50 mL buffycoat (#B2825R00; Sanquin, Nijmegen, The Netherlands) was mixed with 50 mL 2% FBS-DPBS (with Ca^{2+} and Mg^{2+}; #14040-091; ThermoFisher, Waltham, MA, USA), and equally divided over four 50 mL Leucosep tubes (#227290; Greiner Bio-One, Alphen aan den Rijn, The Netherlands). These Leucosep tubes were pre-treated with Ficoll® Reagent (#GE17-1440-03; Merck Life Sciences, Darmstadt, Germany), by adding 15 mL of this reagent to the tube and spinning it at room temperature (RT) for 30 sec at 1,000**g*. The tubes containing buffycoat were centrifuged at 4°C, first for 5 min at 200**g* followed by 15 min at 500**g* (slow brake). Subsequently, the upper plasma layer was removed and the cells were collected and washed by adding 2% FBS-DPBS and centrifuging at RT

for 10 min at 300*g (slow brake). After repeating the washing step, the cell pellet was resuspended in 2 mL of MACS buffer (2% FBS-DPBS (without Ca^{2+} and Mg^{2+}) with 2 mM EDTA (#E6758; Merck Life Sciences, Darmstadt, Germany)). To isolate monocytes, CD14 microbeads (#130-050-201; Miltenyi Biotec, Bergisch Gladbach, Germany) were added according to the manufacturer's protocol. After 15 min incubation at 4°C, 10 mL MACS buffer was added and the suspension was centrifuged at 4°C for 10 min at 300*g (slow brake). The cell pellet was resuspended in 500 µL MACS buffer and loaded onto a LS column with 30 µm pre-separation filter (#130-041-407; Miltenyi Biotec, Bergisch Gladbach, Germany) placed in a QuadroMACS™ separator (#130-090-976; Miltenyi Biotec, Bergisch Gladbach, Germany). The column was washed three times with 3 mL MACS buffer. Then, the column was removed from the MACS separator. MACS buffer (5 mL) was applied to the column and the magnetically labelled cells were immediately flushed out by firmly pushing a plunger into the column. After determining the cell concentration using the Corning® Cell Counter (#734-3259; Avantor/VWR, Radnor, PA, USA), the suspension was centrifuged at 4°C for 10 min at 300*g (slow brake). Until further use, these cells were stored in liquid nitrogen in FBS/10% DMSO.

Differentiation of monocyte to M0 macrophages

For cell culture, primary monocytes from liquid nitrogen were thawed at 37°C and the content was transferred to pre-warmed 9 mL RPMI-1640-Glutamax supplemented with 20% FBS and 1% P/S. The suspension was centrifuged at RT for 8 min at 300*g. The pellet was resuspended in culture medium (RPMI-1640-Glutamax supplemented with 10% FBS and 1% P/S). Next, for flow cytometry analysis of monocytes, cells were seeded at $5.0*10^5$ cells/mL in a 6-well plate (8 mL/well). After overnight resting (37°C, 5% CO_2 at saturating humidity), the monocytes were collected in a 15 mL tube by resuspending and scraping, and flow cytometry protocol was followed. For flow cytometry analysis of M0 macrophages, M-CSF or GM-CSF (resp. #216-MCC and #7954-GM; Bio-Techne, Minneapolis, MN, USA) was added to the culture medium to a final concentration of 50 ng/mL. Instead of overnight resting, cells were cultured for 7 days and, at day 3 and 5 of culturing, medium was refreshed containing new 50 ng/mL M-CSF or GM-CSF. At day 7, M0 cells were trypsinised with 0.25% trypsin-EDTA (2 ml/well) for 10 min (37°C, 5% CO_2 at saturating humidity) and collected by scraping. Immediately thereafter, they were resuspended in culture medium to neutralize the trypsin. Subsequently, the flow cytometry protocol was followed. To test the effects of glycated proteins on M0 macrophages, a similar culture protocol was followed, however cells were

seeded in a 96-well culture plate (200 µL/well). At day 7, supernatant was removed, whereafter experimental conditions were added (100 µL/well) and incubated for 24 h (37°C, 5% CO_2 at saturating humidity).

Flow cytometry protocol for RAGE detection

In order to detect RAGE, cells were centrifuged at RT for 3 min at 300**g* after collection. The pellet was resuspended in 4 mL DPBS and this cell suspension was divided over four 1.5 mL Eppendorf tubes, corresponding to an initial cell count of $1.0*10^6$ cells/Eppendorf. The centrifugation step was repeated and cells were stained with or without being fixed and permeabilized first. In case of fixation-and-permeabilization being applied, which was the case for half of the tubes, each pellet was reconstituted in 100 µL of fixation buffer (2% formaldehyde in DPBS) (made from Pierce™ 16% Formaldehyde (w/v); #28908; ThermoFisher Scientific, Waltham, MA, USA). After 15 min incubation at RT, cells were washed by adding 1 mL DPBS and centrifuging similar to previous steps. Each cell pellet was thereafter reconstituted in 100 µL permeabilization buffer (1% BSA-DPBS with 0.1% saponin) (#47036; Merck Life Sciences, Darmstadt, Germany). After 15 min incubation at RT, the cells were washed once more to finalize the fixation and permeabilization. Subsequently, all samples were reconstituted in 10 µL FcR Blocking Reagent (#130-059-901; Miltenyi Biotec, Bergisch Gladbach, Germany) and incubated for 10 min at 4°C in the dark. Afterwards, 90 µL RAGE polyclonal antibody (1:50 dilution in DPBS; validated for the epitope being on the V-domain of RAGE) (#PA5-24787; ThermoFisher, Waltham, MA, USA) was added a permeabilized and a non-permeabilized sample. To the other two samples, 90 µL DPBS was added which served as negative control to help differentiate non-specific background signal from specific antibody signal. Samples were incubated for 30 min at 4°C in the dark. After washing, all samples were reconstituted in 100 µL Alexa Fluor 647 Goat Anti-Rabbit IgG recombinant antibody (1:200 dilution in DPBS) (#A27040; ThermoFisher, Waltham, MA, USA). After incubating for 30 min at 4°C in the dark, cells were washed and reconstituted in 100 µL DPBS to be analysed on the CytoFLEX Flow Cytometer (Beckman Coulter, Fullerton, CA, USA). For each sample, 10,000 cells were measured at a speed of 10 µL/min. Data was analysed in CytExpert Software (Beckman Coulter, Fullerton, CA, USA). First, debris was excluded based on SSC-A vs FSC-A gating, whereafter doublets were excluded by FSC-H vs FSC-A and SSC-H vs SSC-A gating. Based on this gating strategy, percentage of positive cells and median fluorescent intensity (MFI) (APC channel) were determined. The former parameter is defined as the percentage of positive

cells in the sample of interest relative to 1% positive cells in the corresponding negative control sample (stained without primary antibody), whereas the latter is defined as the MFI of the sample of interest corrected by subtraction for the MFI of the corresponding negative control sample.

Protein glycation

Beta-Lactoglobulin (BLG) (#L0130; Merck Life Sciences, Darmstadt, Germany) was dissolved to 10 mg/mL in DPBS with or without 16 mM D-glucose (#G7021; Merck Life Sciences, Darmstadt, Germany). These solutions were lyophilized in aliquots of 500 µL in 5.0 mL Sterile Eppendorf® tubes (#525-0982; Avantor/VWR, Radnor, PA, USA). Apart from the native protein control, these lyophilized aliquots were heated in a Memmert Environmental Chamber (#10861-384; Avantor/VWR, Radnor, PA, USA) at 60°C and 40% humidity for 9 h, 12 h, and 24 h, to approach temperatures reached during food processing without denaturating BLG. Afterwards, they were redissolved in 500 µL DPBS. Glycated BSA samples were purchased from Sigma (#121800-M) and Abcam (#Ab51995), or prepared in-house. BSA (#A7030; Merck Life Sciences, Darmstadt, Germany) was dissolved to 10 mg/mL in DPBS with 10 mM glycolaldehyde (#G6805; Merck Life Sciences, Darmstadt, Germany). 1 mL aliquots were heated in 1.5 mL Eppendorf tubes in a heating block at 37°C for 24 h. Residual glucose and glycolaldehyde were removed by 10 kDa MWCO, Amicon™ Filter (#UFC9010; Merck Life Sciences, Darmstadt, Germany) according to manufacturer protocol. For each sample, final protein concentration was determined by DUMAS, to be able to account for potential losses. The conversion factor of 6.38 was applied. Samples were stored at -20°C.

Characterization

Glycated samples and their controls were characterized in terms of absorbance, fluorescence, AGE levels, free amino group content, LPS levels, aggregation pattern and sRAGE binding capacity.

Absorbance and fluorescence

Samples (10 mg/mL) were analyzed in duplicate for absorbance and fluorescence in resp. transparent and black 96-well plates (100 µL/well). Fluorescence was measured at λexc 370 nm and λem 440 nm, while absorbance was measured at 300 and 600 nm using a Spectramax® M2.

Free amino group content by OPA

To perform an Phthaldialdehyde (OPA) assay, OPA solution was made by dissolving 3.81 g sodium tetraborate (#1.06308; Merck Life Sciences, Darmstadt, Germany), 88 mg dithiothreitol (#D0632; Merck Life Sciences, Darmstadt, Germany), and 100 mg sodium dodecyl sulphate (#8.22050; Merck Life Sciences, Darmstadt, Germany) in 97 mL UltraPure water at 35–40°C, and subsequently adding a 3 mL ethanol mixture of 80 mg OPA (#1.11452; Merck Life Sciences, Darmstadt, Germany). The OPA solution was kept in the dark and used within 2 h. For the analysis, 10 µL of the glycated samples (10 mg/mL) together with 200 µL of the OPA solution were added to a transparent 96-well plate. For the blank, 10 µL UltraPure water was added to the OPA solution. The plate was incubated for 15 min at RT in the dark, and absorbance was measured at 340 nm. All analysis were performed in duplicate and free amino group content was determined using a six-point two-times serial dilution curve of L-Leucine (2,000 µg/mL) (#L8000; Merck Life Sciences, Darmstadt, Germany) and presented relative to the free amino group content of the untreated (native) sample.

AGE levels (intact Lysine, CML, CEL and furosine) by LC-MS/MS

Protein samples were diluted to 8 mg/mL in DPBS and 50 µL was added to 1 mL 6M HCl in a glass heating tube. The headspace of these tubes was saturated with nitrogen before closing them off with a cap. Tubes were heated at 110°C on a heating block for 22 h. After heating, 400 µL was transferred to a MS vial (#AR0-3921-13; Phenomenex, Woerden, The Netherlands) and dried with a vacuum concentrator (#RVC 2-33 CDplus; CHRIST, Osterode am Harz, Germany) set at 4.5 mbar (2 h, 30°C). Samples were reconstituted in 500 µL UltraPure water and purified by solid phase extraction. In this respect, Oasis HLB 1 cc cartridges (#WAT094225; Waters, Etten-Leur, The Netherlands) were activated by loading and running 1 mL methanol (#0013684101BS; Biosolve, Valkenswaard, The Netherlands) succeeded by 1 mL 10 mM nonafluoropentanoic acid (NFPA) (#396575; Merck Life Sciences, Darmstadt, Germany) in Ultrapure water, before loading the samples. Thereafter, the columns were washed with 1 mL 10 mM NFPA/MeOH (95:5, v/v) and analytes were eluted by running 1 mL 10 mM NFPA/MeOH (1:1, v/v). These eluents were dried in MS vials with a vacuum concentrator set at 4.5 mbar (2 h, 30°C) and reconstituted in 200 µL ultrapure water/acetonitrile (#0001204101BS; Biosolve, Valkenswaard, The Netherlands) (1:1, v/v) containing an internal standard mixture (0.5 ppm) consisting of L-Lysine-4,4,5,5-d4 hydrochloride (#616192; Merck Life Sciences, Darmstadt, Germany), CML-d4 (#HAA2952; Iris Biotech, Marktred-

witz, Germany), CEL-d4 (#HAA2941; Iris Biotech, Marktredwitz, Germany), and Furosine-d4 (#HAA2961; Iris Biotech, Marktredwitz, Germany). The calibration curve for the analysis was a 12-point 3-times serial dilution (2ppm-11.3ppt) of L-Lysine hydrochloride (#4400-M; Merck Life Sciences, Darmstadt, Germany), CML (#HAA2950; Iris Biotech, Marktredwitz, Germany), CEL (#HAA2940; Iris Biotech, Marktredwitz, Germany), and Furosine (#HAA2960; Iris Biotech, Marktredwitz, Germany) in ultrapure water/acetonitrile (1:1, v/v) containing the abovementioned internal standard mixture (0.5 ppm). All samples and calibration solutions were stored at -20°C for maximal one week before LC-MS/MS analysis.

Sample analysis was carried with a Nexera UPLC system (Shimadzu Corporation, Kyoto, Japan) coupled with a LCMS-8050 triple quadrupole mass spectrometer (Shimadzu Corporation, Kyoto, Japan). The UPLC unit consisted of a SIL-30AC autosampler, a LC-20ADXR solvent delivery module, DGU-20ASR degassing unit, a CTO-20AC column oven and an FCV-20AH2 valve unit. The samples (5 µL) were injected on a Kinetex HILIC 2.6 µm, 2.1 mm × 100 mm (Phenomenex B.V., Torrance, CA, USA). The flow rate was set at 0.4 mL/min and the column temperature at 30°C. The mobile phases consisted of 0.1% formic acid (solvent A), acetonitrile with 0.1% formic acid (solvent B) and 50 mmol/L ammonium formate (solvent C) with the following elution profile (t in [min]/[%B]/[%C]): (0/80/10), (0.8/80/10), (3.5/40/10), (6.5/40/10), (8.0/80/10) and (10.0/80/10). MS data was collected for 10 min. Positive ionisation mode was used for all MS analyses. The voltage of the turbo ion-spray ionization was 4.0 kV. The temperature of the electrospray ionization probe, desolvation line, and heat block were set at 300°C, 250°C, and 400°C, respectively. The pressure of the collision-induced dissociation gas was 4 kPa whereas the flow rates of the drying gas, nebulizer gas, and heating gas were set at 10 mL/min, 3 mL/min, and 10 mL/min, respectively. The electrode voltage of Q1 pre bias (collision cell energy entrance potential), collision cell Q2 (collision energy), Q3 pre bias (collision cell energy exit potential), parent and fragment ion m/z of the multiple reaction monitoring transitions were optimized using the support software (LabSolutions, Shimadzu Corporation, Kyoto, Japan). For single reaction monitoring (SRM), the dwell time was set at 32 msec and the most abundant fragment ion was selected for quantitation. The second and third fragments in ion yield were selected as structural confirmation based on the optimized SRM transition (Supplementary Table S4.2).

Analytical data was processed with LabSolutions software (Shimadzu Corporation, Kyoto, Japan). For all samples and calibration solutions, the integrated peak

area of each analyte was divided by the corresponding integrated peak area of the deuterated standard to correct for matrix effects. Analyte content in the samples was quantified by interpolating these corrected integrated peak area from the calibration curve. The limit of detection was defined as the concentration corresponding to the smallest corrected integrated peak area included in the calibration curve (based on the deviation of the slope), which was 0.3 ppb for all analytes corresponding to 0.4 ng/mg protein. Analyte contents are presented as per the amount of protein. As a quality control measure, an additional native BLG sample was spiked with the internal standards (0.5 ppm) prior to SPE and recovery values were calculated:

$$\frac{\text{measured concentration} - \text{theoretical concentration}}{\text{theoretical concentration}} * 100\%.$$

For all analytes, this values was within the acceptable limit of ±20%.

LPS levels by LAL assay

LPS concentrations were determined for the glycated proteins tested in cell culture experiments, using the Pierce LAL Chromogenic Endotoxin Quantitation Kit (A39552; ThermoFisher, Waltham, MA, USA). The test kit was used according to the manufacturer's instructions. To ensure a sterile environment devoid of lipopolysaccharides, LPS-free water, pipette tips, and tubes were employed for the experiment. Additionally, the spatulas were washed with 1 M NaOH before weighing any compounds to mitigate the risk of LPS contamination.

Aggregation pattern by SDS page

6 µL of NuPAGE™ LDS sample buffer (#NP0007; ThermoFisher, Waltham, MA, USA) was added to 1 µg protein and brought to a final volume of 24 µL with deionized water. This mixture was heated for 10 min at 70°C and afterwards, samples were loaded on a NuPAGE™ 12% BisTris 1.0 mm 10-well Gel (#NP0341, ThermoFisher Scientific, Waltham, MA, USA) (18 µL/well; 1.5 µg protein/well). As a reference, 5 µL of a prestained protein standard (#1610377; Bio-Rad, Hercules, CA, USA) was loaded. This gel was run with NuPAGE™ MOPS Running Buffer (#NP0001; ThermoFisher, Waltham, MA, USA) at 120 V in a XCell SureLock™ Mini-Cell (#EI0001; ThermoFisher Scientific, Waltham, MA, USA) until, after approximately 90 min, the dye front reached the bottom of the gel. The gel was washed with deionized water 4 times for 5 min to remove SDS present in the gel before covering the gel with PageBlue™ Protein Staining Solution (#24620; ThermoFisher Scientific, Waltham,

MA, USA) and staining it for 1 h at RT on a shaker. Then, the gel was washed with deionized water 2 times for 5 min before washing it in overnight in deionized water. After overnight washing, gel was put on a white light conversion screen (#1708289; Bio-Rad, Hercules, CA, USA) and picture was taken with ChemiDoc MP machine (Bio-Rad, Hercules, CA, USA) using the Coomassie Blue staining setting.

sRAGE binding capacity by sRAGE ELISA

A Nunc™ Maxisorp™ 96 well plate (#44-2404; ThermoFisher, Waltham, MA, USA) was coated with 40 µg/mL glycated soy extract [51] in 1.5 mM sodium carbonate buffer (6.8 g/L Na_2CO_3 and 11.4 g/L $NaHCO_3$ in UltraPure water, pH 9.6), 80 µL/well, and incubated overnight at 4°C in the dark. Next, the plate was washed three times with 0.05% (v/v) Tween 20-PBS (0.24 g/L KH_2PO_4, 1.78 g/L $Na_2HPO_4 \cdot 2H_2O$, 0.2 g/L KCL, and 8 g/L NaCl in UltraPure Water, pH 7.4), 200 µL/well, and incubated with 3% BSA-PBS (#BSAV-RO (Fraction V); Merck Life Sciences, Darmstadt, Germany), 150 µL/well, for 1 h at RT. Meanwhile, protein samples and amyloid beta 1-42 (Aβ-42) (#HB9805; Hello Bio, Dunshaughlin, Ireland) were 2-times serial diluted (100–3.125 µg/mL) in dilution buffer (1.5% BSA-PBS with 0.0125% Tween 20) with 0.5 µg/mL sRAGE (#RD172116100; BioVendor R&D, Brno, Czech Republic) in a 450 µL Nunc™ Polystyrene dilution plate (200 µL/well final volume) (#267245; ThermoFisher Scientific, Waltham, MA, USA) and incubated for 45 min at 37°C on a shaker. In addition to the protein samples, dilution buffer with and without 0.5 µg/mL sRAGE were included as controls. After incubation, the Maxisorp plate was washed three times, and samples plus controls from the dilution plate were added in duplicate to this Maxisorp plate (80 µL/well). After 1 h incubation at 37°C on a shaker, the plate was washed five times before adding 80 µL/well primary RAGE antibody (#MAB11451; Bio-Techne, Minneapolis, MN, USA) (0.5 µg/mL in dilution buffer). Plate was incubated for 30 min at RT on a shaker and afterwards washed 5 times before adding 80 µL/well Goat Anti-Mouse antibody-HRP (P0447; Agilent, Santa Clara, CA, USA) (1:1,000 in dilution buffer). Plate was incubated for 30 min at RT on a shaker and then washed 4 times before adding 80 µL/well TMB solution (#T4444; Merck Life Sciences, Darmstadt, Germany). After 10 min incubation at RT in the dark, 100 µL/well 2M H_2SO_4 was added. Absorbance was measured at 450 and 540 nm with Spectramax® M2. For the data analysis, OD values of 540 nm were subtracted from OD values of 450 nm and these OD values were averaged for each duplicate. Percentage of Inhibition, as a measure for RAGE binding affinity, was calculated by applying the following formula:

$$\frac{\text{ODdilution buffer with sRAGE} - (\text{ODsample} - \text{ODdilution buffer without sRAGE})}{\text{ODdilution buffer with sRAGE}} * 100\%.$$

The limit of quantification was considered 25%.

Cell culture experiments

To test the inflammatory properties of glycated proteins, M0 macrophages were exposed to a concentration range of 24 hour glucose-glycated BLG (1,000, 100, 10, and 1 µg/mL) and glycolaldehyde-glycated BSA (100, 50, 10, 5, and 1 µg/mL). These preparations were either produced in-house or purchased, as described in the section 'Protein Glycation'. Culture medium and 1 ng/mL LPS (#L3137; Merck Life Sciences, Darmstadt, Germany) served as negative and positive controls, respectively. When preparations showed a pro-inflammatory response, the cells were pre-incubated with different concentrations of FPSZM1 (#6237; Bio-Techne, Minneapolis, MN, USA) (20, 2, 0.2 µM) for 1 h before adding glycated BLG or BSA (resp. 200 and 10 µg/mL). In addition, glycated BLG and BSA were co-incubated with different concentrations of Polymyxin B (PMB) (10, 1, 0.1 µg/mL) (#P4932; Merck Life Sciences, Darmstadt, Germany). In all cases, after 24 h of exposure, a WST-1 assay was performed on the cells and the supernatant was collected and stored at -20°C for further cytokine analysis.

WST-1 assay

Cell proliferation was determined using a WST-1 assay. Briefly, 110 µL/well WST-1 mixture was added to the cells. This mixture consisted of WST-1 reagent (#CELLPRO-RO; Merck Life Sciences, Darmstadt, Germany) added to the culture medium (final dilution 1:10). As a positive control, cells were pre-exposed for 10 seconds to 10 µL 70% 2-propanol (#8167045000; Actu-All Chemicals, Oss, The Netherlands). Cells were incubated with the mixture for 90 min at 37°C (5% CO_2 at saturating humidity), before absorbance was measured at 450 and 540 nm with a Spectramax® M2 (Molecular Devices, San Jose, CA, USA). For data analysis, these OD values at 450 nm were corrected for those at 540 nm. Corrected OD values of duplicate measurements were averaged and expressed as percentage of the negative control (culture medium).

Cytokine ELISA

IL-8, IL-6 and TNF-α levels were quantified with Human Duoset ELISA kits (resp. #DY208, #DY206 and #DY210; Bio-Techne, Minneapolis, MN, USA). Manufacturer protocol was followed, however TMB substrate, supersensitive, for ELISA (#T4444; Merck Life Sciences, Darmstadt, Germany) was used as substrate solution. Absorbance was measured at 450 nm and 540 nm using a Spectramax® M2. For data analysis, the OD values (450–540 nm) of technical duplicates were averaged and corrected for the blank. Sample concentrations were determined by interpolating these OD values against the standard curve by GraphPad Prism 9 (GraphPad Software, La Jolla, CA) and correcting them for the dilution factor. For samples with an average OD value below the LLOQ, the concentration was considered zero.

Statistics

All cell culture experiments were repeated at least 3 times (n=3). Results are stated as mean ± SD from these independent experiments, unless stated otherwise. One-way analysis of variance (ANOVA) followed by Tukey's multiple comparison test was used for statistical analysis in IBM SPSS statistics 25 (SPSS Inc., Chicago, IL, USA). A p-value of ≤0.05 was considered statistically significant. All graphs were created using GraphPad Prism 9 (GraphPad Software, La Jolla, CA).

References

1. Ulrich P, Cerami A. Protein Glycation, Diabetes, and Aging. 2001.
2. Verzijl N, Degroot J, Oldehinkel E, Bank RA, Thorpe SR, Baynes JW, et al. Age-related accumulation of Maillard reaction products in human articular cartilage collagen. vol. 350. 2000.
3. Smuda M, Henning C, Raghavan CT, Johar K, Vasavada AR, Nagaraj RH, et al. Comprehensive analysis of maillard protein modifications in human lenses: Effect of age and cataract. Biochemistry 2015;54:2500–7. https://doi.org/10.1021/bi5013194.
4. Monnier VM, Kohn RR, Cerami A. Accelerated age-related browning of human collagen in diabetes mellitus. Proc Natl Acad Sci U S A 1984;81:583–7. https://doi.org/10.1073/PNAS.81.2.583.
5. Ramasamy R, Vannucci SJ, Yan SS Du, Herold K, Yan SF, Schmidt AM. Advanced glycation end products and RAGE: A common thread in aging, diabetes, neurodegeneration, and inflammation. Glycobiology 2005;15. https://doi.org/10.1093/glycob/cwi053.
6. Ott C, Jacobs K, Haucke E, Navarrete Santos A, Grune T, Simm A. Role of advanced glycation end products in cellular signaling. Redox Biol 2014;2:411–29. https://doi.org/10.1016/J.REDOX.2013.12.016.
7. Sparvero LJ, Asafu-Adjei D, Kang R, Tang D, Amin N, Im J, et al. RAGE (Receptor for advanced glycation endproducts), RAGE ligands, and their role in cancer and inflammation. J Transl Med 2009;7. https://doi.org/10.1186/1479-5876-7-17.
8. Schmidt AM. Isolation and characterization of two binding proteins for advanced glycosylation end products from bovine lung which are present on the endothelial cell surface. Journal of Biological Chemistry 1992;267:14987–97. https://doi.org/10.1016/S0021-9258(18)42137-0.
9. Neeper M, Marie Schmidt A, Brett J, Du YanQ S, Wangll F, Pan Y-CE, et al. Cloning and Expression of a Cell Surface Receptor for Advanced Glycosylation End Products of Proteins. J Biol Chem 1992;267:14998–5004.
10. Stern DM, Yan S Du, Yan SF, Schmidt AM. Receptor for advanced glycation endproducts (RAGE) and the complications of diabetes. vol. 1. 2002.
11. Snelson M, Lucut E, Coughlan MT. The Role of AGE-RAGE Signalling as a Modulator of Gut Permeability in Diabetes 2022.
12. Lin L, Park S, Lakatta EG. RAGE signaling in inflammation and arterial aging. 2009.
13. Kierdorf K, Fritz G. RAGE regulation and signaling in inflammation and beyond. J Leukoc Biol 2013;94:55–68. https://doi.org/10.1189/jlb.1012519.
14. Linkens AMA, van Best N, Niessen PM, Wijckmans NEG, de Goei EEC, Scheijen JLJM, et al. A 4-Week Diet Low or High in Advanced Glycation Endproducts Has Limited Impact on Gut Microbial Composition in Abdominally Obese Individuals: The deAGEing Trial. Int J Mol Sci 2022;23:5328. https://doi.org/10.3390/IJMS23105328.
15. Linkens AMA, Houben AJHM, Niessen PM, Wijckmans NEG, de Goei EEC, Van den Eynde MDG, et al. A 4-week high-AGE diet does not impair glucose metabolism and vascular function in obese individuals. JCI Insight 2022;7. https://doi.org/10.1172/JCI.INSIGHT.156950.
16. Delgado-Andrade C, Fogliano V. Dietary Advanced Glycosylation End-Products (dAGEs) and Melanoidins Formed through the Maillard Reaction: Physiological Consequences of their Intake. Annu Rev Food Sci Technol 2018;9:271–91. https://doi.org/10.1146/ANNUREV-FOOD-030117-012441.
17. Xie J, Reverdatto S, Frolov A, Hoffmann R, Burz DS, Shekhtman A. Structural Basis for Pattern Recognition by the Receptor for Advanced Glycation End Products (RAGE). Journal of Biological Chemistry 2008;283:27255–69. https://doi.org/10.1074/JBC.M801622200.
18. Xue J, Rai V, Singer D, Chabierski S, Xie J, Reverdatto S, et al. Advanced glycation end product recognition by the receptor for AGEs. Structure 2011;19:722–32. https://doi.org/10.1016/j.str.2011.02.013.

19. Zhao D, Sheng B, Wu Y, Li H, Xu D, Nian Y, et al. Comparison of Free and Bound Advanced Glycation End Products in Food: A Review on the Possible Influence on Human Health. J Agric Food Chem 2019;67:14007–18. https://doi.org/10.1021/acs.jafc.9b05891.
20. Dubois C, Litke R, Rianha S, Paul-constant C, Lo Guidice JM, Taront S, et al. Exposure of caenorhabditis elegans to dietary nε-carboxymethyllysine emphasizes endocytosis as a new route for intestinal absorption of advanced glycation end products. Nutrients 2021;13. https://doi.org/10.3390/NU13124398/S1.
21. Wu Y, Zong M, Zhang Z, Wu Y, Li L, Zhang X, et al. Selective transportation and energy homeostasis regulation of dietary advanced glycation end-products in human intestinal Caco-2 cells. Food Chem 2022;391:133284. https://doi.org/10.1016/J.FOODCHEM.2022.133284.
22. Paparo L, Coppola S, Nocerino R, Pisapia L, Picariello G, Cortese M, et al. How dietary advanced glycation end products could facilitate the occurrence of food allergy. Journal of Allergy and Clinical Immunology 2024;153:742–58. https://doi.org/10.1016/j.jaci.2023.11.023.
23. Van Der Lugt T, Weseler AR, Gebbink WA, Vrolijk MF, Opperhuizen A, Bast A. Dietary advanced glycation endproducts induce an inflammatory response in human macrophages in vitro. Nutrients 2018;10. https://doi.org/10.3390/nu10121868.
24. Toyomura T, Watanabe M, Wake H, Nishinaka T, Hatipoglu OF, Takahashi H, et al. Glycolaldehyde-derived advanced glycation end products promote macrophage proliferation via the JAK-STAT signaling pathway. Mol Biol Rep 2023. https://doi.org/10.1007/s11033-023-08509-y.
25. Raupbach J, Müller SK, Schnell V, Friedrich S, Hellwig A, Grune T, et al. The Effect of Free and Protein-Bound Maillard Reaction Products N-ε-Carboxymethyllysine, N-ε-Fructosyllysine, and Pyrraline on Nrf2 and NFκB in HCT 116 Cells. Mol Nutr Food Res 2023;67. https://doi.org/10.1002/mnfr.202300137.
26. Valencia J V., Mone M, Koehne C, Rediske J, Hughes TE. Binding of receptor for advanced glycation end products (RAGE) ligands is not sufficient to induce inflammatory signals: Lack of activity of endotoxin-free albumin-derived advanced glycation end products. Diabetologia 2004;47:844–52. https://doi.org/10.1007/S00125-004-1392-9.
27. Birben E, Şahiner ÜM, Kalayci CÖ. Determination of the effects of advanced glycation end products receptor polymorphisms and its activation on structural cell responses and inflammation in asthma. Turk J Med Sci 2023;53:160–70. https://doi.org/10.55730/1300-0144.5569.
28. Lappas M, Permezel M, Rice GE. Advanced glycation endproducts mediate pro-inflammatory actions in human gestational tissues via nuclear factor-κB and extracellular signal-regulated kinase 1/2. Journal of Endocrinology 2007;193:269–77. https://doi.org/10.1677/JOE-06-0081.
29. Ohtsu A, Shibutani Y, Seno K, Iwata H, Kuwayama T, Shirasuna K. Advanced glycation end products and lipopolysaccharides stimulate interleukin-6 secretion via the RAGE/TLR4-NF-κB-ROS pathways and resveratrol attenuates these inflammatory responses in mouse macrophages. Exp Ther Med 2017:4363–70. https://www.spandidos-publications.com/10.3892/etm.2017.5045.
30. Shu M, Cheng W, Jia X, Bai X, Zhao Y, Lu Y, et al. AGEs promote atherosclerosis by increasing LDL transcytosis across endothelial cells via RAGE/NF-κB/Caveolin-1 pathway. Molecular Medicine 2023;29:1–16. https://doi.org/10.1186/S10020-023-00715-5.
31. Adamopoulos C, Piperi C, Gargalionis AN, Dalagiorgou G, Spilioti E, Korkolopoulou P, et al. Advanced glycation end products upregulate lysyl oxidase and endothelin-1 in human aortic endothelial cells via parallel activation of ERK1/2-NF-κB and JNK-AP-1 signaling pathways. Cellular and Molecular Life Sciences 2016;73:1685–98. https://doi.org/10.1007/S00018-015-2091-Z.
32. Shen C, Ma Y, Zeng Z, Yin Q, Hong Y, Hou X, et al. RAGE-Specific Inhibitor FPS-ZM1 Attenuates AGEs-Induced Neuroinflammation and Oxidative Stress in Rat Primary Microglia. Neurochem Res 2017;42:2902–11. https://doi.org/10.1007/s11064-017-2321-x.

33. Kumar V, Fleming T, Terjung S, Gorzelanny C, Gebhardt C, Agrawal R, et al. Homeostatic nuclear RAGE-ATM interaction is essential for efficient DNA repair. Nucleic Acids Res 2017;45:10595–613. https://doi.org/10.1093/nar/gkx705.
34. Kumar V, Agrawal R, Pandey A, Kopf S, Hoeffgen M, Kaymak S, et al. Compromised DNA repair is responsible for diabetes-associated fibrosis. EMBO J 2020;39. https://doi.org/10.15252/EMBJ.2019103477.
35. Han Z, Andrš M, Madhavan BK, Kaymak S, Sulaj A, Kender Z, et al. The importance of nuclear RAGE-Mcm2 axis in diabetes or cancer-associated replication stress. Nucleic Acids Res 2023;51:2298–318. https://doi.org/10.1093/nar/gkad085.
36. Mosquera-Sulbarán J, Pedreáñez A, Carrero Y, Peña C. Nuclear and cytoplasmic expressions of the receptor for advanced glycation end products (RAGE) in the rat central nervous system. Invest Clin 2023;64:505–12. https://doi.org/10.54817/ic.v64n4a07.
37. Liliensiek B, Weigand MA, Bierhaus A, Nicklas W, Kasper M, Hofer S, et al. Receptor for advanced glycation end products (RAGE) regulates sepsis but not the adaptive immune response. J Clin Invest 2004;113. https://doi.org/10.1172/JCI200418704.
38. Chavakis T, Bierhaus A, Al-Fakhri N, Schneider D, Witte S, Linn T, et al. The Pattern Recognition Receptor (RAGE) Is a Counterreceptor for Leukocyte Integrins: A Novel Pathway for Inflammatory Cell Recruitment. Journal of Experimental Medicine 2003;198:1507–15. https://doi.org/10.1084/jem.20030800.
39. Gao Y, Wake H, Morioka Y, Liu K, Teshigawara K, Shibuya M, et al. Phagocytosis of Advanced Glycation End Products (AGEs) in Macrophages Induces Cell Apoptosis 2017. https://doi.org/10.1155/2017/8419035.
40. Sun F, Suttapitugsakul S, Xiao H, Wu R. Comprehensive Analysis of Protein Glycation Reveals Its Potential Impacts on Protein Degradation and Gene Expression in Human Cells. J Am Soc Mass Spectrom 2019;30:2480. https://doi.org/10.1007/S13361-019-02197-4.
41. Takizawa N, Takada K, Ohkawa K. Inhibitory Effect of Nonenzymatic Glycation on Ubiquitination and Ubiquitin-Mediated Degradation of Lysozyme. Biochem Biophys Res Commun 1993;192:700–6. https://doi.org/10.1006/BBRC.1993.1471.
42. Qiao X, Li W, Zheng Z, Liu C, Zhao L, He Y, et al. Inhibition of the HMGB1/RAGE axis protects against cisplatin-induced ototoxicity via suppression of inflammation and oxidative stress. Int J Biol Sci 2024;20:784–800. https://doi.org/10.7150/ijbs.82003.
43. Yang H, Liu H, Zeng Q, Imperato GH, Addorisio ME, Li J, et al. Inhibition of HMGB1/RAGE-mediated endocytosis by HMGB1 antagonist box A, anti-HMGB1 antibodies, and cholinergic agonists suppresses inflammation. Molecular Medicine 2019;25:1–13. https://doi.org/10.1186/S10020-019-0081-6.
44. Watanabe M, Toyomura T, Tomiyama M, Wake H, Liu K, Teshigawara K, et al. Advanced glycation end products (AGEs) synergistically potentiated the proinflammatory action of lipopolysaccharide (LPS) and high mobility group box-1 (HMGB1) through their direct interactions. Mol Biol Rep 2020;47:7153–9. https://doi.org/10.1007/S11033-020-05783-Y.
45. Dullah EC, Ongkudon CM. Current trends in endotoxin detection and analysis of endotoxin–protein interactions. Crit Rev Biotechnol 2017;37:251–61. https://doi.org/10.3109/07388551.2016.1141393.
46. Goode A, Yeh V, Bonev BB. Interactions of polymyxin B with lipopolysaccharide-containing membranes. Faraday Discuss 2021;232:317–29. https://doi.org/10.1039/d1fd00036e.
47. Boiko A, Fiore A, Hay A, Troise AD, De Pascale S, Scaloni A, et al. The glycation database: from the Maillard reaction in foods to biomolecular insight. Abertay University 2022.
48. Scheijen JLJM, Clevers E, Engelen L, Dagnelie PC, Brouns F, Stehouwer CDA, et al. Analysis of advanced glycation endproducts in selected food items by ultra-performance liquid chromatography tandem mass spectrometry: Presentation of a dietary AGE database. Food Chem 2016;190:1145–50. https://doi.org/10.1016/J.FOODCHEM.2015.06.049.
49. Scheijen JLJM, van de Waarenburg MPH, Stehouwer CDA, Schalkwijk CG. Measurement of pentosidine in human plasma protein by a single-column high-performance liquid chromatography method with fluorescence detection. J Chromatogr B Analyt Technol Biomed Life Sci 2009;877:610–4. https://doi.org/10.1016/j.jchromb.2009.01.022.

50. Moysa A, Hammerschmid D, Szczepanowski RH, Sobott F, Dadlez M. Enhanced oligomerization of full-length RAGE by synergy of the interaction of its domains. Sci Rep 2019;9. https://doi.org/10.1038/s41598-019-56993-9.
51. Zenker HE, Ewaz A, Deng Y, Savelkoul HFJ, Van Neerven RJJ, De Jong N, et al. Differential effects of dry vs. Wet heating of β-lactoglobulin on formation of sRAGE binding ligands and sIgE epitope recognition. Nutrients 2019;11. https://doi.org/10.3390/nu11061432.

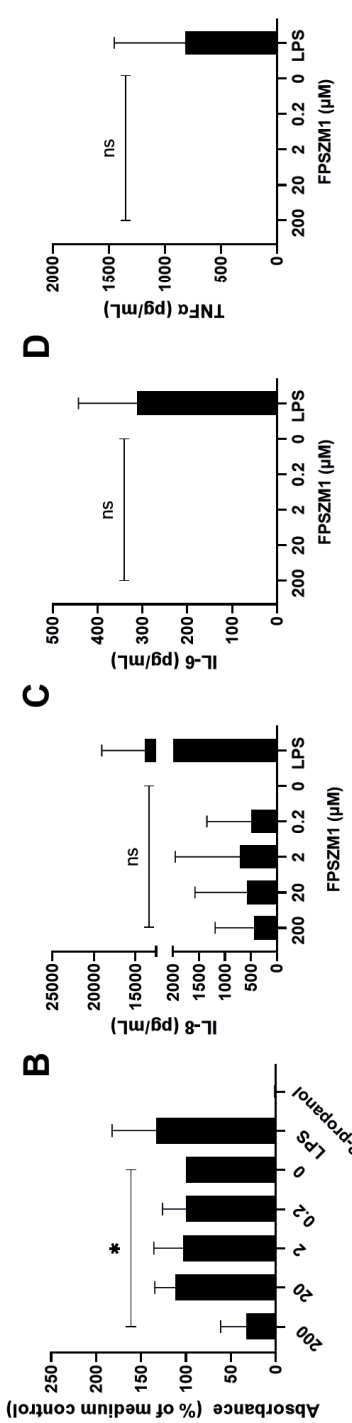
Supplementary information

Supplementary Table S4.1: LPS levels of in-house glucose-glycated BLG and of glycolaldehyde-glycated BSA (Abcam, Sigma, In-house). LPS content was measured with a LAL assay and expressed as EU/mg protein and pg/mg protein. Data are depicted as mean values obtained from a technical duplicate.

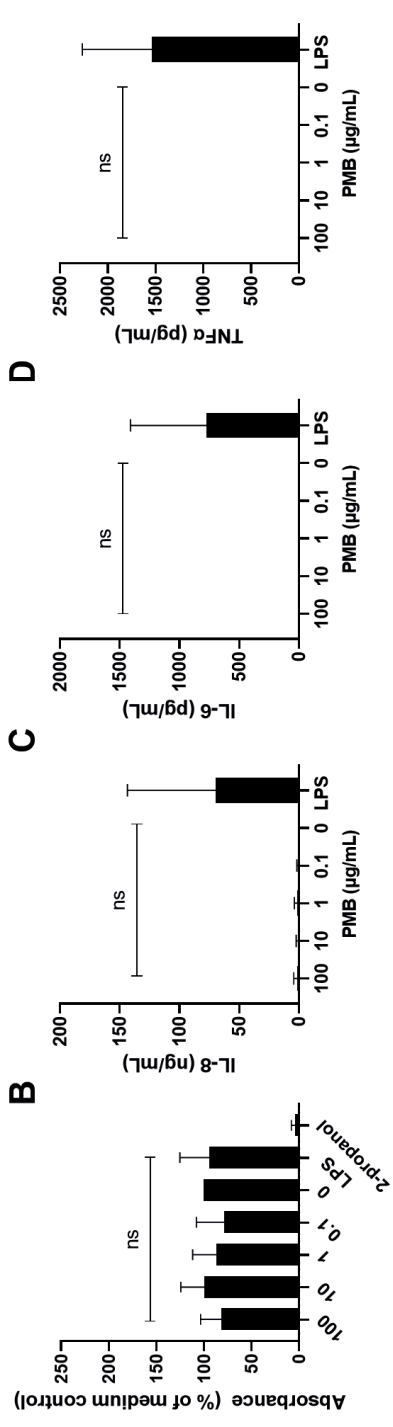
Sample		LPS content (EU/mg protein)	LPS content (pg/mg protein)
Glucose-glycated BLG		0.11	16.5
Glycolaldehyde-glycated BSA	Abcam	0.06	9.0
	Sigma	0.02	3.0
	In-house	2.08	312

Supplementary Table S4.2: Optimized parent and fragment ion (m/z) and electron voltages for single reaction monitoring of analytes of interest (lysine, CEL, CML and Furosine) using LC-MS/MS

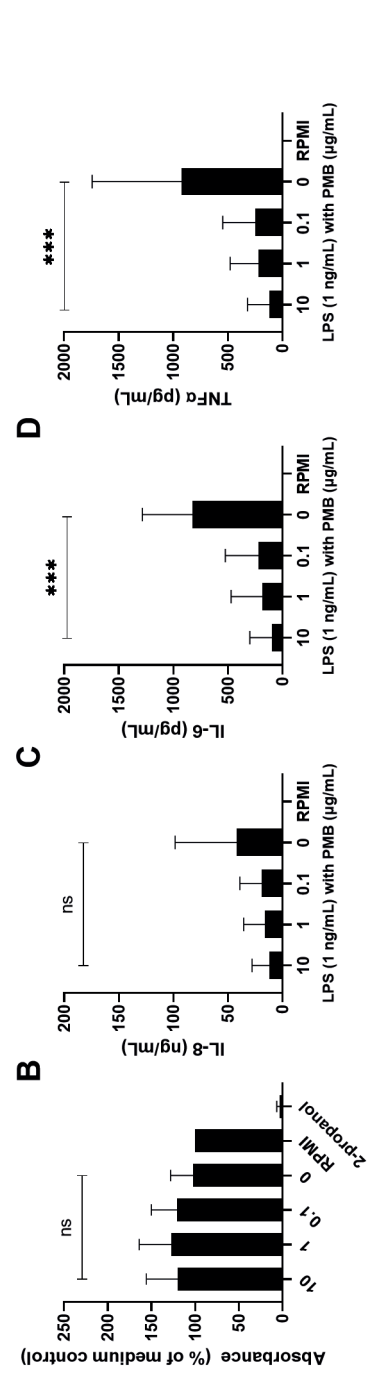
Compound	Precursor ion (m/z)	Product ion (m/z)	Dwell time (ms)	Q1 Pre bias (V)	CE (V)	Q3 Pre bias (V)
Furosine	254.95	83.95	19.0	-13.0	-23.0	-15.0
		130.10	19.0	-13.0	-14.0	-23.0
Furosine-d4	259.15	134.10	19.0	-13.0	-14.0	-26.0
		88.10	19.0	-18.0	-25.0	-10.0
Lysine	146.90	84.10	8.0	-14.0	-19.0	-15.0
		130.25	8.0	-16.0	-16.0	-14.0
Lysine-d4	151.10	88.150	8.0	-20.0	-17.0	-20.0
		134.25	8.0	-25.0	-14.0	-25.0
CML	205.20	84.05	12.0	-13.0	-17.0	-18.0
		130.05	12.0	-14.0	-13.0	-24.0
CML-d4	209.15	88.00	12.0	-11.0	-22.0	-17.0
		134.20	12.0	-23.0	-14.0	-28.0
CEL	219.20	84.00	19.0	-28.0	-19.0	-20.0
		130.00	19.0	-24.0	-12.0	-25.0
CEL-d4	223.00	88.10	19.0	-25.0	-21.0	-14.0
		134.10	19.0	-25.0	-13.0	-26.0



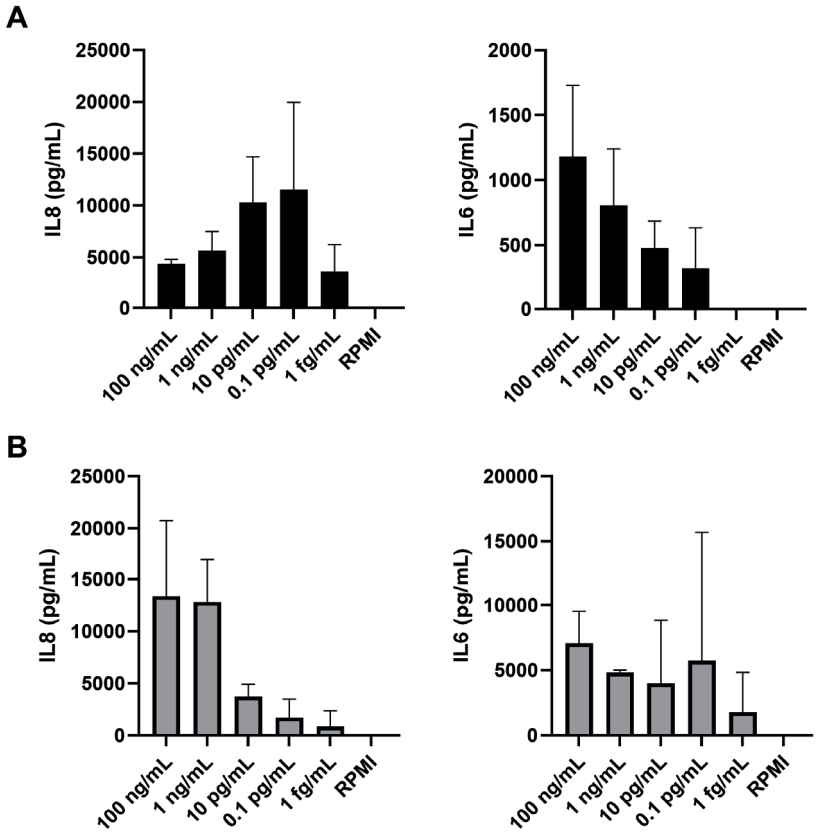
Supplementary Figure S4.1: Cell viability of M-CSF differentiated M0 macrophages **(A)** and their IL-8 **(B)**, IL-6 **(C)** and TNFα **(D)** secretion upon exposure to RAGE antagonist FPS-ZM1. M-CSF differentiated M0 macrophages were exposed to FPSZM1 (0–200 µM) for 24 h at 37°C (5% CO_2, saturated humidity). LPS (1 ng/mL) was included as positive control. Data is mean values ± SD obtained from independent experiments performed with three different donors. P-values (* <0.05) are obtained by a multiple comparisons test (Tukey) following ANOVA.



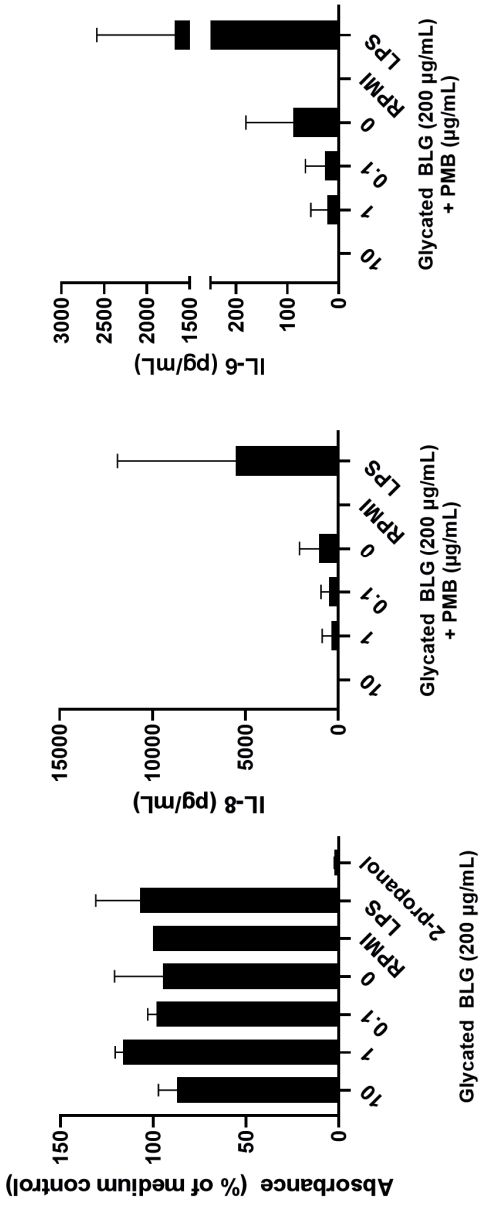
Supplementary Figure S4.2: Cell viability of M-CSF differentiated M0 macrophages **(A)** and their IL-8 **(B)**, IL-6 **(C)** and TNFα **(D)** secretion upon exposure to polymyxin B (PMB). M-CSF differentiated M0 macrophages were exposed to PBS (0–10 µg/mL) for 24 h at 37°C (5% CO_2, saturated humidity). LPS (1 ng/mL) was included as positive control. Data is mean values ± SD obtained from independent experiments performed with three different donors. P-values are obtained by a multiple comparisons test (Tukey) following ANOVA.



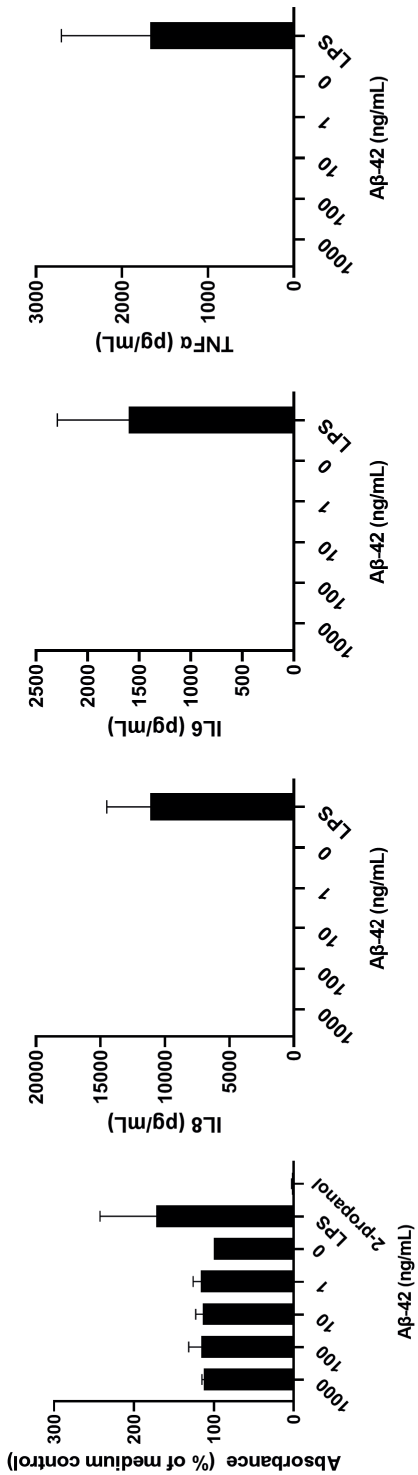
Supplementary Figure S4.3: Cell viability of M-CSF differentiated M0 macrophages **(A)** and their IL-8 **(B)**, IL-6 **(C)** and TNFα **(D)** secretion upon exposure to LPS co-incubated with different concentrations of polymyxin B (PMB). M-CSF differentiated M0 macrophages were exposed to LPS at 1 ng/mL for 24 h at 37°C (5% CO_2, saturated humidity) co-incubated with different concentrations of PMB (0–10 µg/mL). Data is mean values±SD obtained from independent experiments performed with six different donors. P-values (*** <0.001) are obtained by a multiple comparisons test (Tukey) following ANOVA.



Supplementary Figure S4.4: IL-8 and IL-6 response of M-CSF differentiated M0 macrophages **(A)** and GM-CSF differentiated M0 macrophages **(B)** upon exposure to different concentrations of LPS (100 ng/mL – 1 fg/mL) for 24 h. For IL-8, this dose-response curve for LPS follows an inverted U-shape whereas for IL-6 the dose-response relationship is linear in M-CSF differentiated M0 macrophages. Data is mean values±SD obtained from independent experiments performed with three different donors.



Supplementary Figure S4.5: Cell viability of GM-CSF differentiated M0 macrophages and their IL-8 and IL-6 secretion upon exposure to glycated beta-lactoglobulin (BLG) co-incubated with different concentrations of polymyxin B (PMB). BLG was dry heated with glucose for 24 h at 60°C and 40% humidity. Subsequently, GM-CSF differentiated M0 macrophages were exposed to this glycated protein at 200 µg/mL for 24 h at 37°C (5% CO_2, saturated humidity) co-incubated with different concentrations of LPS scavenger PMB (0–10 µg/mL). LPS (1 ng/mL) was included as positive control. Data is mean values ± SD obtained from independent experiments performed with three different donors.



Supplementary Figure S4.6: CWST-1, IL-8, IL-6 and TNFα secretion by M-CSF differentiated M0 macrophages upon exposure to multiple concentrations of RAGE ligand amyloid beta 1-42 (Aβ-42). M-CSF differentiated M0 macrophages were exposed to these recombinant proteins (1,000–0 ng/mL) for 24 h at 37°C (5% CO_2, saturated humidity). LPS (100 ng/mL) was included as positive control. Data is mean values ± SD obtained from independent experiments performed with three different donors.

5

Role of LPS in RAGE activation: confounder or co-factor?

Fleur A.C. Jansen [1] · Klaske van Norren [2] · Josep Rubert [1, 2] · Vincenzo Fogliano [1] · Tamara Hoppenbrouwers [1, 3]

1 Department of Food Quality and Design, Wageningen University & Research, Wageningen, The Netherlands
2 Nutritional Biology, Division of Human Nutrition, Wageningen University & Research, Wageningen, The Netherlands
3 Food and Biobased Research, Wageningen University & Research, Wageningen, The Netherlands

In preparation

Abstract

Food processing generates several compounds which are absent in raw materials, among them those named dietary advanced glycation end products (AGEs). These modified proteins are partially bioavailable and are described to trigger inflammation via RAGE activation, potentially acting primarily within the intestinal tract. Our previous research suggested that LPS may function as a cofactor enabling RAGE agonists to activate this receptor. To investigate this, primary immune cells known to express surface RAGE were exposed to various RAGE agonists, either alone or combined with LPS at different concentrations. Results did not show any effect of RAGE agonists on the inflammatory potency of LPS. Only when NF-κB reporter activity was assessed directly in a genetically modified immune cell line, an amplification of the LPS effect could be observed. This finding suggests that RAGE-dependent NF-κB activation could occur independently of acute inflammation-related cytokines production and may instead involve alternative NF-κB pathways. However, because results in this cell line were inconsistent, no firm conclusions can be drawn. Overall, these preliminary findings suggest that RAGE activation may depend on co-factors or receptor interactions, that may vary with cell type and function, and that downstream immune responses could be mediated through alternative, non-canonical NF-κB signalling.

Introduction

The growing level of processing in our food production system has raised public health concerns due to its generation of deleterious substances. These processing-derived contaminants include for example heterocyclic aromatic amines, polycyclic aromatic hydrocarbons, acrylamide, and advanced glycation end products (AGEs) [1]. The latter is a heterogenous group of compounds formed upon the temperature-driven reaction between animo groups and simple sugars. Most of them are bound to proteins determining their modification, aggregation and altered digestibility. Both human and animal intervention studies have shown that a higher AGEs consumption results in an increase of their concentration in plasma, urine and/or several tissues [2–5] suggesting a certain degree of bioavailability. The health consequences of this accumulation are however not fully clear yet. While some studies fail to demonstrate direct effects on short- and/or long-term health [5], others suggest a link with increased inflammation [2,4]. Taken together, these findings highlight the need to better understand if and how dietary AGEs influence inflammatory processes.

The most likely mechanism by which dietary AGEs modulate inflammation is through their interaction with the receptor for advanced glycation end products (RAGE). When AGEs bind to RAGE, a cascade of events is initiated, including the activation of NF-κB, leading to the production of pro-inflammatory cytokines [6–8]. This mechanism is not fully convincing. Effective binding to RAGE requires a large peptide backbone [9,10], while the majority of dietary AGEs are absorbed as single amino acids glycation products or as di- or tripeptides derivatives [11]. Since the intestine is the organ protein-bound AGEs first and foremost interact with, this might explain why Nogueira Silva Lima et al. [4] only found inflammatory effects on the intestinal level. Thus, dietary AGE-RAGE interaction is an interesting angle to focus on when exploring the health consequences of dietary AGE consumption.

To better understand this relationship between dietary AGEs and (local) inflammation through RAGE, *in vitro* models are a frequently used tool. However, such *in vitro* studies have reported mixed results and are hard to compare due to the use of different dietary proteins, glycation methods and cell models [12]. From our previous attempt to establish a standardized *in vitro* model to study dietary AGE-RAGE signalling [13], we formulated three key messages: 1) RAGE is only expressed as cell surface receptor in specific *in vitro* models, 2) LPS may act as

co-factor to activate RAGE, and 3) commercial dietary AGE preparations are not reliable due to undisclosed methods and potential batch-to-batch variability and/or contamination. Building on these insights, we performed this follow-up study to fill the remaining knowledge gap and identify a biochemical pathway responsible of the RAGE-dependent inflammatory response. To enable direct comparison with our earlier study, and because surface RAGE is only present in certain models, we again used M-CSF differentiated M0 macrophages. This model is physiologically relevant, as we have shown that intact glycated proteins and aggregates can cross the intestinal barrier (Jansen et al., unpublished; Chapter 2), making it plausible that these cells could encounter such proteins *in vivo*. In addition, because a reliable and reproducible source of dietary AGEs is unavailable, we instead used alternative, well-characterized, RAGE agonists: High mobility group box 1 protein (HMGB1) and β-Amyloid 1-42 (Aβ-42). Since our previous study suggested that RAGE activation may require a cofactor, we hypothesis that combining these agonists with LPS in a model expressing surface RAGE will trigger a RAGE-dependent inflammatory response.

Results

Combining RAGE agonists with LPS does not alter the inflammatory response of M-CSF differentiated M0 macrophages

Different concentrations of LPS were combined with HMGB1 and Aβ-42 to test our hypothesis that these RAGE agonists, together with LPS, could enhance LPS's inflammatory potency through RAGE activation. To get a broader view on the processes being involved, not only cytokines were measured but also qPCR analyses were performed on transcription of the individual cytokines as well as the upstream transcription factor NF-κB. Figure 5.1A shows that the RAGE expression of M-CSF differentiated M0 macrophages was substantial in three out of the four different donors, quantified as total RAGE and surface RAGE expression. For surface RAGE, 47.7 ± 7.3% of the cells were positive, with an MFI of 2.7 x 10^5 ± 1.2 x 10^5 RFU. In contrast, the fourth donor showed generally lower RAGE expression, with only 14.0% surface-positive cells and an MFI of 6.5 x 10^3 RFU. Despite confirmed surface expression of RAGE across donors and varying LPS concentrations, neither HMGB1 nor Aβ-42 could enhance the cell's inflammatory response to LPS as the transcription levels of NF-κB, IL-1β, TNFα, and IL-6 remained unchanged (Figure 5.1B, resp. p=0.360, p=0.327, p=0.534, and p=0.418). Cytokine secretion showed the same pattern for TNFα and IL-6 (Figure 5.1C, resp. p=0.419

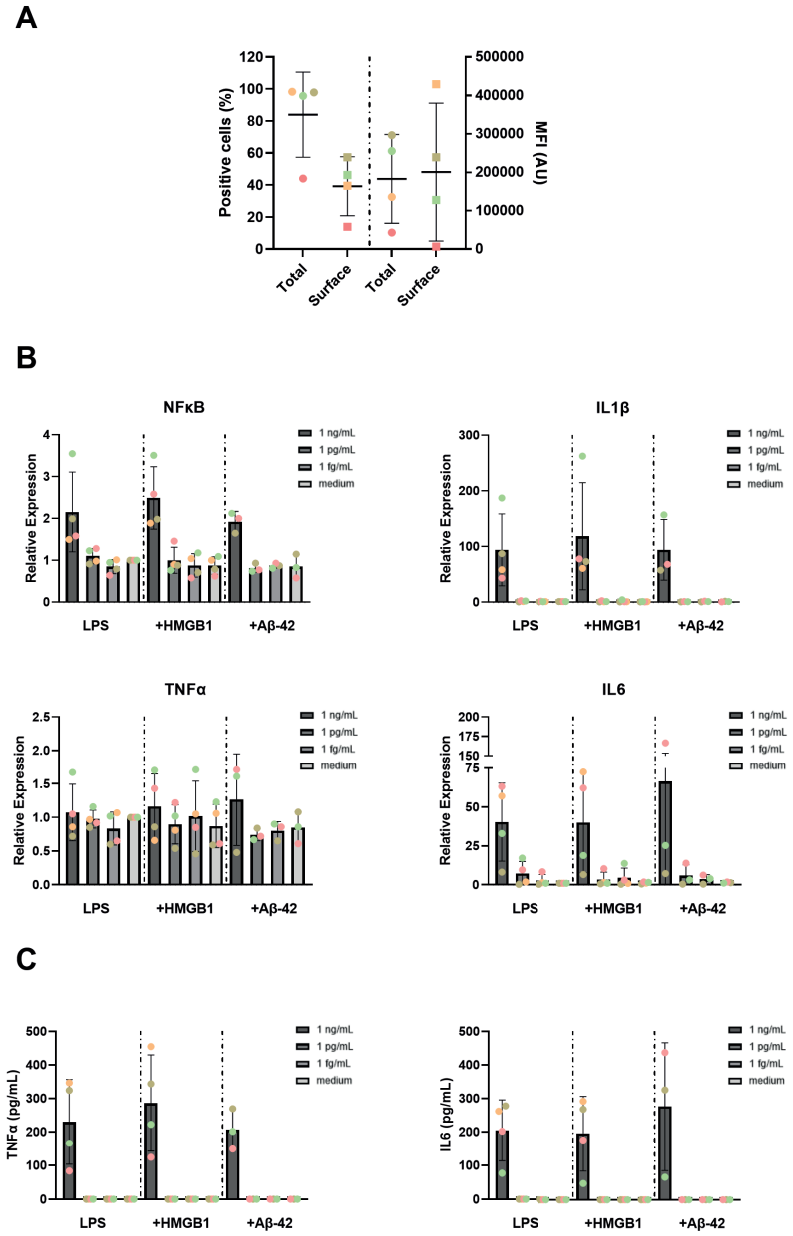


Figure 5.1: RAGE expression of M-CSF differentiated M0 macrophages **(A)**, their relative NF-κB, IL6, TNFα and IL1β gene expression **(B)** and TNFα and IL6 secretion after 24 h exposure to different concentrations of LPS alone or combined with HMGB1 and Aβ-42 (1 µg/mL) **(C)**. RAGE expression was quantified on the cell surface and in totality (i.e. after cell fixation and permeabilization), and shown as percentage of positive cells (left y-axis) and median fluorescent intensity (MFI) (right y-as). These values are relevant to (%) or corrected for (MFI) the unstained control, which implies no staining with the primary RAGE antibody. Gene expression results are expressed relative to medium control. Data are mean ± SD of four independent donor experiments; dots of different colours represent individual donors.

and p=0.300); IL-1β was not detected (data not shown). When the fourth donor with low RAGE expression was excluded from the dataset, similar results were obtained (Supplementary Figure S5.1), suggesting that the observed inflammatory responses are independent of RAGE. Therefore, these findings indicate that the combination of a RAGE agonist with LPS did not induce a RAGE-dependent inflammatory response in this cell model.

One finding that supports the current hypothesis but was non-reproducible

In the abovementioned results, NF-κB transcription levels were measured, however transcription alone does not necessarily reflect NF-κB activity as additional regulatory mechanisms are involved (e.g. IκBα binding). To address this, pilot experiments were conducted using an immune cell line containing a NF-κB-inducible luciferase reporter construct. In this system, NF-κB binding to DNA drives luciferase expression, producing a luminescence signal that directly reflects NF-κB reporter activity. Figure 5.2 shows cytokine and chemokine production in these cells treated with LPS (0.1 ng/mL) combined with the RAGE agonist HMGB1, measured using a multiplex assay that included a wide range of M1 and M2 macrophage-associated analytes. Some analytes, such as the M2 macrophage-associated cytokines IL-4 and IL-10, were below the detection limit. Among the quantifiable analytes (resp. IL-1β, TNFα, IL-6, IL-1RA, and IP-10), only IP-10 showed some minor combination effect. So, also in this model, no profound increase of the inflammatory response was observed by the combination of LPS and HMGB1, regardless of the post-translational modifications of HMGB1 (resp. oxidized, reduced, and disulfide form). However, when analysing the overall NF-κB activity through the luminescence assay, a strong amplification of the LPS effect was observed (Figure 5.3A). These data indicate that NF-κB activity induced by a RAGE agonist combined with low-dose LPS can occur independently of acute inflammation-related cytokine production, in contrast to the robust cytokine response triggered by the positive control, high-dose LPS (50 ng/mL). The reduced form of HMGB1 produced the strongest amplifying effect, with luminescence levels exceeding those of the positive control twice. However, this combination also appeared slightly cytotoxic, as indicated by reduced metabolic activity, an effect also seen with the positive LPS control (Figure 5.3B).

A follow-up experiment suggested that the amplified NF-κB response is likely RAGE-dependent, as pre-incubation with the RAGE antagonist FPS-ZM1 or the RAGE ligand scavenger sRAGE completely blocked the amplification (Figure 5.4A).

Similar effects were observed after pre-incubation with glycated beta-lactoglobulin, suggesting it may also act as a RAGE antagonist. Notably, only FPS-ZM1 showed slight cytotoxicity in this experiment (Figure 5.4B). However, results were inconsistent as some repetitions of the experiments did not show this the amplified effect (data not shown), and therefore no definite conclusions can be drawn.

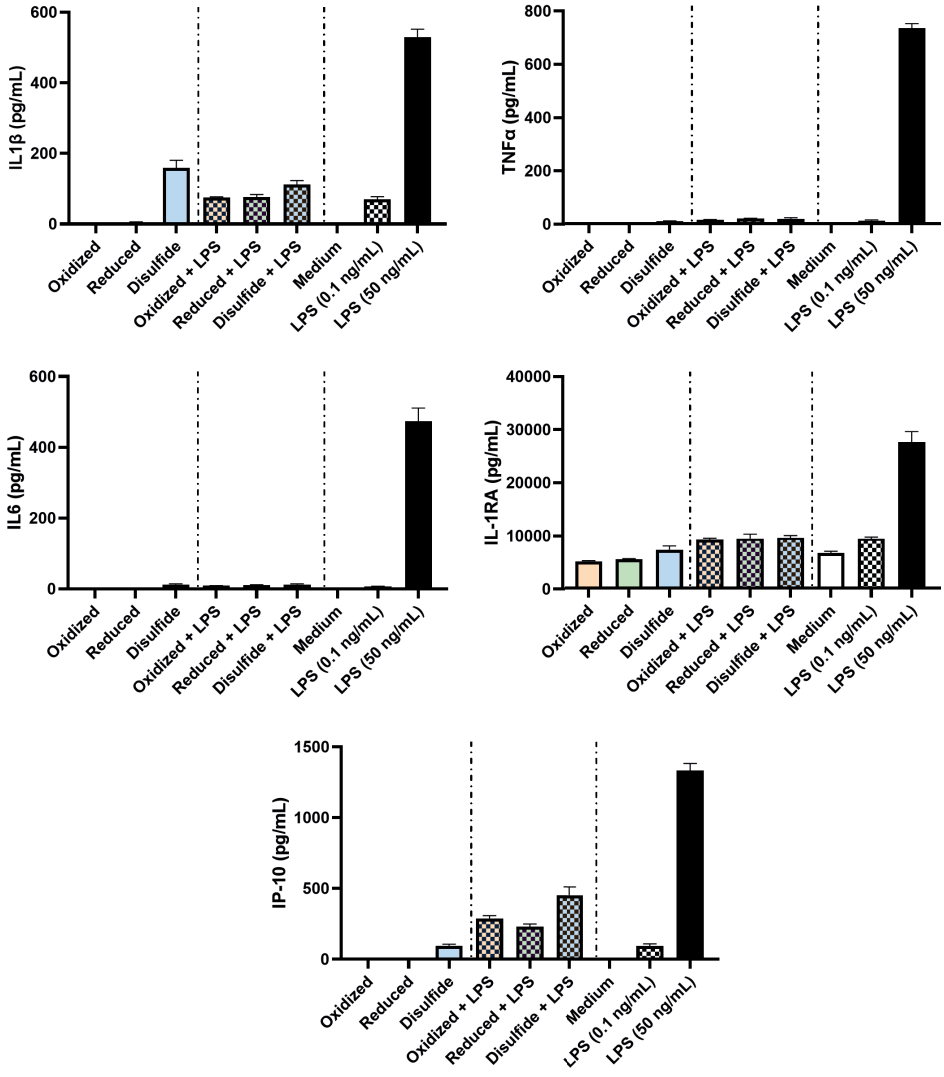


Figure 5.2: Cytokine excretion of THP1-Lucia™ NF-κB cells exposed to the RAGE agonist HMGB1 (1.0 µg/mL) alone or combined with a low dose of LPS (0.1 ng/mL). Different forms of HMGB1 were tested (oxidized, reduced, and disulfide form). IL-1β, TNFα, IL-6, IL-1RA, and IP-10 were quantified by multiplex assay. Data are mean ± SD of a technical duplicate.

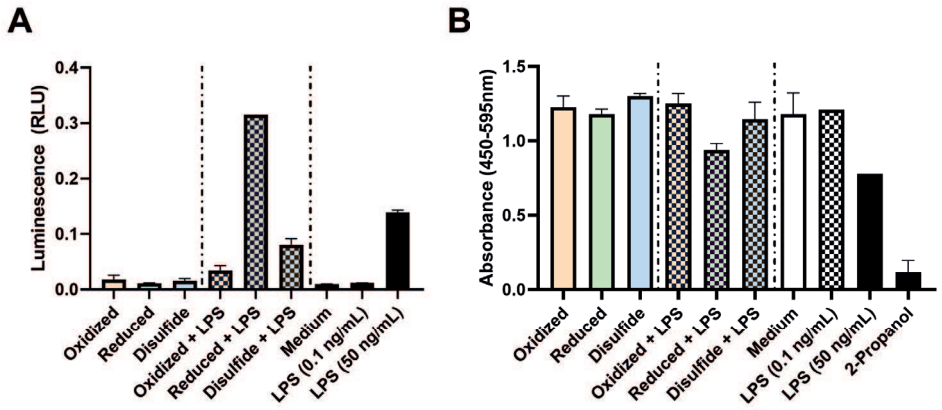


Figure 5.3: NF-κB reporter activity **(A)** and metabolic activity **(B)** of THP1-Lucia™ NF-κB cells exposed to the RAGE agonist HMGB1 (1.0 µg/mL) alone or combined with a low dose of LPS (0.1 ng/mL). Different forms of HMGB1 were tested (oxidized, reduced, and disulfide form). The NF-κB activity was measured by luminescence assay (RLU) and metabolic activity was quantified by WST-1 assay (absorbance). Data are mean ± SD of a technical duplicate.

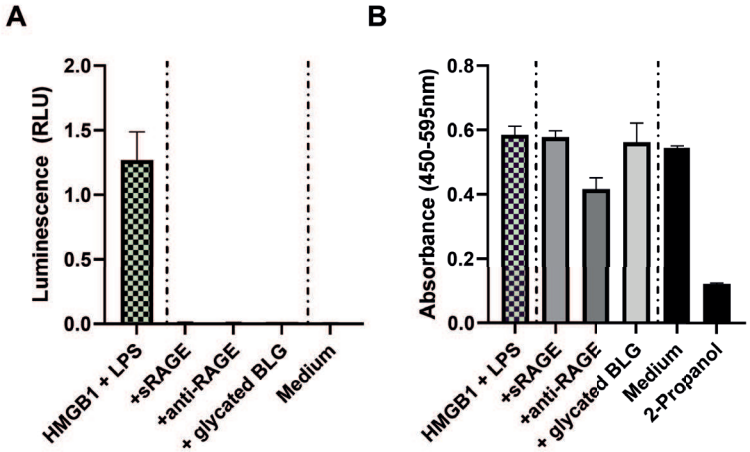


Figure 5.4: NF-κB reporter activity **(A)** and metabolic activity **(B)** of THP1-Lucia™ NF-κB cells exposed to the RAGE agonist reduced HMGB1 (1.0 µg/mL) alone or combined with a low dose of LPS (0.1 ng/mL). The NF-κB activity was measured by luminescence assay (RLU) and metabolic activity was quantified by WST-1 assay (absorbance). Data are mean ± SD of a biological duplicate.

Discussion

The results of this chapter provide only limited support for the hypothesis that RAGE agonists enhance the inflammatory potency of LPS. In primary immune cells, stimulation with LPS in the presence of RAGE agonists did not result in enhanced inflammatory responses, compared to LPS alone. This was observed at both the

protein and gene expression levels for cytokines involved in acute inflammation, as well as for the upstream transcription factor NF-κB. Similar results were obtained in an immune cell line carrying an NF-κB-inducible luciferase reporter construct, where co-treatment with LPS and RAGE agonists did not elevate cytokine production. Only in certain instances, NF-κB reporter activity was amplified in these experiments, suggesting RAGE-dependent NF-κB activation being uncoupled from the production of acute-inflammation-related cytokines. Nevertheless, this effect on NF-κB reporter activity was not consistently reproduced across experiments. So, there is a need to better understand under which circumstances certain effects can be observed regarding RAGE activation.

To connect the mixed results obtained from these two different *in vitro* models, some theories might be formulated. In both models, an attempt to activate RAGE did not result in the production of acute-phase pro-inflammatory cytokines. In the primary cell model, the gene expression of these cytokines was also not upregulated, ruling out the possibility that a lack of effective secretion stimuli is responsible for the absent cytokine secretion. For example, IL-1β is produced as the inactive precursor pro-IL-1β in response to pathogen-associated molecular patterns (PAMPs) and requires an additional stimulus for processing and secretion of active IL-1β [14]. This was also observed in our primary cell model with high-dose LPS (1 ng/mL). However, although the expression and secretion of acute-phase pro-inflammatory cytokines were not increased, the genetically modified cell line did show amplified NF-κB activity. This may be explained by NF-κB regulation at the protein level and the involvement of the alternative non-canonical NF-kB pathway, as our cytokine measurements targeted only those associated with the classic canonical NF-kB pathway. This alternative NF-κB pathway is less well-known and primarily serves as a supplementary axis to coordinate complex immune processes [15]. In contrast, the classic canonical pathway participates in nearly all rapid, transient immune reactions. RAGE has more often been suggested a non-canonical receptor being involved in adaptive immune responses [8]. In addition, RAGE was shown to interact with TLR9 to activate plasmacytoid dendritic cells and B cells, in the presence of nucleic acids and HMGB1 [16]. Therefore, RAGE signaling beyond canonical pathways and its interaction with other receptors could be a direction for follow-up studies to better understand RAGE functionality.

A remaining question is which model is most appropriate and reliable for these studies. Continuing with the genetically-modified cell line is attractive because it allows precise, upstream measurement of NF-kB, without being limited to

specific downstream cytokine measurements. However, cell viability was often problematic, likely due to the high degree of genetic modification. This led to poor proliferation of monocytes, failed differentiation towards macrophages, and macrophages dying during the experimental protocol regardless of conditions, probably due to edge effects (results not shown). In addition, the inconsistent results might potentially be explained by variations in RAGE expression between experiments, however due to the limited amount of available cell material, this could not be checked in each experiment. In contrast, this can easily be done in the primary cell model. While optimizing culture and differentiation conditions, for example using factors other than PMA, might overcome these issues, the highly modified phenotype of the cell line might still raise concerns about the translatability of the results. Therefore, proceeding with the M-CSF differentiated M0 macrophages appears to be the most reliable choice.

In conclusion, in this chapter, we communicated our preliminary data and gave directions on how to continue the research on RAGE functionality. RAGE functionality likely depends on the presence of co-factors or interactions with other receptors, for example Toll-like receptors, G-protein coupled receptors, and/or Tumor Necrosis Factor Receptors. This may require different ligand combinations based on cell type and function. Subsequent immune responses may potentially arise from both canonical and non-canonical pathways. Hopefully, by thoroughly describing methodology and also publishing results not supporting the pending hypothesis, we could move forward finding answers to the outstanding questions regarding RAGE functionality and AGE-RAGE interaction. In this regard, considering our preliminary data, the possibility that (some) glycated proteins may act antagonistically to RAGE should not be ignored.

Materials & methods

Materials

All materials were prepared and/or stored according to manufacturer instructions. The materials mentioned below are applicable to all protocols unless stated otherwise. From Merck Life Sciences (Darmstadt, Germany), Corning® 96-well microplates (#CLS3599), Corning® T25 cell culture flasks (#CLS430639), Dulbecco's Phosphate Buffered Saline (DPBS) without Ca^{2+} and Mg^{2+} (#D857), Bovine Serum Albumin (BSA) (#A3912), and LPS (#L3137) were purchased. RPMI-1640-Glutamax medium (#72400-021), Penicillin-Streptomycin (P/S; 10,000 U/mL)

(#15140122) were obtained from ThermoFisher Scientific (Waltham, MA, USA). From Sarstedt (Nümbrecht, Germany), 15 mL sterile screw cap tubes (#62.554.502) were purchased. From Avantor/VWR (Radnor, PA, USA), Research Grade Foetal Bovine Serum (FBS) (#HYCLSV30160.03; South American Origin) was purchased which was heat inactivated by heating it for 45 min at 56°C. From Greiner Bio-One (Alphen aan den Rijn, The Netherlands), CELLSTAR 24-well microplates (#662160) were purchased.

Primary immune cells

Isolation and differentiation

Monocytes were isolated and subsequently stored in liquid nitrogen according to the protocol described by Jansen et al. [13]. For the experiments, these cells were thawed at 37°C using a water bath, the content of the liquid nitrogen vial was transferred to pre-warmed 9 mL RPMI-1640-Glutamax supplemented with 20% FBS and 1% P/S. The suspension was centrifuged at RT for 8 min at 300*g. The pellet was resuspended in culture medium (RPMI-1640-Glutamax supplemented with 10% FBS and 1% P/S) to a concentration of 5.0 x 10^5 cells/mL and M-CSF (#216-MC; Bio-Techne, Minneapolis, MN, USA) was added (50 ng/mL). Cells were seeded in 24-well plates (750 µL/well) and cultured for 7 days (37°C, 5% CO_2 at saturating humidity). At day 3 and 5 of culturing, medium containing M-CSF was refreshed. At day 7, cells were considered to be M0 macrophages and either used for flow cytometry to quantify RAGE expression or their inflammatory responses to the experimental conditions were tested.

Flow cytometry protocol for RAGE detection

To quantify RAGE expression by flow cytometry, a cell density equivalent to the seeding density of 1.5 x 10^6 cells/mL was required. Cells were detached by incubating with cold FACS buffer (0.5% BSA-DPBS) supplemented with 2 mM EDTA (#E5134; in DPBS; Merck Life Sciences, Darmstadt, Germany) at 4°C for 10–15 min and collected by scraping. The cell suspension was centrifuged at RT for 3 min at 300*g in a 15 mL tube. The pellet was resuspended in 800 µL cold FACS buffer and divided over four 96-wells of a V-bottom plate (#249570; ThermoFisher Scientific, Waltham, MA, USA). The plate was centrifuged at RT for 3 min at 300*g and cells were stained with or without being fixed and permeabilized first. In case of fixation-and-permeabilization being applied, which was the case for half of the wells, each pellet was reconstituted in 100 µL of fixation buffer (2% formaldehyde

in DPBS) (made from Pierce™ 16% Formaldehyde (w/v); #28908; ThermoFisher Scientific, Waltham, MA, USA). After 15 min incubation at RT, cells were washed and reconstituted in 100 µL permeabilization buffer (1% BSA-DPBS with 0.1% saponin) (#47036; Merck Life Sciences, Darmstadt, Germany). After 15 min incubation at RT, cells were washed again. Washing steps consisted of centrifuging the plates at RT for 3 min at 300**g*, reconstituting the pellets in 200 µL FACS buffer and centrifuging again. Subsequently, all samples were reconstituted in 10 µL FcR Blocking Reagent (#130-059-901; Miltenyi Biotec, Bergisch Gladbach, Germany) and incubated for 10 min at 4°C in the dark. Afterwards, 90 µL RAGE polyclonal antibody (1:50 dilution in FACS buffer; validated for the epitope being on the V-domain of RAGE) (#PA5-24787; ThermoFisher, Waltham, MA, USA) was added to a permeabilized and a non-permeabilized sample. To the other two samples, 90 µL FACS buffer was added which served as negative control to help differentiate non-specific background signal from specific antibody signal. Samples were incubated for 30 min at 4°C in the dark. After washing, all samples were reconstituted in 100 µL Alexa Fluor 647 Goat Anti-Rabbit IgG recombinant antibody (1:200 dilution in FACS buffer) (#A27040; ThermoFisher, Waltham, MA, USA). After incubating for 30 min at 4°C in the dark, cells were washed and reconstituted in 100 µL FACS buffer to be analysed on the CytoFLEX Flow Cytometer (Beckman Coulter, Fullerton, CA, USA). For each sample, 10,000 cells were measured at a speed of 10 µL/min. Data was analysed in CytExpert Software (Beckman Coulter, Fullerton, CA, USA). First, debris was excluded based on SSC-A vs FSC-A gating, whereafter doublets were excluded by FSC-H vs FSC-A and SSC-H vs SSC-A gating. Based on this gating strategy, percentage of positive cells and median fluorescent intensity (MFI) (APC channel) were determined. The former parameter is defined as the percentage of positive cells in the sample of interest relative to 1% positive cells in the corresponding negative control sample (stained without primary antibody), whereas the latter is defined as the MFI of the sample of interest corrected by subtraction for the MFI of the corresponding negative control sample.

Experimental exposure

To investigate the inflammatory responses of the primary immune cells to the experimental conditions, supernatant was removed, experimental conditions were added in duplicate (500 µL/well) and incubated for 24 h (37°C, 5% CO_2 at saturating humidity). These experimental conditions included four different LPS concentrations (1 ng/mL, 1 pg/mL, 1 fg/mL, culture medium) combined with a RAGE agonist (HMGB1 or Aβ-42; 1 µg/mL) (resp. #HM-115; HMGBiotech, Milan,

Italy / #HB9805; Hello Bio, Dunshaughlin, Ireland) or not. After the 24 h incubation, supernatant was collected and stored at -20°C. Cells were lysed with 500 µL/well TRIzol (#15596018; ThermoFisher Scientific, Waltham, MA, USA) and RNA extraction was performed subsequently.

RNA extraction, cDNA synthesis, and qPCR analysis

RNA was extracted and purified using a RNeasy kit (#74104; Qiagen, Venlo, The Netherlands) including DNase digestion by the RNase-Free DNase Set (#79256; Qiagen, Venlo, The Netherlands). First, 200 µL chloroform per mL of TRIzol as added and mixed by inverting. After 2–3 min incubation at RT, samples were centrifuged at 12,000**g* for 15 min at 4°C. The aqueous phase was collected and 70% ethanol was added at 1.5 times the volume. This mixture was transferred to the RNeasy kit spin columns and centrifuged at 10,000**g* for 30 sec. Subsequently, 350 µL of buffer RW1 was added and centrifuged at 10,000**g* for 30 sec. DNase stock was diluted 1:7 with buffer RDD (both from DNase kit) and per column, 80 µL was added and incubated for 15 min at RT. Columns were washed once with 350 µL buffer RW1 and twice with 500 µL RPE buffer (centrifugation at 10,000**g* for 30 sec). Spin with open lid at 10,000**g* for 2 min and elute sample by adding 30 µL RNAse-free water to the column and centrifuging it at 10,000**g* for 1 min. RNA quantity was determined using Nanodrop One (ThermoFisher Scientific, Waltham, MA, USA), and cDNA was synthesized using iScript kit (#1708891; Bio-Rad, Hercules, CA, USA). Per six genes of interest, 15 µL of the RNA samples (200 ng RNA in nuclease-free water) was mixed with 5 µL of mastermix (Reverse Transcriptase diluted in iScript reaction mix; 4:1) and incubated in a thermal cycler according to the following protocol: 5 min at 25°C > 20 min at 46°C > 1 min at 95°C > Hold at 4°C. cDNA samples were diluted three-times with nuclease free water and stored at -20°C until further qPCR analysis.

qPCR analysis were performed on a CFX96 Touch Real-Time PCR Detection System (Bio-Rad, Hercules, CA, USA). Each reaction contained 5 µL cDNA, 10 µL iQ™ SYBR Green (#1708882; Bio-Rad, Hercules, CA, USA) and 2.5 µL of forward and reverse primers (3.2 µM), to a total volume of 20 µL. Cycling conditions were as follows: 95°C for 3 min, followed by 39 cycles of 95°C for 10 sec and 60°C for 30 sec. All reactions were run in duplicate. The primers used were designed using primer databases and synthesized by Biolegio (Nijmegen, the Netherlands). Primer efficiency was determined using standard curves from serial dilutions of pooled cDNA samples (1x, 10x, 100x, 1,000x and 10,000x with Ultrapure water). Cycling

conditions were as previously described, but a melting curve was added to check specificity of each pair of primers: 95°C for 10 sec, 65°C for 5 min, and a continuous raise in temperature to 95°C at 0.5°C/s ramp rate followed by 95°C for 5 sec. The PCR products were checked for the absence of primer dimers by electrophoresis (80 V, 25 min) on a 2% agarose gel stained by SYBR™ safe (#S33102; ThermoFisher Scientific, Waltham, MA, USA). The primers with PCR efficiency values between 90% and 110% and R^2 of standard curves higher than 0.98 were selected, leading to the primers as described in Supplementary Table S5.1.

The stability test was performed by qbase+ software (v3.4, Biogazelle, Gent, Belgium). RPLP0, β-actin, and HPRT1 were selected as housekeeping genes (geNorm M value <1.5 and coefficient of variation <0.5). Relative gene expression was calculated using the efficiency-corrected geometric mean normalization approach [17]:

$$\frac{(E_{GOI})^{\Delta Ct\ GOI}}{GeoMean[(E_{REF})^{\Delta Ct\ REF}]}$$

Fold changes in gene expression were expressed relative to the control group (medium control). Ct values >35 were considered below detection limit, which was the case in all samples for NOX1.

Cytokine analysis: ELISAs

IL-1β, IL-6 and TNF-α levels were quantified with Human Duoset ELISA kits (resp. #DY201, #DY206 and #DY210; Bio-Techne, Minneapolis, MN, USA). Manufacturer protocol was followed, however TMB substrate, supersensitive, for ELISA (#T4444; Merck Life Sciences, Darmstadt, Germany) was used as substrate solution. Supernatants were tested at two-times dilution. Absorbance was measured at 450 nm and 540 nm using a Spectramax® M2 (Molecular Devices, San Jose, CA, USA). For data analysis, the OD values (450–540 nm) of technical duplicates were averaged and corrected for the blank. Sample concentrations were determined by interpolating these OD values against the standard curve by GraphPad Prism 9 (GraphPad Software, La Jolla, CA) and correcting them for the dilution factor. For samples with an average OD value below the LLOQ, the concentration was considered zero.

THP1 Lucia's

Culturing and differentiation

THP1-Lucia™ NF-κB cells (#thpl-nfkbv2; InvivoGen, Toulouse, France) were thawed from liquid nitrogen (4.0 x 10^6 cells/mL in 90% FBS-DMSO) at 37°C using a water bath. The suspension was transferred into 9 mL of pre-warmed RPMI-1640-Glutamax supplemented with 20% FBS and 1% P/S, then centrifuged at 300**g* for 3 min at RT. The pellet was resuspended in 5 mL of the same culture medium and maintained in suspension in a T25 flask (37°C, 5% CO_2, saturating humidity). Cells were allowed to recover for two weeks, during which medium was replaced three times a week by centrifugation (3 min, 300**g*, RT), retaining 20% conditioned medium. Following recovery, cell density was determined using a TC-20 Cell Counter (Bio-Rad; Hercules, CA, USA), and cultures were adjusted to 6.0 x 10^5 live cells/mL. Medium replacement (retaining 20% conditioned medium) and density measurements were subsequently performed twice a week. Cultures were kept below 2.0 x 10^6 live cells/mL by subculturing at a 1:2 or 1:3 ratio as needed. Every third passage, Zeocin® (#ant-zn-1; InvivoGen, Toulouse, France) was added to the culture medium at 100 µg/mL. Cell culture experiments were performed only after the second passage post-thaw and up to passage number 22. For experimental use, cells were seeded in 96-well plates at 1.0 x 10^6 live cells/mL (100 µL/well; retaining 20% conditioned medium) and incubated with 100 ng/mL Phorbol 12-myristate 13-acetate (PMA) (P1585; Merck Life Sciences, Darmstadt, Germany). After 48 hours, cells were washed twice with culture medium (100 µL/well) to remove PMA and subsequently maintained until day 7 for experiments.

Experimental exposure

To investigate the inflammatory responses of THP1-Lucia™ NF-κB cells to the experimental conditions, supernatant was removed, experimental conditions were added in duplicate (100 µL/well) and incubated for 24 h (37°C, 5% CO_2 at saturating humidity). These experimental conditions included different RAGE agonists (HMGB1 variants and Aβ-42; 1 µg/mL) (resp. #HM-031; HMGBiotech, Milan, Italy / #HB9805; Hello Bio, Dunshaughlin, Ireland) alone or combined with low-dose LPS (0.1 ng/mL). High-dose LPS (50 ng/mL) was used as positive control for inflammation. In a follow-up experiment, cells were pre-included at 37°C for 30 min with either FPS-ZM1 (10 µM) (#553030; Merck Life Sciences, Darmstadt, Germany) or 24 h-glycated beta-lactoglobulin (100 µg/mL) [13] before being exposed to the combination of reduced HMGB1 and low-dose LPS. In parallel, reduced HMGB1

(#HM-115; HMGBiotech, Milan, Italy) was pre-incubated with sRAGE (5 µg/mL) (#RD172116100; BioVendor R&D, Brno, Czech Republic). After the 24 h exposure period, supernatant was collected and stored at -20°C. To measure their metabolic activity, cells were incubated with 110 µL/well WST-1 mixture, a 1:10 dilution of WST-1 reagent (#CELLPRO-RO; Merck Life Sciences, Darmstadt, Germany) in cell culture medium. As positive control for cell death, 10 seconds pre-exposure to 10 µL 70% 2-propanol (#8167045000; Actu-All Chemicals, Oss, The Netherlands) was included. After 120 min incubation at 37°C (5% CO_2 at saturating humidity), absorbance was measured at 450 and 595 nm with Multiskan Ascent Microplate reader (ThermoFisher Scientific, Waltham, MA, USA). For data analysis, OD values at 450 nm were corrected by subtracting the corresponding values at 595nm, and technical duplicates were averaged.

Cytokine analysis: Legendplex

A panel of inflammatory markers in the supernatant were quantified by LEGENDplex™ Human Macrophage/Microglia Panel (13-plex) (#740503; BioLegend, San Diego, CA, USA). Manufacturer protocol was followed. Samples were diluted two-times and measured in duplicate. The level of eight analytes was either above (arginase) or below detection limit (IL-12p70, IL-4, IL-10, TARC, IL-12p40, IL-23, and IFN-γ) for all samples. Values below detection limit were considered zero, and technical duplicates were averaged.

Luminescence

Supernatant (10 µL, undiluted) was added in duplicate to a white, 96-well plate (#82050-736; Avantor/VWR, Radnor, PA, USA). Luminometric assay was performed with a Fluoroskan Ascent FL (ThermoFisher Scientific, Waltham, MA, USA). Per well, 50 µL Quanti-Luc (rep-qlc1; InvivoGen, Toulouse, France) was automatically injected and 4 sec later luminescent signal was measured for 100 ms, resp. lag and integration time. For data analysis, technical duplicates were averaged.

Statistical analysis

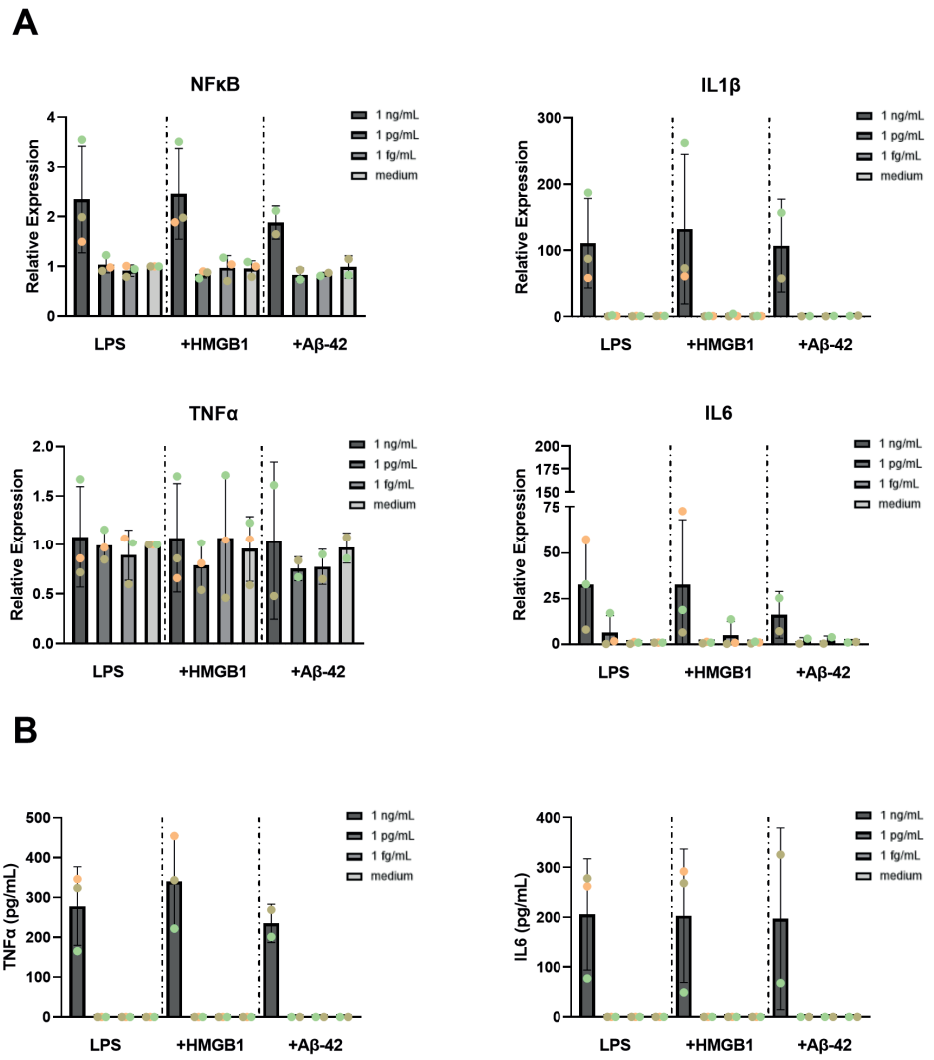
All primary cell culture experiments were repeated at least 3 times (n=3), with different donor material. Results are stated as mean ± SD from these independent experiments. Two-way repeated measure analysis of variance (ANOVA) was used for statistical analysis in IBM SPSS statistics 25 (SPSS Inc., Chicago, IL, USA). The within-subject factors included being LPS concentration and RAGE agonist. Greenhouse-Geisser corrections were applied to account for potential violations

of sphericity due to small sample size. When factors showed significance (p-value of ≤0.05), the LSD method was used for pairwise comparisons. All graphs were created using GraphPad Prism 9 (GraphPad Software, La Jolla, CA).

References

1. Zahir A, Ge Z, Khan IA. Public Health Risks Associated with Food Process Contaminants – A Review. J Food Prot 2025;88:100426. https://doi.org/10.1016/J.JFP.2024.100426.
2. van Dongen KCW, Linkens AMA, Wetzels SMW, Wouters K, Vanmierlo T, van de Waarenburg MPH, et al. Dietary advanced glycation endproducts (AGEs) increase their concentration in plasma and tissues, result in inflammation and modulate gut microbial composition in mice; evidence for reversibility. Food Research International 2021;147:110547. https://doi.org/10.1016/J.FOODRES.2021.110547.
3. Tessier FJ, Niquet-Léridon C, Jacolot P, Jouquand C, Genin M, Schmidt A-M, et al. Quantitative assessment of organ distribution of dietary protein-bound 13C-labeled Nε-carboxymethyllysine after a chronic oral exposure in mice. Mol Nutr Food Res 2016;60:2446–56. https://doi.org/10.1002/MNFR.201600140.
4. Nogueira Silva Lima MT, Delayre-Orthez C, Howsam M, Jacolot P, Niquet-Léridon C, Okwieka A, et al. Early- and life-long intake of dietary advanced glycation end-products (dAGEs) leads to transient tissue accumulation, increased gut sensitivity to inflammation, and slight changes in gut microbial diversity, without causing overt disease. Food Research International 2024;195:114967. https://doi.org/10.1016/J.FOODRES.2024.114967.
5. Linkens AMA, Houben AJHM, Niessen PM, Wijckmans NEG, de Goei EEC, Van den Eynde MDG, et al. A 4-week high-AGE diet does not impair glucose metabolism and vascular function in obese individuals. JCI Insight 2022;7. https://doi.org/10.1172/JCI.INSIGHT.156950.
6. Snelson M, Lucut E, Coughlan MT. The Role of AGE-RAGE Signalling as a Modulator of Gut Permeability in Diabetes 2022.
7. Kierdorf K, Fritz G. RAGE regulation and signaling in inflammation and beyond. J Leukoc Biol 2013;94:55–68. https://doi.org/10.1189/jlb.1012519.
8. Lin L, Park S, Lakatta EG. RAGE signaling in inflammation and arterial aging. Front Biosci 2009;14:1403. https://doi.org/10.2741/3315.
9. Xie J, Reverdatto S, Frolov A, Hoffmann R, Burz DS, Shekhtman A. Structural Basis for Pattern Recognition by the Receptor for Advanced Glycation End Products (RAGE). Journal of Biological Chemistry 2008;283:27255–69. https://doi.org/10.1074/JBC.M801622200.
10. Xue J, Rai V, Singer D, Chabierski S, Xie J, Reverdatto S, et al. Advanced glycation end product recognition by the receptor for AGEs. Structure 2011;19:722–32. https://doi.org/10.1016/j.str.2011.02.013.
11. Zhao D, Sheng B, Wu Y, Li H, Xu D, Nian Y, et al. Comparison of Free and Bound Advanced Glycation End Products in Food: A Review on the Possible Influence on Human Health. J Agric Food Chem 2019;67:14007–18. https://doi.org/10.1021/acs.jafc.9b05891.
12. Jansen FAC, Fogliano V, Rubert J, Hoppenbrouwers T. Dietary Advanced Glycation End products interacting with the intestinal epithelium: What do we really know? Mol Metab 2023;73. https://doi.org/10.1016/J.MOLMET.2023.101734.
13. Jansen FAC, Rubert J, van Norren K, Fogliano V, Hoppenbrouwers T. Seeking standardized in vitro models of AGE-RAGE signaling in the physiological perspective of glycated dietary proteins. Int J Biol Macromol 2025;318. https://doi.org/10.1016/j.ijbiomac.2025.144889.
14. Lopez-Castejon G, Brough D. Understanding the mechanism of IL-1β secretion. Cytokine Growth Factor Rev 2011;22:189. https://doi.org/10.1016/J.CYTOGFR.2011.10.001.
15. Sun SC. The non-canonical NF-κB pathway in immunity and inflammation. Nat Rev Immunol 2017;17:545. https://doi.org/10.1038/NRI.2017.52.
16. Tian J, Avalos AM, Mao S-Y, Chen B, Senthil K, Wu H, et al. Toll-like receptor 9-dependent activation by DNA-containing immune complexes is mediated by HMGB1 and RAGE 2007. https://doi.org/10.1038/ni1457.
17. Vandesompele J, De Preter K, Pattyn F, Poppe B, Van Roy N, De Paepe A, et al. Accurate normalization of real-time quantitative RT-PCR data by geometric averaging of multiple internal control genes. Genome Biol 2002;3:1–12. https://doi.org/10.1186/GB-2002-3-7-RESEARCH0034/COMMENTS.

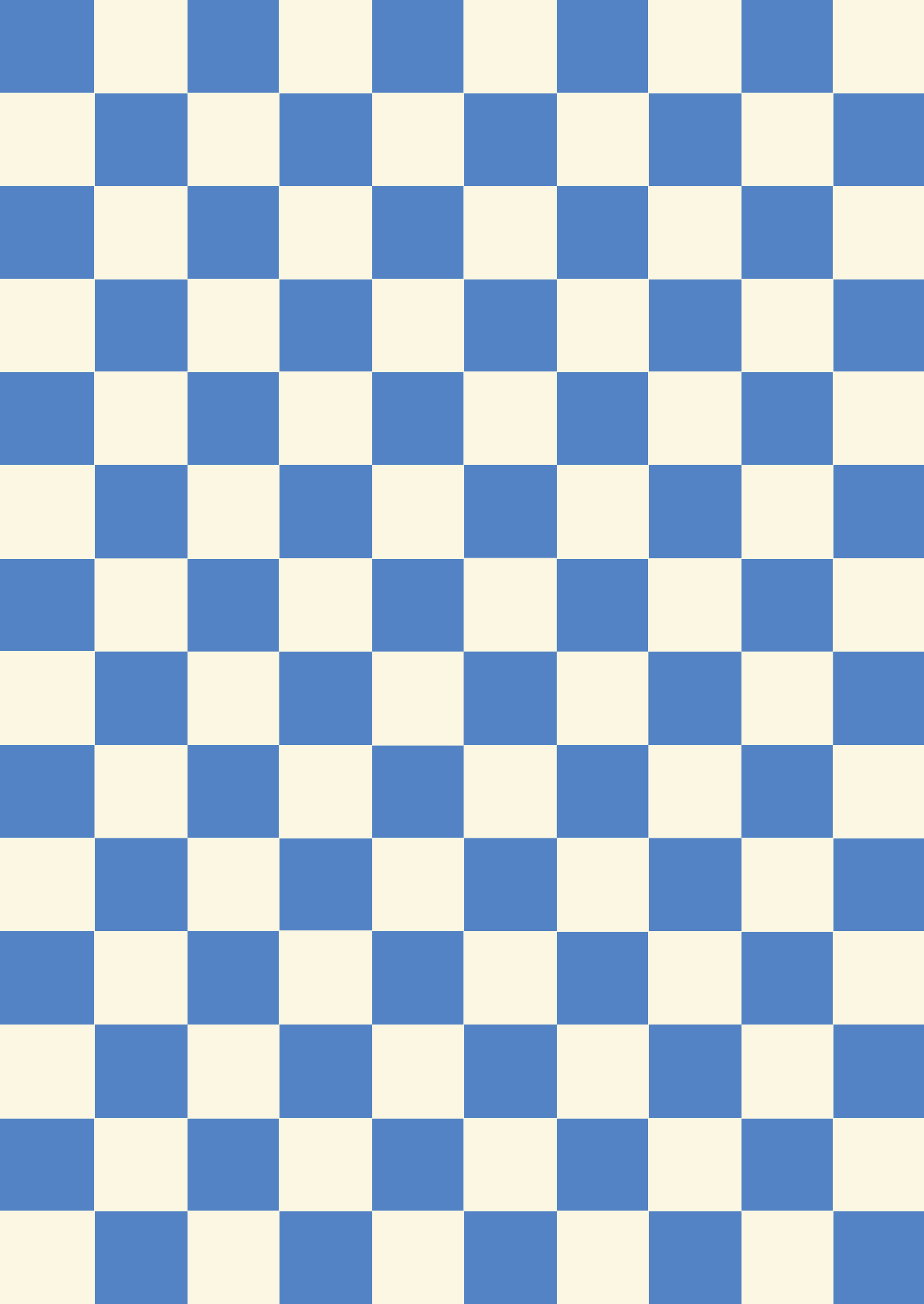
Supplementary information



Supplementary Figure S5.1: Relative NF-κB, IL6, TNFα and IL1β gene expression **(A)** and TNFα and IL6 cytokine secretion **(B)** of M-CSF differentiated M0 macrophages substantially expressing surface RAGE, after 24 h exposure to different concentrations of LPS alone or combined with HMGB1 and Aβ-42 (1 µg/mL). Gene expression results are expressed relative to medium control. Data are mean ± SD of four independent donor experiments; dots of different colours represent individual donors.

Supplementary Table S5.1: qPCR primer information

Gene name	Full name	Direction	Sequence (5' -> 3')	Tm (°C)	Working concentration (µM)	Primer efficiency	Source
NF-κB	Nuclear Factor Kappa B	Forward Reverse	TGAGTCCTGCTCCTTCCA GCTTCGGTGTAGCCCATT	61.0 61.0	3.2	97.4%	Primer Bank (NM_003998.2)
TNFα	Tumor Necrosis Factor Alpha	Forward Reverse	CTGCTGCACTTTGGAGTGAT AGATGATCTGACTGCCTGGG	62.0 63.0	3.2	97.7%	Primer Bank (NM_000594)
IL-6	Interleukin 6	Forward Reverse	AGCCACTCACCTCTTCAGAAC GCCTCTTTGCTGCTTTCACAC	63.0 64.0	3.2	100%	Primer Bank (NM_000600.2)
IL-1β	Interleukin 1 Beta	Forward Reverse	GTGGCAATGAGGATGACTTGTTC TAGTGGTGGTCGGAGATTCGTA	63.0 64.0	3.2	91.8%	Primer Bank (NM_000576.2)
NOX-1	NADPH Oxidase 1	Forward Reverse	CTGCTTCCTGTGTGTCGCAA AGGCAGATCATATAGGCCACC	63.0 60.9	3.2	100%	Primer Bank (NM_007052.4)
β-actin	Bèta-Actin	Forward Reverse	CTGGAACGGTGAAGGTGACA AAGGGACTTCCTGTAACAATGCA	64.0 64.0	3.2	94.3%	Primer Bank (NM_001101)
RPLP0	Ribosomal Protein Lateral Stalk Subunit P0	Forward Reverse	AGCCCAGAACACTGGTCTC ACTCAGGATTTCAATGGTGCC	60.9 60.3	3.2	93.9%	Primer Bank (NM_001002.3)
HPRT1	Hypoxanthine Phosphoribosyltransferase 1	Forward Reverse	CCTGGCGTCGTGATTAGTGAT AGACGTTCAGTCCTGTCCATAA	61.9 60.5	3.2	94.3%	Primer Bank (NM_000194.2)



6

General discussion

Recap of thesis outline

The browning process that gives cooked foods their appealing aromas, flavors and textures is known as the Maillard reaction. This non-enzymatic reaction between proteins and sugars, also referred to as protein glycation, leads to the formation of covalent adducts on lysine and arginine residues. Because many structurally distinct adducts have been identified, they are collectively called advanced glycation end products (AGEs). Following the discovery of glycated hemoglobin (HbA1c) as a diagnostic marker for diabetes in the 1960s, endogenous protein glycation was shown to be relevant to human disease, which subsequently raised concerns about the safety of dietary AGEs. These concerns were reinforced when high consumption of processed foods in the Western diet became associated with an increased risk of the same non-communicable diseases.

Although dietary AGEs are structurally similar to endogenous AGEs, they cannot be considered the same in terms of biological activity. Where endogenous AGEs are generated in the body and directly affect body protein functionality, dietary AGEs enter the body through the digestive tract. In this context, the intestine would be their primary target organ and possibly the only tissue to encounter undigested glycated dietary proteins that can potentially trigger inflammatory processes, possibly mediated by the AGE receptor (RAGE). However, as current literature predominantly focuses on the systemic effects of dietary AGEs, their impact at the intestinal level remains largely unknown. Yet, since intestinal health is known to play a key role in general wellbeing through the gut-brain-axis, it may represent a critical link between dietary AGEs and systemic health outcomes. **Therefore, this thesis aimed to increase our understanding of how intact dietary glycated proteins affect intestinal health at the epithelium and immune level, using *in vitro* models**. This was accomplished by:

- Evaluating the current literature on dietary AGEs and their interaction with the intestinal epithelium. Both *in vivo* and *in vitro* studies were included. Methodological limitations were identified especially considering the published *in vitro* work, including limited chemical characterization of the glycated samples, limited endotoxin quantification of the samples, and no inclusion of an AGE-independent positive control for RAGE activation (e.g. alarmins) (**Chapter 2**);
- Assessing the translocation of a glycated food protein across the intestinal epithelium. In a human ileum-derived 2D organoid model, it was

shown that both glycated monomers as well as high molecular weight aggregates are able to pass this barrier, likely by paracellular transport. Specialized epithelial structures overlaying the Payers patches might favour translocation of glycated monomers, this would facilitate interaction of glycated proteins with the intestinal immune system (**Chapter 3**);

- Testing the inflammatory potency of glycated food proteins in a primary immune cell model. *In vitro* models were shown to primarily express RAGE intracellularly. In primary immune cells with substantial surface RAGE, any pro-inflammatory response observed could be blocked by a LPS scavenger. Since LPS levels in this sample would have been considered neglectable based on its quantification assay, we showed that LPS interference cannot be ruled out solely based on such assays (**Chapter 4**);
- Seeking for an AGE-independent positive control for RAGE activation. RAGE agonists Aβ-42 and HMGB1, either alone or combined with LPS at different concentrations, did not induce a pro-inflammatory response in the primary immune model known to express surface RAGE. Only in one occasion, when NF-κB was assessed directly in a genetically modified immune cell line, an amplification of the LPS effect by HMGB1 could be observed. This indicates that RAGE activation might require a combination of stimulatory factors and that alternative NF-κB pathways might be involved. However, no conclusions can be drawn as the results were inconsistent (**Chapter 5**).

Figure 6.1 summarizes these results in a workflow scheme that integrates the different research chapters of this PhD thesis. In the current chapter, the findings from **Chapters 2–5** discussed in context of the current literature. This chapter aims to extend this discussion beyond the initial scope of this thesis, focusing on the broader perspective of dietary AGE consumption and its implications for human health. To conclude, my perspectives on the future directions of dietary AGE research will be presented.

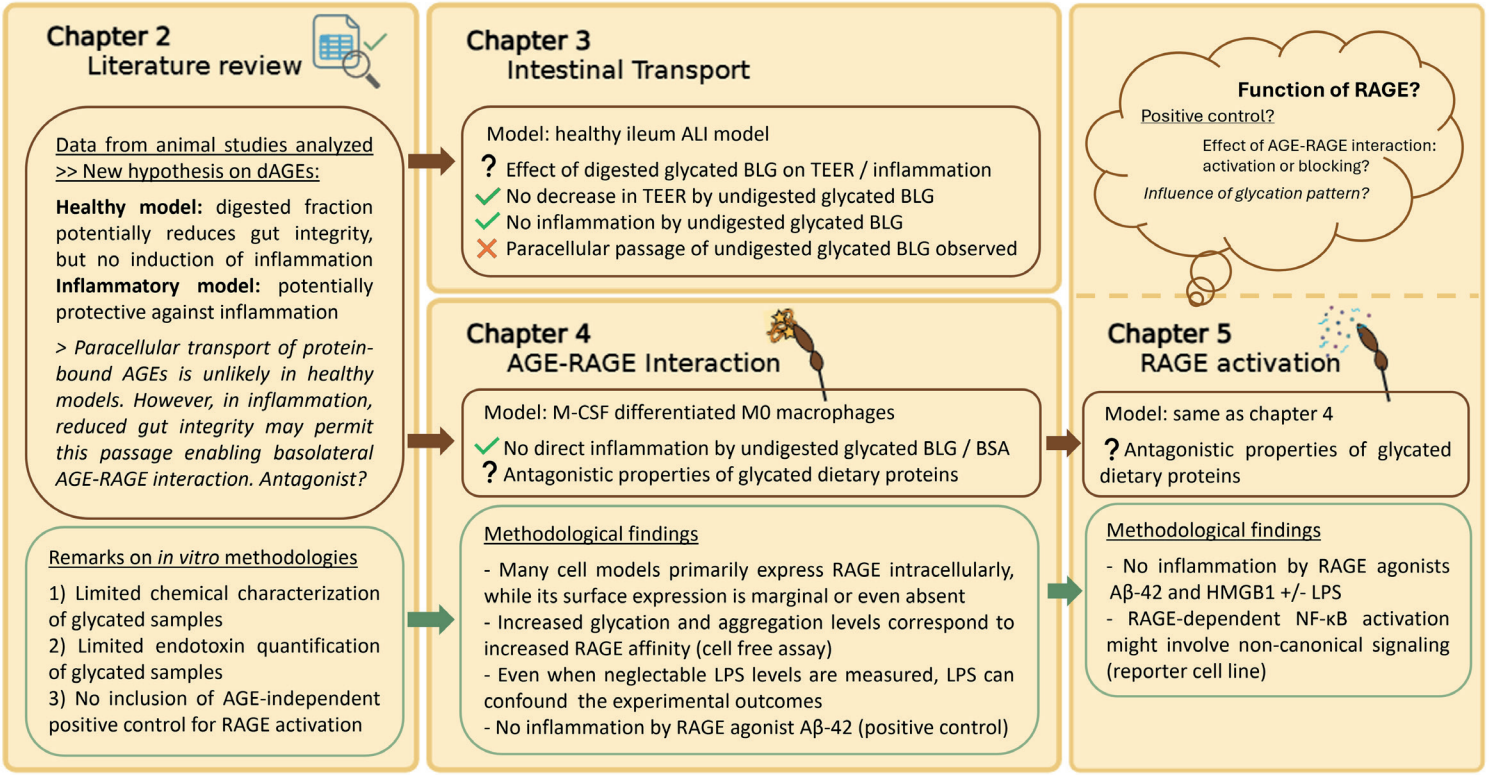


Figure 6.1: Schematic overview of the results from the different research chapters. Aim of the thesis was to increase our understanding of how intact dietary glycated proteins affect intestinal health at the epithelium and immune level, using *in vitro* models. ✗ implies that results did not support statements of Chapter 2, ✓ implies that results support statements of Chapter 2, and ? implies that experiments did not and/or could not cover this statement yet.

Glycated dietary proteins: biological effects of a high-AGE diet

In the research chapters of this thesis (**Chapters 2–5**), we focused on intact glycated dietary proteins related to the intestinal epithelium and intestinal immune system. However, the biological effects of a high-AGE diet go beyond this topic, as it is described to reduce protein digestibility and bioavailability, exert systemic effects, and alter the gut microbiota.

Digestion of dietary AGEs

In our diet, most AGEs are present in protein-bound form [1]. Like all dietary proteins, these glycated proteins are broken down by digestive enzymes (such as pepsin, trypsin and other proteases) into small peptides and single amino acids. These digestion products are then absorbed by enterocytes and enter the systemic circulation, where they are primarily used as building blocks for protein synthesis throughout the body. Early *in vitro* studies showed that protein digestibility decreases with increased level of glycation, mainly because glycation promotes protein aggregation and reduces the accessibility of enzyme cleavage sites [2–5]. Therefore, it was expected that the overall amino acid bioavailability would be lower from glycated proteins, reflected as reduced postprandial plasma levels. However, recent human intervention studies only observed such effect for lysine, which is the only amino acid, together with arginine, directly reacting with sugars to form glycation adducts [6–8]. Thus, although *in vitro* experiments show reduced digestibility of glycated proteins, human data indicates that only the bioavailability of lysine is substantially affected. This suggests that glycation primarily reduces amino acid availability through chemical modification of specific amino acids (mainly lysine), while the impact of reduced protein digestibility is minimal.

Lysine is an essential amino acid for humans. Because we cannot synthesize it ourselves, we have to consume adequate amounts on a daily basis to prevent deficiencies. Long-term deficiency of one or more essential amino acids can lead to for example stunted growth in children and impaired immune function and muscle wasting in adults. The lower an individual's daily protein intake and/or the higher their daily amino acid requirement, the more important protein quality becomes in preventing such deficiencies [9]. This is determined by comparing the essential amino acid profile of a protein source (mg/g protein) to a reference pattern. Glycation lowers this protein quality by reducing the amount of available

lysine and can therefore contribute to protein inadequacy and malnutrition. This was already suggested in 1938 by Greaves et al. [10] who showed that lysine deficiency was the main cause of stunted growth in young rats fed a heated diet. In Western countries, however, protein intake typically exceeds the recommended dietary allowance, making the risk of amino acid deficiency low, even when protein quality is reduced [11]. For example, a standard recovery meal consisting of 20 g protein of reduced quality due to glycation did not impair post-exercise protein synthesis [7]. Nevertheless, decreased protein quality remains relevant for vulnerable populations such as infants, elderly and chronically ill patients [12,13]. In summary, in Western countries, reduced protein quality caused by glycation is primarily concerning for vulnerable individuals who already consume low or inadequate amounts of protein.

Systemic effects of dietary AGEs

In addition to reduced postprandial plasma lysine levels, a high-AGE diet results in increased plasma levels of free AGEs, such as CML, CEL and MG-H1[14]. Although some animal studies have also reported elevated plasma levels of protein-bound AGEs [15,16], most dietary AGEs are absorbed in the free or dipeptide form [4,17,18]. Once absorbed, diet-derived CML is distributed to a wide variety of tissues, excluding adipose tissue, as demonstrated in a mice study using isotopically labelled, dietary protein-bound CML [19]. These tissue CML levels did not differ between wildtype and RAGE knockout mice, showing that CML distribution is independent of RAGE function. In addition, another mice study indicated that this tissue distribution is not limited to only CML, as they reported increased levels of CML but also CEL and/or MG-H1 in liver and kidney upon high AGE intake [15]. In both mice studies, plasma and tissue AGE levels returned to baseline after switching back to a low-AGE diet, demonstrating reversibility [15,19]. This reversibility is likely linked to the absence of a dedicated storage pool for amino acids in the body, and it remains unclear whether deposited AGEs accumulate intra- or extracellularly. Either way, it is unlikely that diet-derived AGEs become incorporated into newly synthesized body proteins, which would lead to an increase in protein misfolding, as protein translation relies on a highly selective system. This system ensures accurate amino acid recognition through binding site composition, non-covalent interactions, error correction mechanisms and steric effects [20]. Thus, while diet-derived AGEs clearly reach multiple tissues, their precise fate and biological activity at the cellular level remain elusive.

Whether a high-AGE diet increases the risk of developing certain diseases remains a topic of debate. A recent well-controlled human intervention study found no effects on vascular parameters, however the intervention period was relatively short as it lasted only a few weeks [14]. Since long-term dietary interventions in humans are often limited by feasibility, we have to rely on animal models to study the long-term consequences of high AGE intake. In recent years, concerns have been raised regarding how these studies should be designed. Ideally, these studies should introduce purified glycated proteins rather than heat-treating the entire diet to avoid confounding factors [21]. In addition, they should quantify AGEs using LC/MS-MS, which is more specific and accurate than ELISA-based methods [22,23]. Many early animal studies reporting detrimental effects of high dietary AGE intake did not yet follow these methodological standards [24–27]. More recent studies show no disease development in healthy mice fed a high-AGE diet [16,28], whereas increased renal injury was observed in diabetic mice [29]. Besides differences in disease models, these divergent findings may relate to the specific AGEs predominant in the diet: CML in the former studies [16,28] vs. MG-H1 in the latter [29]. This is consistent with human observational studies showing that, in diabetic patients, serum MG-H1 but not serum CML is associated with nephropathy, next to serum MG-H1 being a stronger predictor of renal function decline [30,31]. However, LC-MS/MS-based data linking dietary intake of CML or MG-H1 to renal function is still lacking. For other health outcomes, including irritable bowel syndrome, insulin sensitivity, and microvascular function, no associations with habitual dietary AGE intake have been reported [32–34]. Overall, nephropathy is the only condition that has been linked to high AGE intake and more specifically to high MG-H1 intake. Although these findings are of interest, particularly considering the severity of the condition, they should be interpreted with caution at this stage as the available evidence is limited to a single study in diabetic mice and still lacks robust observational human data.

The fate of undigested dietary AGEs

Earlier, we discussed the fate and biological effects of dietary AGEs after digestion, which applies to the majority of dietary proteins. However, a fraction of the dietary protein also remains undigested and reaches the large intestine [35]. The size of this fraction varies by protein source and food processing methods [36]. A recent mice study shows that this fraction is below 12.5% for most protein sources, however in case of brown rice values over 50% were reported [37]. These differences were rather linked to individual protein characteristics than the overarching

plant vs. animal protein dichotomy. These undigested glycated proteins will move to the colon, where they can undergo microbial fermentation and can alter the abundance of different strains [38,39]. The related health implications of these microbiota shifts are still unclear and should not be necessarily negative.

Alternatively, the undigested glycated proteins could pass the intestinal barrier through the paracellular route. Initially, this only seemed relevant during disease, when leakiness of the intestinal barrier increases, as the space between epithelial cells was considered too narrow during homeostasis [40], as discussed in **Chapter 2**. However, contrary to these common assumptions [4], **Chapter 3** demonstrated that intact glycated proteins and their aggregates can pass the intestinal barrier of a healthy ileum ALI model, likely through paracellular transport. Although our model lacked some physiological complexity, such as food-matrix interactions and epithelial-mesenchymal crosstalk, this is consistent with reports showing that peanut proteins are detectable in human blood, with increased levels if gut integrity is compromised, for example upon strenuous exercise [41,42]. Furthermore, **Chapter 3** also suggested that passage of glycated monomers might be favored by the follicle-associated epithelium, which is overlaying intestinal lymphoid follicles. Together, these observations imply that dietary glycated proteins can come in physical contact with both intestinal epithelial cells and intestinal immune cells, most apparently facilitating dietary AGE-RAGE signaling which will be addressed later in this chapter.

Glycated dietary proteins: inflammatory properties

The research chapters of this thesis specifically addressed questions regarding the interaction of glycated dietary proteins with the intestinal epithelium and intestinal immune system. Firstly, by evaluating the current literature on this topic, background knowledge was provided in **Chapter 2**, including both animal and *in vitro* studies. The prevailing statement in literature is that both endogenous and dietary protein-bound AGEs drive inflammation through the receptor for advanced glycation end products (RAGE). Upon its activation, the production of pro-inflammatory cytokines and reactive oxygen species (ROS) gets increased through NADPH oxidases (NOX) and NF-κB signaling. However, based on data from animal studies, we concluded that, although the digested fraction might slightly compromise gut integrity, there is no concrete evidence that dietary glycated proteins induce inflammation in healthy models. This aligns with the findings of

the recent systematic literature review by Hellwig et al. [38], also reporting no increased intestinal inflammation upon high intake of dietary AGEs. Our *in vitro* work of **Chapter 3** further supported this conclusion as 2D human ileum organoids did not respond inflammatory to glycated beta-lactoglobulin. However, **Chapter 2** also presented an overview of the current *in vitro* evidence regarding the inflammatory properties of glycated dietary proteins, revealing inconsistent results across studies: while some papers reported pro-inflammatory responses, others observed no effect. Based on these publications, several methodological factors were identified that may have contributed to these mixed findings, including differences in glycation protocol, endotoxin contamination of the sample, and inadequate inclusion of the appropriate experimental controls. **Chapters 4 and 5** built on this foundation by experimentally investigating these methodological considerations, seeking for a standardized *in vitro* model to study the inflammatory properties of dietary AGEs.

Glycation protocol

Frequently used reducing sugars for the glycation of dietary proteins include glucose, glyceraldehyde, glycolaldehyde, methylglyoxal, glyoxal, and glyoxylic acid. In **Chapter 2**, we mentioned that removal of their residuals after the glycation process is necessary since especially highly potent glycating agents can be cytotoxic to cells. As a proof of principle, we confirmed this for glycolaldehyde in a preliminary experiment (Figure 6.2). We also mentioned that glycated proteins should be physiochemically characterized to be able to link specific modifications to observed effects, since the abundance of these modifications differs per glycation protocol. The type of reducing sugar used strongly affects the outcome, as they differ in potency and glycation pattern. For example, glyoxal favors the development of CML, while glyceraldehyde drives MG-H1 formation [29]. Moreover, also conditions such as temperature, heating time, pH, and moisture content affect the glycation outcome, for example related to denaturation and aggregation of the protein [43]. In **Chapter 4**, we heated beta-lactoglobulin with glucose at 40% humidity for different time periods. The longer the glycation protocol, the higher the levels of furosine, CML and CEL, the higher the amount of high molecular weight structures and the higher its affinity to sRAGE. When evaluating the overall glycation level of our model protein, this can be considered high, but not unrealistic. While our sample showed glycation levels up to 50% blocked lysine, dairy products like infant formula and sports supplements report values up to 44% [44,45]. Since the focus of this thesis directed towards evaluating RAGE-dependent

pro-inflammatory properties of these glycated proteins, and we already generated a glycated protein showing high RAGE affinity, we did not further evaluate how different reducing sugars or glycation conditions would affect this feature and/or its inflammatory potency. However, based on literature, certainly not all glycated proteins seem to bind RAGE, as for example CML-modified BLG and BSA lacked affinity to RAGE in a cell-free assay [46]. This might relate to CML being a non-crosslinking AGE. Therefore, glycation protocol and glycation pattern should be taken into consideration when designing certain experiments.

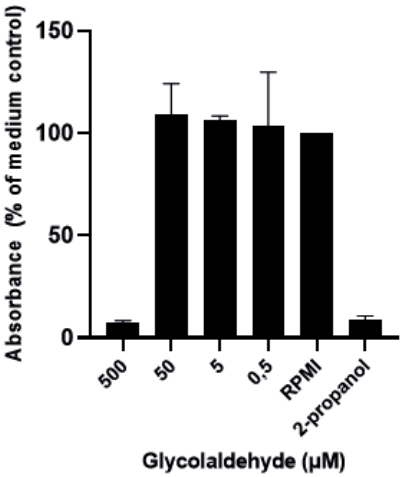


Figure 6.2: Cell viability of THP1 monocytes upon exposure to glycolaldehyde. Cells were exposed to glycolaldehyde (µM) for 24 h at 37°C (5% CO_2, saturated humidity). 2-propanol was included as positive control for cell death. Data is mean values ± SD obtained from technical duplicates.

Endotoxin contamination

In **Chapter 2**, we stated that *in vitro* studies should only be conducted after quantification of endotoxins in the sample and that, if they are detected, they need to be removed or neutralized first before conducting any experiment. In current literature, this measurement is only performed by part of the studies interested in the pro-inflammatory properties of glycated dietary proteins. Among the studies that quantified endotoxin levels and classified their samples as endotoxin-free, some reported pro-inflammatory responses [47,48], while others observed no effect [49]. The maximum endotoxin exposure of the cell cultures in these studies ranges from 0.6 pg/mL to 40 pg/mL, which is comparable to the levels reported in **Chapter 4** (0.3–31 pg/mL). Since these studies employed different immune models and used different cut-off values for classifying samples as endotoxin-free, direct

comparison of their outcomes is challenging. Nevertheless, when the data are considered together, glycated dietary proteins with the lowest maximal endotoxin levels (0.6 pg/mL) induced an inflammatory response in an immortalized cell line [47], whereas glycated dietary proteins with higher maximal endotoxin exposure (40 pg/mL) did not induce inflammation in a primary immune cell model that is generally considered more sensitive [49]. Although these studies did not determine whether the observed inflammatory response was attributed to endotoxin activity, this pattern aligns with our observation that endotoxin concentrations measured using commercial in-house quantification assays do not reliably predict whether an endotoxin-driven inflammatory response will occur, especially when levels are near the detection limit. Therefore, our statement in **Chapter 2** "If endotoxins are detected, …" should be rephrased: "Even if endotoxin levels appear neglectable or below detection limit, the possibility of endotoxin interference should be checked."

In our view, co-incubation with a LPS scavenger is the preferred strategy to assess potential endotoxin interference, as it allows dose-response testing without directly affecting receptor function. In our experiments, we used polymyxin B because it shows high specificity for LPS [50] and, to our knowledge, does not bind dietary proteins. However, when endotoxin concentrations are high, PMB may not fully neutralize its biological activity, as we observed when M-CSF differentiated M0 macrophages were exposed to 1 ng/mL LPS (Chapter 4, Supplementary Figure S4.3). Samples of glycated dietary proteins containing substantial amounts of endotoxin would therefore require an additional purification step. Several purification methods are being used, however because high endotoxin burdens are often accompanied by other contaminants, extraction with Triton X-114 has been described as superior to affinity column-based methods, as this method also removes other hydrophobic compounds [51]. Overall, implementing effective endotoxin removal and/or neutralization strategies is necessary to notice potential endotoxin-related cellular responses. This is primarily relevant in *in vitro* experiments, as in animal experiments the natural endotoxin exposure is already much higher through the diet and the microbiome-gut environment.

Positive controls

Besides AGEs, several other ligands are described to activate RAGE, most notably DAMPs,such as HMGB1, S100 proteins, heat-shock proteins, and cell-free DNA and mRNA [52]. As discussed in **Chapter 2**, when evaluating the pro-inflammatory effects of dietary AGEs *in vitro*, these DAMPs should serve as positive

controls to verify RAGE functionality in the chosen cell model, independent of the dietary AGEs being tested. However, we concluded that such controls are rarely included in the current literature. In our own preliminary experiments that aimed at selecting an appropriate positive control, we tested several commercial RAGE ligands (Aβ-42, S100A12, S100B, and different HMGB1 isoforms) in THP1-Lucia™ NF-κB monocytes. None of these ligands triggered a pro-inflammatory response, as assessed by NF-κB-dependent luciferase activity. To investigate this unexpected result, we examined RAGE expression by flow cytometry, and found that THP1-Lucia™ NF-κB monocytes primarily expressed RAGE intracellularly, with little to no surface expression. Although RAGE is widely depicted as a cell-surface receptor in the AGE literature [53–55], **Chapter 4** demonstrated that this predominant intracellular expression of RAGE is the norm for the majority of cell lines. We then found an *in vitro* model with clear surface expression of RAGE: primary M-CSF differentiated M0 macrophages. However, RAGE ligands (Aβ-42 and HMGB1) still failed to induce RAGE-dependent inflammation in these cells, either alone or in combination with LPS, as measured by both mRNA expression and protein secretion of pro-inflammatory cytokine (**Chapter 4 and 5**) (Figure 6.3).

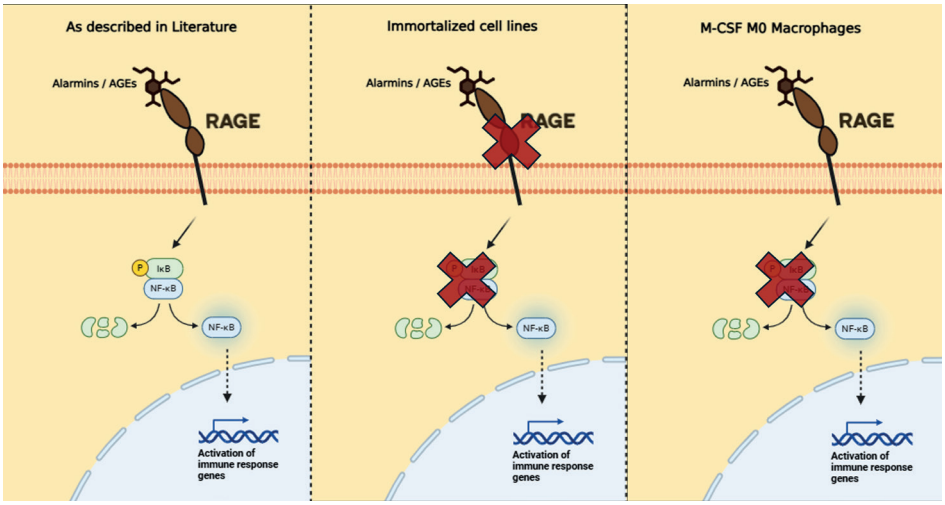


Figure 6.3: Schematic overview of RAGE localization and inflammatory signalling. In the AGE literature, RAGE is described as a cell surface receptor activating NF-κB signaling upon single ligand binding (e.g. AGEs and multiple alarmins). However, in our immortalized cell models, RAGE ligands failed to induce an inflammatory response. We found that this was related to RAGE being predominantly expressed intracellularly, with little to no surface expression. However, when we found a cell model with clear surface expression of RAGE – primary M-CSF differentiated M0 macrophages – these ligands still did not trigger inflammation. Figure created with BioRender.com.

In **Chapter 5**, we did observe one instance in which HMGB1 combined with LPS enhanced NF-κB activity in THP1-Lucia™ NF-κB M0 macrophages, however this response was not accompanied by increased levels of pro-inflammatory cytokines or chemokines. Taken together, these findings suggest that RAGE signaling may be more complex than the classical model of a surface receptor directly triggering innate immune pathways upon single ligand binding, which is the case for e.g. LPS-TLR4 interaction. Instead, RAGE activation may depend on a combination of inflammatory stimuli and/or affect alternative outcome measures.

RAGE functionality: DAMP transporter facilitating the activation of intracellular TLRs and the potential role of dietary glycated proteins

The function of RAGE has been extensively investigated across a wide range of diseases using RAGE knockout mice models, including pulmonary disease, cardiovascular disease, diabetes, and cancer. In general, RAGE deficiency exerted a protective effect on disease progression and/or complications. One of the main mechanisms involved is the recruitment and infiltration of immune cells into damaged or stressed tissue. RAGE deficiency has been shown to drastically reduce this infiltration, across multiple organ systems and disease models [56–66]. A possible link with DAMP signaling was hypothesized as DAMPs are known to be released through uncontrolled cell death upon acute tissue damage. In several studies, an increase of local and circulating DAMPs upon tissue injury was confirmed [61,64,66–68] and DAMP-neutralizing approaches were applied to further investigate RAGE-dependent DAMP signalling in immune cell recruitment [64]. It was shown that neutralization of either HMGB1 or cell-free DNA, released from ischemic myocardium, abolished myocardial infarct size in wildtype mice to a similar extent as knockout of RAGE achieved. In addition, combined administration of HMGB1 and cell-free DNA significantly increased infarct size, while administration of a single DAMP had no effect. This is in line with our observations in **Chapters 4 and 5** that administration of a single DAMP does not induce inflammation *in vitro*. Since the exacerbating effect was only observed in wildtype mice and not in RAGE deficient mice [64], a RAGE-dependent mechanism was suggested in which these DAMPs act interdependently to ensure immune cell infiltration.

That a combination of DAMPs is required to evoke a RAGE-dependent inflammatory response might relate to their ability to also activate other pattern recognition receptors such as TLR4 and TLR9 [69]. Interestingly, next to RAGE deletion, also deletion of these receptors seems to prevent DAMP-driven exaggerated tissue damage [64,68,70]. This suggests that RAGE and TLRs collectively contribute to the observed response. In this respect, RAGE has been described to facilitate the internalization of DAMPs, where they can more potently interact with TLRs [64,71–73]. For example, HMGB1-RAGE interaction is thought to facilitate cell-free DNA entering the cell and binding to intracellular TLR9 [64]. In this context, TLR9 ligand binding led to the immune cell activation, while RAGE rather acts as a transport protein instead of a receptor. RAGE facilitating the transport of DAMPs to enable the activation of cytosolic receptors was also suggested by Yang et al. [72], using a mice immune cell line. In **Chapter 5**, using primary human immune cells, we however failed to replicate their observation that TNFα mRNA expression is amplified by the combination of HMGB1 and LPS. A range of LPS concentrations was tested since such mechanisms might especially be relevant at suboptimal DAMP concentrations [74]. However, including other DAMPS able to activate TLR4/TLR9, such as heat-shock proteins, S100 proteins, and cell-free DNA, might have been more relevant to immune cell activation and recruitment upon sterile tissue injury, as LPS is not a DAMP being excreted by necrotic cells but a pathogen-associated molecular pattern. Since DAMP-driven immune cell activation has been shown to upregulate adhesion markers such as P-selectin glycoprotein ligand-1 (PSGL-1) and formyl peptide receptor 1 (FPR1) [75,76], to facilitate leukocyte rolling on vascular endothelium and chemotaxis towards sites of injury, the surface expression of these markers would also be an outcome measure of interest. So, combining our *in vitro* data with findings reported by *in vivo* studies, we propose that RAGE acts as a transporter requiring a specific combination of DAMPs to facilitate their internalization and subsequently activate intracellular TLRs, as depicted in Figure 6.4A.

In the context of this proposed mechanism, the role of glycated AGEs in shaping RAGE-mediated inflammation has to be re-evaluated. Possibly, RAGE is also involved in internalizing glycated proteins, however, since these proteins are not able to activate TLRs, this would not trigger TLR-signalling pathways as described for DAMPs like cell-free DNA and S100 proteins. Alternatively, the glycated protein aggregates might accumulate within the cell. At high concentrations, this might lead to increased cellular stress and apoptosis, since AGE modifications block lysine residues possibly impairing the ubiquitination and subsequent autophagic

degradation of these aggregates [77–79]. However, despite high levels of blocked lysine in our model protein, no reduction of mitochondrial activity was observed in primary human M0 macrophages under the experimental conditions of **Chapter 4**. Furthermore, we speculated in **Chapter 2** that undigested glycated proteins might act as partial agonists or even antagonists of RAGE, since an animal study reported that a diet high in glycated dietary proteins reduced inflammation in a DSS-induced colitis model [80]. This would imply that when glycated dietary proteins bind to RAGE, its capacity to transport TLR-activating DAMPs gets limited, as depicted in Figure 6.4B. However, currently, this hypothesis cannot be tested since a model robustly showing RAGE function is not yet available.

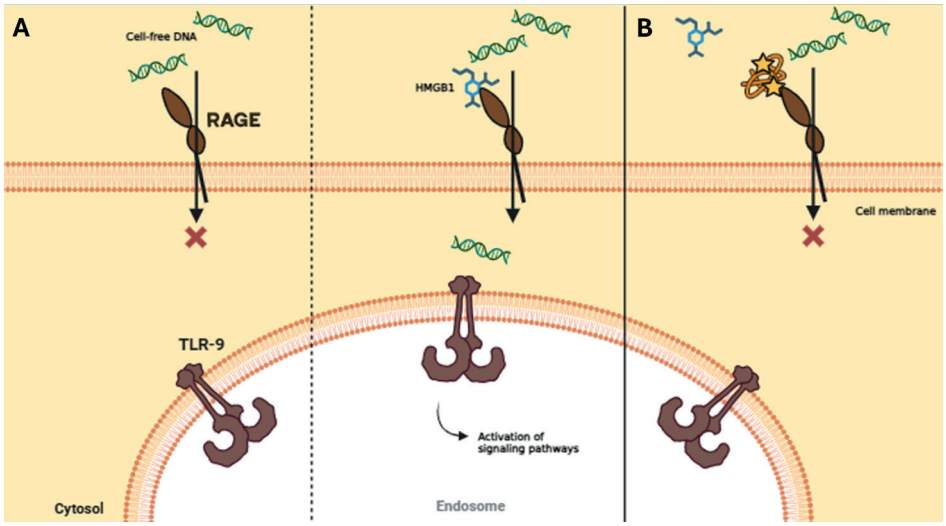


Figure 6.4: Hypothesis on RAGE functionality **(A)** and the role of glycated dietary proteins **(B)**. RAGE is suggested to act as a transport protein facilitating internalization of DAMPs, activating intracellular TLRs. For this mechanism, a combination of DAMPs is thought to be required, for example HMGB1 forming a complex with cell-free DNA that can be transported or HMGB1 changing the conformation of RAGE enabling cell-free DNA to enter the cell. In this context, glycated proteins might block the binding sites for the DAMPs, therefore hampering this transport. Figure created with BioRender.com.

Next to our attempt to develop such a model, combining RAGE agonists with LPS, targeting DAMP signaling, also alternative strategies to identify RAGE functionality to study the role of dietary glycated proteins *in vitro* could be proposed based on literature. Since RAGE has been proposed to also act as adhesion molecule itself [81], cell adhesion assays using different extracellular coatings (including glycated proteins) may be informative. Furthermore, in line with the transporter hypothesis,

RAGE has been suggested to the transcellular transport of oxytocin in epithelial and endothelial cells [82–87]. This could be evaluated using a transwell model, although the relevance of glycated proteins in this context is less clear. The same applies to the proposed role of RAGE in pathogen phagocytosis [88–91], which can be examined using a flow-cytometry-based live-bacteria phagocytosis assay. Other potential RAGE functions, such as its involvement in mitochondrial energy production [92] or epithelial-to-mesenchymal transition [63,93], are more challenging to model and manipulate *in vitro*. Taken together, DAMP-driven immune responses are most relevant and feasible to study the inflammatory potency of dietary glycated proteins in our view.

Future directions and societal relevance

So, supported by literature, RAGE has been proposed to function as a transporter that facilitates the internalization of DAMPs, rather than as a classical receptor that directly initiates inflammatory signaling upon ligand binding. These DAMPs would subsequently activate intracellular TLRs leading to an inflammatory response. Future *in vitro* studies should focus on establishing a reliable model showing this mechanism, for example by visualizing the internalization of DAMPs with fluorescent microscopy in combination with quantifying inflammatory outcome measures. In this regard, next to the standard NF-κB-signaling pathway readouts, tracking the expression of cell adhesion markers through flow cytometry could also be of interest considering the role of RAGE in immune cell recruitment. Subsequently, RAGE dependency could be confirmed by pre-incubation with known RAGE antagonists or RAGE deletion in the employed cell model.

Extending this concept to future *in vivo* studies on glycated dietary proteins and intestinal health, research should prioritize models of intestinal disease or injury (e.g. colitis) where endogenous DAMP levels are elevated, since glycated dietary proteins alone are unlikely to trigger immune activation in healthy individuals. However, in these diseased models, the overall picture becomes more complex as increased levels of sRAGE also modulate inflammatory responses by scavenging multiple RAGE ligands [94]. Therefore, to be able to design meaningful studies, the effect of dietary AGEs on RAGE-mediated pathways must be clarified first, specifically their function (co-factor, agonist, or inhibitor) and how this depends on the glycation protocol. As discussed before, developing a standardized *in vitro* model for RAGE function is an essential first step in this regard.

Nevertheless, the societal relevance of such studies can be questioned. Although scientifically interesting, the overall health impact of dietary AGEs is probably small, especially in the general population. In contrast, the consequences of endogenous AGE formation are well established, as glycation of endogenous proteins contributes to a broad spectrum of non-communicable diseases [95]. Accelerated AGE formation in diabetes, driven by increased glucose and MGO concentrations, is also a major contributor to diabetes-related complications [96]. Notably, a low-AGE diet did not improve renal burden or mitochondrial superoxide production in diabetic mice, whereas reducing endogenous AGE accumulation with alagebrium show protective effects [97], highlighting the clear discrepancy between dietary and endogenous AGEs in terms of biological impacts. Taken together, these observations suggest that further large-scale research efforts specifically targeting dietary AGEs are unlikely to yield substantial public health benefits. Overall, Western dietary patterns are far more harmful due to their high caloric density, high sugar content and low fiber intake, being key drivers of insulin resistance, than because of their AGE content per se. Yet, despite the well-established health consequences of these dietary patterns, adherence to healthier dietary choices remains a major challenge, as reflected by the rising prevalence of obesity and diabetes. Accordingly, additional research on dietary AGEs should be evaluated critically and is warranted only when driven by clearly defined research questions and well-founded hypotheses that justify its societal relevance.

Summary and concluding remarks

In summary, several mechanisms can be considered when evaluating how a high-AGE diet might influence health. First, it could contribute to lysine deficiency, as this essential amino acid becomes modified through glycation. However, in Western populations, the risk of lysine deficiency is low because total protein intake generally exceeds requirements. Second, some absorbed free AGEs, such as MG-H1, may have nephrotoxic effects, as suggested by a small number of mice studies [29]. Yet, LC-MS/MS-based human data linking the intake of specific dietary AGEs to renal function are still lacking. Moreover, observational and intervention studies using the well-established Maastricht University AGE database [22] have reported no associations between habitual dietary AGE intake and other health outcomes, including irritable bowel syndrome, insulin sensitivity, and microvascular function. A third potential route concerns the interaction between glycated dietary proteins and RAGE-expressing cells. Our *in vitro* data suggest that these

proteins can cross the intestinal barrier, however based on subsequent chapters, we propose that a combination of stimuli is required to induce RAGE-dependent inflammatory signaling, implying that glycated proteins alone are unlikely to induce inflammation in healthy individuals. Consequently, reducing total energy and sugar intake would likely yield greater health benefits than limiting dietary AGE intake. From this perspective, the societal relevance of further dietary AGE research, particularly in healthy populations, is limited.

References

1. Yuan X, Nie C, Liu H, Ma Q, Peng B, Zhang M, et al. Critical Reviews in Food Science and Nutrition Comparison of metabolic fate, target organs, and microbiota interactions of free and bound dietary advanced glycation end products Comparison of metabolic fate, target organs, and microbiota interactions of free and bound dietary advanced glycation end products. Food Sci Nutr 2021;63:3612–33. https://doi.org/10.1080/10408398.2021.1991265.
2. Zhao D, Li L, Le TT, Larsen LB, Xu D, Jiao W, et al. Digestibility of glycated milk proteins and the peptidomics of their in vitro digests. J Sci Food Agric 2019;99:3069–77. https://doi.org/10.1002/JSFA.9520.
3. Van Der Lugt T, Venema K, Van Leeuwen S, Vrolijk MF, Opperhuizen A, Bast A. Gastrointestinal digestion of dietary advanced glycation endproducts using an in vitro model of the gastrointestinal tract (TIM-1). Food Funct 2020;11:6297–307. https://doi.org/10.1039/D0FO00450B.
4. Zhao D, Sheng B, Wu Y, Li H, Xu D, Nian Y, et al. Comparison of Free and Bound Advanced Glycation End Products in Food: A Review on the Possible Influence on Human Health. J Agric Food Chem 2019;67:14007–18. https://doi.org/10.1021/acs.jafc.9b05891.
5. van Lieshout GAA, Lambers TT, Bragt MCE, Hettinga KA. How processing may affect milk protein digestion and overall physiological outcomes: A systematic review. Crit Rev Food Sci Nutr 2020;60:2422–45. https://doi.org/10.1080/10408398.2019.1646703.
6. Nyakayiru J, Van Lieshout GAA, Trommelen J, Van Kranenburg J, Verdijk LB, Bragt MCE, et al. The glycation level of milk protein strongly modulates post-prandial lysine availability in humans. British Journal of Nutrition 2020;123:545–52. https://doi.org/10.1017/S0007114519002927.
7. van Lieshout GA, Trommelen J, Nyakayiru J, van Kranenburg J, Senden JM, Gijsen AP, et al. Protein glycation compromises the bioavailability of milk protein-derived lysine in vivo in healthy adult males: a double-blind, randomized cross-over trial. Am J Clin Nutr 2025. https://doi.org/10.1016/J.AJCNUT.2025.01.025.
8. van Lieshout GA, Trommelen J, Hendriks FK, Nyakayiru J, van Kranenburg J, Senden JM, et al. Milk Protein Glycation Compromises Postprandial Lysine Bioavailability but does not Modulate Postprandial Muscle Protein Synthesis Rates In Vivo in Males: A Double-blind, Randomized Parallel Trial. J Nutr 2025;155:2215–26. https://doi.org/10.1016/J.TJNUT.2025.05.032.
9. Matthews JJ, Arentson-Lantz EJ, Moughan PJ, Wolfe RR, Ferrando AA, Church DD. Understanding Dietary Protein Quality: Digestible Indispensable Amino Acid Scores and Beyond. J Nutr 2025;155:3152–67. https://doi.org/10.1016/J.TJNUT.2025.07.005.
10. Greaves EO, Morgan AF, Loveen MK. The Effect of Amino-Acid Supplements and of Variations in Temperature and Duration of Heating Upon the Biological Value of Heated Casein: Two Figures. J Nutr 1938;16:115–28. https://doi.org/10.1093/JN/16.2.115.
11. Maleky F, Ahmadi L. Adhering to recommended dietary protein intake for optimizing human health benefits versus exceeding levels. RSC Adv 2025;15:9230–42. https://doi.org/10.1039/D4RA08221D.
12. Faiad J, Andrade MF, de Castro G, de Resende J, Coêlho M, Aquino G, et al. Muscle loss in cancer cachexia: what is the basis for nutritional support? Front Pharmacol 2025;16:1519278. https://doi.org/10.3389/FPHAR.2025.1519278.
13. Mendonça N, Granic A, Mathers JC, Hill TR, Siervo M, Adamson AJ, et al. Prevalence and determinants of low protein intake in very old adults: insights from the Newcastle 85+ Study. Eur J Nutr 2018;57:2713–22. https://doi.org/10.1007/S00394-017-1537-5.
14. Linkens AMA, Houben AJHM, Niessen PM, Wijckmans NEG, de Goei EEC, Van den Eynde MDG, et al. A 4-week high-AGE diet does not impair glucose metabolism and vascular function in obese individuals. JCI Insight 2022;7. https://doi.org/10.1172/JCI.INSIGHT.156950.

15. van Dongen KCW, Linkens AMA, Wetzels SMW, Wouters K, Vanmierlo T, van de Waarenburg MPH, et al. Dietary advanced glycation endproducts (AGEs) increase their concentration in plasma and tissues, result in inflammation and modulate gut microbial composition in mice; evidence for reversibility. Food Research International 2021;147:110547. https://doi.org/10.1016/J.FOODRES.2021.110547.
16. Teissier T, Quersin V, Gnemmi V, Daroux M, Howsam M, Delguste F, et al. Knockout of receptor for advanced glycation end-products attenuates age-related renal lesions. Aging Cell 2019;18. https://doi.org/10.1111/ACEL.12850.
17. Hellwig M, Geissler S, Matthes R, Peto A, Silow C, Brandsch M, et al. Transport of Free and Peptide-Bound Glycated Amino Acids: Synthesis, Transepithelial Flux at Caco-2 Cell Monolayers, and Interaction with Apical Membrane Transport Proteins. ChemBioChem 2011;12:1270–9. https://doi.org/10.1002/CBIC.201000759.
18. Grunwald S, Krause R, Bruch M, Henle T, Brandsch M. Transepithelial flux of early and advanced glycation compounds across Caco-2 cell monolayers and their interaction with intestinal amino acid and peptide transport systems. British Journal of Nutrition 2006;95:1221–8. https://doi.org/10.1079/BJN20061793.
19. Tessier FJ, Niquet-Léridon C, Jacolot P, Jouquand C, Genin M, Schmidt A-M, et al. Quantitative assessment of organ distribution of dietary protein-bound 13C-labeled Nε-carboxymethyllysine after a chronic oral exposure in mice. Mol Nutr Food Res 2016;60:2446–56. https://doi.org/10.1002/MNFR.201600140.
20. Kaiser F, Krautwurst S, Salentin S, Haupt VJ, Leberecht C, Bittrich S, et al. The structural basis of the genetic code: amino acid recognition by aminoacyl-tRNA synthetases. Scientific Reports 2020 10:1 2020;10:12647-. https://doi.org/10.1038/s41598-020-69100-0.
21. Delgado-Andrade C, Fogliano V. Dietary Advanced Glycosylation End-Products (dAGEs) and Melanoidins Formed through the Maillard Reaction: Physiological Consequences of their Intake. Annu Rev Food Sci Technol 2018;9:271–91. https://doi.org/10.1146/ANNUREV-FOOD-030117-012441.
22. Scheijen JLJM, Clevers E, Engelen L, Dagnelie PC, Brouns F, Stehouwer CDA, et al. Analysis of advanced glycation endproducts in selected food items by ultra-performance liquid chromatography tandem mass spectrometry: Presentation of a dietary AGE database. Food Chem 2016;190:1145–50. https://doi.org/10.1016/J.FOODCHEM.2015.06.049.
23. Charissou A, Ait-Ameur L, Birlouez-Aragon I. Evaluation of a gas chromatography/mass spectrometry method for the quantification of carboxymethyllysine in food samples. J Chromatogr A 2007;1140:189–94. https://doi.org/10.1016/J.CHROMA.2006.11.066.
24. Sandu O, Song K, Cai W, Zheng F, Uribarri J, Vlassara H. Insulin Resistance and Type 2 Diabetes in High-Fat–Fed Mice Are Linked to High Glycotoxin Intake. Diabetes 2005;54:2314–9. https://doi.org/10.2337/DIABETES.54.8.2314.
25. Cai W, He JC, Zhu L, Chen X, Zheng F, Striker GE, et al. Oral Glycotoxins Determine the Effects of Calorie Restriction on Oxidant Stress, Age-Related Diseases, and Lifespan. Am J Pathol 2008;173:327–36. https://doi.org/10.2353/AJPATH.2008.080152.
26. Lin RY, Choudhury RP, Cai W, Lu M, Fallon JT, Fisher EA, et al. Dietary glycotoxins promote diabetic atherosclerosis in apolipoprotein E-deficient mice. Atherosclerosis 2003;168:213–20. https://doi.org/10.1016/S0021-9150(03)00050-9.
27. Hofmann SM, Dong HJ, Li Z, Cai W, Altomonte J, Thung SN, et al. Improved Insulin Sensitivity Is Associated With Restricted Intake of Dietary Glycoxidation Products in the db/db Mouse. Diabetes 2002;51:2082–9. https://doi.org/10.2337/DIABETES.51.7.2082.
28. Nogueira Silva Lima MT, Delayre-Orthez C, Howsam M, Jacolot P, Niquet-Léridon C, Okwieka A, et al. Early- and life-long intake of dietary advanced glycation end-products (dAGEs) leads to transient tissue accumulation, increased gut sensitivity to inflammation, and slight changes in gut microbial diversity, without causing overt disease. Food Research International 2024;195:114967. https://doi.org/10.1016/J.FOODRES.2024.114967.

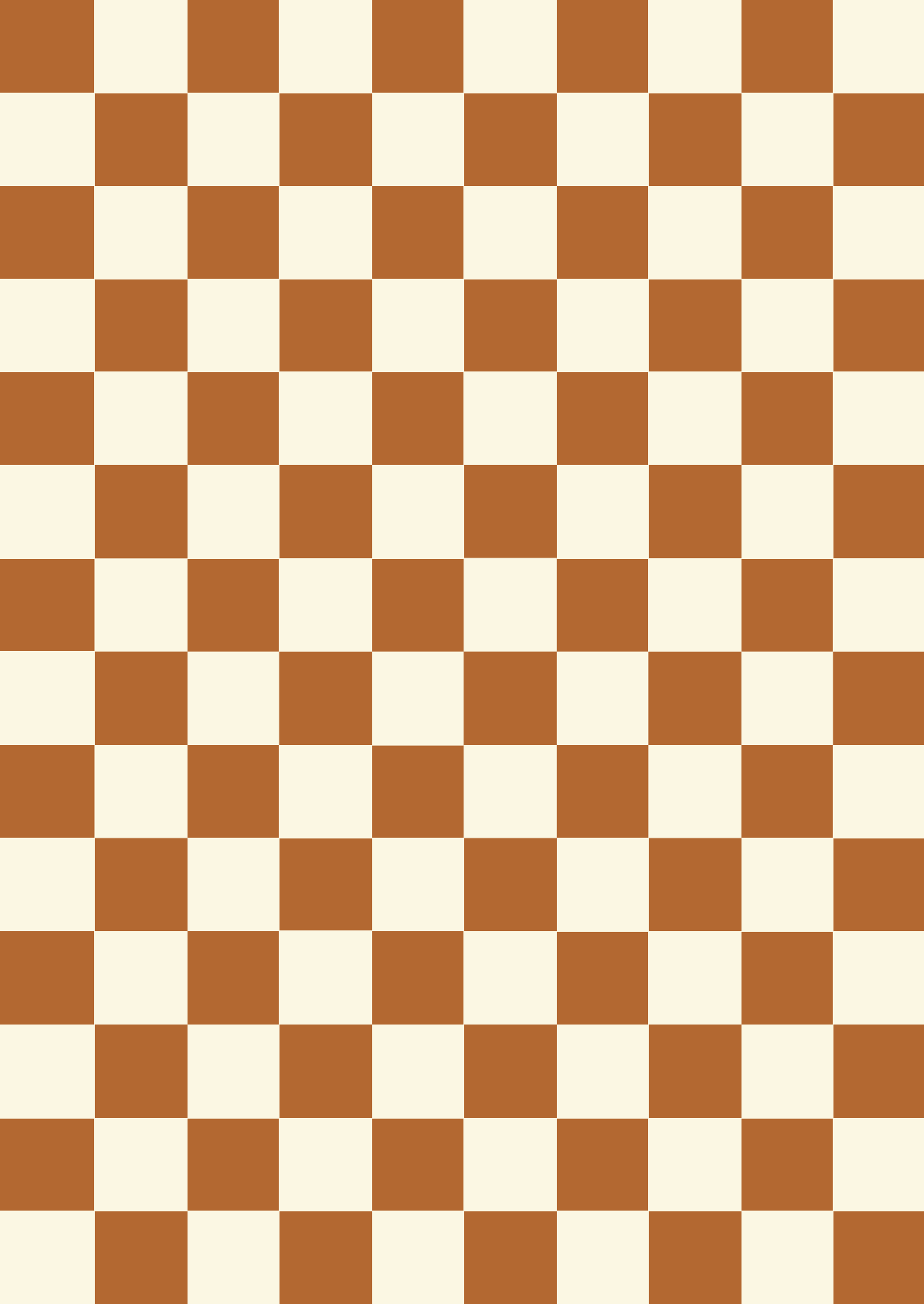
29. Lee HW, Gu MJ, Kim D, Han EH, Kim Y, Ha SK. Effect of advanced glycation end products formed methylglyoxal, a food-borne dicarbonyl precursor, on the exacerbation of diabetic kidney disease by NOX4/Nrf2/NLRP3 inflammasome signaling pathway in db/db mice. Applied Biological Chemistry 2025 68:1 2025;68:38-. https://doi.org/10.1186/S13765-025-01011-Y.
30. Saulnier PJ, Wheelock KM, Howell S, Weil EJ, Tanamas SK, Knowler WC, et al. Advanced glycation end products predict loss of renal function and correlate with lesions of diabetic kidney disease in American indians with type 2 diabetes. Diabetes 2016;65:3744–53. https://doi.org/10.2337/DB16-0310/-/DC1.
31. Diallo AM, Jaisson S, Barriquand R, Lukas C, Barraud S, Decoudier B, et al. Association Between the Tissue and Circulating Advanced Glycation End-Products and the Micro- and Macrovascular Complications in Type 1 Diabetes: The DIABAGE Study. Diabetes Therapy 2022 13:8 2022;13:1531–46. https://doi.org/10.1007/S13300-022-01285-1.
32. de Graaf MCG, Scheijen JLJM, Spooren CEGM, Mujagic Z, Pierik MJ, Feskens EJM, et al. The Intake of Dicarbonyls and Advanced Glycation Endproducts as Part of the Habitual Diet Is Not Associated with Intestinal Inflammation in Inflammatory Bowel Disease and Irritable Bowel Syndrome Patients. Nutrients 2023;15. https://doi.org/10.3390/NU15010083.
33. Linkens AMA, Eussen SJMP, Houben AJHM, Mari A, Dagnelie PC, Stehouwer CDA, et al. Habitual intake of advanced glycation endproducts is not associated with worse insulin sensitivity, worse beta cell function, or presence of prediabetes or type 2 diabetes: The Maastricht Study. Clin Nutr 2023;42:1491–500. https://doi.org/10.1016/J.CLNU.2023.05.021.
34. Linkens AMA, Houben AJHM, Kroon AA, Schram MT, Berendschot TTJM, Webers CAB, et al. Habitual intake of dietary advanced glycation end products is not associated with generalized microvascular function—the Maastricht Study. Am J Clin Nutr 2022;115:444–55. https://doi.org/10.1093/AJCN/NQAB302.
35. Bartlett A, Kleiner M. Dietary protein and the intestinal microbiota: An understudied relationship. IScience 2022;25:105313. https://doi.org/10.1016/J.ISCI.2022.105313.
36. Xie Y, Wang C, Zhao D, Zhou G, Li C. Processing Method Altered Mouse Intestinal Morphology and Microbial Composition by Affecting Digestion of Meat Proteins. Front Microbiol 2020;11:528031. https://doi.org/10.3389/FMICB.2020.00511/BIBTEX.
37. Awan A, Bartlett A, Blakeley-Ruiz JA, Richie T, Theriot CM, Kleiner M. Dietary protein from different sources escapes host digestion and is differentially modified by gut microbiota. Food Funct 2025;16:7154. https://doi.org/10.1039/D5FO01132A.
38. Hellwig M, Diel P, Eisenbrand G, Grune T, Guth S, Henle T, et al. Dietary glycation compounds – implications for human health. Crit Rev Toxicol 2024:1–133. https://doi.org/10.1080/10408444.2024.2362985.
39. Hellwig M, Bunzel D, Huch M, Franz CMAP, Kulling SE, Henle T. Stability of Individual Maillard Reaction Products in the Presence of the Human Colonic Microbiota. J Agric Food Chem 2015;63:6723–30. https://doi.org/10.1021/ACS.JAFC.5B01391.
40. Snoeck V, Goddeeris B, Cox E. The role of enterocytes in the intestinal barrier function and antigen uptake. Microbes Infect 2005;7:997–1004. https://doi.org/10.1016/J.MICINF.2005.04.003.
41. Janssen Duijghuijsen LM, Van Norren K, Grefte S, Koppelman SJ, Lenaerts K, Keijer J, et al. Endurance exercise increases intestinal uptake of the peanut allergen Ara h 6 after peanut consumption in humans. Nutrients 2017;9. https://doi.org/10.3390/nu9010084.
42. Jansen FAC, van Norren K, Baumert JL, van den Bos A, Jacobs JFM, Koppelman SJ. Peanut allergen Ara h 6 is detectable in blood transfusion products. Clin Transl Allergy 2023;13. https://doi.org/10.1002/CLT2.12307.
43. Lund MN, Ray CA. Control of Maillard Reactions in Foods: Strategies and Chemical Mechanisms. J Agric Food Chem 2017;65:4537–52. https://doi.org/10.1021/ACS.JAFC.7B00882.
44. Mehta BM, Deeth HC. Blocked Lysine in Dairy Products: Formation, Occurrence, Analysis, and Nutritional Implications. Compr Rev Food Sci Food Saf 2016;15:206–18. https://doi.org/10.1111/1541-4337.12178.

45. Sánchez-Oliver AJ, Contreras-Calderón J, Puya-Braza JM, Guerra-Hernández E. Quality analysis of commercial protein powder supplements and relation to characteristics declared by manufacturer. LWT 2018;97:100–8. https://doi.org/10.1016/J.LWT.2018.06.047.
46. Buetler TM, Leclerc E, Baumeyer A, Latado H, Newell J, Adolfsson O, et al. Nε-carboxymethyllysine-modified proteins are unable to bind to RAGE and activate an inflammatory response. Mol Nutr Food Res 2008;52:370–8. https://doi.org/10.1002/MNFR.200700101.
47. Toyomura T, Watanabe M, Wake H, Nishinaka T, Hatipoglu OF, Takahashi H, et al. Glycolaldehyde-derived advanced glycation end products promote macrophage proliferation via the JAK-STAT signaling pathway. Mol Biol Rep 2023. https://doi.org/10.1007/s11033-023-08509-y.
48. Van Der Lugt T, Weseler AR, Gebbink WA, Vrolijk MF, Opperhuizen A, Bast A. Dietary advanced glycation endproducts induce an inflammatory response in human macrophages in vitro. Nutrients 2018;10. https://doi.org/10.3390/nu10121868.
49. Valencia J V., Mone M, Koehne C, Rediske J, Hughes TE. Binding of receptor for advanced glycation end products (RAGE) ligands is not sufficient to induce inflammatory signals: Lack of activity of endotoxin-free albumin-derived advanced glycation end products. Diabetologia 2004;47:844–52. https://doi.org/10.1007/S00125-004-1392-9.
50. Goode A, Yeh V, Bonev BB. Interactions of polymyxin B with lipopolysaccharide-containing membranes. Faraday Discuss 2021;232:317–29. https://doi.org/10.1039/d1fd00036e.
51. Buetler TM, Latado H, Leclerc E, Weigle B, Baumeyer A, Heizmann CW, et al. Glycolaldehyde-modified β-lactoglobulin AGEs are unable to stimulate inflammatory signaling pathways in RAGE-expressing human cell lines. Mol Nutr Food Res 2011;55:291–9. https://doi.org/10.1002/MNFR.201000140.
52. Snelson M, Lucut E, Coughlan MT. The Role of AGE-RAGE Signalling as a Modulator of Gut Permeability in Diabetes 2022.
53. Schmidt AM, Hofmann M, Taguchi A, Shi Du Yan, Stern DM. RAGE: a multiligand receptor contributing to the cellular response in diabetic vasculopathy and inflammation. Semin Thromb Hemost 2000;26:485–93. https://doi.org/10.1055/S-2000-13204.
54. Bierhaus A, Humpert PM, Morcos M, Wendt T, Chavakis T, Arnold B, et al. Understanding RAGE, the receptor for advanced glycation end products. Journal of Molecular Medicine 2005 83:11 2005;83:876–86. https://doi.org/10.1007/S00109-005-0688-7.
55. Thornalley PJ. Glycation in diabetic neuropathy: Characteristics, consequences, causes, and therapeutic options. Int Rev Neurobiol 2002;50:37–57. https://doi.org/10.1016/S0074-7742(02)50072-6.
56. Hirschi-Budge KM, Tsai KYF, Curtis KL, Davis GS, Theurer BK, Kruyer AMM, et al. RAGE signaling during tobacco smoke-induced lung inflammation and potential therapeutic utility of SAGEs. BMC Pulm Med 2022;22:1–12. https://doi.org/10.1186/S12890-022-01935-X.
57. Englert JM, Kliment CR, Ramsgaard L, Milutinovic PS, Crum L, Tobolewski JM, et al. Paradoxical function for the receptor for advanced glycation end products in mouse models of pulmonary fibrosis. Int J Clin Exp Pathol 2011;4:241.
58. Perkins TN, Oczypok EA, Milutinovic PS, Dutz RE, Oury TD. RAGE-dependent VCAM-1 expression in the lung endothelium mediates IL-33-induced allergic airway inflammation. Allergy: European Journal of Allergy and Clinical Immunology 2019;74:89–99. https://doi.org/10.1111/ALL.13500.
59. Oczypok EA, Milutinovic PS, Alcorn JF, Khare A, Crum LT, Manni ML, et al. Pulmonary receptor for advanced glycation end-products promotes asthma pathogenesis through IL-33 and accumulation of group 2 innate lymphoid cells. Journal of Allergy and Clinical Immunology 2015;136:747-756.e4. https://doi.org/10.1016/J.JACI.2015.03.011.
60. Al-Robaiy S, Kindermann A, Wodischeck S, Simm A, Treede H, Bartling B. Long-term endurance running activity causes pulmonary changes depending on the receptor for advanced glycation end-products. Pflugers Arch 2018;470:1543–53. https://doi.org/10.1007/S00424-018-2175-3.

61. Bangert A, Andrassy M, Müller AM, Bockstahler M, Fischer A, Volz CH, et al. Critical role of RAGE and HMGB1 in inflammatory heart disease. Proc Natl Acad Sci U S A 2016;113:E155–64. https://doi.org/10.1073/PNAS.1522288113.
62. Bi C, Liu B, Gao P, Wang C, Fang S, Huo Z, et al. RAGE deficiency ameliorates abdominal aortic aneurysm progression. Inflammation Research 2025;74:1–17. https://doi.org/10.1007/S00011-025-02027-2.
63. Kwak T, Drews-Elger K, Ergonul A, Miller PC, Braley A, Hwang GH, et al. Targeting of RAGE-ligand signaling impairs breast cancer cell invasion and metastasis. Oncogene 2017;36:1559–72. https://doi.org/10.1038/ONC.2016.324.
64. Tian Y, Charles EJ, Yan Z, Wu D, French BA, Kron IL, et al. The myocardial infarct-exacerbating effect of cell-free DNA is mediated by the high-mobility group box 1–receptor for advanced glycation end products–Toll-like receptor 9 pathway. J Thorac Cardiovasc Surg 2019;157:2256-2269.e3. https://doi.org/10.1016/J.JTCVS.2018.09.043.
65. He J, Wei L, Tan S, Liang B, Liu J, Lu L, et al. Macrophage RAGE deficiency prevents myocardial fibrosis by repressing autophagy-mediated macrophage alternative activation. The FASEB Journal 2023;37:e23259. https://doi.org/10.1096/FJ.202300173RR.
66. Liu S, Song Y, Zhang IY, Zhang L, Gao H, Su Y, et al. RAGE Inhibitors as Alternatives to Dexamethasone for Managing Cerebral Edema Following Brain Tumor Surgery. Neurotherapeutics 2022;19:635–48. https://doi.org/10.1007/S13311-022-01207-W.
67. Hansen LM, Gupta D, Joseph G, Weiss D, Taylor WR. The receptor for advanced glycation end products impairs collateral formation in both diabetic and non-diabetic mice. Laboratory Investigation 2017;97:34–42. https://doi.org/10.1038/LABINVEST.2016.113.
68. Nadatani Y, Watanabe T, Tanigawa T, Ohkawa F, Takeda S, Higashimori A, et al. High-Mobility Group Box 1 Inhibits Gastric Ulcer Healing through Toll-Like Receptor 4 and Receptor for Advanced Glycation End Products. PLoS One 2013;8:e80130. https://doi.org/10.1371/JOURNAL.PONE.0080130.
69. von Bauer R, Oikonomou D, Sulaj A, Mohammed S, Hotz-Wagenblatt A, Gröne H-J, et al. CD166/ALCAM Mediates Proinflammatory Effects of S100B in Delayed Type Hypersensitivity. The Journal of Immunology 2013;191:369–77. https://doi.org/10.4049/JIMMUNOL.1201864.
70. Mazarati A, Maroso M, Iori V, Vezzani A, Carli M. High-mobility group box-1 impairs memory in mice through both toll-like receptor 4 and Receptor for Advanced Glycation End Products. Exp Neurol 2011;232:143–8. https://doi.org/10.1016/J.EXPNEUROL.2011.08.012.
71. Riva M, Källberg E, Björk P, Hancz D, Vogl T, Roth J, et al. Induction of nuclear factor-κB responses by the S100A9 protein is Toll-like receptor-4-dependent. Immunology 2012;137:172–82. https://doi.org/10.1111/J.1365-2567.2012.03619.X.
72. Yang H, Liu H, Zeng Q, Imperato GH, Addorisio ME, Li J, et al. Inhibition of HMGB1/RAGE-mediated endocytosis by HMGB1 antagonist box A, anti-HMGB1 antibodies, and cholinergic agonists suppresses inflammation. Molecular Medicine 2019;25:1–13. https://doi.org/10.1186/S10020-019-0081-6.
73. Sun C, Yang Y, Liu G, Nakanishi H. Activation of receptor for advanced glycation end products by histone to induce the inflammatory response. Food and Fermentation Industries 2024;50:78–84. https://doi.org/10.13995/J.CNKI.11-1802/TS.035362.
74. Paz S, Hsiao J, Cauntay P, Soriano A, Bai L, Machemer T, et al. The Distinct and Cooperative Roles of Toll-Like Receptor 9 and Receptor for Advanced Glycation End Products in Modulating In Vivo Inflammatory Responses to Select CpG and Non-CpG Oligonucleotides. Https://Home-Liebertpub-ComEzproxyLibraryWurNl/Nat 2017;27:272–84. https://doi.org/10.1089/NAT.2017.0668.
75. Ye D, Miyoshi A, Ushitani T, Kadoya M, Igeta M, Konishi K, et al. RAGE in circulating immune cells is fundamental for hippocampal inflammation and cognitive decline in a mouse model of latent chronic inflammation. Brain Behav Immun 2024;116:329–48. https://doi.org/10.1016/J.BBI.2023.12.022.

76. Tian Y, Pan D, Chordia MD, French BA, Kron IL, Yang Z. The spleen contributes importantly to myocardial infarct exacerbation during post-ischemic reperfusion in mice via signaling between cardiac HMGB1 and splenic RAGE. Basic Res Cardiol 2016;111:62. https://doi.org/10.1007/S00395-016-0583-0.
77. Gao Y, Wake H, Morioka Y, Liu K, Teshigawara K, Shibuya M, et al. Phagocytosis of Advanced Glycation End Products (AGEs) in Macrophages Induces Cell Apoptosis 2017. https://doi.org/10.1155/2017/8419035.
78. Sun F, Suttapitugsakul S, Xiao H, Wu R. Comprehensive Analysis of Protein Glycation Reveals Its Potential Impacts on Protein Degradation and Gene Expression in Human Cells. J Am Soc Mass Spectrom 2019;30:2480. https://doi.org/10.1007/S13361-019-02197-4.
79. Takizawa N, Takada K, Ohkawa K. Inhibitory Effect of Nonenzymatic Glycation on Ubiquitination and Ubiquitin-Mediated Degradation of Lysozyme. Biochem Biophys Res Commun 1993;192:700–6. https://doi.org/10.1006/BBRC.1993.1471.
80. Al Amir I, Dubayle D, Héron A, Delayre-Orthez C, Anton PM. Maillard reaction products from highly heated food prevent mast cell number increase and inflammation in a mouse model of colitis 2017;48:26–32. https://doi.org/10.1016/J.NUTRES.2017.10.005.
81. Ahrens I, Chen YC, Topcic D, Bode M, Haenel D, Hagemeyer CE, et al. HMGB1 binds to activated platelets via the receptor for advanced glycation end products and is present in platelet rich human coronary artery thrombi. Thromb Haemost 2015;114:994–1003. https://doi.org/10.1160/TH14-12-1073.
82. Yamamoto Y, Liang M, Munesue S, Deguchi K, Harashima A, Furuhara K, et al. Vascular RAGE transports oxytocin into the brain to elicit its maternal bonding behaviour in mice. Commun Biol 2019;2. https://doi.org/10.1038/s42003-019-0325-6.
83. Cherepanov SM, Gerasimenko M, Yuhi T, Shabalova A, Zhu H, Yokoyama S, et al. An improved sample extraction method reveals that plasma receptor for advanced glycation end-products (RAGE) modulates circulating free oxytocin in mice. Peptides (NY) 2021;146:170649. https://doi.org/10.1016/J.PEPTIDES.2021.170649.
84. Munesue S ichi, Liang MK, Harashima A, Zhong J, Furuhara K, Boitsova EB, et al. Transport of oxytocin to the brain after peripheral administration by membrane-bound or soluble forms of receptors for advanced glycation end-products. J Neuroendocrinol 2021;33. https://doi.org/10.1111/JNE.12963.
85. Higashida H, Furuhara K, Yamauchi AM, Deguchi K, Harashima A, Munesue S, et al. Intestinal transepithelial permeability of oxytocin into the blood is dependent on the receptor for advanced glycation end products in mice. Sci Rep 2017;7. https://doi.org/10.1038/S41598-017-07949-4.
86. Sakatani S, Yamada K, Homma C, Munesue S, Yamamoto Y, Yamamoto H, et al. Deletion of RAGE causes hyperactivity and increased sensitivity to auditory stimuli in mice. PLoS One 2009;4. https://doi.org/10.1371/JOURNAL.PONE.0008309.
87. Gerasimenko M, Lopatina O, Munesue S, Harashima A, Yokoyama S, Yamamoto Y, et al. Receptor for advanced glycation end-products (RAGE) plays a critical role in retrieval behavior of mother mice at early postpartum. Physiol Behav 2021;235:113395. https://doi.org/10.1016/J.PHYSBEH.2021.113395.
88. Na M, Mohammad M, Fei Y, Wang W, Holdfeldt A, Forsman H, et al. Lack of receptor for advanced glycation end products leads to less severe staphylococcal skin infection but more skin abscesses and prolonged wound healing. Journal of Infectious Diseases 2018;218:791–800. https://doi.org/10.1093/INFDIS/JIY007.
89. He M, Kubo H, Morimoto K, Fujino N, Suzuki T, Takahasi T, et al. Receptor for advanced glycation end products binds to phosphatidylserine and assists in the clearance of apoptotic cells. EMBO Rep 2011;12:358–64. https://doi.org/10.1038/EMBOR.2011.28.
90. Achouiti A, De Vos AF, Van'T Veer C, Florquin S, Tanck MW, Nawroth PP, et al. Receptor for advanced glycation end products (RAGE) serves a protective role during Klebsiella pneumoniae-induced pneumonia. PLoS One 2016;11. https://doi.org/10.1371/JOURNAL.PONE.0141000.

91. van Zoelen MAD, Schouten M, de Vos AF, Florquin S, Meijers JCM, Nawroth PP, et al. The Receptor for Advanced Glycation End Products Impairs Host Defense in Pneumococcal Pneumonia. The Journal of Immunology 2009;182:4349–56. https://doi.org/10.4049/JIMMUNOL.0801199.
92. Palmer IL, Parker G, Chiu AT, Beus CG, Evans EP, Radford JH, et al. RAGE Knockout Mitigates Diet-Induced Obesity and Metabolic Disruption. Metabolites 2025, Vol 15, Page 524 2025;15:524. https://doi.org/10.3390/METABO15080524.
93. Zhang L, He J, Wang J, Liu J, Chen Z, Deng B, et al. Knockout RAGE alleviates cardiac fibrosis through repressing endothelial-to-mesenchymal transition (EndMT) mediated by autophagy. Cell Death Dis 2021;12:1–13. https://doi.org/10.1038/S41419-021-03750-4.
94. Schmidt AM. Soluble RAGEs – Prospects for Treating & Tracking Metabolic and Inflammatory Disease. Vascul Pharmacol 2015;72:1. https://doi.org/10.1016/J.VPH.2015.06.011.
95. Zhang Y, Zhang Z, Tu C, Chen X, He R. Advanced Glycation End Products in Disease Development and Potential Interventions. Antioxidants 2025, Vol 14, Page 492 2025;14:492. https://doi.org/10.3390/ANTIOX14040492.
96. Ahmed N, Thornalley PJ. Advanced glycation endproducts: what is their relevance to diabetic complications? Diabetes Obes Metab 2007;9:233–45. https://doi.org/10.1111/J.1463-1326.2006.00595.X.
97. Tan ALY, Sourris KC, Harcourt BE, Thallas-Bonke V, Penfold S, Andrikopoulos S, et al. Disparate effects on renal and oxidative parameters following RAGE deletion, AGE accumulation inhibition, or dietary AGE control in experimental diabetic nephropathy. Am J Physiol Renal Physiol 2010;298. https://doi.org/10.1152/AJPRENAL.00591.2009.



7

English summary

Background and aim

The browning process that gives cooked foods their appealing aromas, flavors and textures is known as the Maillard reaction. This non-enzymatic reaction between proteins and sugars, also referred to as protein glycation, leads to the formation of covalent adducts on lysine and arginine residues; a heterogenous group of compounds collectively called advanced glycation end products (AGEs). Following the discovery of glycated hemoglobin (HbA1c) as a diagnostic marker for diabetes in the 1960s, endogenous protein glycation was shown to be relevant to human disease, which subsequently raised concerns about the safety of dietary AGEs. These concerns were reinforced when high consumption of processed foods in the Western diet became associated with an increased risk of the same non-communicable diseases.

Dietary AGEs enter the body through the digestive tract. After digestion, they are mainly absorbed as free AGEs or dipeptides, and current literature on the health effects of high AGE intake therefore predominantly focuses on the systemic effects of these bioavailable forms. However, only protein-bound AGEs are able to bind to the receptor for AGEs (RAGE), which is involved in inflammatory signaling. In this context, the intestine would be the primary target organ, as it might be the only tissue to encounter undigested glycated dietary proteins. However, their impact at the intestinal level remains largely unknown. Yet, intestinal health is known to play a key role in general wellbeing, so this interaction might be of influence to systemic health outcomes. Therefore, the aim of this thesis was to increase our understanding of how intact dietary glycated proteins affect intestinal health at the epithelium and immune level, using *in vitro* models.

Main findings

The currently available *in vitro* studies on the inflammatory effects of glycated dietary proteins on the intestinal epithelium face multiple methodological limitations and should therefore be interpreted with caution (**Chapter 2**). Key concerns include the limited chemical characterization of the glycated samples, including insufficient endotoxin quantification, and the absence of appropriate positive controls for RAGE activation. The subsequent chapters of this thesis aimed to address these uncertainties. In **Chapter 3**, both monomers and aggregates of undigested glycated proteins (beta-lactoglobulin) were shown to cross a conventional air-liquid interface monolayer, mimicking the ileal villous epithelium, most likely via paracellular transport. This finding challenges the prevailing assumption

that undigested glycated proteins are not bioavailable, leaving open the possibility that they might interact with cell types beyond the epithelium, for example intestinal immune cells. Since protein-bound AGEs are thought to induce inflammation through interaction with RAGE, these glycated proteins were subsequently tested on primary immune cells in **Chapter 4**. Some notable observations emerged. First, RAGE appeared predominantly expressed intracellularly across multiple cell models, while RAGE was only substantially expressed on the cell surface of specific *in vitro* models, for example in M-CSF differentiated M0 macrophages. Second, LPS scavenging drastically reduced the inflammatory responses attributed to glycated dietary proteins, despite endotoxin levels being considered neglectable based on common quantification methods. In contrast, a RAGE antagonist did not attenuate these responses, suggesting that LPS may act as a confounding factor in such experiments. Furthermore, stimulation with known RAGE agonists (e.g. HMGB1 or Aβ-42) did not induce an inflammatory response, raising the question whether LPS might function as a necessary co-factor in RAGE-mediated processes. This hypothesis was explored in **Chapter 5**, but the preliminary results obtained were mixed. RAGE agonists did not enhance the inflammatory potency of LPS in the primary cell model used previously, but occasional amplification of NF-kB activity was observed in NF-kB-reporter cells. This result was however not consistently reproducible and was not accompanied by increased pro-inflammatory cytokines production, as would be expected, suggesting that alternative downstream outcome may be involved.

Discussion and conclusion

Based on the main findings of this thesis, it is proposed that a combination of stimuli is required to induce RAGE-dependent inflammatory signalling, suggesting that glycated dietary proteins alone are unlikely to induce inflammation in healthy individuals. When placed in the broader context of dietary AGE consumption and its implications for human health, glycation can also contribute to lysine deficiency and some absorbed free AGEs (particularly HMGB1) are suggested to exert nephrotoxic effects. However, as discussed in **Chapter 6**, the consequences of a high-GI diet and endogenous AGE formation appear to be far more pronounced. From this perspective, the societal relevance of further dietary AGE research, particularly in healthy populations, seems limited.

A

Acknowledgements
About the author
List of publications
Training activities

Acknowledgements

The completion of this PhD thesis marks the end of more than a decade at Wageningen University. I began this journey in September 2015 as a first-year bachelor's student. Over time, the inspiring learning environment, together with the many wonderful people I met along the way, made me want to stay, eventually carrying me through every stage of my academic training. These years have been filled with joy, growth, and personal development, although they also came with their fair share of challenges and setbacks. In these acknowledgements, I would like to express my gratitude to the people who have supported and accompanied me throughout this memorable journey.

First of all, I would like to thank my supervisory team. **Vincenzo**, you are one of a kind and I truly enjoyed working with you! From your (unintended?) funny emails and occasional pep talks to your quick, straight-to-the-point feedback, I never left a meeting disappointed. You gave me the trust and freedom to follow the direction I believed was needed to move my research forward. Although this path has been frustrating at times and some of my questions still remain unanswered, I would choose it again without hesitation. Thank you for making this possible. **Tamara**, ik wist (en weet) dat ik altijd bij je terecht kan. Ondanks alle kopzorgen die dit project soms met zich meebracht, hebben we er samen iets moois van gemaakt. Je dacht altijd in mijn belang, en daar ben ik je heel dankbaar voor. Je voelde feilloos aan wanneer het nodig was om even een keer extra in te checken. Blijf doen waar je hart ligt en laat je niet gek maken! Thanks for having my back! **Klaske**, wat ben ik blij dat jij het team wilde komen versterken tijdens het tweede deel van mijn promotieonderzoek. Je bent een echte vakvrouw, en jouw betrokkenheid en input hebben veel betekend voor de afronding van dit proefschrift. Waar een MSc thesis allemaal niet toe kan leiden... Ik vond het toen heel spannend om aan 'het echte werk' te beginnen, maar jij en Xiaolin geloofden in mij waardoor ik ook in mezelf begon te geloven. Mijn MSc thesis is daarmee echt een van de waardevolste periodes van mijn studie geweest. Bedankt daarvoor! **Josep**, you are definitely not afraid to think big! I really admire your ambition and energy. I'll remember our in-depth conversations about science, often just spontaneously in the corridor. Take good care of yourself, your students, and of course your new family!

Then my dear paranymphs, **Marialena and Susanne**, I cannot imagine having done this without you! Marialena, my dear partner in crime, perhaps I should have mentioned you first, because without you this thesis would not be there. We spent

many hours together in the lab, discussing cells, assays, and unexpected results, while repeatedly questioning our beliefs and assumptions. And, somehow, we also kept ending up together in Maastricht, which turned out to be quite the conference hotspot… Not to forget our trip to Dundee and the PhD trip to Spain and Mexico. Thank you for being my roommate, thank you for all the adventures. You are one of the purest and kindest people I know! Susanne, my organoid whisperer, het was een feestje om met jou aan het project te werken. Samen puzzelen blijft toch echt het leukste! Je bent zo goed in wat je doet, bedankt voor wat ik van je heb mogen leren. Oh en die whatsapp stickers… die zijn nog steeds mijn favoriet! Ik kan nooit meer normaal naar een pipet kijken. Bedankt voor de vrolijke noot, de flauwe grapjes. Zorg goed voor jezelf, ik gun je de wereld!

Also a special thanks to Tamara's FQD team: **Danielle, Xiangnan, Marit, and Karen**. I really enjoyed working with all of you. Thank you for the help, coffees, conversations, gossip and all the fun along the way. You are amazing. Danielle, that Italian restaurant in Mexico is still one of the most memorable dinners I've ever had. Its owner was absolutely adorable, and we had such a great time. Xiangnan, I have so much respect for you and for the way you are chasing your dreams. Marit and Karen, I only wish you had joined the group years earlier, I really enjoyed your personalities and would have loved to spend more time working together.

The **HNH Corner Office**, dear Cornies, thanks for adopting me, it was a pleasure to be part of the office when I was working in the HNH cell culture lab. A special thanks to **Aina** and **Mieke**. Aina, we started our PhDs around the same time, and it meant a lot to me to have each other as a sounding board along the way. Good luck with the final stretch, you've got this and I'm proud of you! Mieke, wat zouden wij PhD studenten zonder jou moeten, onze rots in de branding! Het bloemetje op de boekenlegger is een knipoog naar jouw tekeningetjes op mijn pakketjes, labspullen en de random briefjes op mijn bureau. Bedankt voor je eindeloze steun en betrokkenheid!

FQD office and technicians, thanks for your kind support and efforts to keep everything running smoothly behind the scenes. A special thanks to **Nienke** for helping to get the FQD cell culture lab up and running and **Christos** for helping with the UPLC-MS/MS analysis.

Mijn studiemaatjes, **Rianne, Monique en Annelien**, hoe bijzonder dat we elkaar in het eerste jaar van onze bachelor tegen zijn gekomen en praktisch de hele opleiding zij-aan-zij hebben doorlopen. Elk van ons met een compleet andere

achtergrond, maar dat maakte het juist zo leuk! Bedankt voor de mooie gesprekken en alles wat ik van jullie heb mogen leren. Ik kon me ook geen leukere practicum / project partners wensen. Jullie fanatisme was aanstekelijk, als we ergens onze zinnen op hadden gezet...! Ik mis de studie-break brownies trouwens wel nog steeds, eeuwig zonde dat die niet meer verkocht worden in Forum.

Last but not least, mijn lieve vrienden thuis! Bedankt voor alle gezelligheid en relativering onderweg. **Kim**, wat hebben we samen veel meegemaakt de afgelopen 10 jaar. Ik ben trots op ons en op hoe ver we al gekomen zijn. Ik weet dat ik altijd op je kan rekenen, bedankt voor je onvoorwaardelijke vriendschap, gelukkig is onze bingokaart nog lang niet vol (en anders verzinnen we er gewoon weer iets bij)! **Ellie en Robert-Jan**, bij jullie voelt het echt als een tweede thuis. Bedankt voor alle gezelligheid, de spelletjesavonden, zondag frietdag, de wijze raad op z'n tijd, en nog zoveel meer, maar bovenal voor jullie vriendschap! **Marjolein en Martijn**, ik bewonder hoe jullie altijd zoveel warmte en gezelligheid brengen, ik ben blij jullie vriendin te zijn! Bedankt voor de goede gesprekken, bitterballen, en buitenritten. Ohja, en natuurlijk de wodka slush puppies! **Joeri**, ik denk dat je half niet weet hoeveel je voor me betekent. Na de Knip zijn we elk onze eigen weg ingeslagen, maar gelukkig zijn we elkaar niet uit het oog verloren.

Chris, je hebt de gave om me te laten lachen, ook als ik soms sip, teleurgesteld, of gefrustreerd ben. Ik hou van onze pesterijtjes, fietsritten, hardlooprondjes, (ski-)vakanties, avonden bij Bella of gewoon op de bank. Ik wil geen bakkies meer eten zonder jou! **Claudia en Arjan**, bedankt voor alle gezelligheid en dat jullie me altijd met open armen hebben ontvangen!

Ans en Wil, mam en pap, bedankt voor alles wat jullie me geleerd hebben, kansen die jullie mogelijk hebben gemaakt. Bedankt voor jullie liefde en tijd. Bedankt dat ik mijn hart mag volgen, al weet ik soms zelf (nog) niet waar dat toe leidt. Ik kom altijd graag thuis, en hopelijk kan dat nog vele jaren!

About the author

Fleur Jansen was born on November 26, 1997, in Geldrop, the Netherlands. She completed her secondary school education at the Dr. Knippenbergcollege in Helmond, where she obtained her VWO diploma in 2015. She continued her education at Wageningen University and Research, pursuing a Bachelor's and Master's degree in Nutrition & Health, specializing in Molecular Nutrition and Toxicology. Both degrees were obtained *cum laude*. During her MSc thesis at the Nutritional Biology group, she investigated the mechanisms underlying hypothalamic inflammation in cancer cachexia using *in vitro* models. She completed her internship during the COVID-19 pandemic, during which she conducted a systematic literature while also gaining hands-on experience with UPLC-MS/MS analysis. The data and findings from both her thesis and internship contributed to several scientific publications. Starting her scientific career, she remained affiliated with the Nutritional Biology group as a research assistant, where she was responsible for analysing biological samples from several clinical studies and contributed to teaching in various BSc and MSc courses, before starting her PhD at the Food Quality and Design group in September 2021. The scientific results of this PhD trajectory are presented in this thesis.

List of publications

This thesis

Jansen, F.A.C., Fogliano, V., Rubert, J., & Hoppenbrouwers, T. (2023). Dietary Advanced Glycation End products interacting with the intestinal epithelium: What do we really know? *Molecular Metabolism*, *73*. https://doi.org/10.1016/J.MOLMET.2023.101734

Jansen, F.A.C., Rubert, J., van Norren, K., Fogliano, V., & Hoppenbrouwers, T. (2025). Seeking standardized in vitro models of AGE-RAGE signaling in the physiological perspective of glycated dietary proteins. *International Journal of Biological Macromolecules*, *318*(Pt 1). https://doi.org/10.1016/j.ijbiomac.2025.144889

Other publications

Jansen, F.A.C., van Norren, K., Baumert, J. L., van den Bos, A., Jacobs, J. F. M., & Koppelman, S. J. (2023). Peanut allergen Ara h 6 is detectable in blood transfusion products. *Clinical and Translational Allergy*, *13*(11). https://doi.org/10.1002/CLT2.12307

Li, X.*, Holtrop, T.*, **Jansen, F.A.C.***, Olson, B., Levasseur, P., Zhu, X., Poland, M., Schalwijk, W., Witkamp, R. F., Marks, D. L., & van Norren, K. (2022). Lipopolysaccharide-induced hypothalamic inflammation in cancer cachexia-anorexia is amplified by tumour-derived prostaglandin E2. *Journal of Cachexia, Sarcopenia and Muscle*, *13*(6), 3014–3027. https://doi.org/10.1002/jcsm.13093

van Krimpen, S.J.*, **Jansen, F.A.C.***, Ottenheim, V.L.*, Belzer, C., van der Ende, M., & van Norren, K. (2021). The effects of pro-, pre-, and synbiotics on muscle wasting, a systematic review—gut permeability as potential treatment target. *Nutrients*, *13*(4), 1115. https://doi.org/10.3390/nu13041115

van der Ende, M., Li, X., Poland, M., **Jansen, F.A.C.**, Meijerink, J., Keijer, J., Witkamp, R. F., Grefte, S., & van Norren, K. (2026). Assessing the involvement of tumor-secreted factors in the inhibition of muscle differentiation. *Biochimica et Biophysica Acta - Molecular Cell Research*, *1873*(2), 120093. https://doi.org/10.1016/j.bbamcr.2025.120093

Li, X., Zhu, X., Diba, P., Shi, X., Vrieling, F., **Jansen, F.A.C.**, Balvers, M. G. J., de Bus, I., Levasseur, P. R., Sattler, A., Arneson-Wissink, P. C., Poland, M., Witkamp, R. F., van Norren, K., & Marks, D. L. (2025). Tumor-derived cyclooxygenase-2 fuels

hypothalamic inflammation. *Brain, Behavior, and Immunity*, *123*, 886–902. https://doi.org/10.1016/j.bbi.2024.11.002

* These authors have contributed equally to this work

Training activities

Discipline specific activities	Organizer and location	Year
Summer school “Glycation, Maillard Reaction & Carbamylation”	Université de Lille, Lille, FR (online)	2021
IMARS-14	International Maillard Reaction Society, Doha, QA (online)	2021
European summer school on stem cell biology and regenerative medicine	Stem Cell Education & Research, Hydra, GR	2022
Young AGErs Symposium 2022	University of Edinburgh, Edinburgh, UK	2022
OrganoidNL Symposium 2023	AMOLF, Amsterdam, NL	2023
Young AGErs Symposium 2023	Maastricht University, Maastricht, NL	2023
IMARS-15	International Maillard Reaction Society, Maastricht, NL	2024
OrganoidNL Symposium 2025	AMOLF, Amsterdam, NL	2025
Dutch Nutritional Immunology Conference	Utrecht University / Wageningen University & Research, Wageningen, NL	2025

General courses	Organizer and location	Year
PhD Competence Assessment	WGS, Wageningen, NL	2021
Reviewing a Scientific Manuscript	WGS, Wageningen, NL	2022
VLAG PhD week	VLAG, Baarlo, NL	2022
PhD Workshop Carousel	WGS, Wageningen, NL	2022
Project and Time Management	WGS, Wageningen, NL	2022
Effective Behaviour in Professional Surroundings	WGS, Wageningen, NL	2022
Scientific Integrity	WGS, Wageningen, NL	2022
Critical Thinking and Argumentation	WGS, Wageningen, NL	2022
LaTex Introduction	WGS, Wageningen, NL	2023
PhD on Track	VLAG, Wageningen, NL	2023
Career Orientation	WGS, Wageningen, NL	2024

Other activities	Organizer and location	Year
Preparation of research proposal	FQD, Wageningen, NL	2021
PhD Excursion	FQD, Madrid / Murcia / Valencia / Barcelona, ES	2022
PhD Excursion	FQD, Mexico-Stad, MX	2024
Research group discussion meetings	FQD, Wageningen, NL	2021–2025

A

Funding statement
The research described in this thesis was directly funded by the research department.

Cover design: Kira van Landschoot | Vankira.nl
Layout: Renate Siebes | Proefschrift.nu
Printed by: ProefschriftMaken on FSC-certified paper